Characterizing and exploiting genetic trajectories towards antibiotic resistance

Jahn, Leonie Johanna

Publication date:
2019

Document Version
Publisher's PDF, also known as Version of record

Characterizing and exploiting genetic trajectories towards antibiotic resistance

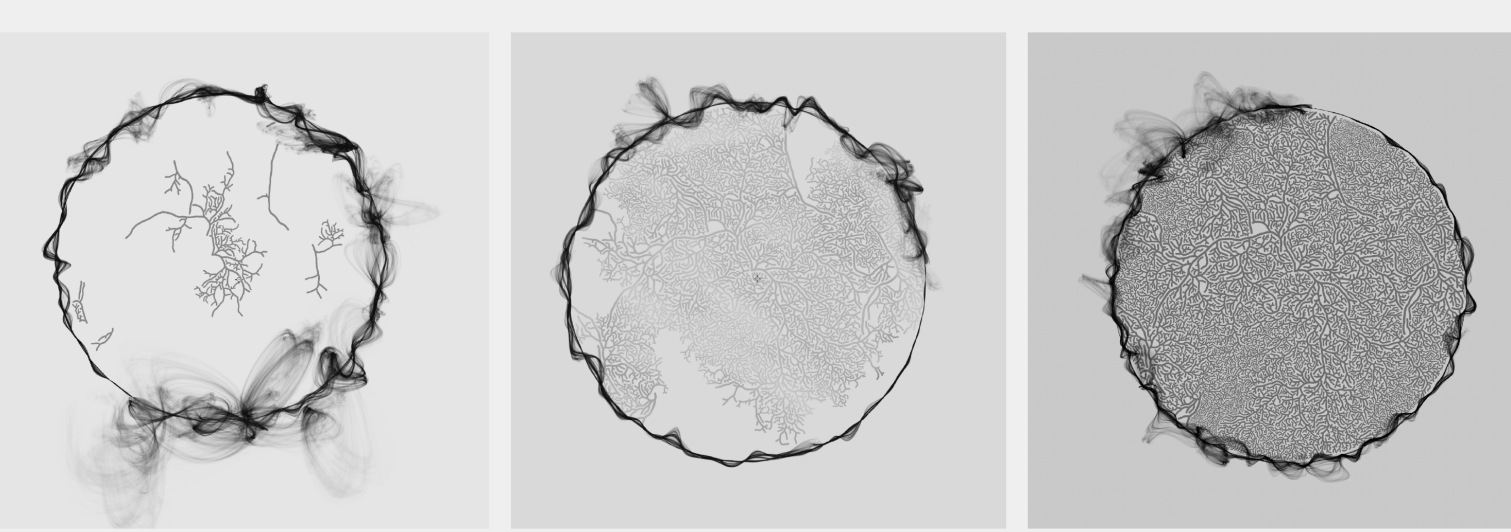

Leonie Johanna Jahn

PhD Thesis
May 2019

The Novo Nordisk Foundation Center for Biosustainability
The Technical University of Denmark

Preface

The work presented in this thesis was conducted from the 1st of July 2015 to the 4th of May 2019 with a period of maternity/parental leave between the 1st of July 2016 and the 9th of May 2017. The work was primarily based at the Novo Nordisk Foundation Center for Biosustainability at the Technical University of Denmark (DTU) and included a three-month research stay at the Broad Institute and the Massachusetts Institute of Technology (MIT) in the laboratory of Professor Jim Collins. The work was supervised by Professor Morten Otto Alexander Sommer, affiliated to the Novo Nordisk Foundation Center for Biosustainability at the DTU, and co-supervised by Professor Matthias Heinemann, affiliated to the University of Groningen. The work was funded by the European Union through the "metaRNA" Marie Curie Fellowship.

Leonie Johanna Jahn, 4th of May 2019

Novo Nordisk Foundation Center for Biosustainability, DTU, Kgs. Lyngby

Abstract

Bacteria have an enormous genetic plasticity and adaptive potential that enables them to inhabit almost every ecological niche on this planet and respond to drastic environmental changes. While this bacterial diversity and flexibility is highly fascinating and provides us with immense resources, it can also put human health at risk, e.g. when pathogenic bacteria adapt to antibiotics and become resistant. As antibiotic resistant bacteria increase human morbidity and mortality it is crucial to take action. The antibiotic resistance crisis is addressed on multiple levels including governmental and non-governmental programs, education, public-health campaigns as well as academic and industrial research in epidemiology, medicine, pharmacology, biology and chemistry. The work conducted in this thesis contributes to the antibiotic resistance research by providing novel tools to study *de novo* antibiotic resistance evolution in a more systematic and high-throughput fashion. Moreover, these tools were utilized to characterize the genetic trajectories of *de novo* antibiotic resistance evolution, predominantly in the model organism *Escherichia coli*. Genetic constrains were identified, like negative epistatic interactions between different resistance modes or collateral sensitivity, and subsequently exploited by creating a framework to rationally design drug combinations in order to limit *de novo* resistance evolution. Finally, limitations in efficiency and genetic responses to novel CRISPR-based antimicrobials were studied and based on the findings factors crucial to optimize killing efficiency were identified. In short, this thesis contributes to our understanding of antibiotic resistance evolution, providing suggestions for novel and improved treatment options that likely contribute to limiting resistance evolution and treatment of resistant bacteria.

Dansk Resumé

Bakterier har en enorm genetisk plasticitet og adaptivt potentiale, der gør dem i stand til at kolonisere stort set alle økologiske nicher på jordkloden samt reagere på drastiske ændringer i deres omgivelser. Denne bakterielle mangfoldighed og fleksibilitet er ikke kun fascinerende men udgør en vigtig genetisk ressource i bioteknologien, men den kan også sætte menneskers sundhed i fare, f.eks. når patogene bakterier tilpasser sig til antibiotika og bliver resistente. Da antibiotikaresistente bakterier sætter flere menneskeliv på spil end nogensinde før, er det afgørende at tage handling. Antibiotikaresistens-krisen kan behandles på flere niveauer, herunder statslige og ikke-statslige programmer, uddannelse, offentlige sundhedskampagner samt akademisk og industriel forskning inden for epidemiologi, medicin, biologi og kemi. Arbejdet i denne afhandling bidrager til antibiotikaresistensforskningen ved at tilvejebringe nye værktøjer til at studere antibiotikaresistensevolution på en mere systematisk og effektiv facon. Desuden blev disse værktøjer udnyttet til at karakterisere de genetiske udviklingsmønstre i antibiotikaresistensudvikling, overvejende i modelorganismen *Escherichia coli*. Her blev genetiske begrænsninger identificeret, f.eks. negative epistatiske interaktioner mellem forskellige genetiske tilpasninger, også kaldet ”collateral sensitivity” og senere udnyttet ved at skabe rammer for rationelt at designe lægemiddelkombinationer for at begrænse resistensevolutionen. Afslutningsvis blev genetiske tilpasninger som respons på nye CRISPR-baserede antibiotika undersøgt, og baseret på resultaterne blev systemets antibiotiske effektivitet optimeret. Kort sagt bidrager denne afhandling til vores forståelse af udviklingen af antibiotikaresistens og foreslår nye og forbedrede behandlingsmuligheder, som sandsynligvis kan bidrage til at begrænse udviklingen af resistens og til behandling af resistente bakterier.

Outline of the PhD thesis

The PhD thesis is divided into five Chapters. In the first chapter a general introduction to the work conducted for this PhD thesis is presented. In the following three chapters specific introductions are provided as well as between one and three manuscripts in form of research articles that cover the research findings of this PhD thesis. The thesis closes with a short summary and perspective in the last chapter.

Chapter I gives an overview of the antibiotic resistance crisis. The burden, prevalence and routes of dissemination of antibiotic resistance are shortly discussed and an overview of the evolutionary principles that shape and drive resistance evolution is presented. The chapter ends with a summary of actions that are taken in the fight against antibiotic resistance.

Chapter II focuses on methodological aspects of antibiotic resistance research. The organisms *Escherichia coli* and *Pseudomonas aeruginosa* as well as techniques that were central to the work in this thesis are presented in more detail. A special focus lies on adaptive laboratory evolution as a tool to study antibiotic resistance. The chapter rounds off with two peer-reviewed articles. In **manuscript 1**, the impact of the adaptive laboratory evolution protocol on resulting geno-and phenotypes was studied. It was found that the methodology used for evolution does impact the evolved lineages, however the key features and mutations arise regardless of the selection method used. Since many different adaptive laboratory evolution protocols are routinely used in antibiotic resistance research this work reassured that the methodology is not biasing the results to a large extent. This provided hope that the results from laboratory-evolved lineages were also comparable to clinically evolving strains. In **manuscript 2**, a method for the marker-free insertion of a genetic barcode was developed and shown to ease the characterization of multiple lineages upon adaptive laboratory evolution in a multiplexed fashion. Moreover, the presented technique allows the in depth characterization, simplifies competition experiments and opens up ways to easily study population dynamics or multiple environments. Consequently, it is a valuable tool to help answer multiple questions in antibiotic resistance research.

Chapter III is the core of this thesis and focuses on the understanding of antibiotic resistance adaptations and tries to explore whether evolutionary trajectories to resistance can be manipulated or exploited in order to limit resistance evolution. At first an overview of a central concept for this idea is given, namely collateral sensitivity, followed by a short

literature review of different studies that explored the suppression of resistance previously. The introduction is followed by three manuscripts that are either submitted or still in preparation. In **manuscript 3** the potential of antibiotic combinations in limiting resistance evolution in *E. coli* was explored and linked to phenotypic and genotypic features of drug combinations. We found that exposure to antibiotic combinations in general limits resistance evolution. In addition, we clarified contradictory findings in the literature regarding the potential of phenotypic features in predicting resistance evolution and found that phenotypic characteristics such as epistatic interactions or collateral sensitivity are only weak predictors for resistance evolution. Instead, we proposed a novel framework for the identification of resistance suppressing drug combinations based on the genotype of lineages evolved to drug pairs relative to those of individual-drug evolved lineages. Drug combinations that required a novel genetic response displayed significantly limited and decelerated resistance evolution. The manuscript is followed by **manuscript 4** in which we performed a similar analysis on the evolvability to drug combinations in *P. aeruginosa*. We also concluded that resistance evolution is limited in *P. aeruginosa* through drug combinations. While collateral sensitivity between the drug pairs predicted resistance evolution to combination therapy only to a certain extend, we identified and presented examples in which genetic incompatibilities caused by collateral sensitivity or resistance shaped the evolution towards drug combinations. **Manuscript 5** explored the interaction between vertically and horizontally acquired resistance features in *E. coli* and found that while many resistance features act neutral or additive, some exhibit strong negative epistasis. The results help to understand prevalence and dominance of specific resistance features over others and might also contribute to our ability to understand and predict resistance evolution. All three manuscripts aim to identify genetic constrains in resistance evolution that might be exploited in future to decelerate and limit resistance evolution.

Chapter IV further deals with resistance adaptations and their exploitation with a focus on CRISPR- based antimicrobials. First an introduction to alternatives to antibiotics like CRISPR-based antimicrobials is provided. The second part of this chapter contains **manuscript 6**, in which the genetic responses to CRISPR imposed killing were analyzed and implemented in the CRISPR system in order to increase killing efficiency.

In **chapter V** a short summary and perspective on the work conducted in this thesis is outlined and a few general trends regarding the antibiotic resistance crisis are described.

List of manuscripts

Overview of published and unpublished scientific manuscripts included in this PhD synopsis:

Manuscript 1:

Adaptive Laboratory Evolution of Antibiotic Resistance Using Different Selection Regimes Lead to Similar Phenotypes and Genotypes, Leonie J. Jahn, Christian Munck, Mostafa M. H. Ellabaan and Morten O. A. Sommer (2017). *Frontiers in Microbiology*, Vol. 8

Manuscript 2:

Chromosomal barcoding as a tool for multiplexed phenotypic characterization of laboratory evolved lineages, Leonie J. Jahn, Andreas Porse, Christian Munck, Daniel Simon, Svetlana Volkova and Morten O. A. Sommer (2018). *Scientific Reports*, Vol. 8, Article number: 6961

Manuscript 3:

Compatibility of evolutionary responses drive resistance evolution during combination therapy, Leonie J. Jahn, Daniel Simon, Mia Jensen, Charles Bradshaw, Mostafa M. H. Ellabaan and Morten O. A. Sommer (2019), manuscript currently under review

Manuscript 4:

Genetic constrains limit resistance evolution in *P. aeruginosa*, Leonie J. Jahn, Daniel Simon, Mia Jensen, Charles Bradshaw, Mostafa M. H. Ellabaan and Morten O. A. Sommer (2019), Manuscript in preparation

Manuscript 5:

Dominant resistance and negative epistasis limit the co-selection of vertically and horizontally acquired antibiotic resistance factors, Andreas Porse*, Leonie J. Jahn*, Mostafa M. H. Ellabaan and Morten O. A. Sommer (2019), Manuscript in preparation

Manuscript 6:

Resistance mechanisms against CRISPR-mediated DNA damage, Ruben Vazquez-Uribe*, Christin Rathmer*, Leonie J. Jahn*, Simone Li and Morten O. A. Sommer (2019), Manuscript in preparation

* denotes equal contribution

Acknowledgements

For the opportunity to conduct a PhD and to work as a scientist I am extremely grateful, as I love the variability in tasks associated with my daily work such as reading, discussing, formulating hypothesis, planning as well as conducting experiments, data analysis, data visualization and communication in form of talks, posters and scientific publications, but also learning in courses and from the scientific community on conferences and finally teaching. Moreover, I highly appreciate the freedom in terms of research questions and daily flexibility that I experienced. Obviously, science can also be challenging and demanding and I hope that I grew personally as well as scientifically by overcoming or dealing with these obstacles. On my way to and through the PhD I had help from many wonderful people that I would like to thank in the following:

I would like to thank my former supervisors **Lena** Studt, **Bertina** Tudzynsky, **Reiner** Schulz and **Genevieve** Thon for their efforts in teaching me scientific thinking and laboratory skills, for supporting me during different steps in my career and for enthusing me about science.

For my thesis I am extremely grateful that you, **Morten,** gave me the opportunity to join your lab. Thank you for the delightful time, a lot of inspiration and all your support and trust in me. Furthermore, I would like to thank **Christian** for helping me getting started in the lab, for his talent to calm me down when I am stressed and for many interesting discussions on our bus rides to and from Hørsholm. **Gitte** – thank you so much for all your administrative efforts and all the help you provided in correctly filling in expense or absence reports. I would also like to thank all the members of the metaRNA network – it was a great experience to meet so many talented and wonderful people and to share experiences and challenges.

A huge thanks goes to all the former and current members of the Sommer lab that created a helpful, welcoming and fun environment that made the PhD such an amazing and unique experience. Special thanks to **Andreas** for many helpful discussions about our research and way beyond. I would like to thank **Mari** for her great organization skills and her support whenever I was in the middle of a high-throughput experiment and in need of more materials or equipment but also for many meaningful conversations and a great time in Paris on the AMR conference. Special thanks also to **Ruben** for his wonderful positive energy, the great atmosphere he created at work and a lot of fun experiences. I would also like to thank **Daniel** for the excellent collaboration and all his efforts continuing my project while I was on

maternity leave. Special thanks to **Carola** for many helpful early morning talks about the challenges of being a scientist and a mum at the same time. Thanks also to **Mostafa**, who is always helpful and a great support for any problem in bioinformatics. Last but not least I would like to thank the students that I supervised during my PhD: thanks to **Mia** and to **Christin**, who did not only contribute enormously to the work of the CRISPR project but also to the good atmosphere in the lab!

I also like to thank the entire CFB for the collaborative work environment. Special thanks to **Charles**, **Olivier**, **Anna** and **Ann** for their support of my high-throughput work.

I would also like to thank **Jim** Collins, **Allison** and **Jason** for the opportunity to experience the inspiring scientific world at the Broad Institute and the MIT.

Finally, I want to thank my entire **family,** especially **Susanne**, **Holger**, **Lisa**, **Stefan**, **Laura** and **Klaus**, for their support and love – knowing that you are there means the world to me. The biggest thanks goes to **Alex** for helping me living my dreams and for countless adventures on earth and beyond. I also thank **Linnea** for helping me creating a new perspective on the world and for finding out what really matters. Moreover, I want to thank my former flatmates **Caro**, **Moritz**, **Theo**, **Karma**, **Adam**, **Katie**, **Andrea**, **Niklas**, **Mathilde**, **Signe** and **Ebbe** for the wonderful time and for making me feel at home here in Copenhagen. Finally, special thanks to **Sara** for her endless support.

Table of contents

Chapter I – Introduction

Antibiotic resistance crisis

Many critical human diseases are caused by large populations of asexually dividing cells such as viruses, bacteria, fungi, protozoa or cancer cells[1]. Except for the latter, all of them cause infectious diseases that can spread between humans but can also be transmitted through animals or environmental sources[2–4]. Bacteria cause a large proportion of infectious diseases and, bacterial infections are very common. Before antibiotics were discovered many simple infections could become deadly and were consequently one of the leading causes of mortality[5]. The discovery of penicillin by Alexander Fleming in 1928 marks a turning point in human history, saving millions of lives from the consequences of bacterial infections[6]. Thereafter, many antibiotics have been discovered that potently kill (bactericidal) or inhibit the growth (bacteriostatic) of bacteria (Figure 1).

The antibiotics differ both in their mechanism of action (Figure 1) as well as in the spectrum of bacteria affected by the drug. Important drug classes include beta-lactam antibiotics that target the bacterial cell wall, aminoglycosides, tetracyclines and macrolides that all inhibit translation, fluorquinolones that disturb the DNA gyrase, rifampicins that target the RNA-polymerase, as well as antibiotics that inhibit essential folate-metabolism (Figure 1). Most antibiotics, like penicillin, are secondary metabolites of fungi or bacteria[7]. The environmental role of these substances remains controversial[8–10]. It was suggested that antimicrobials provide a fitness advantage when multiple species compete for resources in an ecological niche[11]. However, it was considered doubtful that concentrations would achieve high enough levels to kill or reduce the growth of adjacent bacteria[11]. An alternative hypothesis was, that they were used as signaling molecules, since it was shown that antimicrobials altered gene expression profiles of bacteria when applied at low concentrations[11].

A substantial part of functionally different antimicrobials was discovered in the golden age, the 1950´s, in large screens of fungal or soil extracts (Waksmann screening platform[12]). However, this approach did not continuously succeed but rather repeatedly returned already known compounds[7]. Thereafter, the science of protein structures and genome sequencing advanced and these techniques were used to identify potential targets in bacteria. Subsequently, biochemical assays were developed to screen for inhibitors based on huge libraries of natural compounds[7]. Many compounds were successfully discovered, yet they often failed in inhibiting *in vitro* growth of the entire cell[7].

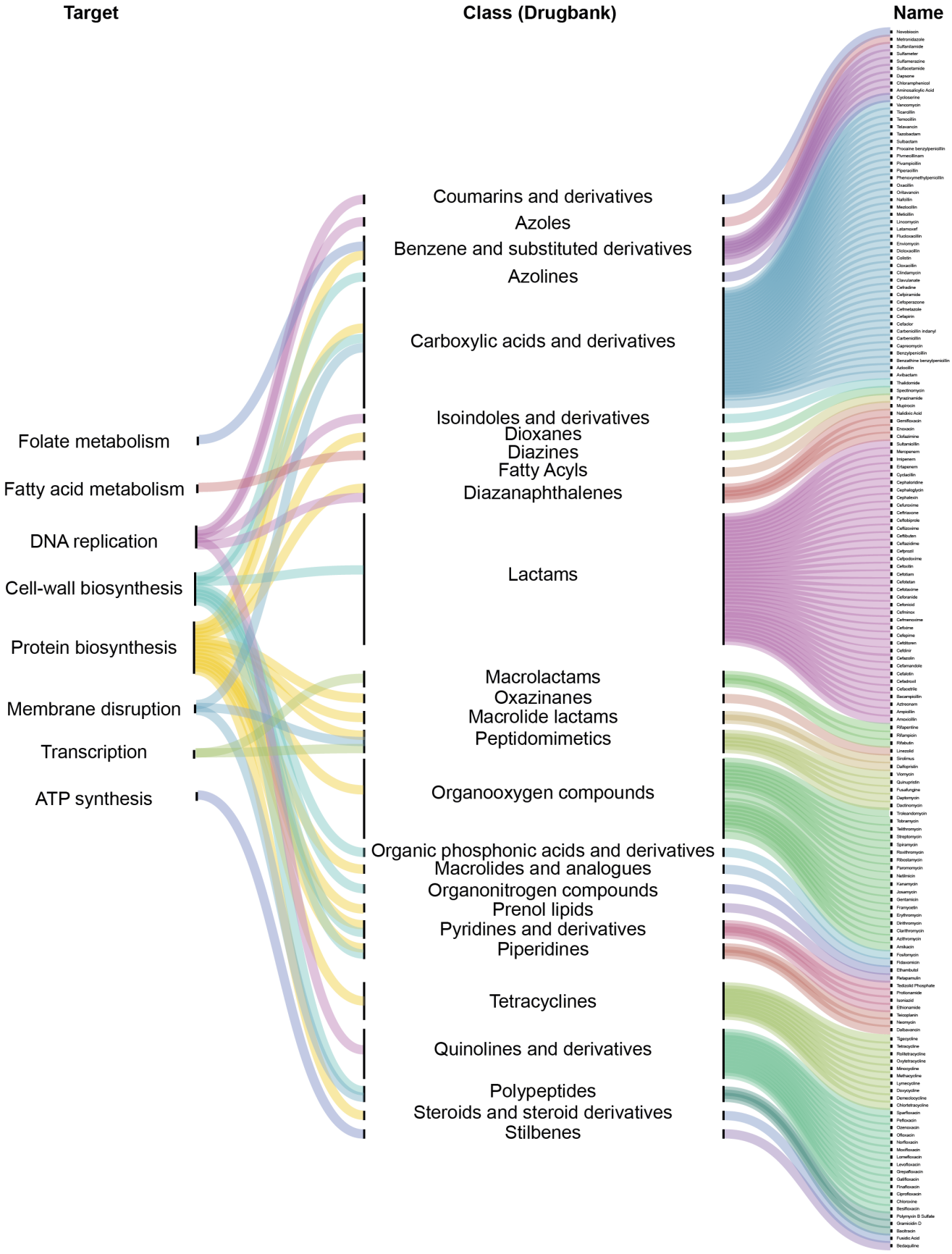

Figure 1: All FDA approved drugs, drug classes and cellular targets according to DrugBank. All FDA approved antibiotics target only eight different molecular processes in bacterial cells. The antibiotics can be distinguished in different classes. The classes used in DrugBank are chemical classes and are not entirely

overlapping with the classification system usually used for antibiotics that also considers mode of action and activity spectrum[13]. For example Macrolide and Aminoglycoside antibiotics both group into the organooxygen compounds. In total more than 150 different antibiotics are listed as FDA approved antibiotics at DrugBank. Data for this figure was obtained from DrugBank[14] (April 2018).

Consequently, the entire cell, ideally a biosensor carrying reporter strain, was again used for screenings of natural compound libraries[7]. In addition, virtual screening through the use of molecular docking was utilized to discover novel antimicrobials[15].

Besides natural compounds that are often synthetically optimized, there are also entirely synthetic antibiotics, such as quinolones[16,17]. Once an antibiotic compound is newly discovered either through screenings or synthesis, further steps e.g. validating the activity and testing for toxicity are required. These steps are performed according to specific protocols of hit, lead and candidate declaration that are then followed by clinical trials (Figure 2)[7]. It was estimated that pharmaceutical companies pay about 1.5 billion USD for the development of a single antibiotic (Figure 2)[18].

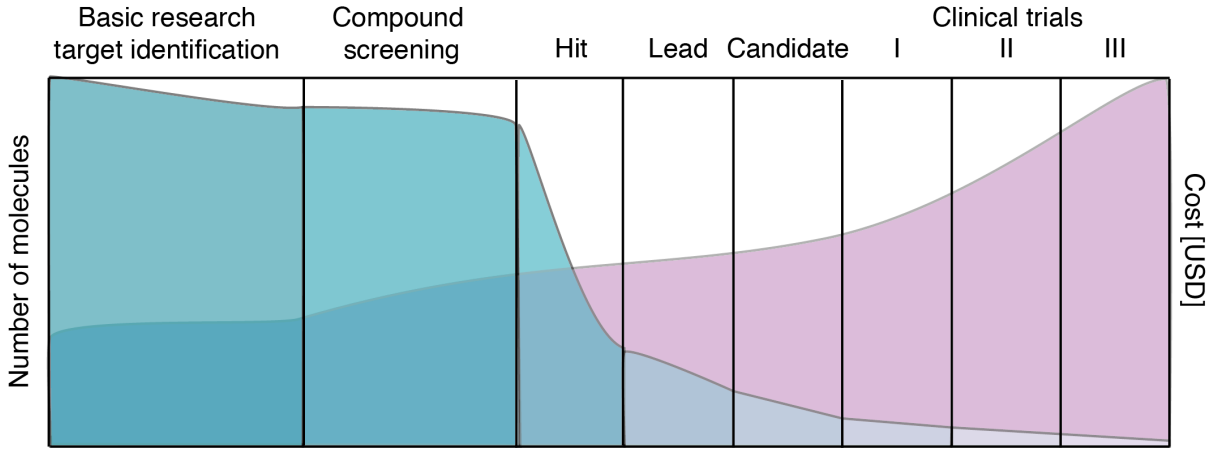

Figure 2: Number of potential antibiotic compounds and cost over different steps of drug discovery. This is a schematic illustration that shell visualize that the number of potential compounds with antibacterial properties decreases drastically at each step, while the cost of the identification and testing of the compounds increases. While there are many compounds of potential interest studied in basic research and in compounds screens, only few will then be selected for hit, lead, candidate testing and subsequently for clinical trials. Often only resulting in a single compound that will be approved as antibiotic. However, the costs for research, subsequent tests and especially for clinical trials are very high and increase at each step.

This is a huge cost for a fairly unlucrative drug that is mainly used for short durations against acute infections. Moreover, new antibiotics are often held back from the market so that they can be used as last resort antibiotics[19]. While this is important to be able to cure infections by multi-drug resistant pathogens, it further decreases the monetary value for pharmaceutical companies. Consequently, it is not of economic interest to invest in the discovery of novel

antibiotics, wherefore many companies have stopped their efforts in this field[5]. This resulted in more than a 50% decrease of the approval of novel antibiotics in the first ten years of the 21st century compared to the preceding 10 years (Figure 3).

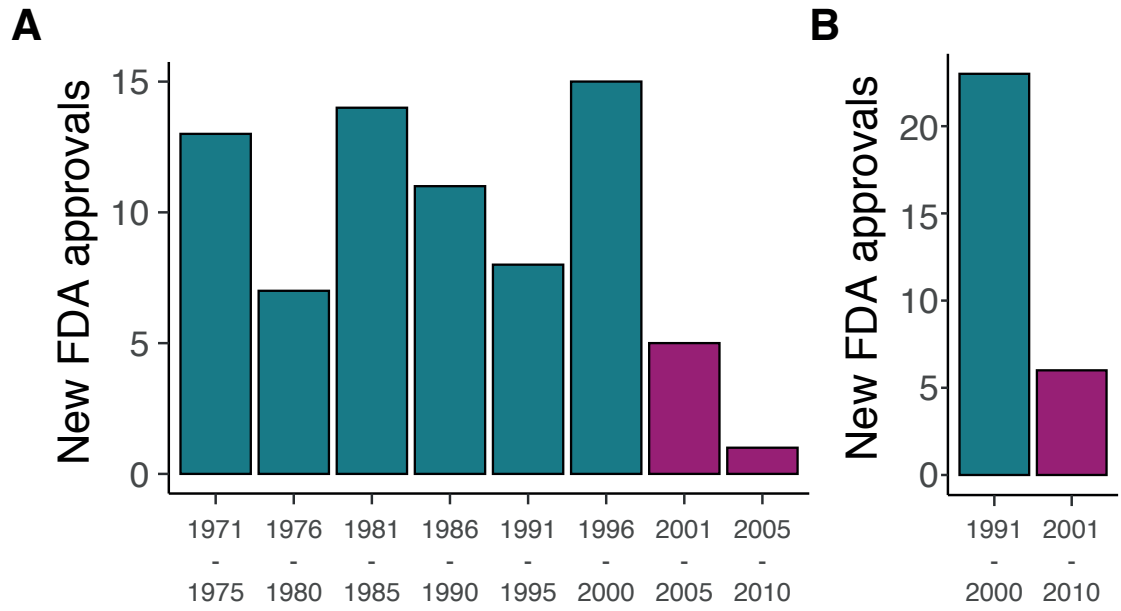

Figure 3: FDA approval of antimicrobials between 1971 and 2010. A) Number of newly FDA approved dugs for every 5 years between 1971 and 2010. While the approval rate was fairly constant in the 20th century, it dropped in the beginning of the 21st century. **B)** Number of newly FDA approved antibiotics for 10 years in the 90s and early 2000. Data for this figure was obtained based on a list of antibacterial agents from DrugBank searched in the orange book database of the FDA[20].

Nonetheless, the discovery of novel antibiotics is crucial due to antibiotic resistance. Already in his acceptance speech for the Nobel prize in 1945, Alexander Fleming pointed out that antibiotic resistance emerges quickly and that the novel drugs should be used cautiously in order to preserve their live saving properties[21]. As many antibiotics are naturally produced by bacteria they carry resistance genes to ensure their own survival[22]. In addition, these resistance genes have also been found in bacteria that do not produce antibiotics but rather protect themselves from exposure to antibiotics in the environment[23]. The massive use of antibiotics in humans, animals including livestock, as well as environmental pollution through antibiotic production companies, resulted in the increased selection of antibiotic resistance and the high abundance of resistance genes, including those in human pathogens[24,25]. It was estimated that at least 700,000 people die annually of infections by antibiotic resistant pathogens[26]. Moreover, it was predicted that this number would increase to 10,000,000 people by 2050, if the suboptimal use of antibiotics along with the decreasing number of approved antibiotics

continues[26]. Consequently, the global emergence of multi-drug resistant bacteria that cannot be treated with currently available antibiotics puts human health at risk.

The burden of antibiotic resistance

The burden of antibiotic resistance has been assessed in multiple studies[27]. Various organisms and measures of burden (economic, healthcare or health) as well as methodology were used for these estimates[27]. When focusing on patient health, the majority of studies suggest that the mortality rate was increased in patients due to antibiotic resistance[27]. In addition, secondary effects of antibiotic resistance on prophylactic antibiotic use after surgery or during chemotherapy was estimated to result in 6,300 additional deaths per year in the US when antibiotic efficiency was reduced by 30%[28]. Further studies explored the impact of resistance on the healthcare system. The majority of studies found an excess length of hospital stays caused by infections with antibiotic resistant bacteria ranging between 2 to 17 additional days[27]. The monetary costs for the healthcare system were estimated to be between non-significant up to 28,553 USD per case of an antibiotic resistant infection[27]. The economic burden of resistance was estimated to be in whole percent points of the GDP only due to reduced labour supply[29]. The immense burden of antibiotic resistant infections was further highlighted by the fact that alone methicillin-resistant *Staphylococcus aureus* infections were estimated to cost multiple million USD per year[30]. However, a systematic study including a global take on all organisms, for whose antibiotic resistance is reported, is missing, making it difficult to assess the actual burden. Moreover, smaller impacts such as treatment failure, change of treatment strategy, and prolonged illness in less severe but more common infections, such as skin or acute urinary tract infections, were usually not taken into consideration. Overall, it can be concluded that antibiotic resistance significantly impacts human health and is associated with an immense economic cost.

Evolution of antibiotic resistance

Antibiotic resistance is a result of the enormous genetic flexibility of microorganisms to adapt even to harsh and sudden environmental changes. Consequently, antibiotic resistance is an evolutionary result and the evolutionary forces that drive this adaptation need to be depicted in evolutionary medicine in order to counter act the resistance crisis[31]. The evolutionary theory proposed by Charles Darwin in 1858/1859, explains that populations are often heterogeneous due to mutations or recombination. Also, that the fittest individuals of these populations have a reproductive advantage making them likely to pass on their genetic traits to the next

generation[32]. Different mechanisms drive the selection of the fittest individuals. Some mechanisms are directed such as natural selection, in which a selection pressure is imposed on a population and the individuals that are the fittest under these conditions survive and reproduce[33,34]. Whilst other mechanisms include elements of chance, such as genetic drift or gene hitchhiking[35]. It is likely that natural selection is the most important driver as antibiotic exposure represents a strong selection pressure and requires adaptation for survival[36]. Even sublethal antibiotic concentrations were shown to impose a selection pressure on bacteria favoring low-resistance conferring adaptations[37]. In the following paragraphs, the different ways of adaptation and the selection process of the fittest individuals are described in more detail.

Modes of resistance acquisition

Bacteria have a fast genetic and phenotypic plasticity. In the following it will be described how this adaptive potential assists bacteria to evolve antibiotic resistance. First of all, bacteria can be intrinsically resistant to antibiotics due to an interplay between bacterial physiology and antibiotic properties (Figure 4). For example, the antibiotic Linezolid is effective against most Gram-positive bacteria but due to efflux activity most Gram-negative bacteria are intrinsically resistant[38].

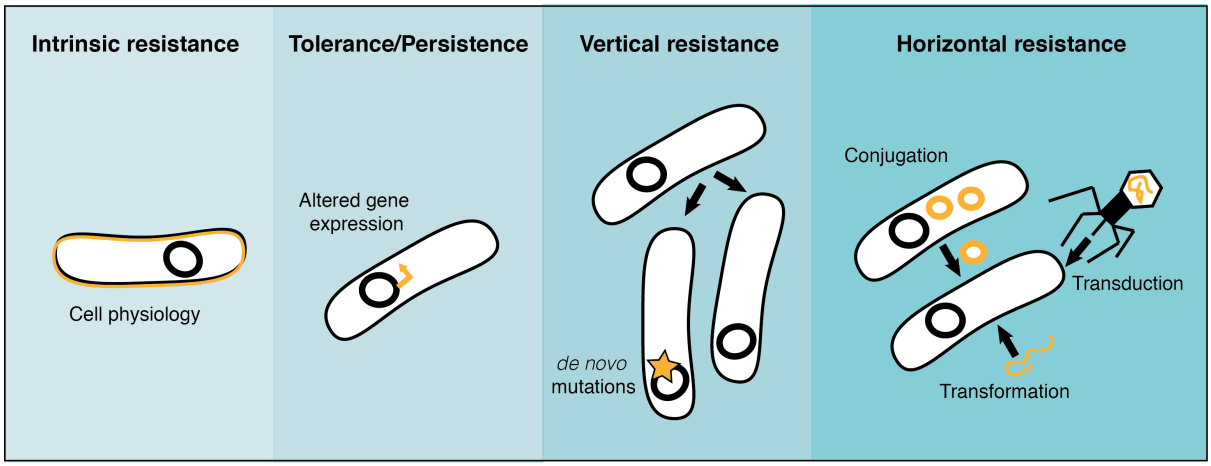

Figure 4: Overview of different mechanisms of antibiotic resistance. Bacteria can be intrinsically resistant to antibiotics due to their physiology or they can develop resistance, either through phenotypic adaptations resulting in persistence or tolerance of the antibiotic or by genetic alterations. Bacteria can mutate their core genome in order to adapt to antibiotics or they can take up foreign DNA, including mobilized antibiotic resistance genes, through conjugation, transduction or transformation, resulting in horizontally acquired antibiotic resistance.

Apart from intrinsic resistance, bacteria can adapt to antibiotics phenotypically by changing their gene expression. These phenotypic alterations are usually triggered through specific environmental conditions[39,40] and population dynamics,[38–40] and can result in the survival of

high antibiotic concentrations of the entire bacterial population (tolerance) or a subset of a population (persistence) (Figure 4). Genetically, bacteria can become resistant either through the uptake of genetic material (horizontal resistance) or through changes in their core genome (vertical resistance) (Figure 4).

As mentioned above, antibiotic resistance genes have been found in antibiotic-producing microorganisms but more concerning also in other bacteria from environmental sources[23]. Consequently, many antibiotic resistance mechanisms have evolved long before the use of antibiotics by humans[44]. Resistance genes can be passed between individuals of the same bacterial species as well as among bacteria of different species[45]. Even gene exchange between bacteria and eukaryotes has been discussed previously[46,47]. Exchange of genetic material happens through different modes. Either through transformation, a process in which free floating DNA is taken up by a bacterium while it is in a specific phenotypic state called natural competence; through transduction, where genetic material enters the bacteria and is inserted into the bacterial genome upon phage infection; or through conjugation, the exchange of plasmids between bacteria (Figure 4)[48]. Besides horizontally acquired resistance genes, also vertical resistance through genomic mutations plays a role in antibiotic resistance (Figure 4)[49]. Both modes, horizontal and vertical acquisition of antibiotic resistance, are likely to contribute to the antibiotic resistance crisis. While some bacteria seem to prefer one mode over the other, they can also exist in parallel[50].

Vertical resistance evolution in *E. coli* and *P. aeruginosa*

Since *de novo* resistance evolution is the focus of this thesis, different aspects of vertical resistance evolution are presented in more detail in the following. Two important parameters to access the evolutionary capacity of vertical resistance evolution in bacteria are the population size and the mutation rate. It was estimated that the world wide population size of the common bacteria and pathogen *Escherichia coli* (~10^{20} cells)[51] equates with the number of stars in the universe[52], illustrating the dimensions of bacterial populations. In addition, bacterial population sizes upon infection can be large, e.g. an urinary tract infection caused by *E. coli* can reach densities of 10^{10} cells per mL[53] and sputum samples of cystic fibrosis patients were reported to contain 10^{9} cells per ml of *P. aeruginosa*[54], suggesting an even larger total population size in the lung. Mutation rates are anticipated to be around 10^{-10} per nucleotide per cell division[55]. These mutation rates in combination with the population sizes suggest an immense heterogeneity and evolutionary capacity of bacteria. Population sizes of 10^{10} cells,

would likely contain mutants that confer antibiotic resistance even before antibiotic treatment was started[53]. In addition, bacteria can also accumulate mutations in genes like *mutD*, *mutL*, *mutH* and *mutS* encoding for the proteins that ensure genetic stability through proofreading activity or methyl-directed mismatch repair[56]. Mutations in these genes can increase mutation rates 10- to 1000-fold[56], resulting in so called hypermutator strains. Interestingly, the prevalence of hypermutators was high (~17-23% of isolates) within infections by uropathogenic *E. coli* and *P. aeruginosa* infected lungs of cystic fibrosis patients[57–59]. While hypermutation can be connected to a fitness cost[60], contrastingly the hypermutators ability to respond faster to stronger environmental changes has been discussed as an adaptation strategy[61]. Consequently, it was proposed to be an important mechanism for the adaptation of bacteria to antibiotics in the human host[62]. Besides mutations that increase the mutation rate, the environment, including the stress imposed through antibiotics, can increase the mutation rate mainly through the radical-induced SOS response[63,64]. In addition to single nucleotide polymorphisms, other genetic rearrangements can also cause antibiotic resistance. Tandem duplications enabled through recombination between short randomly occurring homologues sequences can also contribute to antibiotic resistance. For example, the copy number of the *ampC* gene, encoding a beta-lactamase in the *E. coli* core genome, is directly linked to the level of beta-lactam resistance[65]. Even though gene duplications occur with a high frequency of 10^{-5}- 10^{-2} dependent on the genetic region, they are often unstable, wherefore they are hard to detect and to characterize[66]. Moreover, gene deletions also occur with frequencies of about $3x10^{-8}$ per generation[67] and have been found to contribute to antibiotic resistance of clinical isolates[68]. Finally, mobile genetic elements such as insertion elements can also impact antibiotic resistance evolution (**manuscript 1** and **manuscript 3**). Insertion elements are the smallest transposable elements in bacteria and they care flanked by short terminal inverted repeats and contain only genetic material that allows their mobility within the genome[69]. They were found to play a role in antibiotic resistance both in *E. coli*, for which clinical isolates with insertions in *ompR*, affecting expression of porins, were reported; and in clinical isolates of *P. aeruginosa* with insertion sequences found in the porin encoding gene *oprD* or *mexR,* encoding a suppressor of efflux pumps[69]. Interestingly, it was reported for *E. coli* that mutations in *lon*, encoding a protease, could induce a mutator phenotype through an increased frequency of insertion element transposition and other genome rearrangements[70].

Persistence of antibiotic resistance in bacterial populations

Since antibiotics impose such a strong selection pressure on bacteria and many antibiotic resistance features are connected to a fitness cost in the absence of antibiotic, it was believed that reducing the use and pollution with antibiotics alone would be sufficient to counter select and to decrease the prevalence of antibiotic resistant bacteria[71,72]. However, experimental work and epidemiological studies suggest that antibiotic resistance often persists in bacterial populations even in the absence of antibiotics[73]. Reasons for the persistence of antibiotic resistance in bacterial populations will be briefly discussed in the following.

Persistence of antibiotic resistance in light of fitness

A fundamental principle of evolution is the selection of the fittest[32]. This principle holds also true for antibiotic resistance evolution. Most resistance mechanisms come with a fitness cost in the absence of antibiotics[74], but allow survival under antibiotic exposure resulting in a vast fitness advantage in certain environments (Figure 5).

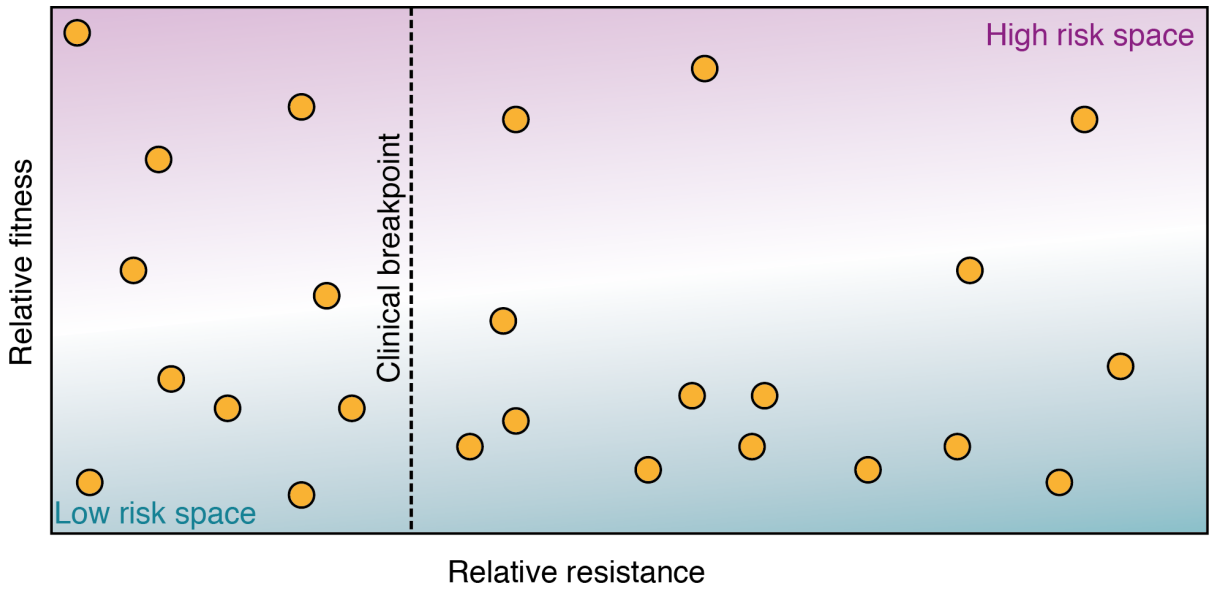

Figure 5: Fitness and resistance level determine evolutionary success of antibiotic resistant bacteria. Isolated bacteria, illustrated in orange dots, have different resistance levels connected to a specific fitness cost in absence of the antibiotic. Bacteria with little resistance at a high fitness cost are in a low-risk space as they are likely to be outcompeted in a bacterial population and do not confer an essential benefit even under selecting conditions. However, bacteria that have a high resistance level at a low fitness cost are in a high-risk space as they will likely persist in bacterial populations even without selection. The figure is based on figure 2 of Sommer et al. (2017)[43].

The fitness landscape of antibiotic resistance is complex: Certain resistance mechanisms, both horizontally and vertically acquired, are not connected to a high fitness cost or actually confer a fitness advantage even without presence of the respective antibiotic[75]. In general, the fitness is highly dependent on the environment wherefore it is likely that most antibiotic resistance

adaptations are favorable in multiple different environments, allowing their selection and persistence in bacterial populations[73]. Moreover, the expression of some mobilized antibiotic resistance genes is coupled to the presence of the antibiotic[76] facilitating optimal fitness conditions in multiple environments. Furthermore, resistance genes can also be physically linked to each other or to other genetic features, allowing co-selection of the costly gene in favor of the beneficial genetic feature[53]. The fitness cost of antibiotic resistance both horizontally or vertically acquired can also be ameliorated through compensatory mutations[75]. In addition, there are also epistatic interactions between different mutations, core genome and the accessory genome, that can render a costly resistance adaptation more favorable[77].

Additional factors contributing to the persistence of horizontally acquired resistance genes

Besides fitness with and without selection also the rate at which horizontally acquired genes spread is an important factor determining the persistence of antibiotic resistance. It was shown that conjugation rates for some plasmids without antibiotic selection can be sufficiently high under certain conditions in order to preserve antibiotic resistance genes in bacterial populations[78], wherefore resistance genes are unlikely to be lost in bacterial populations even in absence of antibiotic induced selection pressure. In addition, plasmid loss rates are anticipated to be fairly low[79], favoring the maintenance of antibiotic resistance in bacterial populations.

Reversion rate of vertical acquired resistance

While conjugation and plasmid loss rates are important for the evolution of horizontally acquired resistance features, reversion rates of genomic rearrangements and single nucleotide polymorphisms are important for the evolution of vertically acquired resistance. Reversion of antibiotic resistance mutations has been observed both in clinical settings as well as in the laboratory[80–82] but experimental and theoretical models have predicted that reversion rates are generally low and that mutants would rather be outcompeted by the ancestor wild type[73,83]. A study that utilized mathematical modeling found that the reversion rate is highly dependent on the relative fitness between the mutant, a mutant with compensatory mutations and the wild type. In addition, the rate at which bacteria die in a population also influenced the reversion rate according to the model[84]. However, the actual reversion rates after antibiotic treatment of a patient, not only for single nucleotide polymorphisms but also for other genetic

rearrangements, need to be further studied to fully understand the factors that drive persistence of resistance features.

Population dynamics in the host

In addition to the described forces that influence the persistence of antibiotic resistance in bacteria, population dynamics are important to understand persistence of antibiotic resistance. Interestingly, it was reported that in a substantial proportion of infections different sub-populations of bacteria co-exist, such as resistant and susceptible populations[85,86]. Mathematical modeling could explain why this co-occurrence might be as frequent and why resistant bacteria are not outcompeted in the absence of antibiotic treatment[85]. It was found that frequency-dependent selection causes and stabilizes the co-occurrence of susceptible and resistant sub-populations in and within human hosts[85]. Consequently, the fitness within bacterial populations also determines the persistence of antibiotic resistance.

Dissemination of antibiotic resistance

The persistence but also the spread of antibiotic resistance is linked to the fitness of the resistance feature and those with a high fitness under selective conditions will likely be the most prevalent[75]. Horizontal gene transfer promotes resistance features within and across bacterial populations and was shown to be only limited by the ecological niche of the bacteria as well as by the biochemistry of the resistance mechanism[87]. Another aspect of the dissemination of resistant bacteria are the environmental reservoirs and the cross-talk between them. While some studies provide evidence that antibiotic resistant bacteria can be transferred to humans from livestock[88], the overall impact of animal-human transmission was found to be low[89]. Therefore, human-human transmissions of pathogenic drug resistant bacteria are a key problem. Poor sanitary conditions in many parts of the world alleviate fecal-oral contact allowing the spread of resistant Enterococci. Some drug resistant pathogens like *Neisseria gonorrhoeae* can also be sexually transmitted[90]. Moreover, transmission of drug resistant bacteria in hospitals through health care workers has been extensively studied[91,92]. In addition, traveling was shown to impact the spread and dissemination of antibiotic resistant bacteria, as the frequency of antibiotic resistance genes in the human gut changes significantly upon traveling to regions in which antibiotic resistance is more frequent[93,94].

The prevalence of antibiotic resistance

Antibiotic resistance genes are found in many environments at different frequencies[17,95–100] (Figure 6).

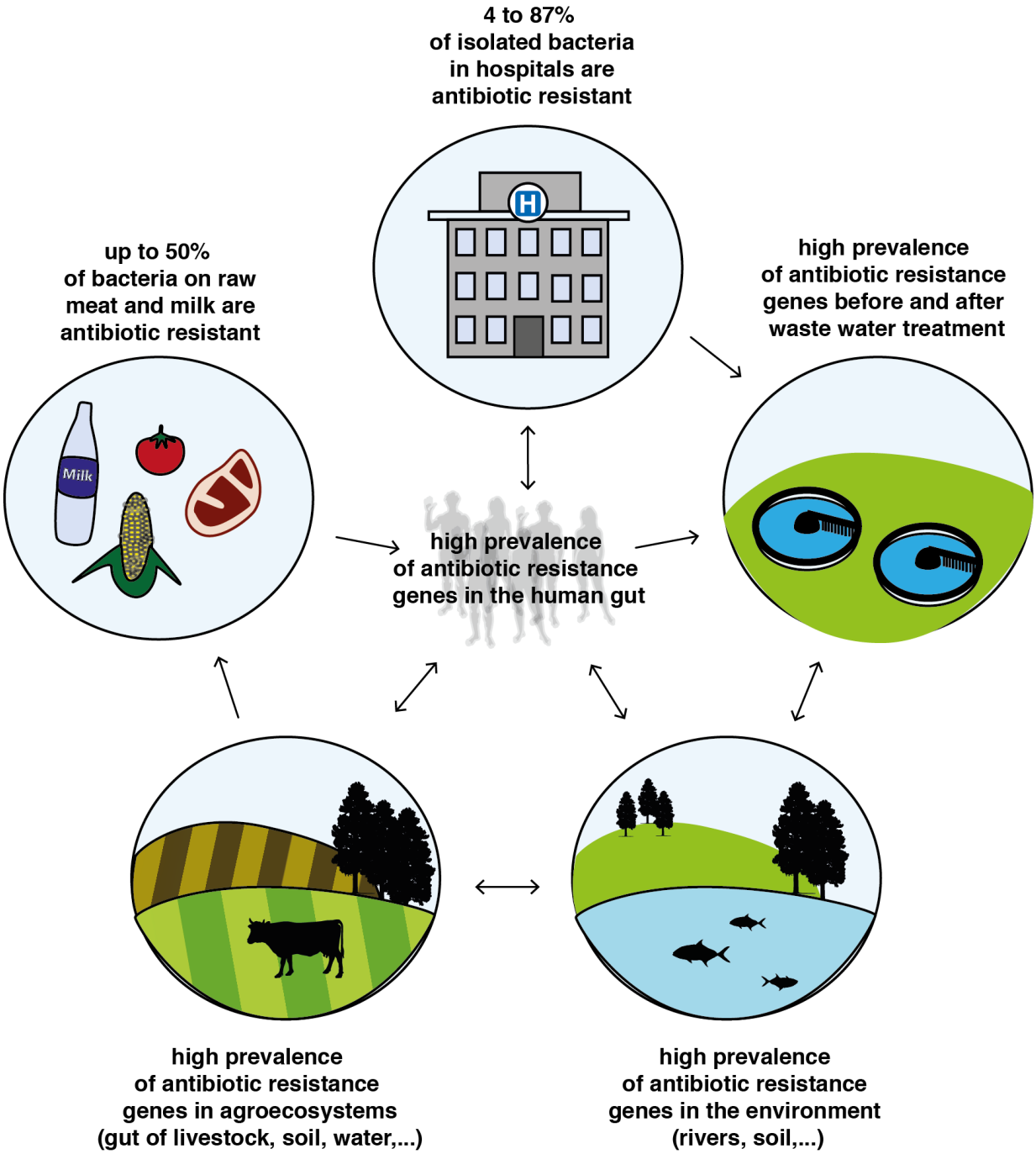

Figure 6: Prevalence of antibiotic resistance in multiple environments. Antibiotic resistance genes have been identified in multiple environments such as wastewater, fresh water, soil, animals, food, the human community and hospitals.

In human pathogens the frequency of drug resistance differs from pathogen to pathogen, from country to country and changes over time (Figure 7).

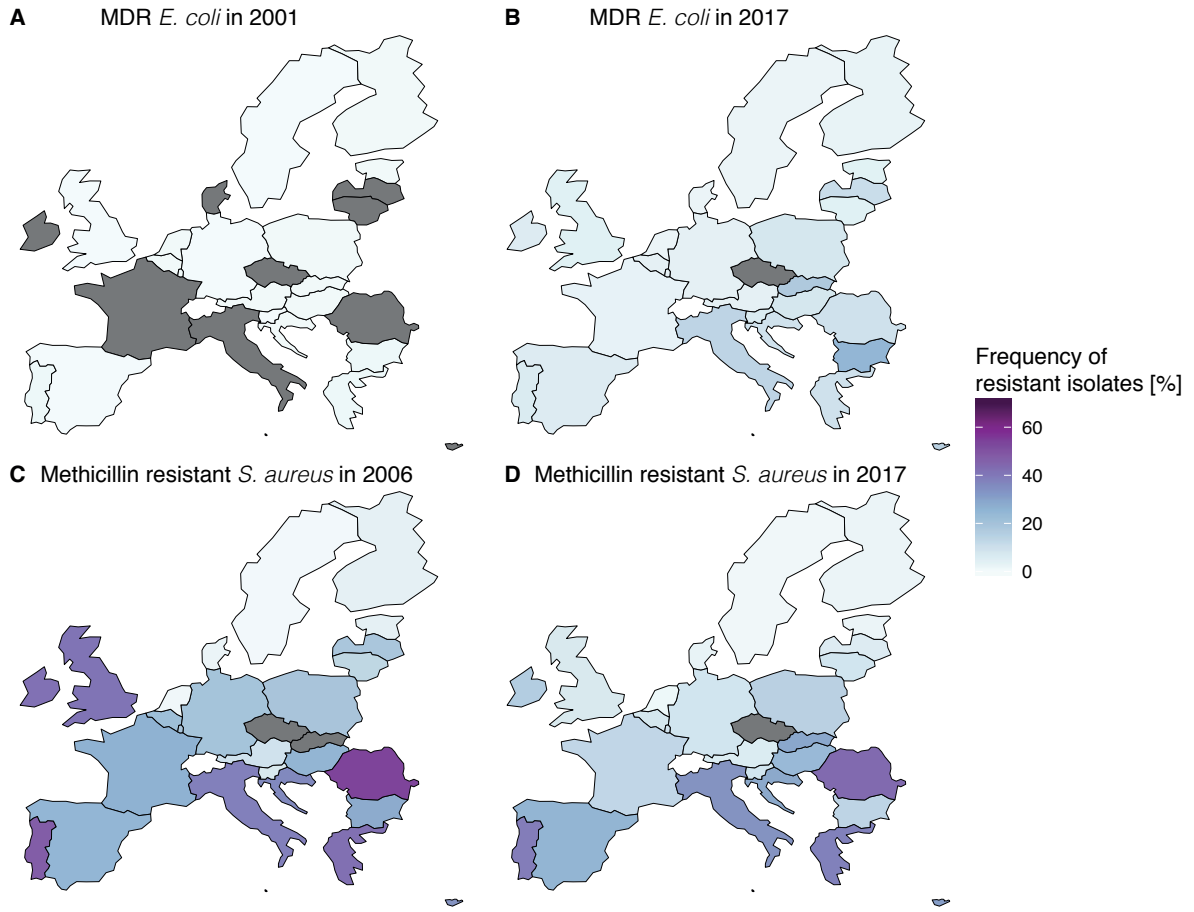

Figure 7: Frequency of multi-drug resistant (MDR) *E. coli* and Methicillin resistant *S. aureus* (MRSA) isolates in different European countries. A) Frequency of *E. coli* isolates resistant to third-generation cephalosporins, flourquinolones and aminoglycoside antibiotics in Europe in 2001. **B)** Frequency of *E. coli* isolates resistant to third-generation cephalosporins, flourquinolones and aminoglycoside antibiotics in Europe in 2017. While MDR in *E. coli* remains low, it is rising over time. **C)** Frequency of MRSA isolates in Europe in 2006. **D)** Frequency of MRSA isolates in Europe in 20017. While MRSA is more common than MDR *E. coli*, the frequency is decreasing over time.

The prevalence of horizontally transferred resistance genes is better studied for *E. coli* compared to vertical acquired resistance. However, reports reveal that between 45 to 100% of quinolone resistant clinical *E. coli* isolates carry mutations in the drug target *gyrA*[101–103]. Mutations involved in the upregulated efflux and a multi-drug resistance phenotype are also found in clinical isolates, yet, at lower frequencies of about 10%[101]. However, clinical isolates are not routinely screened for these mutations wherefore the actual frequency might indeed be higher. In *P. aeruginosa* vertical resistance evolution is more common than horizontal gene acquisition[104]. About 20% of *P. aerugonosa* isolates are multi-drug resistant often associated with mutations in the genes *gyrA*, *mexB* or *oprD,* encoding the DNA gyrase, a component of a multi-drug efflux pump and a porin that are known drug targets, involved in drug efflux and entry, respectively[105,106].

Antibiotic resistance Mechanisms

Different molecular mechanisms have been described for how antibiotic resistance can be achieved by bacteria[107]. First of all, there is intrinsic resistance defining the initial resistance level of bacteria to an antibiotic according to the combination of drug properties and cell physiology such as the presence of a cell wall[107]. Furthermore, there is acquired resistance that functions either through efflux of the drug, decreased drug uptake, inactivation of the drug, modification of the drug target, bypassing of the drug or through changes of global gene expression (Figure 8)[107].

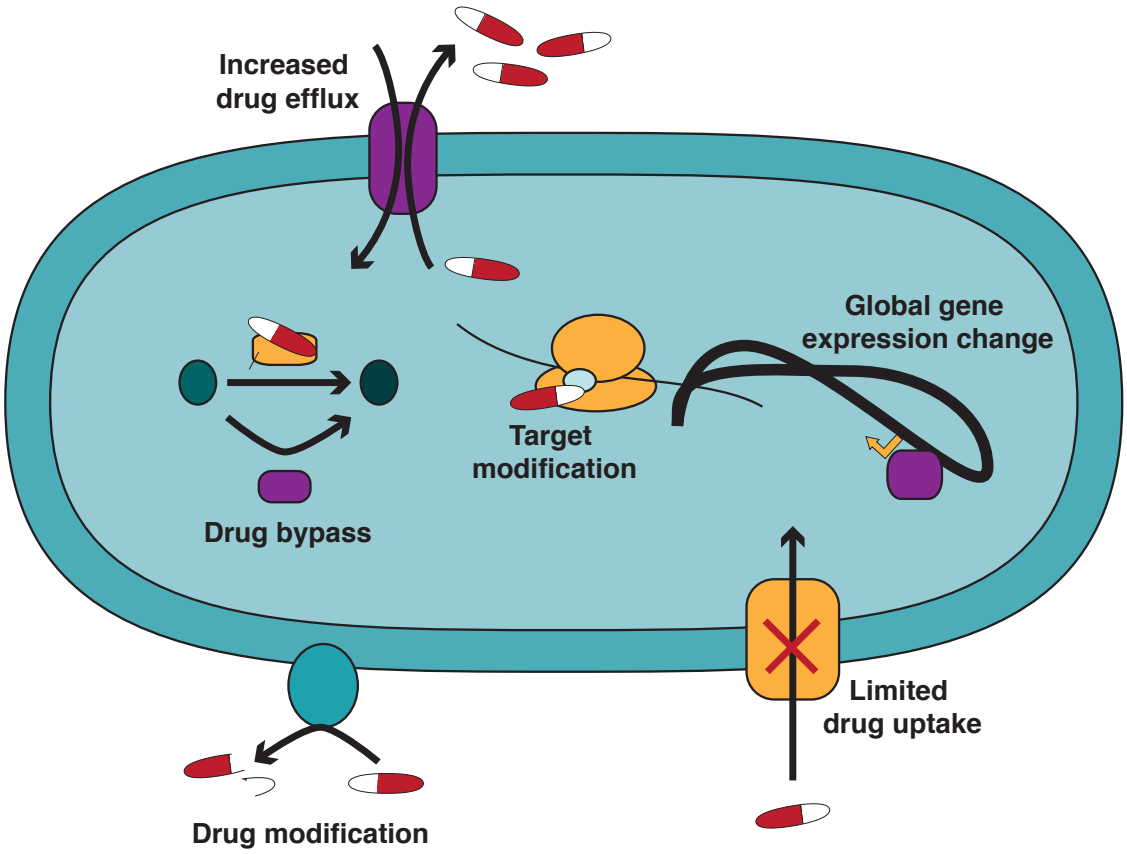

Figure 8: Overview of different molecular resistance mechanisms in bacteria. Bacteria can gain resistance through limiting the uptake of the drug, by increasing the efflux of antibiotics, by modifying or inactivating the antibiotic, by modifying or shielding of the drug target, through bypass of the drug or through global changes in the gene expression.

Efflux and limited drug uptake

Most antibiotics have intracellular targets and need to enter the bacterial cell in order to be effective. The cell wall of Gram-negative bacteria is a natural barrier for some antibiotics

resulting in no or limited effects of the drug[108]. Most antibiotics, active against Gram-negative bacteria, are diffusing through the outer cell-wall through porins[109]. In *E. coli* and *P. aeruginosa* the most important porins for antibiotic uptake are OmpF, OmpC, PhoE and OprD, respectively[108]. Mutations affecting drug uptake usually either reduce the expression of the porin, shift abundances of different porins or alter the porins and accordingly substrate specificity[108]. These modifications usually result in a moderate resistance level[108]. Once an antibiotic entered the cell, efflux pumps can limit the intracellular concentration of the drug effectively[110]. Many bacteria have efflux pumps encoded in their core genome that contribute to their intrinsic resistance level. However, gene expression of efflux pumps can be increased through mutations in multiple regulators resulting in increased drug efflux and resistance[111–113]. In addition, efflux pumps can be localized on mobile genetic elements and confer an additional increase in resistance[114]. Efflux pumps vary in their substrate specificity. While some have a very narrow spectrum of ligand molecules, others transport a broad range of molecules often resulting in multi-drug resistance[115].

Inactivation and destruction of the antibiotic

Another resistance mechanism is the inactivation of the antibiotic. This can happen through chemical modifications of the drug like acetylation, often observed in aminoglycoside or chloramphenicol resistance mediated through horizontally acquired resistance genes[116]. Moreover, antibiotics can also be inactivated through destruction. The most abundant and troublesome is the destruction of beta-lactam antibiotics through beta-lactamases. Some bacteria like *E. coli* or *P. aeruginosa* contain beta-lactamases encoded in their core genome. Mutations or gene-duplications facilitating the over expression of these enzymes can result in resistance[117]. However, mobilized beta-lactamase genes, usually termed *bla* genes, impact antibiotic resistance the most[118]. More than 1000 different beta-lactamases have been described[116]. Beta-lactamases differ in their spectrum range but unfortunately, beta-lactamases effective against all know beta-lactam antibiotics have been described, questioning the future reliability of one of the most valuable drug classes for humans[119].

Modification of the drug target

Besides the drug, the drug target site can also be modified to render a bacterial cell resistant. Target protection is often achieved by proteins encoded in horizontally acquired resistance genes like TetO, TetM or Qnr that compete with the drug for interaction with the target site. Due to higher affinities these proteins can protect the antibiotic target from the drug[116].

However, the drug target can also be modified either through point mutations, like the well-studied *gyrA* mutations that confer flourquinolone resistance as discussed above[120], or through enzymatic target modification, e.g. by methylation of the ribosome resulting in macrolide resistance[121].

Drug target bypass

Resistance can also be mediated by bypassing the drug target. Bacteria can acquire resistance genes that encode a protein with similar or identical function to the drug target that is not targeted by the antibiotic via horizontal gene transfer. Prominent examples include the *mecA* gene in *S. aureus* that encodes a penicillin binding protein that is not targeted by methicillin; or the *van* gene cluster, whose gene expression results in an altered peptidoglycan structure ultimately promoting vancomycin resistance[116]. Bypassing can also be achieved through vertical resistance mechanisms, such as mutations in the promoter region of enzymes involved in folate synthesis. The overexpression of these enzymes can lead to an access of the target molecule, so that the drug combination sulfamethodoxazole-trimethoprim cannot reach sufficient concentrations to kill the bacteria effectiely[116].

Regulation of gene expression

Finally, bacteria can also mutate specific regulators that alter overall gene expression in the bacterial cell resulting in reduced antibiotic susceptibility[122,123]. One such regulator is the Cpx-two-component-regulator in *E. coli* that has been shown to influence the expression of various genes affecting not only antibiotic susceptibility but also virulence and general stress adaptation[124]. Mutations in the two-component system are linked to increased antibiotic resistance to multiple bactericidal antibiotics[125].

Strategies to combat antibiotic resistance

As antibiotic resistance is a severe threat to global human health, international and national guidelines have been developed in order to tackle the antibiotic crisis. In 2016 antibiotic resistance gained a high level of attention as it was discussed by the general assembly of the United-Nations[126]. The previously created Action Plan on Antimicrobial Resistance (AMR) was rated to have a central role in combating the antibiotic resistance crisis. The World Health Organization (WHO) was chosen to implement and develop strategies to combat the crisis[126]. Apart from its official role for the United-Nations, the WHO had already started to develop

action plans against AMR in 2001[126]. The central points for combatting the crisis are: effective communication and education about AMR, knowledge gain through surveillance and research, reduction of AMR spread through controlled antibiotic usage, prevention of new infections with antibiotic resistant pathogens and financial support for the development of novel antibiotics and diagnostic tools[126]. Based on these goals all nations were supposed to develop national plans to combat the antibiotic crisis, however, the implementation of such national plans has only been successful in about half of the member states of the United-Nations[126].

In this thesis research was conducted to strengthen the knowledge about antibiotic resistance in two important Gram-negative human pathogens *E. coli* and *P. aeruginosa* to contribute to the fight against the global antibiotic resistance crisis.

Chapter II – Development of new tools to study antibiotic resistance

Methodological aspects of antibiotic resistance research

Research on antibiotic resistance is manifold, elucidating various aspects of the problem including a broad range of different disciplines and methodologies. Disciplines include epidemiology, medicine, biology, chemistry and pharmacology. While methodologies range from mathematical modeling over systems biology to molecular and synthetic biology, including *in silico*, *in vitro* and *in vivo* work. The work conducted for this thesis was mainly performed around three major techniques: phenotypic characterization of bacterial resistance, whole-genome-sequencing and adaptive laboratory evolution. In addition, two Gram-negative model organisms *E. coli* and *P. aeruginosa* were utilized in this thesis, wherefore these organisms and techniques shall be introduced in more detail in the following. The remainder of the chapter focuses on research performed during this thesis that advances our understanding and the applicability of laboratory evolution.

Model organism *Escherichia coli*

According to the WHO *E. coli* and *P. aeruginosa* are among the 10 most troublesome bacteria in regards to antibiotic resistance[127]. *E. coli* colonizes the lower-intestine of warm-blooded animals and humans, and can also be found in the environment[128]. While most *E. coli* are non-pathogenic and important members of the healthy gut microbiome, there are at least six pathotypes that cause enteric disease and further pathotypes cause extra-intestinal infections, such as urinary tract infections or meningitis[129]. While some infections caused by *E. coli*, such as meningitis or sepsis, are rare, they are often deadly (36% of meningitis infections)[130]; other infections caused by *E. coli,* such as urinary tract infections (UTIs), are among the most common infections in humans[131]. In UTIs *E. coli* is the most important causal pathogen[132]. UTIs can also occur in a chronic form requiring long durations of antibiotic treatment[133]. As *E. coli* is an important human pathogen, involved in rare deadly and very common less severe infections, it is important to study resistance evolution in *E. coli* in order to keep our ability to treat these infections also successfully in future. Due to the physiology of the bladder in accumulating and discharging liquid, it seems fairly well suited to use adaptive laboratory evolution with serial transfers in order to study antibiotic resistance evolution under controlled conditions. Moreover, *E. coli* serves as a model organism and production strain for many academic and industrial purposes, providing a vast amount of background information

in ecology[128], physiology[134] and genetics[135,136] that allows interpreting results from adaptive laboratory evolution experiments in the best-possible way.

Model organism Pseudomonas aeruginosa

P. aeruginosa is also a well studied model organism for antibiotic resistance research[137–140]. It is an ubiquitous Gram-negative bacteria that is not pathogenic in healthy adults. However, in immune-compromised patients it can cause severe diseases. Moreover, it can colonize the mucus in the lung of cystic fibrosis patients[141]. Bacterial lung infections in cystic fibrosis patients are associated with a higher mortality, wherefore it is crucial to study *P. aeruginosa* in more detail to prevent human deaths[142]. Lung infections in cystic fibrosis are often treated with long exposure of antibiotics, frequently followed by vertically acquired resistance[143]. In addition, *P. aeruginosa* has a high-level of intrinsic antibiotic resistance and is even less susceptible to antibiotics when it grows in a biofilm formation[144], as it likely does in its human host[145]. A lot of research efforts have been conducted in order to study antibiotic resistance and tolerance in *P. aeruginosa*[137,139,140]. Some studies have provided hope for improved treatment[39,146], yet, more research is needed to fully understand and target antibiotic resistance evolution in *P. aeruginosa*.

Resistance determination in bacteria

Defining the resistance level of bacteria is crucial to study antibiotic resistance. The minimal inhibitory concentration (MIC) of an antibiotic needed in order to prevent growth of bacteria is usually determined according to standard protocols either using bacteria growing on solid media utilizing an e-test or diffusion tests or in a dilution series in liquid media with increasing antibiotic concentrations[147]. The lowest concentration with no visible bacterial growth after 24 hours is called the MIC. While the MIC is widely used in order to describe the resistance level of the bacterium, it is not very precise. Therefore, a variation of the liquid MIC determination method, also used in other scientific studies[148–150], was used in this thesis to characterize the resistance level. Bacterial cells were inoculated in a 10-step 2-fold dilution of antibiotic in media and the bacterial growth after 18 hours of incubation at 37 °C was measured with a plate reader. Based on the growth of the bacteria without antibiotic exposure the growth inhibition was calculated for each antibiotic concentration and a dose response curve was fitted in the data. The antibiotic concentration at which only 10% of growth compared to the growth in media without antibiotic was reached, was called the IC90 (inhibitory concentration for 90% inhibition) and used as a measure to quantify the resistance

level of the bacteria[149]. Fitting of a dose response curve and computing the resistance level might be more robust and reproducible compared to MIC determination that relies on visible growth. However, it shall be noted that regardless of the method used for determination of the resistance level, it is sensitive to specific factors such as the inoculum size, duration of growth or the media used[151,152]. Consequently, I have tried to be as consistent and precise as possible during the work for this thesis to keep these parameters constant. Moreover, also the drug batch, drug stock concentration and individual dilution series are variable and can cause technical variation between experiments that is likely to result in a two-fold variation range[147].

Whole-genome sequencing

Whole-genome sequencing techniques have advanced tremendously over the past decades: whole-genome sequencing became faster and more affordable; longer read length options[153] as well as small, portable sequencing machines[153], deep sequencing protocols[154] or smaller input DNA quantities[155] broaden the use of whole-genome sequencing for a number of biological questions. In microbiology, especially in regards to antibiotic resistance, whole-genome sequencing has proven to be extremely valuable both in the clinic and laboratory. Whole-genome sequencing is either coupled with epidemiology for a detailed surveillance[156] or transmission records, for screening for resistance markers and subsequent treatment recommendations,[157] as well as for the identification of novel resistance markers[158] and for the study of the evolution of antibiotic resistance[159,160]. However, time and a certain unpredictability in phenotype genotype links especially in regards to antibiotic susceptibility need to be further improved[161]. In this thesis, illumina sequencing was performed to analyze hundreds of genomes of antibiotic resistant bacteria in order to derive information about the evolution of antibiotic resistance and resistance mechanisms and to identify genetic constrains in the evolutionary trajectories towards resistance (**manuscript 1**, **3**, **4** and **6**).

Adaptive laboratory evolution

Adaptive laboratory evolution has been proven to be a valuable tool to study different aspects of antibiotic resistance. It has helped to determine novel resistance mechanisms; elucidate evolutionary trajectories of antibiotic resistance adaptations; shed light on evolutionary dynamics and principles; identify population dynamics upon resistance evolution; study persistence and tolerance in bacteria; and to identify constrains in resistance evolution (Table 1). Identifying these constrains then allows rational design of improved treatment regimes

such as drug cycling or combination therapy (Table 1). Overall, adaptive laboratory evolution provides us with crucial information to study evolution of antibiotic resistance systematically and under controlled conditions; therefore it is an important supplement to clinical research[31].

Table 1: Overview of research questions addressed by various forms of adaptive laboratory evolution experiments.

Aspect of resistance evolution	ALE method	Organism	Reference
Plasmid host interaction	serial passaging	*E. coli* *K. pneumoniae*	[160]
Plasmids and adaptation speed	increment	*E. coli*	[162]
Collateral sensitivity	increment, gradient plate, serial passaging, liquid gradient	*P. aeruginosa* *E. coli*	[163] [164] [165] [146] [166]
Combination therapy	liquid gradient	*E. coli* *S. aureus*	[149] [167,168]
Evolutionary trajectories	gradient plate, morbidostat	*E. coli*	[169] [170]
Resistance evolution	plates, serial passaging	*P. aeuginosa* *E. coli* *S. enterica*	[171] [172]
Population dynamics	continuous growth, serial passaging	*E. coli* *P. aeruginosa*	[41] [173]
Tolerance and persister	alternating antibiotic exposure	*E. coli*	[174] [175]
Bacterial hysteresis	serial passaging	*P. aeruginosa*	[176]
Resistance mechanism	plates, increment	*S. typhimurium* *E. coli*	[177] [178]
Parallel evolution	antibiotic exposure in liquid and on plates	*P. aeruginosa*	[179]
Compensatory evolution	serial passaging	*E. coli*	[180]

Adaptive laboratory evolution is a valuable tool, yet no standardized protocols exist. Table 1 demonstrates that different studies utilizing adaptive laboratory evolution vary tremendously in the protocols they use. Some differences in protocols were needed to elucidate a specific research question, e.g. selection for persisters likely requires a different protocol than studies that want to explore novel resistance mechanisms based on genetic adaptations. However, even studies that were elucidating similar research questions used different methodologies (Table 1). Various different protocols for adaptive laboratory evolution exist (Table 1, Figure 9): it can be performed on agar plates[171,181], on gradient plates[169,182], in liquid in a morbidostat[170], in liquid with serial passaging based on a gradient[149,167] or increment[164] approach. It can be speculated that the growth conditions in solid and liquid media are different and that the strength of the selection pressure likely differs between the listed approaches, which has previously been shown to impact results of adaptive laboratory evolution experiments[166].

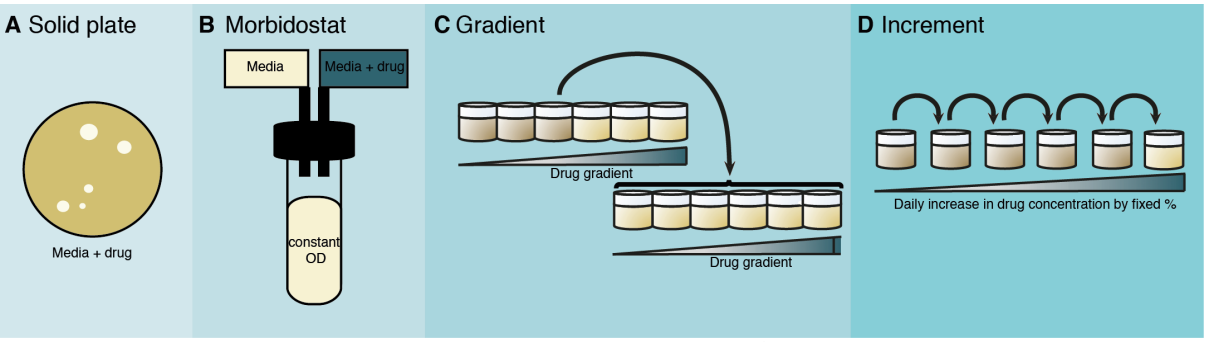

Figure 9: Different adaptive laboratory evolution techniques. A) Solid plate: Adaptive evolution can be performed on solid agar plates on which bacteria are exposed to high antibiotic concentrations and growth is permitted for multiple days. The protocol can also be varied and agar plates with antibiotic gradients can be used. **B) Morbidostat:** Growth in a morbidostat fixates the growth rate and the antibiotic concentration is adjusted to keep the population at a defined size. Due to adaptation of the bacteria to the antibiotic, the antibiotic concentration is increased over time. **C) Liquid gradient:** A gradient of antibiotic concentrations in liquid media is inoculated and the well with the highest antibiotic concentration that shows growth is usually used to inoculate a fresh gradient after a defined growth period. **D) Liquid increment:** The antibiotic concentration is increased at each transfer by a fixed increment.

In addition, important parameters for adaptive evolution are the population size[183], the bottleneck[184] and the dilution[185]. All of these parameters vary widely between the different approaches used for adaptive evolution (Table 1). Moreover, other parameters vary between different experimental setups and it can be assumed that they also impact evolution. One of these parameters is the media used for the experiment as it likely determines the metabolic activity of bacteria, which in turn was shown to be important for antibiotic resistance[39,186,187].

Another variation concerns the number of biological replicates that is used to access the evolutionary robustness of the study. Different evolution protocols also allow different growth phases, which have been previously linked with different antibiotic susceptibility profiles and might therefore also impact resistance evolution[188–190]. These observations raise the question whether the outcomes from these different studies utilizing various methodologies are comparable or biased by the method. Comparing the genes mutated in *E. coli* in response to exposure to doxycycline and chloramphenicol either in a morbidostat, gradient approach or increment methodology[149,170](**manuscript 3**) reveals that key mutations are overlapping across different methodologies. Moreover, mutations identified in response to trimethoprim based on a gradient approach on solid media, a morbidostat and an increment approach[169,170](**manuscript 3**) were to a large extend overlapping. In addition, we studied the outcome of experimental differences on the evolved geno-and phenotypes of multiple parallel evolved lineages as presented in **manuscript 1** and found that key features are selected regardless of the methodology. Besides the comparability between different evolution experiments, it is also important to consider the comparability between experimental and clinical data, as most experiments aim to explain naturally occurring phenomenons. The transferability of knowledge from adaptive evolution to the in-host evolution is controversial and might depend on the organism and adaptive laboratory evolution protocol used. While one study compared the evolution of *E. coli in vitro* and in the human host upon an urinary tract infection both challenged with antibiotic exposure, they found little overlap between the mutations that conferred resistance[191]. As the mutations that occurred *in vitro* were associated with a high fitness cost they speculated that these mutations could not be selected under natural conditions as the growth rate is critical for pathogens in urinary tract infections[191]. On the other hand many mutations frequently identified in laboratory evolution experiments with *E. coli* in genes like *gyrA*, *marR* or *acrR*[149,170], were also observed in clinical isolates[120,192,193]. The same is true for mutations known to be involved in resistance of *P. aeruginosa*[194]. Recently, it was also shown that a specific genetic resistance marker in *P. aeruginosa* could be counter selected upon antibiotic treatment in the laboratory and also in patients[146], highlighting that results from adaptive laboratory evolution experiments potentially depict evolutionary processes occurring in the human host.

Adaptive laboratory evolution of antibiotic resistance using different selection regimes lead to similar phenotypes and genotypes

Authors:

Leonie J. Jahn*

Christian Munck*[1]

Mostafa M. H. Ellabaan*

Morten O. A. Sommer*[§]

[§]Corresponding author: msom@bio.dtu.dk

*Author affiliation:

Novo Nordisk Foundation Center for Biosustainability, Technical University of Denmark, Kemitorvet 220, 2800 Kgs. Lyngby, DK

[1]Current affiliation:

Department of Systems Biology, Columbia University, Irving Cancer Research Center 1130 St. Nicholas Avenue, New York, NY 10032, USA

frontiers in Microbiology

ORIGINAL RESEARCH
published: 11 May 2017
doi: 10.3389/fmicb.2017.00816

Adaptive Laboratory Evolution of Antibiotic Resistance Using Different Selection Regimes Lead to Similar Phenotypes and Genotypes

*Leonie J. Jahn, Christian Munck, Mostafa M. H. Ellabaan and Morten O. A. Sommer**

Novo Nordisk Foundation Center for Biosustainability, Technical University of Denmark, Hørsholm, Denmark

Antibiotic resistance is a global threat to human health, wherefore it is crucial to study the mechanisms of antibiotic resistance as well as its emergence and dissemination. One way to analyze the acquisition of *de novo* mutations conferring antibiotic resistance is adaptive laboratory evolution. However, various evolution methods exist that utilize different population sizes, selection strengths, and bottlenecks. While evolution in increasing drug gradients guarantees high-level antibiotic resistance promising to identify the most potent resistance conferring mutations, other selection regimes are simpler to implement and therefore allow higher throughput. The specific regimen of adaptive evolution may have a profound impact on the adapted cell state. Indeed, substantial effects of the selection regime on the resulting geno- and phenotypes have been reported in the literature. In this study we compare the geno- and phenotypes of *Escherichia coli* after evolution to Amikacin, Piperacillin, and Tetracycline under four different selection regimes. Interestingly, key mutations that confer antibiotic resistance as well as phenotypic changes like collateral sensitivity and cross-resistance emerge independently of the selection regime. Yet, lineages that underwent evolution under mild selection displayed a growth advantage independently of the acquired level of antibiotic resistance compared to lineages adapted under maximal selection in a drug gradient. Our data suggests that even though different selection regimens result in subtle genotypic and phenotypic differences key adaptations appear independently of the selection regime.

Keywords: adaptive laboratory evolution, antibiotic resistance, selection pressure, collateral sensitivity, evolutionary constrains

OPEN ACCESS

Edited by:
Rakesh Sharma, Institute of Genomics and Integrative Biology (CSIR), India

Reviewed by:
Remy Froissart, Centre National de la Recherche Scientifique (CNRS), France
Raghavan Varadarajan, Indian Institute of Science, India
Cristian Ruiz Rueda, California State University, Northridge, USA

****Correspondence:***
Morten O. A. Sommer
msom@bio.dtu.dk

Specialty section:
This article was submitted to Evolutionary and Genomic Microbiology, a section of the journal Frontiers in Microbiology

Received: *20 December 2016*
Accepted: *21 April 2017*
Published: *11 May 2017*

Citation:
Jahn LJ, Munck C, Ellabaan MMH and Sommer MOA (2017) Adaptive Laboratory Evolution of Antibiotic Resistance Using Different Selection Regimes Lead to Similar Phenotypes and Genotypes. Front. Microbiol. 8:816. doi: 10.3389/fmicb.2017.00816

INTRODUCTION

Ecosystems continuously undergo changes in their physical and chemical properties resulting in shifts of ecological niches and living conditions (Hoffmann and Parsons, 1997; Elmqvist et al., 2003; Fine, 2015). Bacterial populations can respond to these environmental changes via both temporary and permanent adaptation. Temporary adaptation includes modulation of gene expression resulting in phenotypic changes, driven by changes in environmental signals, that are sensed by the bacteria (López-Maury et al., 2008). In contrast, selection of beneficial mutations or horizontal acquisition of advantageous genes represent permanent, genetic adaptations to a changed environment. Whether an environmental change is met by a temporary or a permanent

adaptation largely depends on the strength and duration of the selection pressure. Substantial changes in the environment, as in the case of antibiotic treatment, can result in both temporary adaptations like metabolic alterations resulting in antibiotic persistent bacteria (Levin et al., 2014) and permanent adaptations that sometimes give rise to antibiotic resistant bacteria (Carroll et al., 2014; Dhawale and Rath, 2014).

This adaptive potential of microorganisms is increasingly explored in biotechnology by adaptive laboratory evolution (ALE) experiments (Blum et al., 2016). ALE can be utilized to improve production strains by increasing their tolerance to the metabolic product (Hu et al., 2016; Lennen, 2016), by activating latent pathways (Wang et al., 2016) or by enabling the utilization of non-native substrates (Lee and Palsson, 2010). In addition, ALE experiments can improve our understanding of fundamental evolutionary principles that might help us solve rising global challenges of undesirable adaptations like drug resistances in microbial pathogens (Anderson et al., 1950; Govan and Fyfe, 1978; Cohen et al., 1989; Donald and van Helden, 2009; Wensing et al., 2015), cancer (Riganti et al., 2015) or insect resistance toward pesticides (Georghiou, 2012). Usually, ALE experiments focus on the adaptation to specific physical or chemical factors such as temperature (Tenaillon et al., 2012; Sandberg et al., 2014) or antibiotic tolerance (Hegreness et al., 2008; Toprak et al., 2012; Lázár et al., 2014; Munck et al., 2014; Rodriguez de Evgrafov et al., 2015). Various ALE setups have been used to study similar environmental perturbations like exposure to different antibiotics (Hegreness et al., 2008; Toprak et al., 2012; Lázár et al., 2014; Munck et al., 2014; Rodriguez de Evgrafov et al., 2015), yet, the influence of the experimental setup on the resulting adaptations remains poorly understood.

In this study we use evolution of antibiotic resistance as a model for studying the impact of the experimental setup on evolved phenotypes and genotypes. Prior studies have evolved bacteria to high level antibiotic resistance using different methodologies, including gradients of increasing drug concentrations (Kim et al., 2014; Munck et al., 2014; Oz et al., 2014; Rodriguez de Evgrafov et al., 2015), step-wise exposure to antibiotics (Lázár et al., 2014) or gradual increase in drug concentration in a morbidostat (Toprak et al., 2012). These different approaches utilize varying selection pressures, population sizes, and bottlenecks–all known to impact evolution (Nei et al., 1975; Levin et al., 2000; Wahl et al., 2002; Charlesworth, 2009). The influence of the selection pressure on the resulting pheno- and genotypes has been assessed by comparing bacteria exposed to mild and strong selection in a gradient approach (Oz et al., 2014) as well as by challenging bacteria with drug increments, varying in the steepness of drug increase (Lindsey et al., 2013). Differences in the number of mutations, growth rate, and resistance phenotypes were detected dependent on the methodology used (Lindsey et al., 2013; Oz et al., 2014). While the gradient method applies maximal selection pressure resulting in rapid generation of highly resistant lineages, the increment approach requires fewer laboratory resources, allowing for investigations of larger number of replicates and conditions such as different antibiotics, without increased handling time. Yet, the rate of drug increase is fixed in the increment approach, which can result in low as well as too high selection pressure dependent on the adaptation level of the bacteria.

In this study, we compare different increment approaches, varying in the steepness of drug increase, with the gradient approach to investigate how the selection regime defined by the ALE methodology influences the resulting geno- and phenotypes.

MATERIALS AND METHODS

Laboratory Adaptive Evolution in Drug Gradients

Escherichia coli K12 (MG1655) was evolved for 14 days to three different antibiotics: Amikacin sulfate (AMK) (Sigma), Piperacillin sulfate (PIP) (Sigma), and Tetracycline hydrochloride (TET) (Sigma), covering three major classes of antibiotics, including both bactericidal and bacteriostatic drugs. The antibiotics were dissolved in water (10 mg/l) and the stock solutions were stored at −20°C. Four replicate lineages were evolved in parallel for each drug. 96-well plates (Almeco), containing 1 ml Mueller-Hinton broth II (MHBII) (Sigma) per well and a 2-fold antibiotic gradient in 10 dilutions, were prepared at the start of the experiment and stored at −20°C. The minimal inhibitory concentration (MIC) of the wild type, as defined by the European Committee on Antibiotic Susceptibility Testing (EUCAST), was located in the second well, allowing growth of the wild type in the first well under sub-inhibitory conditions (exact plate setup and drug concentrations are given in Supplementary Table 1). Plates were defrosted at the day of usage, pre-heated to 37°C, inoculated with 50 μl of freshly growing cells and incubated at ∼900 r.p.m. and 37°C for 22 h. One hundred fifty microliters of each well were transferred into a 96-well microtiter plate and the optical density was measured at a wavelength of 600 nm (OD_{600}) by an ELx808 Absorbance Reader (BioTek). Based on the OD measurement a cut-off value, that was the minimal growth that clearly set itself apart from the background growth, was chosen to define distinct growth for each drug (Supplementary Figure 1). An $OD_{600} > 0.1$ corresponding to $\sim 8.0 \times 10^7$ CFU/ml defined distinct growth for AMK and TET and an $OD_{600} > 0.3$ equivalent to about 2.4×10^8 CFU/ml defined growth for PIP due to a background growth level of around $OD_{600} = 0.18$. Fifty microliters of the well with the highest drug concentration that showed distinct growth in the deep-well plate were used to inoculate a fresh gradient (exact OD_{600} values and corresponding drug concentrations of the well chosen for each transfer are given in Supplementary Table 2). Remaining cells in these wells were mixed to a final glycerol concentration of 20% and stored at −80°C. On each plate 16 wells served as negative control resulting in a total of 448 wells during the course of the experiment, of which 1% showed growth. For each lineage seven colonies were isolated for genomic and phenotypic characterization from the population that had been maintained for two passages at or above the clinical breakpoint as defined by EUCAST for the specific antibiotic. The clinical breakpoint is the drug concentration that is used as

a cut-off value to classify pathogens as susceptible or resistant toward a specific drug (Turnidge and Paterson, 2007).

Laboratory Adaptive Evolution in Drug Increments and Media Control

E. coli K12 (MG1655) was not only evolved in drug gradients but also to a daily relative increase of drug concentration. Three different approaches were used (exact drug concentrations for each day for the different increment approaches and drugs are given in Supplementary Table 3). The lineages in the "Increment 100" setting were exposed to a 100% increase in drug concentration. Under this regime the drug concentration was consequently doubled every day, applying a constantly strong selection pressure to the lineages. The clinical breakpoint was supposed to be reached after 7 days of the ALE experiment. "Increment 50" lineages were also exposed to a rather high environmental change rate by growth in a 50% higher drug concentration every day, reaching the clinical breakpoint on the 9th day of the experiment. The drug concentration was raised by 25% for the "Increment 25" lineages, allowing a mild selection and twice as much time to adapt to the clinical breakpoint concentration compared to the "Increment 100" lineages. Eight lineages were evolved in parallel in each setting to AMK, PIP, and TET. The experiment was designed that all experimental setups reached the MIC as defined by EUCAST at the 4th day. As control for media adaptations eight wild type lineages were evolved to the media without antibiotics. The MHBII antibiotic mixture was prepared in falcon tubes for each day, drug and experimental setup in the beginning of the experiment and stored at −20°C. The drug containing media was defrosted on the day of usage and pre-heated to 37°C. The lineages were grown in 1 ml MHBII and antibiotic in a 96-deep-well dish for 22 h at 37°C and ∼900 r.p.m. 50 μl of cells were transferred every 22 h. The remaining cells were mixed to a final concentration of 20% glycerol and stored at −80°C. The adaptive evolution was stopped after 14 days when the "Increment 25" lineages had passed the clinical breakpoint. During the experiment ∼3% of 1,152 negative controls showed growth. Cells were streaked on LB plates and identified by visual investigation as *E. coli*. All colonies looked identical, suggesting that there was no contamination. Once the adaptive evolution experiment was ended, lineages that were adapted to the clinical breakpoint were streaked on LB agar and seven isolated colonies were used for further analysis. If lineages died out before they had reached the clinical breakpoint, the last possible time point was chosen.

IC_{85} Determination

Isolated colonies were used to inoculate a 96-well microtiter plate containing 150 μl MHBII. About 10^5 cells of an overnight culture were transferred with a 96-pin replicator to 10 dilutions of a 2-fold drug gradient spanning from 0.5 to 256 mg/l AMK and 0.25 to 128 mg/l of PIP or TET, respectively. For each lineage one isolated colony was tested in two technical replicates against all three antibiotics. Eight inoculated wells containing MHBII served as positive control while eight wells only filled with MHBII served as negative control. The plates were incubated at 37°C and 900 r.p.m. for 18 h and subsequently the OD_{600} was measured by an ELx808 Absorbance Reader (BioTek). The data was further analyzed using R (Team R Core, 2014). The average OD_{600} values of the negative controls were subtracted from all remaining OD_{600} values. Percent inhibition was calculated by subtraction of the OD_{600} values divided through the average of the OD_{600} values of the positive controls from 1.

$$\textit{Percent inhibition} = 1 - \frac{OD_{600}\ (\textit{growth}) - OD_{600}\ (\textit{negative control})}{OD_{600}\ (\textit{positive control}) - OD_{600}\ (\textit{negative control})} \quad (1)$$

A dose-response curve was fitted to the values using a logistic model from the drc package (Ritz and Streibig, 2005), with x for the molar drug concentration and default values for the other variables, where b describes the steepness of the curve, c and d the lower and upper asymptotes and e the effective dose (Munck et al., 2014; Ritz et al., 2015):

$$f\left(x\left(b,\ c,\ d,\ e\right)\right) = c + \frac{(d-c)}{1+\exp\left(b*\left(\log\left(x\right)-\log\left(e\right)\right)\right)} \quad (2)$$

Dose-response curves were plotted with the package ggplot (Wickham, 2009). The drug concentration causing 85% growth inhibition (IC_{85}) was calculated with the inverted function, normalized to the wild type, and plotted grouped by drug using ggplot (Wickham, 2009). A non-parametric distribution of parallel lineages was observed for some experimental setups and drugs wherefore the non-parametric Kruskal-Wallis one-way analysis of variance was applied in R to detect significant ($P < 0.05$) differences between the four experimental setups adapted to each drug.

Growth Rate Measurements

A 96-well microtiter plate, containing 200 μl MHBII per well, was inoculated with cells in exponential growth phase using a 96-pin replicator. All seven isolated colonies per lineages were included in the growth measurement. OD_{600} was measured in a ELx808 Absorbance Reader (BioTek) every 5 min for 10 h at 37°C and 650 r.p.m. The data was analyzed with R (Team R Core, 2014). The growth rate was calculated based on the steepest part of the growth curve during exponential growth. The doubling time was normalized to the wild type and plotted grouped by drug with the package ggplot (Wickham, 2009). To test whether the observed differences in growth rate were significant ($P < 0.05$) the non-parametric Kruskal-Wallis one-way analysis of variance was applied in R.

Whole-Genome Sequencing

One isolated colony of each of the 92 lineages, that was also used to measure the IC_{85} and growth rate, was grown in LB and DNA was extracted with the A & A Genomic Mini kit (A&A Biotechnology). The DNA was sent to Macrogen, who prepared genomic libraries with the TruSeq DNA Nano (550 bp) kit from Illumina and sequenced them by Illumina MiSeq 300 bp paired ends.

Identification of Single Nucleotide Polymorphisms and Small INDEL Sequences

The reads were aligned to *E. coli* K12 U00096 reference genome with CLC Genomics Workbench (Escherichia coli Str. K-12 Substr, 2014). On average each base was covered at least 37.5 times (Supplementary Table 4). SNP and INDEL sites were determined with CLC Genomics Workbench. Only loci with a phred score of 30 at the variable position as well as at the three neighboring bases occurring at least with a frequency of 80% were included in the analysis. Single nucleotide polymorphisms (SNPs) that were detected in all lineages including the media adapted wild type were considered mutations that had occurred before the start of the experiment and were therefore excluded. If two lineages shared two identical SNPs they were considered cross-contaminated and one of them was excluded from further analysis.

Detection of Large Deletions

Large deletions were identified with a workflow in CLC workbench. The reads of all genomes were assembled *de novo* and used as reference genomes to map the reads from one of the media adapted wild type strains. The reads from the media adapted strain that did not map to the *de novo* assembled antibiotic evolved genome were collected and also *de novo* assembled into contigs. Contigs larger than 1 kb with a coverage > 30 were considered large deletions.

Detecting Large DNA Insertions by Insertion Elements

We downloaded both the complete genome of *E. coli* K12 MG1655, with accession U00096, and the corresponding ORFs from the NCBI Nucleotide Archive. The ORFs were then clustered together using cd-hit (Li and Godzik, 2006), allowing ORFs with at least 90% identity and coverage to be in the same cluster. The reads of the sequenced strains were filtered using the FASTX-Toolkit package and a minimum quality of 30. The quality-filtered reads were blasted against the clustered ORFs by setting the word_size to 10 and the e-value to 100 allowing accurate short sequence mapping. Reads mapping to at least two ORFs of different clusters with a minimum of 30 and a maximum of 70% coverage of each cluster were further considered potential large insertion reads. These reads were blasted against the whole genome to confirm that the two genes were not adjacent on the genome. Reads that covered the reference genome with more than 90% were expected to contain two adjacent genes, wherefore they were excluded from the analysis. It was further explored whether the remaining hits overlapped with insertion elements. Reads that aligned to one ORF annotated as insertion element were included for further analysis. Only insertion reads that were detected in more than 10 reads were considered as large DNA insertions.

Identification of Gene Duplications

Gene duplications were identified with CLC Genomics Workbench using the coverage analysis tool by calling for regions with at least 700 bp of significantly ($P < 0.001$) increased coverage. The identified regions were mapped to the reference genome U00096 in R and genes that overlapped with at least 95% with the region of high coverage were identified as duplicated genes.

RESULTS

Four Different Strategies of Adaptive Laboratory Evolution

To compare the effect of the ALE methodology on final pheno- and genotypes we evolved *E. coli* to three different antibiotics using four different ALE strategies. The antibiotics chosen for this experiment represent three major groups of antibiotics. Two of the drugs, amikacin (AMK) and tetracycline (TET), target the ribosome with the former being bactericidal and the latter being bacteriostatic. The third drug, piperacillin (PIP), is a bactericidal drug targeting cell-wall biosynthesis. The four different selection regimes can be divided into two categories: (1) A gradient approach in which the population that tolerates the highest drug concentration is passed to a fresh drug gradient every 22 h; and (2) an increment approach in which the evolving population is passed every 22 h to a new drug concentration increased by fixed increments (**Figure 1**).

A 20-fold dilution of the gradient evolved populations was chosen based on a model by Wahl et al. (2002), to allow a high variation in the transferred population and to base fixation of mutations on the optimal adaptation rather then on limiting bottlenecks. According to Wahl et al. (2002) a 10-fold dilution of the population would be optimal but previous experiments in the laboratory showed a small increase in the inhibitory drug concentration for AMK and TET when a 10-fold dilution was used. To avoid an inoculum effect, which is a significant increase in the inhibitory concentration caused by a larger amount of organisms in the inoculum (Brook, 1989), we chose a 20-fold dilution (Supplementary Figure 2).

After 14 days of adaptive evolution in the gradient setup, the populations exposed to AMK tolerated on average 512 mg/l of the drug, corresponding to a 170-fold increase compared to the media adapted wild type ($P = 2.89654\text{E}^{-27}$, student's *t*-test) (**Figure 2A**). The PIP evolved lineages grew in drug concentrations of 192 mg/l on day 14 of the ALE experiment, equal to a 80-fold increase compared to the media adapted wild type ($P = 0.00109527$, student's *t*-test). However, large oscillations in resistance were observed for the PIP evolved lineages during the course of the experiment (**Figure 2B**). This variation could be explained by an inoculum effect, which is more frequently observed for beta-lactam antibiotics (Eng et al., 1984, 1985; Brook, 1989). Lineages evolved to TET did not reach the same drug tolerance compared to AMK or PIP evolved lineages, but still grew in 15 mg/l TET, exceeding the media adapted wild type inhibitory concentration (IC) by 15 times ($P = 2.04072\text{E}^{-06}$, student's *t*-test) (**Figure 2C**). These values are in accordance with previous findings where the IC_{90} values (the drug concentration at which growth of 90% of the population is inhibited) of isolated colonies were determined after 14 days of adaptive evolution in a

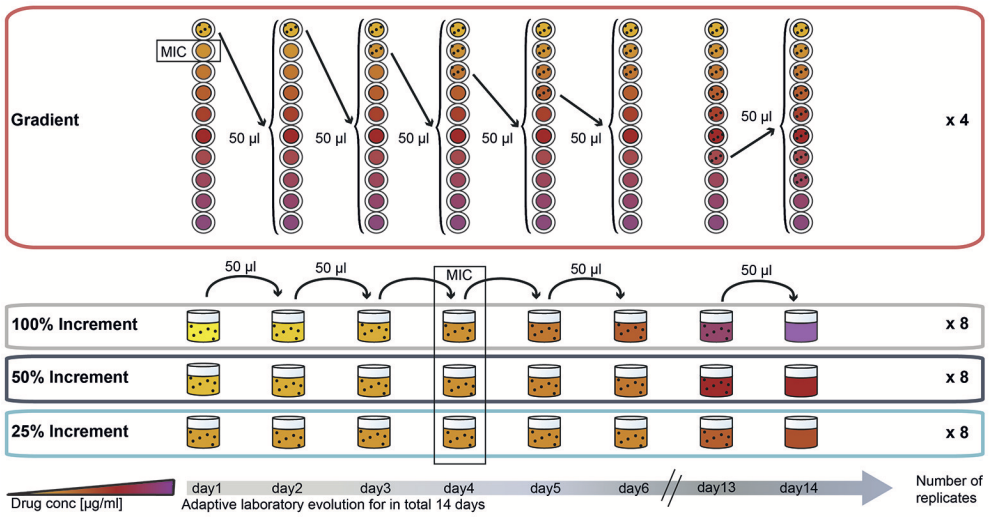

FIGURE 1 | Experimental design of the study: adaptation of *E. coli* K12 to three antibiotics following four adaptation protocols with different selection strengths. The four selection systems are named "gradient," "100% increment," "50% increment," and "25% increment." In the gradient approach, cells were inoculated into a 2-fold, 10-step drug gradient and cells growing in the highest concentration were used for inoculation of a fresh gradient. In the increment approaches the drug concentration was raised with every transfer either by 100, 50, or 25%. The wild type minimal inhibitory concentration (MIC) was reached on the fourth day of the experiment for all increment lineages.

gradient system using the same strain and drugs (Munck et al., 2014). Only PIP evolved lineages appear more resistant in the present study, which is attributed to the inoculum effect caused by the larger passaging volume.

In the increment approach three different rates of environmental change were tested (**Figure 1**), for which the selective pressure (e.g., antibiotic concentration) was increased by 100, 50, or 25% every day. Similar to the gradient approach the 100% increment setup applies a high selection pressure with the risk of exceeding the adaptive potential of the bacterium leading to extinction of the lineages (**Figure 1**).

Extinction of Increment Lineages after Exceeding the Adaptation Maximum Defined by Gradient Lineages

We speculated that the increment-evolved lineages would die out when the drug concentrations they were exposed to exceeded the adaptation level of the gradient evolved lineages as a maximal selection pressure was applied to the gradient evolved lineages. Our observations during the ALE experiment support this hypothesis (**Figures 2A–C**). Whenever the antibiotic concentration of the drugs in the increment evolution experiments exceeded the maximal concentration of at least one of the gradient evolved lineages, some of the parallel increment lineages became extinct. For instance, the remaining 100% increment lineages adapted to AMK became extinct after they grew in 32 mg/l on day 8 of the experiment but one of the gradient adapted lineages only grew in 16 mg/l. All increment lineages died out when exposed to a drug concentration above the drug concentration to which all of the gradient lineages were adapted to (**Figures 2A–C**). For example all remaining increment 50% lineages died out when they passed an PIP concentration of ∼32 mg/l on day 13 of the adaptive evolution experiment when lineages adapted in the gradient approach only grew in PIP concentrations of 8 mg/l. Since the antibiotic exposure for the 100 and 50% increment lineages exceeded the maximum evolutionary potential exhibited by the relevant gradient evolved lineages all 100 and 50% increment lineages went extinct before the end of the experiment (**Figures 2A–C**). Notably, only 4 out of the 24 lineages that were exposed to 100% increments reached the clinical breakpoint before extinction. A decrease in population density (OD_{600}) often preceded extinction (Supplementary Figure 3). In contrast, all 50 and 25% lineages reached the clinical breakpoint. The ability to adapt appeared to be drug specific. The different adaptation potentials are reflected in the extinction of the increment lineages. For instance, 100 and 50% increment lineages died out later when adapted to AMK compared to TET (**Figures 2A–C**).

Similar Resistance Levels Can Be Accompanied by Different Fitness Costs

We were interested in observing how the different rates of environmental change affected the final genotypes and phenotypes. By design, lineages would be adapted to different antibiotic concentrations at the end of the experiment, depending on the specific ALE approach. Accordingly, we decided to compare the lineages when they had reached the clinical breakpoint (defined by EUCAST, 2016). Gradient evolved lineages were analyzed at the time point when they had reached or exceeded the clinical breakpoint for 2 consecutive days. Increment evolved lineages were analyzed at the time point when the lineage had reached the clinical breakpoint. As most of the

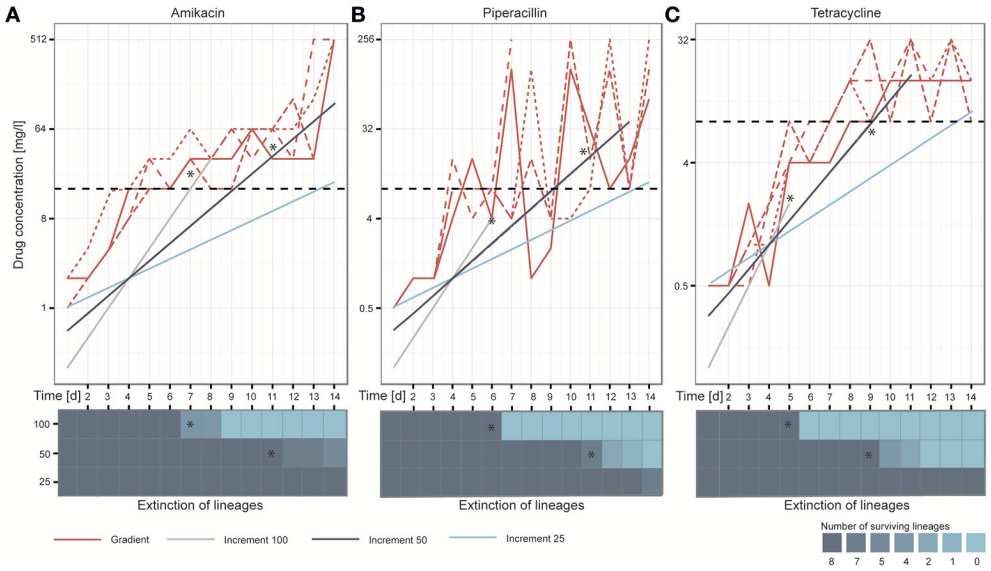

FIGURE 2 | Overview of the adaptation potential over time for each drug: (A) amikacin, **(B)** piperacillin, and **(C)** tetracycline. The lineages adapted under the gradient method follow the maximal selection pressure wherefore it can be observed that lineages from the increment approaches (100, 50, and 25) die out when they exceed the natural selection maximum defined by the gradient approach, indicated with stars in the figure. Replicates are represented in different line styles. The clinical breakpoint is indicated with a dotted line in black. The heatmaps illustrate the extinction of lineages over time.

100% increment lineages failed to reach the clinical breakpoint we excluded these lineages from the analysis.

One colony was obtained from each lineage at the time point where the population had reached the clinical breakpoint and the antibiotic tolerance was determined. The IC_{85} values were normalized to the average IC_{85} of the media adapted strains (**Figure 3A**).

For AMK and TET adapted strains the resistance level of the gradient evolved strains was above the clinical breakpoint (**Figure 3A**). In contrast, only one of the strains adapted to PIP was above the clinical breakpoint. High fluctuations in resistance level were observed in the PIP adapted lineages (**Figure 2B**) suggesting that an inoculum effect rather than real adaptation contributed to the population tolerance. The inoculum used in this study corresponded to about 10^8 CFU/ml and did not indicate inoculum effect in previous experiments (Supplementary Figure 2). Yet, it is exceeding the reported CFU/ml concentration causing inoculum effect for PIP (Bryson and Brogden, 2012).

The resistance levels of the 25% increment evolved strains displayed a normal distribution around the clinical breakpoint for TET and PIP and were above the clinical breakpoint for AMK, whereas the 50% increment strains displayed a slightly lower tolerance (**Figure 3A**). However, when comparing gradient and increment adapted strains, only TET evolved strains showed a significant ($P < 0.05$ Kruskal-Wallis one-way analysis of variance) difference in their resistance levels (**Figure 3A**).

Many resistance-conferring mutations are known to confer a fitness cost, which can often be detected by a reduced growth rate (Linkevicius et al., 2013). Since the selection regime seems to influence the fitness of the resulting lineages (Lindsey et al., 2013), we measured the growth rate of the same isolated colonies that were used for the IC_{85} determination and an additional six isolated colonies for each lineage, resulting in 28 clones for the gradient approaches and 56 clones for the increment experiments (**Figure 3B**). Adaptation to AMK generally seemed to be connected with a reduced growth rate compared to the other drugs.

For all three drugs the 25% increment strains grew significantly (Kruskal-Wallis one-way analysis of variance $P < 0.05$) faster than the gradient adapted strains (**Figure 3B**). The growth advantage of the increment lineages could be due to a larger number of generations that they underwent compared to the gradient evolved lineages providing better opportunity for fitter mutants to outcompete resistant mutants with larger fitness costs and to accumulate compensatory mutations that can balance the fitness costs of resistance conferring mutations. However, the time that a population was evolved for and the doubling time are not significantly correlated ($R = -0.019$, Pearson's product-moment correlation coefficient, $P = 0.71$). Accordingly, it is likely that the shorter doubling time of the increment lineages is due to a lower selection pressure toward drug resistance, resulting in an increased selection for high growth rate. This finding is in line with previous studies reporting that *E. coli* lineages evolved to rifampicin under sudden drug increase have a significantly reduced growth rate compared to lineages evolved to more gradual drug increases (Lindsey et al., 2013) and that *E. coli* lineages adapted to 22 different antibiotics under mild selection have an elevated growth rate compared to lineages evolved under strong selection regimes (Oz et al., 2014). Yet, no correlation was found between the resistance level and the growth rate suggesting that a mutation that confers high-level

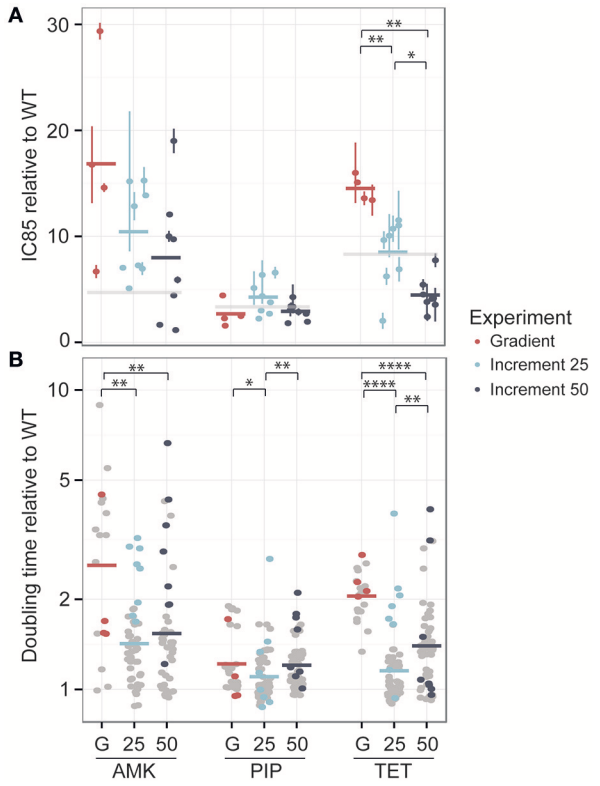

FIGURE 3 | Phenotypic changes in drug resistance and growth rate after the adaptive laboratory evolution experiment. (A) The fold-increase of the IC_{85} compared to the wild type (WT) is displayed for each drug. The evolved resistance levels are not significantly different for amikacin (AMK) and piperacillin (PIP) across different experimental setups, which are referred to as G for the gradient approach, 25 for the 25% increment and 50 for the 50% increment method. However, strains adapted to tetracycline (TET) display significant changes in drug resistance. The clinical breakpoint normalized to fold-increase to the media adapted wild type (WT) of each drug is marked with a light gray panel. **(B)** The doubling time relative to the wild type is shown for the same isolated colony used for the IC_{85} determination as well as for six additional colonies, colored in gray. A significantly lower doubling time for the 25% increment lineages compared to the gradient evolved lineages can be observed for all drugs. $^{*}P < 0.05$, $^{**}P < 0.01$, $^{***}P < 0.001$, $^{****}P < 0.0001$.

resistance is not necessarily linked to a high fitness cost and *vice versa* (Supplementary Figure 4).

Different Selection Regimes Do Not Substantially Influence Collateral Sensitivity and Cross-Resistance Phenotype

Antibiotic resistant bacteria often show cross-resistance to similar drugs (Szybalski and Bryson, 1952). Interestingly, increased susceptibility toward other antibiotics can also frequently be observed (Szybalski and Bryson, 1952; Imamovic and Sommer, 2013; Lázár et al., 2014; Munck et al., 2014), a phenomenon commonly referred to as collateral sensitivity. In order to test if the cross-resistance and collateral sensitivity phenotype is influenced by the selection regime we determined the drug resistance profiles for each evolved strain toward each of the three drugs tested (**Figure 4**). All lineages adapted to AMK showed collateral sensitivity toward PIP. However, the gradient and 25% increment AMK adapted strains differed in their collateral sensitivity toward TET ($P < 0.05$, Kruskal-Wallis one-way) (**Figure 4**). It should be noted that the end point of the gradient adapted AMK lineages showed collateral sensitivity toward TET in accordance with previous studies (Munck et al., 2014), suggesting that the number of generations that a lineage was allowed to undergo before testing the collateral sensitivity was important. Isolates from gradient and increment lineages all showed collateral sensitivity against AMK when evolved to TET and cross-resistance between PIP and TET (**Figure 4**). However, strains adapted to PIP in the gradient approach were slightly less resistant ($P < 0.05$, Kruskal-Wallis one-way) to TET than the strains adapted in the 25% increment approaches (**Figure 4**). While, Oz et al. (2014) highlights differences in collateral sensitivity in mildly and strongly selected lineages, our results are in line with findings by Lázár et al. (2014) suggesting that phenotypic similarities dominate over differences.

Overall it can be concluded that the cross-resistance was very similar between gradient and increment approaches. The main phenotypic difference between gradient and increment evolved lineages is a slower growth rate of the gradient evolved lineages.

Genotypes of Lineages Adapted under Different Selection Pressures Overlap

The strains used for IC_{85} determination and growth rate measurements were sequenced in order to uncover the underlying genetic changes. We identified a total of 173 mutations across 92 sequenced strains (Supplementary Table 5). Large insertions and deletions made up 26.5% of the total number of mutations (Supplementary Figure 5A). These larger genetic rearrangements are frequently overlooked but can play important roles in the genetic adaptation process. Two of the eight parallel strains adapted in a 25% increment to AMK have three identical SNPs in common, suggesting potential cross-contamination between the lineages. Therefore, only one of the strains was used for the following analysis.

On average we identified about two mutations in each strain across the different experiments (Supplementary Figure 5B). Even though the 25% increment lineages were evolved for more generations until they reached the clinical breakpoint there was no significant difference in the number of mutations between experimental setups ($P > 0.5$, Students *t*-test) and the number of mutations in the sequenced isolates did not correlate significantly with the number of generations ($R = 0.19$, Pearson's correlation, $P = 0.097$).

Whether a mutation confers resistance, compensates fitness costs of other mutations or hitchhikes with a resistance mutation is difficult to determine without re-introducing specific mutations alone and in combinations into the non-evolved wild type. However, if a gene is mutated in more than one independent strain it is likely that the mutation was selected for (Lieberman et al., 2011; Yang et al., 2011; Sandberg et al., 2014). We filtered our dataset according to this criterion and found that 88.8% of

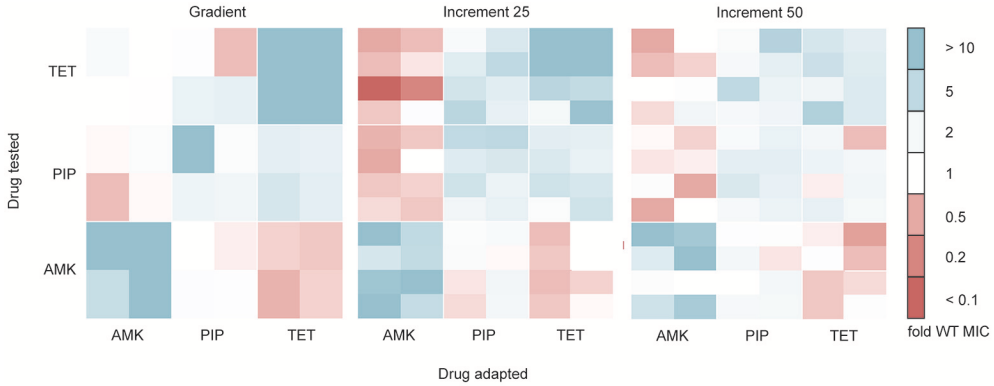

FIGURE 4 | Cross-resistance and collateral sensitivity phenotypes of the gradient, 25 and 50% increment evolved strains. Fold increase (blue) or decrease (red) of the IC_{85} compared to the wild type (WT) is indicated for each individual strain. The collateral sensitivity as well as cross-resistance is similar across experimental setups. Collateral sensitivity toward tetracycline (TET) of strains adapted to amikacin (AMK) under the 25% increment approach is elevated ($P < 0.05$) compared to strains evolved to the drug gradient. The cross-resistance of strains evolved to piperacillin (PIP) tested against TET is increased ($P < 0.05$) in the 25% increment adapted strains compared to the gradient evolved strains.

genes mutated in the gradient evolved strains were also mutated in the increment strains (**Figure 5**). Except mutations in the ATP synthase gamma chain (*atpG*) and the cytochrome bo(3) ubiquinol oxidase subunit 2 (*cyoA*), all mutated genes of the gradient strains in the filtered dataset have also been found to be mutated in the 25% increment strains (**Figure 5**). The clones carrying one of the two mutations have an average doubling time that is four times higher than the wild type and twice as high as the average of all strains adapted to AMK. Therefore, it is likely that these mutations come with a high fitness cost, and accordingly were not fixed in the 25% increment lineages.

Interestingly, the increment-adapted strains carried not only most of the mutations found in the gradient adapted strains, but also many mutations that were solely identified in the increment strains (**Figure 5**). Such mutated genes are for example *nuoB*, *nuoC*, and *nuoH*, subunits of the NADH-quinone oxidreductases that shuttle electrons from NADH to quinones in the respiratory chain that have been identified to confer resistance toward AMK in previous studies (Kohanski et al., 2007; Schurek et al., 2008; Girgis et al., 2009; Wong et al., 2014). In addition, these mutations were linked to the collateral-sensitivity phenotypes of aminoglycosides toward many other classes of antibiotics (Lázár et al., 2014), suggesting that mutations in these genes are relevant for the collateral sensitivity phenotype toward TET, that was not observed in the gradient lineages when they reached the clinical breakpoint, but only in strains isolated from the end point of the gradient evolved lineages.

Mutations in the genes *fusA, sbmA* as well as in two different two component systems, *cpxRA* and *arcAB* appeared to be the dominating mutations in all strains adapted to AMK (**Figure 5**). All mutations have been previously linked to AMK resistance (Laviña et al., 1986; Busse et al., 1992; Johanson and Hughes, 1994; Salomón and Farías, 1995; Macvanin and Hughes, 2005; Kohanski et al., 2008, 2010; Pena-Miller et al., 2013; Lázár et al., 2014; Munck et al., 2014). Mutations in the elongation factor G encoding gene *fusA* have been shown to result in collateral sensitivity toward beta-lactam antibiotics, as observed in this study for PIP (Macvanin and Hughes, 2005).

acrR was found to be the predominantly mutated gene in the PIP evolved lineages regardless of the experimental setup (**Figure 5**). Mutations in *acrR* as well as in *marR* and *rob*, also identified to be mutated in the increment strains adapted to PIP, lead to the multiple antibiotic resistance (mar) phenotype, which was described to confer resistance toward a variety of drugs including beta-lactam antibiotics and tetracyclines. This finding explains the cross-resistance observed for TET and PIP evolved lineages in this experiment (George and Levy, 1983; Cohen et al., 1989; Ariza et al., 1995; Maneewannakul and Levy, 1996; Oethinger et al., 1998). The lack of mutations in *marR* and *rob* in the gradient adapted strains might account for the difference in cross-resistance toward TET compared to the 25% increment adapted strains. However, it can be speculated that these mutations would also occur in a gradient system if the inoculum effect can be avoided, since they were observed previously in an experiment following the gradient approach (Munck et al., 2014). Another frequently observed mutation in PIP adapted strains affects the drug target, the peptidoglycan synthase *ftsI* (penicillin-binding protein 3) (**Figure 5**) (Matic et al., 2003; Blázquez et al., 2006). Interestingly, mutations in *cpxA* were solely found in 25 and 50% increment strains adapted to PIP (**Figure 5**). Mutations in this gene can confer up to 2-fold increases in resistance to beta-lactam antibiotics (Srinivasan et al., 2012; Bernal, 2014). Since a 2-fold increase in drug resistance is moderately low, it can explain why the mutation was only found in 25 and 50% increment lineages that were exposed to low antibiotic concentrations and why it was not identified in the gradient or 100% increment lineages.

The lineages adapted to TET showed, similar to PIP, mutations in genes belonging to the mar phenotype (**Figure 5**). In addition to mutations belonging to the mar phenotype, two other mutated genes, *dksA* and *waaP*, were identified which were previously only indirectly linked to antibiotic susceptibility (Yethon et al.,

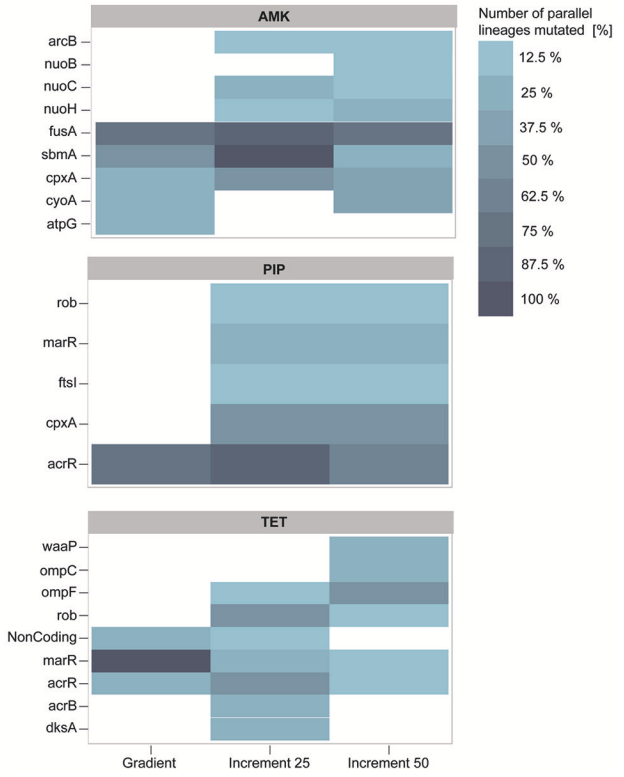

FIGURE 5 | Genetic adaptations to the antibiotics amikacin (AMK), piperacillin (PIP), and tetracycline (TET). The color represents the number of strains in percent that harbor a mutation, identified in at least two independent lineages. Almost all mutations identified in the gradient approach are also present in at least one of the increment strains. PIP and TET evolved lineages display similar genotypes with mutations predominantly affecting the mar phenotype.

1998; Yethon and Whitfield, 2001; Hansen et al., 2008; Tamae et al., 2008; Liu et al., 2010). Interestingly, the only gene duplications observed in this experiment were all found in three different lineages in the 50% increment strains adapted to TET. Two genes, *yicS* and *yibT*, with uncharacterized gene products, were duplicated as well as *phoU,* whose deletion mutant was more susceptible toward antibiotics suggesting a potential role in antibiotic tolerance (Li and Zhang, 2007).

The significant difference in resistance between gradient and increment evolved lineages might be explained by the abundance of mutations in *marR.* Almost all strains adapted under the gradient approach carry a mutation in *marR,* whereas this genetic change was only observed in a few lineages evolved in the increment regime (**Figure 5**). Lineages harboring mutated *marR* were overall 15% more resistant to TET than all TET adapted lineages on average. However, they also had an increased doubling time by ∼27% compared to the average. Δ*marR* mutants were previously linked to an impaired fitness (Marcusson et al., 2009), suggesting that mutations in *marR* are more likely to dominate a population under strong selection.

The clones adapted under the gradient approach seem to have fewer mutations in the filtered data set in comparison to the increment lineages. However, they often carry mutations that were only detected once in the whole experiment (Supplementary Table 5), therefore the gradient adapted lineages display a higher diversity in unique mutations. In order to quantify the similarity and dissimilarity between genotypes in the different experimental setups, we did a pairwise comparison between all strains using the unfiltered data set. The overlap of mutated genes between the pairs was calculated in percent of the total number of mutated genes found in the two strains. We chose to analyze the similarity on the gene level and not on SNP or gene family level, since it was suggested as appropriate measure to detect parallel or convergent evolution (Achaz et al., 2014). The genetic similarity within the gradient evolved replicates was on average around 30–50% (**Figure 6**). The strains adapted under the 25 and 50% increments were about 45 and 30% similar to each other when adapted to AMK and PIP and only around 20 and 10% alike when evolved to TET (**Figure 6**). Interestingly, the genetic similarity of strains evolved using different selection regimens was comparable to the similarity within replicates from the same selection regimen (**Figure 6**). The similarity of the gradient and the 25% increment strains was maximal about 3% below and 12% above the group internal similarity of either the gradient or the increment 25 strains (**Figure 6**). This result underlines that the genetic similarity between the different selection regimens is similar to the genetic similarity observed between parallel lineages that were evolved under identical conditions.

DISCUSSION

In this study we analyzed the impact of the selection regimen in different ALE methodologies on the resulting phenotypes and genotypes. As expected, the rate of environmental change is a crucial parameter for the extinction of populations. Environmental changes, that exceed the adaptation capability of an organism or that allow too little time for adaptation, result usually in extinction. A decrease of the OD often preceded extinction of lineages, indicating that the mean fitness of the population was reduced preceding extinction (Lynch and Lande, 1993). The reduction in population size also lowered the number of cells transferred to the next drug concentration, reducing the genetic variability (Frankham, 2005; Bell and Collins, 2008). Under these conditions the mean population fitness is impaired and can only be enhanced through a lowered environmental change rate (Lynch and Lande, 1993). In our case the constantly high rate of environmental change in the 100 and 50% increment lineages led to extinction of the evolving population. We observed an evolutionary limit for adaptation that was defined by the gradient evolved lineages. If the rate of environmental change of the 50 and 100% increment lineages exceeded this maximum, strains became extinct. These findings can be implemented in the design of an ALE experiment for industrial purposes where the extinction of lineages should typically be prevented. Therefore, it can be suggested to either use a milder rate of environmental change or a higher number of replicates in order to compensate for lineage extinction.

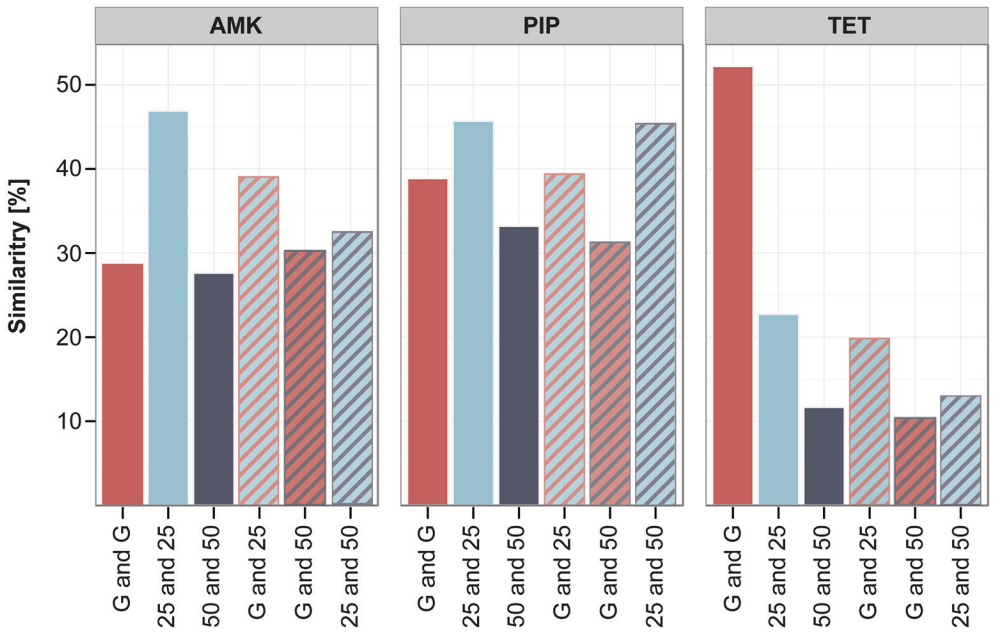

FIGURE 6 | Similarity of lineages evolved to different selection strengths. The similarity between different strains was calculated in pairwise comparisons by analyzing the percentage of genes that were mutated in both strains compared to the total number of mutations found in the two strains. The average of the pairwise similarity is displayed for different groups of strains: either within one experimental setup like the gradient (G) (red) or the increment approaches (25 and 50) (blue and gray) or between those experimental setups (stripes), comparing similarity of the gradient and increment lineages or the increment approaches with each other.

We expected, that the gradient evolved lineages would indicate the evolutionary capacity of *E. coli* to adapt to a certain drug as we constantly applied maximal selection pressure in the gradient setup. However, in case of Piperacillin we observed large oscillations of the drug tolerance in all parallel evolving populations during the 14 days of the adaptive evolution experiment. The inoculum varied during the cause of the experiment and sometimes exceeded the inoculum that was used for the initial test that did not suggest inoculum effect for any of the three drugs. In addition, beta-lactam antibiotics are known to be more prone to cause inoculum effect (Eng et al., 1985; Brook, 1989), wherefore we conclude that inoculum effect is the likeliest explanation for the oscillations. Yet, other scenarios such as (1) clonal interference (de Visser and Rozen, 2006), where several mutations conferring resistance, tolerance or growth advantageous compete against each other, (2) disruptive frequency dependent selection (Levin et al., 1988), where only common mutations are fixed in the population or (3) phenotypic tolerance, that temporarily allows bacteria to survive in antibiotic concentrations without conferring resistance (Brauner et al., 2016) could potentially account for the oscillations as well.

Once a given phenotypic level has been reached, different paths of selection lead to similar phenotypes and genotypes. The similar outcomes of variations in selection pressure strength can be explained by the concept of evolutionary constrains (Losos, 2011). Due to a limited number of accessible changes to adapt to a certain selection pressure, evolution is biased toward these mutations, resulting in similar changes in organisms exposed to comparable environments (Losos, 2011).

We found that differing selection strength, applied through a daily increase in drug concentration by 25% or a drug gradient, follows similar evolutionary trajectories, resulting in similar phenotypes and genotypes. The cross-resistance and collateral sensitivity patterns appear very similar between both approaches. This is in line with previous findings, where lineages evolved to sub-inhibitory drug concentrations were compared to those adapted under strong selection (Lázár et al., 2014). Yet, also opposing results have been reported, showing differences in mildly and strongly selected lineages (Oz et al., 2014). However, the cross-resistance and collateral sensitivity differences observed by Oz et al. were mildly connected to the final resistance level of the strain to the adapted drug, which could account for these phenotypic differences (Oz et al., 2014). To limit these confounding factors we sought to investigate lineages as they had reached similar resistance levels toward the adapted drug. The phenotypic differences observed by Oz et al. were explained by genotypic variations. A larger number of mutations was reported for the strongly selected lineages including a higher variety of mutations concerning the drug targets. These findings contrast other studies claiming that the stronger the selection pressure, the less evolutionary trajectories are open to meet the adaptation requirements, resulting in fewer but more impactful mutations in strongly evolved lineages (Barrick and Lenski, 2013; Lindsey et al., 2013) and may result from differences in the finally evolved phenotypes of the strains compared to the present study. In our study we find a similar number of mutations in strongly and mildly adapted lineages. However, when filtering our genomic data for recurring mutations, we find a smaller number of

mutations in the gradient evolved lineages compared to the increment adapted lineages, suggesting that fewer resistance conferring mutations are selected for under strong selection. In spite of this small difference, the genetic similarity between replicates within one selection approach is comparable to the similarity between different selection approaches. These findings suggest that ALE experiments conducted with varying protocols are indeed comparable. Accordingly, one doesn't loose genetic or phenotypic information when using a high throughput applicable increment approach compared to gradient systems.

Nonetheless, one important difference with implications for ALE experiments was detected in this study: Lineages adapted with the 25% increment method consistently displayed a higher growth rate compared to the growth rate of isolates from lineages evolved to stronger selection pressure. The growth advantage of strains adapted with the 25% increment method can be explained by the mild selection regime that increases the selection pressure on fitness rather than on highest resistance levels, possibly selecting for mutations that compensate fitness costs or generally increase the fitness. When the sequencing data was filtered to consider only mutations that have been detected in more than two individual lineages, clones adapted in 25% increments carried almost all mutations that were found in the gradient lineages. These mutations are therefore likely to be most important for the resistance phenotype. A number of additional mutations were solely identified in the increment lineages. These mutations may confer resistance at a lower fitness cost or balance out fitness disadvantages of the resistance conferring mutations. Depending on the aim of the ALE experiment, attention should be paid to the impact of the method on the growth rate. Especially, if the ALE experiment is conducted to improve a biotechnological production strain, the growth rate of the evolved strains can be an important factor to select for (O'Brien et al., 2016).

In case of antibiotic resistance, ALE experiments can be useful to explore the evolutionary potential of a species to develop antibiotic resistance. Some of the mutated genes that were identified in this and previous studies, like the *marR*, *rob,* or *acrAB* loci, have been reported to carry mutations also in clinical isolates (Oethinger et al., 1998; Sáenz et al., 2004; Buffet-Bataillon et al., 2012). However, other mutations identified by ALE experiments do not occur in natural environments. Regardless, ALE experiments can provide a better understanding of the genetic and phenotypic flexibility of the organism and its adaptation potential in response to challenging environmental conditions.

We were interested to see if both, the gradient as well as the increment approach, mimic natural occurring resistance evolution similarly. To investigate the generality of the identified SNPs we mined all sequenced *E. coli* genomes for non-conservative SNPs in coding regions. More than 50% of the mutated genes in both the increment 25% and gradient approach and all of the genes that the approaches have in common overlap with the mutated genes in the database (Supplementary Figure 6), indicating that both methodologies simulate natural resistance evolution to a similar extend. Obviously, it remains to be clarified if these SNPs actually confer resistance or other advantages in the host environment. Yet, the occurrence of such mutations in both natural isolates as well as laboratory-evolved populations suggests a biological importance.

Our results demonstrate that key adaptations to AMK, PIP and TET in *E. coli* are independent of the selection regimen and that mutations that robustly occur regardless of the selection regime or ALE methodology are also more likely to be selected for in the clinic than mutations that are selected only under very specific selection conditions.

AUTHOR CONTRIBUTIONS

MS, CM, and LJ planned the project and designed the experiments. LJ conducted the experiments and carried out the data analysis with help from CM. ME contributed by identifying large insertion sequences and by writing the Material and Methods section about his analysis. LJ wrote the manuscript, which was critically reviewed by CM and MS.

FUNDING

This work was supported by the European Union's Horizon 2020 research and innovation program under the Marie Sklodowska-Curie grant agreement No 642738, MetaRNA as well from the European Union's Horizon 2020 (ERC-2014-StG) under grant agreement 638902, LimitMDR. In addition, funding was received from the Danish Free Research Council and from the Novo Nordisk Foundation through the Novo Nordisk Foundation Center for Biosustainability.

ACKNOWLEDGMENTS

We would like to thank A. Porse for helpful discussions and for supplying us with an R script to determine the growth rate accurately.

SUPPLEMENTARY MATERIAL

The Supplementary Material for this article can be found online at: http://journal.frontiersin.org/article/10.3389/fmicb.2017.00816/full#supplementary-material

REFERENCES

Achaz, G., Rodriguez-Verdugo, A., Gaut, B. S., and Tenaillon, O. (2014). The reproducibility of adaptation in the light of experimental evolution with whole genome sequencing. *Adv. Exp. Med. Biol.* 781, 211–231. doi: 10.1007/978-94-007-7347-9_11

Anderson, W., Jansen, M. G., and Wicks, C. A. (1950). Para-aminosalicylic acid with streptomycin in Tuberculosis. *Can. Med. Assoc. J.* 62, 231–235.

Ariza, R. R., Li, Z., Ringstad, N., and Demple, B. (1995). Activation of multiple antibiotic resistance and binding of stress-inducible promoters by *Escherichia coli* Rob protein. *J. Bacteriol.* 177, 1655–1661.

Barrick, J. E., and Lenski, R. E. (2013). Genome dynamics during experimental evolution. *Nat. Rev. Genet.* 14, 827–839. doi: 10.1038/nrg3564

Bell, G., and Collins, S. (2008). Adaptation, extinction and global change. *Evol. Appl.* 1, 3–16. doi: 10.1111/j.1752-4571.2007.00011.x

Bernal, M. M. (2014). *The Cpx Pathway Causes Changes in Peptidoglycan Structure, Turnover, and Recycling*. Master's thesis, University of Alberta.

Blázquez, J., Gómez-Gómez, J. M., Oliver, A., Juan, C., Kapur, V., and Martín, S. (2006). PBP3 inhibition elicits adaptive responses in *Pseudomonas aeruginosa*. *Mol. Microbiol.* 62, 84–99. doi: 10.1111/j.1365-2958.2006.05366.x

Blum, P., Rudrappa, D., Singh, R., McCarthy, S., and Pavlik, B. (2016). "Experimental microbial evolution of extremophiles," in *Biotechnology of Extremophiles: Grand Challenges in Biology and Biotechnology*, *Vol. 1*, ed P. H. Rampelotto (Cham; Heidelberg; New York, NY; London; Dordrecht: Springer International Publishing), 619–636.

Brauner, A., Fridman, O., Gefen, O., and Balaban, N. Q. (2016). Distinguishing between resistance, tolerance and persistence to antibiotic treatment. *Nat. Rev. Microbiol.* 14, 320–330. doi: 10.1038/nrmicro.2016.34

Brook, I. (1989). Inoculum effect. *Rev. Infect. Dis.* 11, 361–368.

Bryson, H. M., and Brogden, R. N. (2012). Piperacillin/tazobactam. *Drugs* 47, 506–535. doi: 10.2165/00003495-199447030-00008

Buffet-Bataillon, S., Le Jeune, A., Le Gall-David, S., Bonnaure-Mallet, M., and Jolivet-Gougeon, A. (2012). Molecular mechanisms of higher mics of antibiotics and quaternary ammonium compounds for *Escherichia coli* isolated from bacteraemia. *J. Antimicrob. Chemother.* 67, 2837–2842. doi: 10.1093/jac/dks321

Busse, H. J., Wöstmann, C., and Bakker, E. P. (1992). The bactericidal action of streptomycin: membrane permeabilization caused by the insertion of mistranslated proteins into the cytoplasmic membrane of *Escherichia coli* and subsequent caging of the antibiotic inside the cells due to degradation of these proteins. *J. Gen. Microbiol.* 138, 551–561. doi: 10.1099/00221287-138-3-551

Carroll, S. P., Søgaard Jørgensen, P., Kinnison, M. T., Bergstrom, C. T., Denison, R. F., Gluckman, P., et al. (2014). Applying evolutionary biology to address global challenges. *Science* 346:1245993. doi: 10.1126/science.1245993

Charlesworth, B. (2009). Effective population size and patterns of molecular evolution and variation. *Nat. Rev. Genet.* 10, 195–205. doi: 10.1038/nrg2526

Cohen, S. P., McMurry, L. M., Hooper, D. C., Wolfson, J. S., and Levy, S. B. (1989). Cross-resistance to fluoroquinolones in multiple-antibiotic-resistant (Mar) *Escherichia coli* selected by tetracycline or chloramphenicol: decreased drug accumulation associated with membrane changes in addition to OmpF reduction. *Antimicrob. Agents Chemother.* 33, 1318–1325. doi: 10.1128/AAC.33.8.1318

de Visser, J. A., and Rozen, D. E. (2006). Clonal interference and the periodic selection of new beneficial mutations in *Escherichia coli*. *Genetics* 172, 2093–2100. doi: 10.1534/genetics.105.052373

Dhawale, A., and Rath, A. (2014). Antibiotic resistance: a threat and challenge to society. *Ann. Appl. Biosci.* 1, R1–R6.

Donald, P. R., and van Helden, P. D. (2009). The global burden of Tuberculosis — combating drug resistance in difficult times. *N. Engl. J. Med.* 360, 2393–2395. doi: 10.1056/NEJMp0903806

Elmqvist, T., Folke, C., Nyström, M., Peterson, G., Bengtsson, J., Walker, B., et al. (2003). Response diversity, ecosystem change, and resilience. *Front. Ecol. Environ.* 1, 488–494. doi: 10.1890/1540-9295(2003)001[0488:RDECAR]2.0.CO;2

Eng, R. H., Cherubin, C., Smith, S. M., and Buccini, F. (1985). Inoculum effect of beta-lactam antibiotics on Enterobacteriaceae. *Antimicrob. Agents Chemother.* 28, 601–606. doi: 10.1128/AAC.28.5.601

Eng, R. H., Smith, S. C., and Cherubin, C. (1984). Inoculum effect of new beta-lactam antibiotics on *Pseudomonas aeruginosa*. *Antimicrob. Agents Chemother.* 26, 42–47. doi: 10.1128/AAC.26.1.42

Escherichia coli Str. K-12 Substr (2014). *Escherichia coli Str. K-12 Substr. MG1655, Complete Genome.*

"EUCAST" (2016). EUCAST. Available online at: http://www.eucast.org/ (Accessed July, 25).

Fine, P. V. A. (2015). Ecological and evolutionary drivers of geographic variation in species diversity. *Annu. Rev. Ecol. Evol. Syst.* 46, 369–392. doi: 10.1146/annurev-ecolsys-112414-054102

Frankham, R. (2005). Genetics and extinction. *Biol. Conserv.* 126, 131–140. doi: 10.1016/j.biocon.2005.05.002

George, A. M., and Levy, S. B. (1983). Gene in the major cotransduction gap of the *Escherichia coli* K-12 linkage map required for the expression of chromosomal resistance to tetracycline and other antibiotics. *J. Bacteriol.* 155, 541–548.

Georghiou, G. P. (2012). *Pest Resistance to Pesticides*. Riverside, CA: Springer Science and Business Media.

Girgis, H. S., Hottes, A. K., and Tavazoie, S. (2009). Genetic architecture of intrinsic antibiotic susceptibility. *PLoS ONE* 4:e5629. doi: 10.1371/journal.pone.0005629

Govan, J. R. W., and Fyfe, J. A. M. (1978). Mucoid *Pseudomonas aeruginosa* and cystic fibrosis: resistance of the mucoid form to carbenicillin, flucloxacillin and tobramycin and the isolation of mucoid variants *in vitro*. *J. Antimicrob. Chemother.* 4, 233–240. doi: 10.1093/jac/4.3.233

Hansen, S., Lewis, K., and Vulić, M. (2008). Role of global regulators and nucleotide metabolism in antibiotic tolerance in *Escherichia coli*. *Antimicrob. Agents Chemother.* 52, 2718–2726. doi: 10.1128/AAC.00144-08

Hegreness, M., Shoresh, N., Damian, D., Hartl, D., and Kishony, R. (2008). Accelerated evolution of resistance in multidrug environments. *Proc. Natl. Acad. Sci. U.S.A.* 105, 13977–13981. doi: 10.1073/pnas.0805965105

Hoffmann, A. A., and Parsons, P. A. (1997). *Extreme Environmental Change and Evolution*. Cambridge, UK: Cambridge University Press.

Hu, B., Yang, Y. M., Beck, D. A. C., Wang, Q. B., Chen, W. J., Yang, J., et al. (2016). Comprehensive molecular characterization of methylobacterium extorquens AM1 adapted for 1-butanol tolerance. *Biotechnol. Biofuels* 9:84. doi: 10.1186/s13068-016-0497-y

Imamovic, L., and Sommer, M. O. A. (2013). Use of collateral sensitivity networks to design drug cycling protocols that avoid resistance development. *Sci. Transl. Med.* 5:204ra132. doi: 10.1126/scitranslmed.3006609

Johanson, U., and Hughes, D. (1994). Fusidic acid-resistant mutants define three regions in elongation factor g of Salmonella Typhimurium. *Gene* 143, 55–59.

Kim, S., Lieberman, T. D., and Kishony, R. (2014). Alternating antibiotic treatments constrain evolutionary paths to multidrug resistance. *Proc. Natl. Acad. Sci.U.S.A.* 111, 14494–14499. doi: 10.1073/pnas.1409800111

Kohanski, M. A., DePristo, M. A., and Collins, J. J. (2010). Sublethal antibiotic treatment leads to multidrug resistance via radical-induced mutagenesis. *Mol. Cell* 37, 311–320. doi: 10.1016/j.molcel.2010.01.003

Kohanski, M. A., Dwyer, D. J., Hayete, B., Lawrence, C. A., and Collins, J. J. (2007). A common mechanism of cellular death induced by bactericidal antibiotics. *Cell* 130, 797–810. doi: 10.1016/j.cell.2007.06.049

Kohanski, M. A., Dwyer, D. J., Wierzbowski, J., Cottarel, G., and Collins, J. J. (2008). Mistranslation of membrane proteins and two-component system activation trigger antibiotic-mediated cell death. *Cell* 135, 679–690. doi: 10.1016/j.cell.2008.09.038

Laviña, M., Pugsley, A. P., and Moreno, F. (1986). Identification, mapping, cloning and characterization of a gene (sbmA) required for microcin B17 action on *Escherichia coli* K12. *J. Gen. Microbiol.* 132, 1685–1693. doi: 10.1099/00221287-132-6-1685

Lázár, V., Pal, G. S., Spohn, R., Nagy, I., Horvath, B., Hrtyán, M., Busa-Fekete, R., et al. (2014). Bacterial evolution of antibiotic hypersensitivity. *Mol. Syst. Biol.* 9, 700–700. doi: 10.1038/msb.2013.57

Lee, D. H., and Palsson, B. Ø. (2010). Adaptive evolution of *Escherichia coli* K-12 MG1655 during growth on a nonnative carbon source, L-1,2-Propanediol. *Appl. Environ. Microbiol.* 76, 4158–4168. doi: 10.1128/AEM.00373-10

Lennen, R. (2016). "Adaptive laboratory evolution of product-tolerant hosts for biobased chemical production," in *2016 SIMB Annual Meeting and Exhibition* (New Orleans, LA).

Levin, B. R., Antonovics, J., and Sharma, H. (1988). Frequency-dependent selection in bacterial populations [and discussion]. *Philos. Trans. R. Soc. B Biol. Sci.* 319, 459–472. doi: 10.1098/rstb.1988.0059

Levin, B. R., Concepción-Acevedo, J., and Udekwu, K. I. (2014). Persistence: a copacetic and parsimonious hypothesis for the existence of non-inherited

resistance to antibiotics. *Curr. Opin. Microbiol. Antimicrob.* 21, 18–21. doi: 10.1016/j.mib.2014.06.016

Levin, B. R., Perrot, V., and Walker, N. (2000). Compensatory mutations, antibiotic resistance and the population genetics of adaptive evolution in bacteria. *Genetics* 154, 985–997.

Li, W., and Godzik, A. (2006). Cd-Hit: a fast program for clustering and comparing large sets of protein or nucleotide sequences. *Bioinformatics* 22, 1658–1659. doi: 10.1093/bioinformatics/btl158

Li, Y., and Zhang, Y. (2007). PhoU is a persistence switch involved in persister formation and tolerance to multiple antibiotics and stresses in *Escherichia coli*. *Antimicrob. Agents Chemother.* 51, 2092–2099. doi: 10.1128/AAC.00052-07

Lieberman, T. D., Michel, J. B., Aingaran, M., Potter-Bynoe, G., Roux, D., Davis, M. R., et al. (2011). Parallel bacterial evolution within multiple patients identifies candidate pathogenicity genes. *Nat. Genet.* 43, 1275–1280. doi: 10.1038/ng.997

Lindsey, H. A., Gallie, J., Taylor, S., and Kerr, B. (2013). Evolutionary rescue from extinction is contingent on a lower rate of environmental change. *Nature* 494, 463–467. doi: 10.1038/nature11879

Linkevicius, M., Sandegren, L., and Andersson, D. I. (2013). Mechanisms and fitness costs of tigecycline resistance in *Escherichia coli*. *J. Antimicrob. Chemother.* 68, 2809–2819. doi: 10.1093/jac/dkt263

Liu, A., Tran, L., Becket, E., Lee, K., Chinn, L., Park, E., et al. (2010). Antibiotic sensitivity profiles determined with an *Escherichia coli* Gene knockout collection: generating an antibiotic bar code. *Antimicrob. Agents Chemother.* 54, 1393–1403. doi: 10.1128/AAC.00906-09

López-Maury, L., Marguerat, S., and Bähler, J. (2008). Tuning gene expression to changing environments: from rapid responses to evolutionary adaptation. *Nat. Rev. Genet.* 9, 583–593. doi: 10.1038/nrg2398

Losos, J. B. (2011). Convergence, adaptation, and constraint. *Evolution* 65, 1827–1840. doi: 10.1111/j.1558-5646.2011.01289.x

Lynch, M., and Lande, R. (1993). Evolution and extinction in response to environmental change. *Biotic Interact. Glob. Change* 234–50.

Macvanin, M., and Hughes, D. (2005). Hyper-susceptibility of a fusidic acid-resistant mutant of Salmonella to different classes of antibiotics. *FEMS Microbiol. Lett.* 247, 215–220. doi: 10.1016/j.femsle.2005.05.007

Maneewannakul, K., and Levy, S. B. (1996). Identification for mar mutants among quinolone-resistant clinical isolates of *Escherichia coli*. *Antimicrob. Agents Chemother.* 40, 1695–1698.

Marcusson, L. L., Frimodt-Møller, N., and Hughes, D. (2009). Interplay in the selection of fluoroquinolone resistance and bacterial fitness. *PLoS Pathog.* 5:e1000541. doi: 10.1371/journal.ppat.1000541

Matic, V., Bozdogan, B., Jacobs, M. R.,Ubukata, K., and Appelbaum, P. C. (2003). Contribution of β-Lactamase and PBP amino acid substitutions to amoxicillin/clavulanate resistance in β-lactamase-positive, amoxicillin/clavulanate-resistant *Haemophilus influenzae*. *J. Antimicrob. Chemother.* 52, 1018–1021. doi: 10.1093/jac/dkg474

Munck, C., Gumpert, H. G., Nilsson Wallin, A. I., Wang, H. H., and Sommer, M. O. A. (2014). Prediction of resistance development against drug combinations by collateral responses to component drugs. *Sci. Transl. Med.* 6:262ra156. doi: 10.1126/scitranslmed.3009940

Nei, M., Maruyama, T., and Chakraborty, R. (1975). The bottleneck effect and genetic variability in populations. *Evolution* 29, 1–10. doi: 10.2307/2407137

O'Brien, E. J., Utrilla, J., and Palsson, B. Ø. (2016). Quantification and classification of *E. coli* proteome utilization and unused protein costs across environments. *PLOS Comput Biol* 12:e1004998. doi: 10.1371/journal.pcbi.1004998

Oethinger, M., Podglajen, I., Kern, W. V., and Levy, S. B. (1998). Overexpression of the marA or soxS regulatory gene in clinical topoisomerase mutants of *Escherichia coli*. *Antimicrob. Agents Chemother.* 42, 2089–2094.

Oz, T., Guvenek, A., Yildiz, S., Karaboga, E., Tamer, Y. T., Mumcuyan, N., et al. (2014). Strength of selection pressure is an important parameter contributing to the complexity of antibiotic resistance evolution. *Mol. Biol. Evol.* 31, 2387–2401. doi: 10.1093/molbev/msu191

Pena-Miller, R., Laehnemann, D., Jansen, G., Fuentes-Hernandez, A., Rosenstiel, P., Schulenburg, H., et al. (2013). When the most potent combination of antibiotics selects for the greatest bacterial load: the smile-frown transition. *PLoS Biol.* 11:e1001540. doi: 10.1371/journal.pbio.1001540

Riganti, C., Mini, E., and Nobili, S. (2015). Editorial: multidrug resistance in cancer: pharmacological strategies from basic research to clinical issues. *Front. Oncol.* 5:105 doi: 10.3389/fonc.2015.00105

Ritz, C., and Streibig, J. C. (2005). Bioassay analysis using RJ Stat. *Software* 12, 1–22.

Ritz, C., Baty, F., Streibig, J. C., and Gerhard, D. (2015). Dose-response analysis using R. *PLoS ONE* 10:e0146021. doi: 10.1371/journal.pone.0146021

Rodriguez de Evgrafov, M., Gumpert, H., Munck, C., Thomsen, T. T., and Sommer, M. O. A. (2015). Collateral resistance and sensitivity modulate evolution of high-level resistance to drug combination treatment in *Staphylococcus aureus*. *Mol. Biol. Evol.* 32, 1175–1185. doi: 10.1093/molbev/msv006

Sáenz, Y., Briñas, L., Domínguez, E., Ruiz, J., Zarazaga, M., Vila, J., et al. (2004). Mechanisms of resistance in multiple-antibiotic-resistant *Escherichia coli* strains of human, animal, and food origins. *Antimicrob. Agents Chemother.* 48, 3996–4001. doi: 10.1128/AAC.48.10.3996-4001.2004

Salomón, R. A., and Farías, N. R. (1995). The peptide antibiotic microcin 25 is imported through the tonb pathway and the SbmA protein. *J. Bacteriol.* 177, 3323–3325.

Sandberg, T. E., Pedersen, M., LaCroix, R. A., Ebrahim, A., Bonde, M., Herrgard, M. J., et al. (2014). Evolution of *Escherichia coli* to 42°C and subsequent genetic engineering reveals adaptive mechanisms and novel mutations. *Mol. Biol. Evol.* 31. 2647–2662. doi: 10.1093/molbev/msu209

Schurek, K. N., Marr, A. K., Taylor, P. K., Wiegand, I., Semenec, L., Khaira, B. K., et al. (2008). Novel genetic determinants of low-level aminoglycoside resistance in *Pseudomonas aeruginosa*. *Antimicrob. Agents Chemother.* 52, 4213–4219. doi: 10.1128/AAC.00507-08

Srinivasan, V. B., Vaidyanathan, V., Mondal, A., and Rajamohan, G. (2012). Role of the two component signal transduction system CpxAR in conferring cefepime and chloramphenicol resistance in *Klebsiella pneumoniae* NTUH-K2044. *PLoS ONE* 7:e33777. doi: 10.1371/journal.pone.0033777

Szybalski, W., and Bryson, V. (1952). Genetic studies on microbial cross resistance to toxic agents i.: cross resistance of *Escherichia coli* to fifteen antibiotics1, 2. *J. Bacteriol.* 64:489.

Tamae, C., Liu, A., Kim, K., Sitz, D., Hong, J., Becket, E., et al. (2008). Determination of antibiotic hypersensitivity among 4,000 single-gene-knockout mutants of *Escherichia coli*. *J. Bacteriol.* 190, 5981–5988. doi: 10.1128/JB.01982-07

Team R Core (2014). *R: A Language and Environment for Statistical Computing*. Vienna: R Foundation for Statistical Computing.

Tenaillon, O., Rodríguez-Verdugo, A., Gaut, R. L., McDonald, P., Bennett, A. F., Long, A. D., et al. (2012). The molecular diversity of adaptive convergence. *Science* 335, 457–461. doi: 10.1126/science.1212986

Toprak, E., Veres, A., Michel, J.-B., Chait, R., Hartl, D. L., and Kishony, R. (2012). Evolutionary paths to antibiotic resistance under dynamically sustained drug selection. *Nat. Genet.* 44, 101–105. doi: 10.1038/ng.1034

Turnidge, J., and Paterson, D. L. (2007). Setting and revising antibacterial susceptibility breakpoints. *Clin. Microbiol. Rev.* 20, 391–408. doi: 10.1128/CMR.00047-06

Wahl, L. M., Gerrish, P. J., and Saika-Voivod, I. (2002). Evaluating the impact of population bottlenecks in experimental evolution. *Genetics* 162, 961–971.

Wang, Z., Wu, J.,Zhu, L., and Zhan, X. (2016). Activation of glycerol metabolism in *Xanthomonas campestris* by adaptive evolution to produce a high-transparency and low-viscosity xanthan gum from glycerol. *Bioresour. Technol.* 211, 390–397. doi: 10.1016/j.biortech.2016.03.096

Wensing, A. M., Calvez, V., Günthard, H. F., Johnson, V. A., Paredes, R., Pillay, D., et al. (2015). 2015 Update of the drug resistance mutations in HIV-1. *Top. Antivir. Med.* 24, 132-133.

Wickham, H. (2009). *ggplot2: Elegant Graphics for Data Analysis*. New York, NY: Springer Science and Business Media.

Wong, K. S., Snider, J. D., Graham, C., Greenblatt, J. F., Emili, A., Babu, M., et al. (2014). The MoxR ATPase RavA and its cofactor viaA interact with the NADH:ubiquinone oxidoreductase I in *Escherichia coli*. *PLoS ONE* 9:e85529. doi: 10.1371/journal.pone.0085529

Yang, L., Jelsbak, L., Lykke Marvig, R., DamkiÃęr, S., Workman, C. T., Holm Rau, M., et al. (2011). Evolutionary dynamics of bacteria in a

human host environment. *Proc. Natl. Acad. Sci.U.S.A.* 108, 7481–7486. doi: 10.1073/pnas.1018249108

Yethon, J. A., and Whitfield, C. (2001). Purification and characterization of WaaP from *Escherichia coli*, a lipopolysaccharide kinase essential for outer membrane stability. *J. Biol. Chem.* 276, 5498–5504. doi: 10.1074/jbc.M008255200

Yethon, J. A., Heinrichs, D. E., Monteiro, M. A., Perry, M. B., and Whitfield, C. (1998). Involvement of waaY, waaQ, andwaaP in the modification of *Escherichia coli* lipopolysaccharide and their role in the formation of a stable outer membrane. *J. Biol. Chem.* 273, 26310–26316. doi: 10.1074/jbc.273.41.26310

Conflict of Interest Statement: The authors declare that the research was conducted in the absence of any commercial or financial relationships that could be construed as a potential conflict of interest.

Supplementary figures

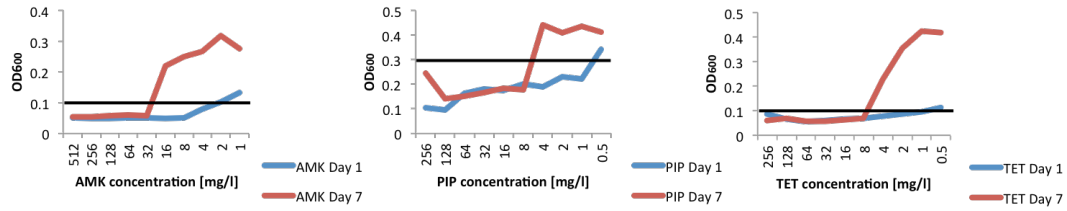

SI Figure 1: Growth in the different drug concentrations of the gradient. For each drug, amikacin (AMK), piperacillin (PIP) and tetracycline (TET) OD_{600} values for each drug concentration in the 10 dilutions of a two-fold gradient are shown in order to illustrate how we chose our cut-off value to define distinct growth. As it can be seen higher OD_{600} values are reached during the course of the experiment but OD_{600} values in the beginning are fairly low. In order to be able to use the same cut off value for one drug for the entire experiment we chose the lowest possible OD_{600} value that shows distinct growth compared to the background we chose $OD_{600} > 0.1$ for AMK and TET and $OD_{600} > 0.3$ for PIP.

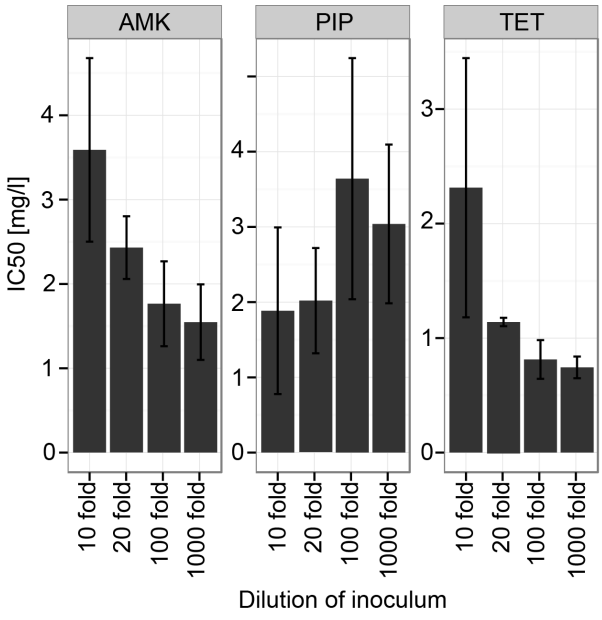

SI Figure 2: Effect of the dilution or inoculum size on the IC_{50}. Freshly growing MG1655 was inoculated into 10 dilutions of a two-fold gradient for three different drugs: amikacin (AMK) with an EUCAST MIC of 2 mg/l, piperacillin (PIP) with an EUCAST MIC of 1-2 mg/l and tetracycline (TET) with an EUCAST MIC of 1 mg/l. From the well with the highest drug concentration that showed growth (as defined in

Materials & Methods) new gradients were inoculated in triplicates with 10, 20, 100 and 1000 fold dilution. The IC_{50} values of these gradients were determined and are presented in this graph. A 10-fold dilution seems to elevate the IC_{50} values for AMK and TET, suggesting inoculum effect. Therefore, a 20-fold dilution was chosen for the adaptive laboratory evolution experiment.

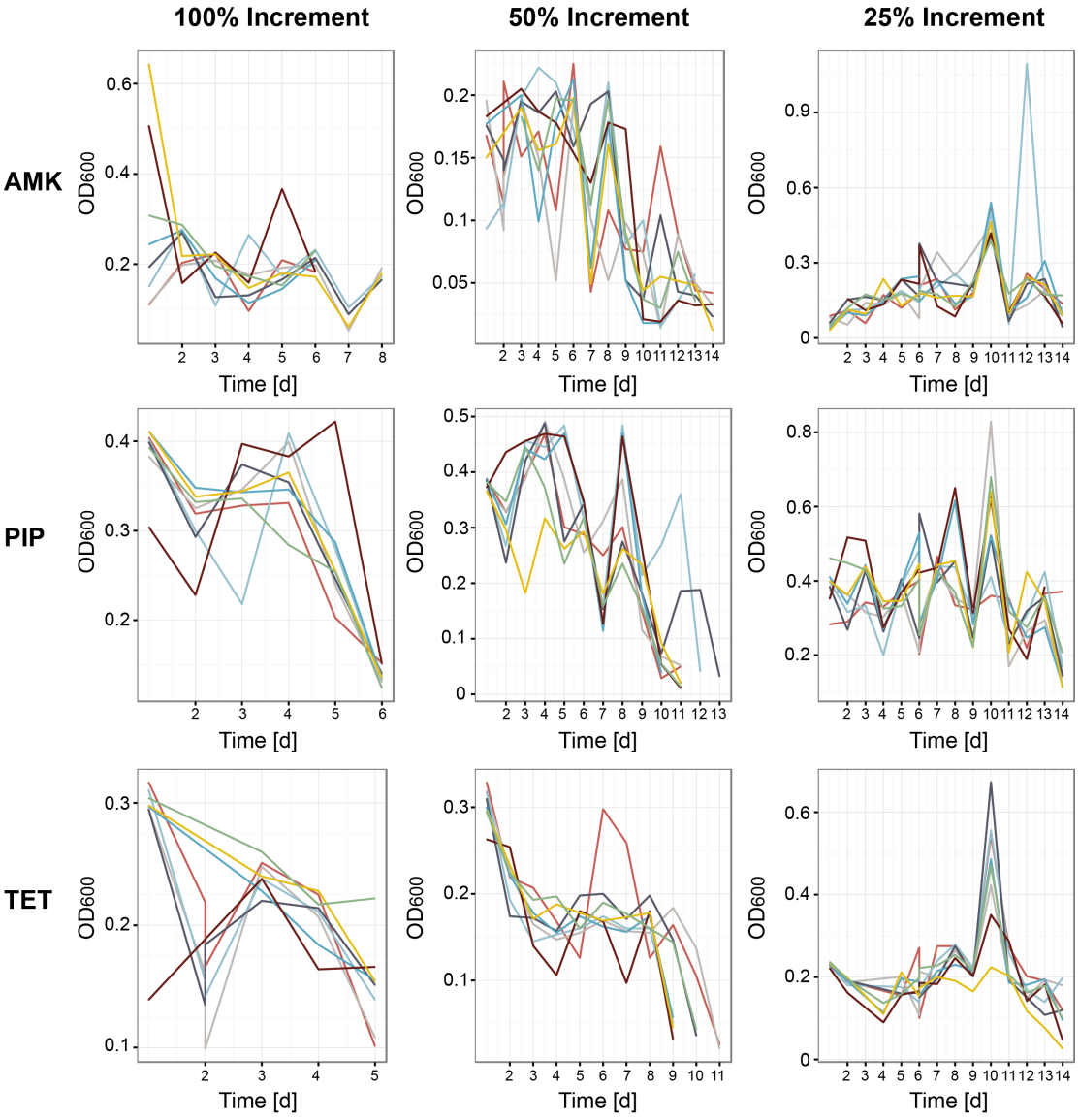

SI Figure 3: OD_{600} of increment lineages before daily transfer. The OD_{600} is displayed for all increment lineages grouped by experimental setup (25, 50 and 100 % increments) and the three drugs they have been adapted to: amikacin (AMK), piperacillin (PIP) and tetracycline (TET). In most cases the OD_{600} declined before extinction of the lineages. The different colors represent the eight different replicates.

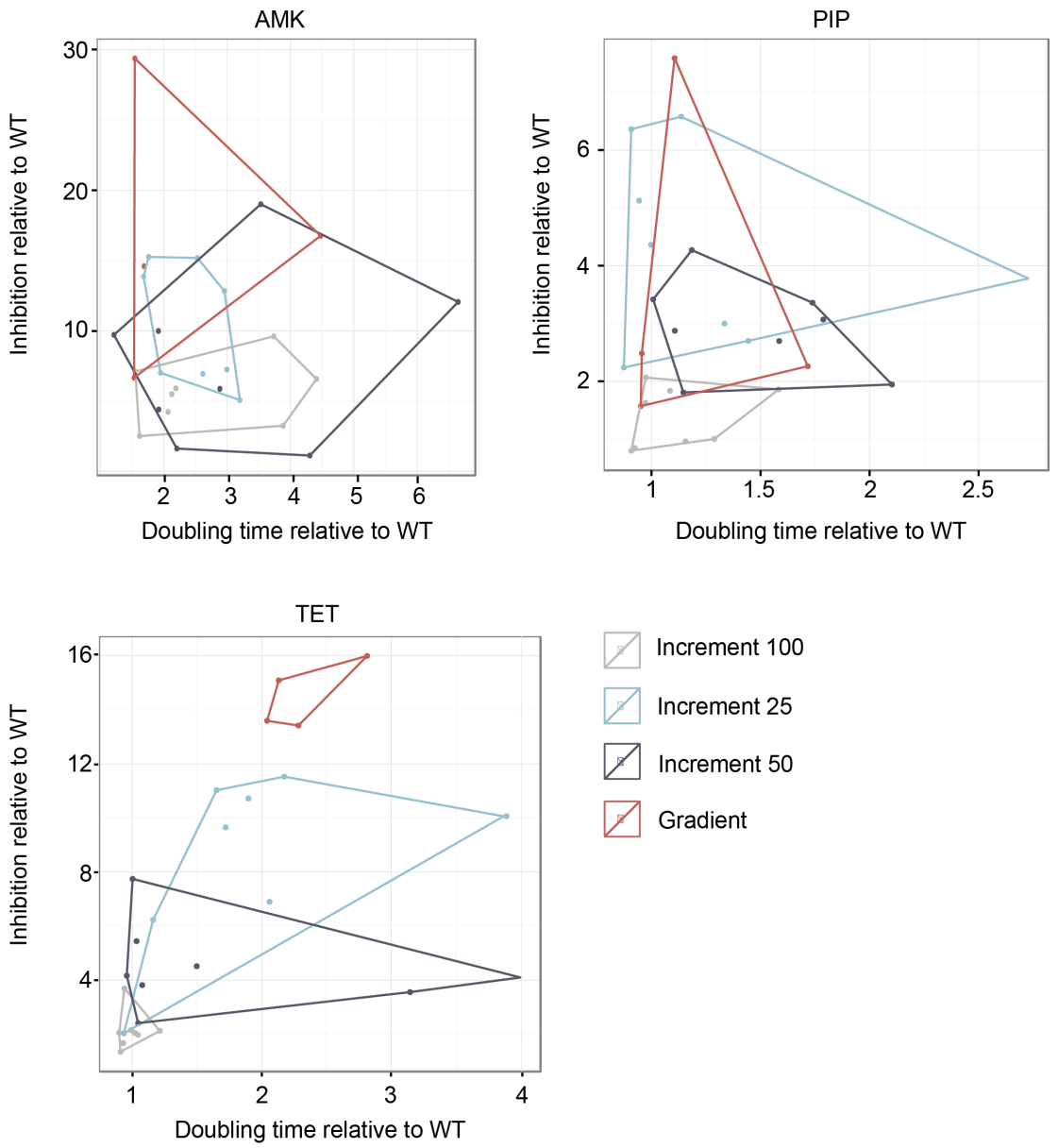

SI Figure 4: IC_{85} relative to the wild type compared to the doubling time relative to the wild type. The three plots are divided by the three drugs amikacin (AMK), piperacillin (PIP) and tetracycline (TET). The different colors represent the different experimental setups. Strains are plotted according to their relative resistance compared to the wild type (WT) and their relative doubling time. The strains marking the outer area of all strains belonging to one experimental setup are connected. No distinct correlation between high resistance with longer doubling time and low resistance with shorter doubling time can be identified.

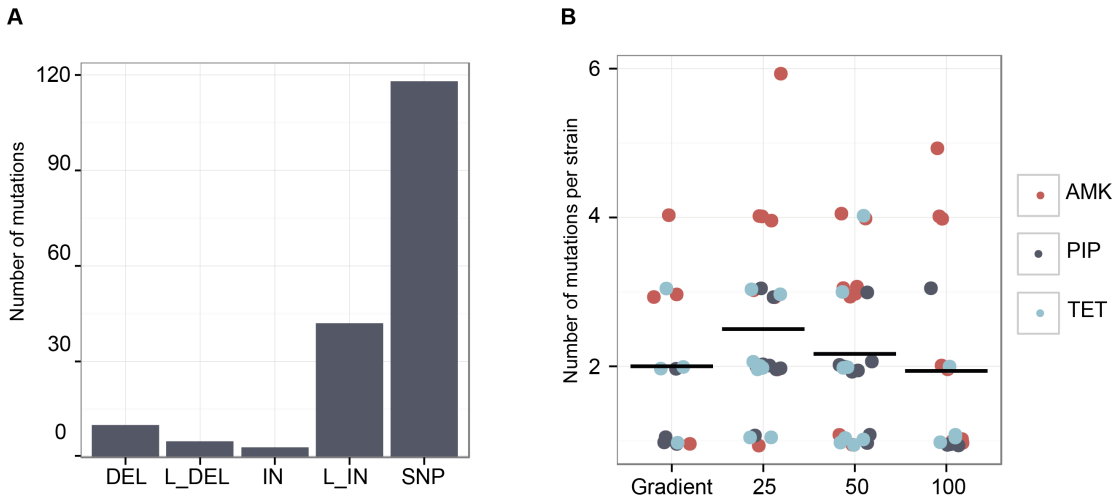

SI Figure 5: Meta-analysis of the sequencing data. (A) Number of different mutation types, discriminating between deletions (DEL), large deletions (L_DEL), insertions (IN), large insertions (L_IN) and single nucleotide polymorphisms (SNP). (B) Number of mutations per strain discriminating the lineages in color by the drugs they have been adapted to (amikacin (AMK), piperacillin (PIP) and tetracycline (TET)). According to a t.test no significant ($P > 0.5$) difference can be detected between the experiments.

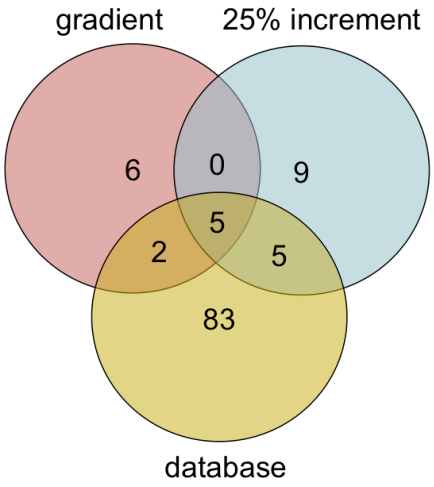

SI Figure 6: Overlap of mutated genes between the gradient evolved lineages, the clones adapted to 25 % increments and a database. In total 13 different genes have been found to be mutated in clones evolved in the gradient system and 19 different genes were mutated in lineages adapted with the 25 % increments. 90 genes were found to be mutated in 5 % of sequenced clinical *E. coli* strains. More than half of the mutations found in the gradient (7) and increment 25 % (10) adapted clones

overlap with the database and all genes (5) that were mutated in both approaches overlap with the database.

Table legends

SI Table 1: Plate design and drug concentrations of the gradient adaptive laboratory evolution experiment.

https://www.dropbox.com/s/mmacwahfojkgwzm/Gradient_concentrations.xlsx?dl=0

SI Table 2: OD600 values at each transfer of the gradient adaptive evolution experiment. This table contains all OD600 values and drug concentrations of the well that was chosen to inoculate a new gradient during the adaptive laboratory evolution experiment.

https://www.dropbox.com/s/esgdsc2mqyl54vu/OD_values_at_each_transfer.xlsx?dl=0

SI Table 3: Drug concnetrations of the increment approaches. This table gives the drug concentrations of each antibiotic for the adaptive laboratory evolution experiment for the three increment approaches.

https://www.dropbox.com/s/xgvp3rpcyxw23kp/Increment_concnetrations.xlsx?dl=0

SI Table 4: Sequencing data analysis. The table contains information about the average coverage, quality (phred score) and mapping properties of the sequencing data for every strain.

https://www.dropbox.com/s/y2ifxkq2zok81ez/Sequencing_analysis.xlsx?dl=0

SI Table 5: List of all mutations identified in the sequenced strains. Information about all mutations identified in the sequenced strains, including position of the mutation, frequency, type of mutation, annotated gene, coverage and a reference explaining the potential role in antibiotic resistance, is listed in the table.

https://www.dropbox.com/s/vxzyioycy9uq48q/Genotypic_changes.xls?dl=0

Chromosomal barcoding for multiplexed phenotyping upon adaptive laboratory evolution

Authors:
Leonie J. Jahn*
Andreas Porse*[1]
Christian Munck*[2]
Daniel Simon*[3]
Svetlana Volkova*
Morten O. A. Sommer*[§]

[§]Corresponding author: msom@bio.dtu.dk

*Author affiliation:
Novo Nordisk Foundation Center for Biosustainability, Technical University of Denmark, Kemitorvet 220, 2800 Kgs. Lyngby, DK

[1]Current affiliation:
SNIPR Biome, Lersø Parkallé 44, 2100 Copenhagen, Denmark

[2]Current affiliation:
Department of Systems Biology, Columbia University, Irving Cancer Research Center 1130 St. Nicholas Avenue, New York, NY 10032, USA

[3]Current affiliation:
Department of Computer Science, New York University Shanghai, 1555 Century Ave, Pudong Xinqu, Shanghai Shi, China, 200122

SCIENTIFIC REPORTS

OPEN

Chromosomal barcoding as a tool for multiplexed phenotypic characterization of laboratory evolved lineages

Received: 11 January 2018
Accepted: 4 April 2018
Published online: 03 May 2018

Leonie Johanna Jahn[1], Andreas Porse[1], Christian Munck[1,2], Daniel Simon[1], Svetlana Volkova[1] & Morten Otto Alexander Sommer[1]

Adaptive laboratory evolution is an important tool to evolve organisms to increased tolerance towards different physical and chemical stress. It is applied to study the evolution of antibiotic resistance as well as genetic mechanisms underlying improvements in production strains. Adaptive evolution experiments can be automated in a high-throughput fashion. However, the characterization of the resulting lineages can become a time consuming task, when the performance of each lineage is evaluated individually. Here, we present a novel method for the markerless insertion of randomized genetic barcodes into the genome of *Escherichia coli* using a novel dual-auxotrophic selection approach. The barcoded *E. coli* library allows multiplexed phenotyping of evolved strains in pooled competition experiments. We use the barcoded library in an adaptive evolution experiment; evolving resistance towards three common antibiotics. Comparing this multiplexed phenotyping with conventional susceptibility testing and growth-rate measurements we can show a significant positive correlation between the two approaches. Use of barcoded bacterial strain libraries for individual adaptive evolution experiments drastically reduces the workload of characterizing the resulting phenotypes and enables prioritization of lineages for in-depth characterization. In addition, barcoded clones open up new ways to profile community dynamics or to track lineages *in vivo* or *situ*.

Lineage tracking is a valuable tool used to answer many fundamental biological questions regarding the evolutionary forces and principles behind adaptation processes[1]. Tracking of lineages resulted in the identification of key parameters for evolutionary dynamics[2], shed light on the deterministic character of evolution[3], deepened our knowledge in dynamic genetic interactions[4] and helped us to characterize genetic functions[5–7] as well as specific mutations in more detail in direct competition experiments[8] or complex environments such as the gut[9–11].

Different methods have been utilized to track the population dynamics of co-existing lineages. The first studies applied light microscopy to track cells[12,13]. Later fluorescent tags were used in microscopy to follow specific phenotypes over time[14,15], during development *in vivo*[16–18], in cancer models[17] or to trace individual lineages of cells in a population[19,20]. Fluorescent tags have also been used for evolution experiments[2] and for allele tracking with qPCR[8]. More recently, genetic approaches have been used for lineage tracking. Whole genome sequencing enabled researchers to follow the evolution of individual MRSA strains in a human host during antibiotic treatment[21], to characterize the colonialization of the infant gut[10,11] or to perform multiplexed phenotyping of different gut microbiome species[22]. In addition, the insertion of genetic elements such as microsatellite regions[23] or genetic barcodes[3] has broadened our understanding of evolutionary dynamics. While whole genome sequencing is needed to track unmodified bacterial strains in *in situ*, tracking genetically barcoded clones by amplicon sequencing provides a cheaper and faster alternative when the strains can be genetically manipulated.

Here, we present a novel method describing the markerless integration of genomic barcodes at a specific location in the genome of *E. coli* without inserting selection markers or altering the genomic sequence except for the additional nucleotides of the barcode. We created a library composed of more than 400 clones carrying unique 12-nucleotide barcodes, that is available upon request, and used a subset of these clones in an adaptive laboratory

[1]Novo Nordisk Foundation Center for Biosustainability, Technical University of Denmark, DK-2800, Kongens Lyngby, Denmark. [2]Present address: Department of Systems Biology, Columbia University, New York, NY, USA. Correspondence and requests for materials should be addressed to M.O.A.S. (email: msom@bio.dtu.dk)

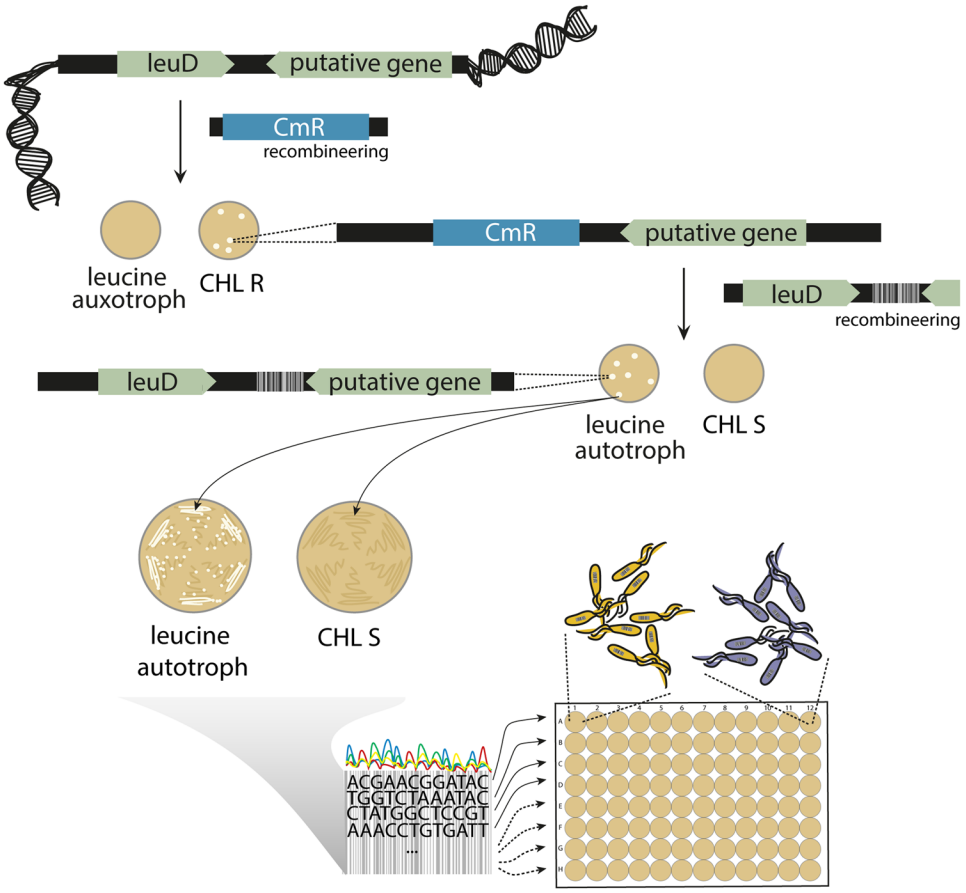

Figure 1. Cloning strategy for creating the barcoded library. *leuD*, part of the leucine operon and essential to produce leucine, was replaced with a chloramphenicol resistance gene through recombeneering[51]. Clones were screened for leucine auxotrophy and chloramphenicol resistance (CHL R). In a next step the replacement was reverted using the native *leuD* gene attached to a random 12-nucleotide long genetic barcode. Clones were selected when they were leucine autotroph and chloramphenicol sensitive (CHL S). Barcode integration was confirmed via Sanger sequencing. A library of 445 uniquely barcoded clones was compiled and cured from the recombeneering plasmid.

evolution (ALE) experiment towards antibiotic resistance. Finally, we showed, as a proof of concept that the multiplexed phenotyping enabled through the barcoding scheme presented here, correlates well with traditional phenotyping methods based on individual clones and allows deeper insights into the population dynamics that would not be detected by traditional growth assays.

Results

Dual-auxotrophic selection allows for markerless insertion of genetic barcodes. To develop a tool for elucidating the dynamics of clonal populations we engineered a library of uniquely barcoded *E. coli* strains. As selection markers, especially those that confer antibiotic resistance, could potentially interfere with our interest of studying *de novo* antibiotic resistance mutations, we developed a protocol that allows the marker-free insertion of genetic barcodes into the genome of *E. coli*. Insertion of the unique barcodes occurred in a two-step process; first *leuD* of the leucine operon was knocked out with a chloramphenicol resistance gene resulting in a leucine auxotroph and chloramphenicol resistant clone. In the second step the *leuD* gene was reintroduced with a fragment containing a random 12-nucleotide barcode removing the chrolamphenicol marker and restoring leucine autotrophy (Fig. 1). The fragment was created with a primer containing an overhang of 12 random nucleotides allowing us to introduce up to 4^{12} unique barcodes in a single step. We then selected clones that were chloramphenicol sensitive and leucine autotroph. A region including the barcode and part of *leuD* was sequenced to confirm the correct insertion of the *leuD* gene and the specific sequence of each barcode. From the sequencing data we compiled a library composed of 445 clones each harboring a unique barcode at the same position in the genome (SI Table 1).

Evolution of antibiotic resistance using uniquely barcoded parallel evolving lineages. ALE experiments are commonly applied to study the evolution of antibiotic resistance[24–29]. To illustrate the potential of a library with unique barcodes that allow the tracking and comparison of evolving populations, a subset of the library was used in an antibiotic ALE experiment.

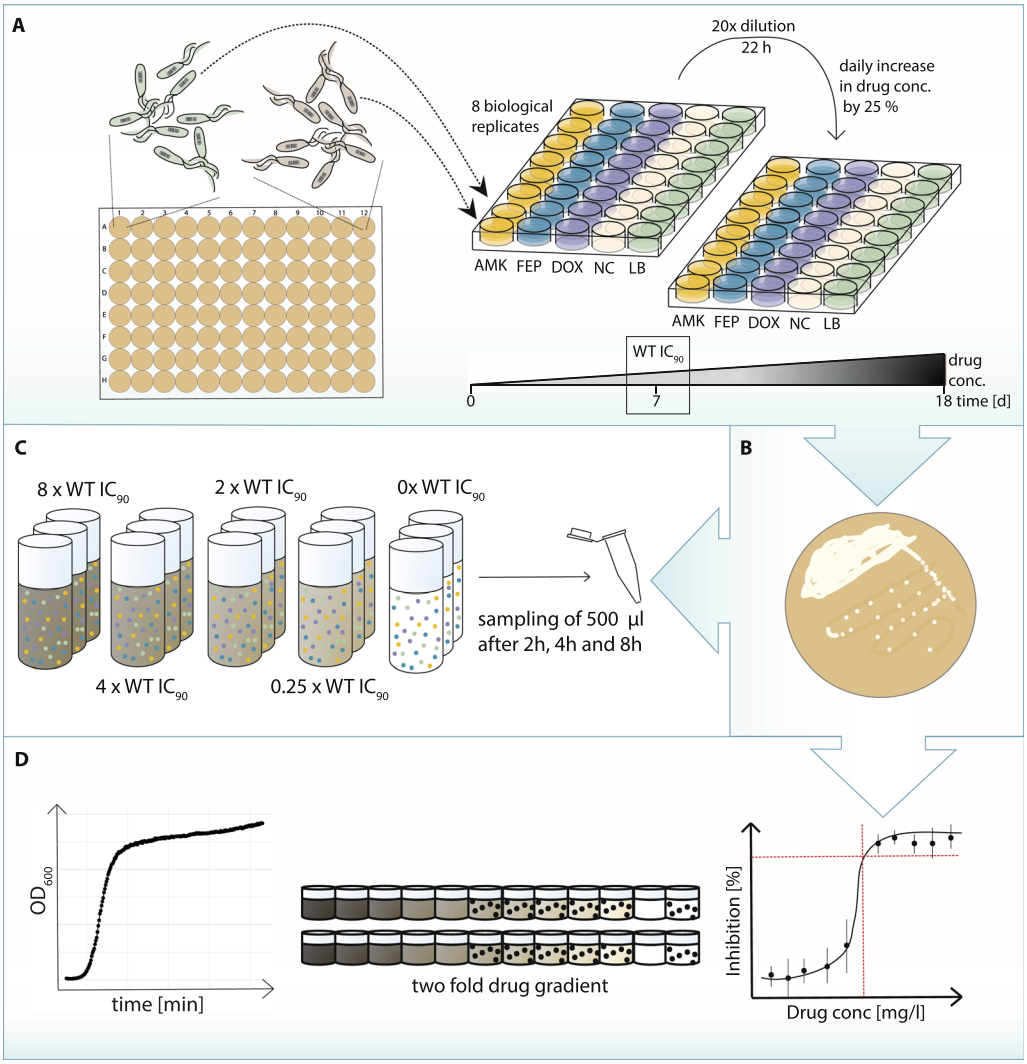

Figure 2. Workflow of the adaptive laboratory evolution (ALE) and subsequent phenotyping. **(A)** ALE towards amikacin (AMK), cefepime (FEP) and doxycycline (DOX) resistance. Uniquely barcoded *Escherichia coli* K12 clones were adapted to AMK, FEP, DOX and the media (LB) for 18 days in 8 replicates. Each replicate carried a unique chromosomal barcode. The populations were transferred every 22 hours with a 20-fold dilution to an increased drug concentration of 25%. The drug concentration at which the OD_{600} of the WT was 10% of the OD_{600} of the positive control before the evolution experiment was started (WT IC_{90}) was reached on the 7th day of the evolution experiment. The drug concentration of the last day of the experiment was more than 10-fold higher than the WT IC_{90}. **(B)** After the completion of the ALE each lineage was streaked on LB and a single colony was chosen for further experiments. **(C)** Competition experiment of evolved barcoded clones in different antibiotic concentrations. Outgrown cultures of all clones were mixed with equal volumes and used to inoculate media with five different drug concentrations for each antibiotic, as well as without antibiotic (in triplicates). Samples were taken after 2, 4 and 8 hours. **(D)** Traditional phenotyping methods such as growth kinetics in different antibiotic concentrations and resistance level determination in a drug gradient were performed for each clone.

We adapted 8 parallel lineages to 3 different antibiotics, the aminoglycoside amikacin (AMK), the tetracycline doxycycline (DOX) and the beta-lactam antibiotic cefepime (FEP) as well as to lysogenic broth (LB) medium as a control (Fig. 2A). The 3 drugs represent 3 major antibiotic drug classes with different mechanisms of action, including both bactericidal as well as bacteriostatic drugs. For the ALE experiment, we inoculated each replicate with a uniquely barcoded clone. Therefore, 32 different genetically barcoded lineages were required and randomly selected from the barcoded library. The ALE was carried out for 18 days and was started at sub-inhibitory antibiotic concentrations. The drug concentrations were increased by 25% at every daily transfer as previously described[29]. The IC_{90} of the wild type (WT) was reached on the 7th day of evolution. The IC_{90} is defined as the drug concentration at which the optical density (OD_{600}) of the tested strain is 10% of the OD_{600} of the WT grown without exposure to the respective drug[8]. On the last day of the evolution experiment, lineages were exposed to drug concentrations exceeding the WT IC_{90} by at least 10-fold. Exact drug concentrations for each day and each drug can be found in SI Table 2. A single colony was isolated at the end of the evolution experiment for each replicate lineage (Fig. 2B).

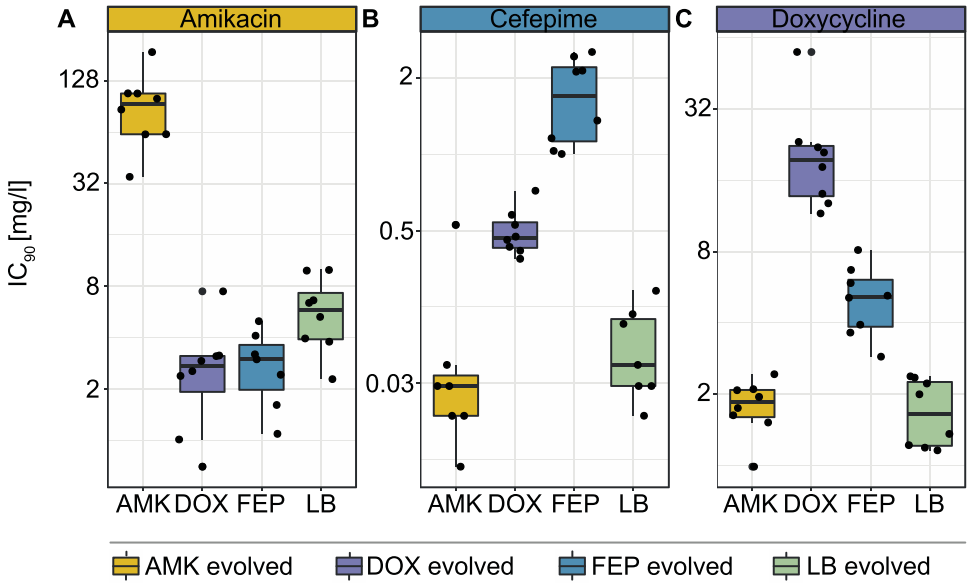

Figure 3. Antibiotic susceptibility of evolved isolates. Inhibitory drug concentrations (IC_{90}) of **(A)** amikacin, **(B)** cefepime and **(C)** doxycycline after the adaptive laboratory evolution (ALE) experiment. The IC_{90} was measured for all 8 biological replicates after the adaptive evolution experiment for all 3 drugs. Clones adapted to amikacin (AMK), cefepime (FEP), doxycycline (DOX) and medium (LB) are displayed in yellow, blue, purple and green, respectively.

Traditional phenotyping methods reveal cross-resistance between DOX and FEP evolved lineages. Traditionally the resistance level of a single clone is determined by measuring the minimal inhibitory concentration in microbroth dilutions. We measured the IC_{90} of all lineages towards the 3 antibiotics using 2-fold microbroth drug dilutions. All lineages evolved high-level resistance to the drug they were exposed to during the evolution experiment (Fig. 3). The IC_{90} values of the media adapted WT were comparable to the IC_{90} values of the ancestor WT, measured before the experiment started, as the average of the media adapted IC_{90} values were less than 2-fold different from the original IC_{90} values (SI Table 3). Yet, a variability among biological replicates was observed that might be accounted by media adaptations potentially altering the susceptibility profiles[30]. The most resistant clones for each drug were ~50 (AMK), ~60 (FEP) and ~30 (DOX) fold more resistant compared to the WT, while the least resistant clones were only 5-fold more resistant than the ancestor (Fig. 3). This highlights that adaptive evolution towards these drugs can follow a wide range of evolutionary trajectories.

Lineages that become resistant to one antibiotic often display either resistance or increased susceptibility to other antibiotics[25,26,31]. These phenotypes are referred to as collateral resistance and sensitivity, respectively. In this study, clones evolved to FEP displayed an elevated resistance towards DOX and *vice versa*. DOX and FEP evolved lineages were on average slightly more susceptible towards AMK than the media adapted WT (Fig. 3). Mutations increasing drug efflux through AcrAB are commonly found in antibiotic resistant bacteria[8,26,32]. While increased efflux confers resistance towards many different antibiotics, it is not effective against aminoglycosides[26]. An interaction between the membrane potential, crucial for the uptake of aminoglycosides, and AcrAB mediated efflux has previously been documented to explain the collateral sensitivity of aminoglycoside resistant strains towards other antibiotics such as DOX and FEB[26]. This well explained mechanism of collateral sensitivity was also observed in this study between cells adapted to AMK tested in FEP. Yet, it does not explain the observed collateral sensitivity between DOX and FEP evolved lineages towards AMK. We speculate that cells adapted to a high AcrAB mediated efflux are also adapted to sustain a high membrane potential to fuel the high efflux rate. This in turn could result in a higher uptake of aminoglycosides, explaining the slightly increased susceptibility of DOX and FEP evolved lineages towards AMK.

Growth-rate measurements are another standard experiment used as a proxy for the fitness in the characterization of mutants resulting from ALE experiments[33–35]. We assessed the growth rate of the evolved clones in a sub-inhibitory concentration as well as in 2, 4 and 8 fold of the WT IC_{90} drug concentrations for all three drugs in 2 technical replicates (Fig. 4A–C). The doubling time was normalized with the doubling time of the ancestor (WT) growing in LB medium without antibiotics (Fig. 4A–C, SI Table 4). The medium adapted lineages had a similar doubling time compared to the ancestral WT (Fig. 4A–C). The drug-evolved clones had slower growth rates compared to the media evolved lineages (SI Tables 4 and 5, Mann-Whitney-U-test, $p < 2.2e^{-16}$). All lineages were capable of growing in the sub-inhibitory drug concentrations of all 3 drugs; indicating the absence of strong evolved collateral sensitivity. As a general trend it can be noticed that the doubling time increases with the antibiotic concentration; also for the clones that were adapted to the respective drug. We observed some exceptional clones (biological replicates 1 and 6 of AMK evolved lineages, biological replicate 2 of FEP evolved lineages and biological replicate 6 of DOX evolved lineages, SI Table 4) with a stable doubling time independent of the drug concentration for all 3 drugs. For AMK and DOX adapted lineages those clones were among the most resistant

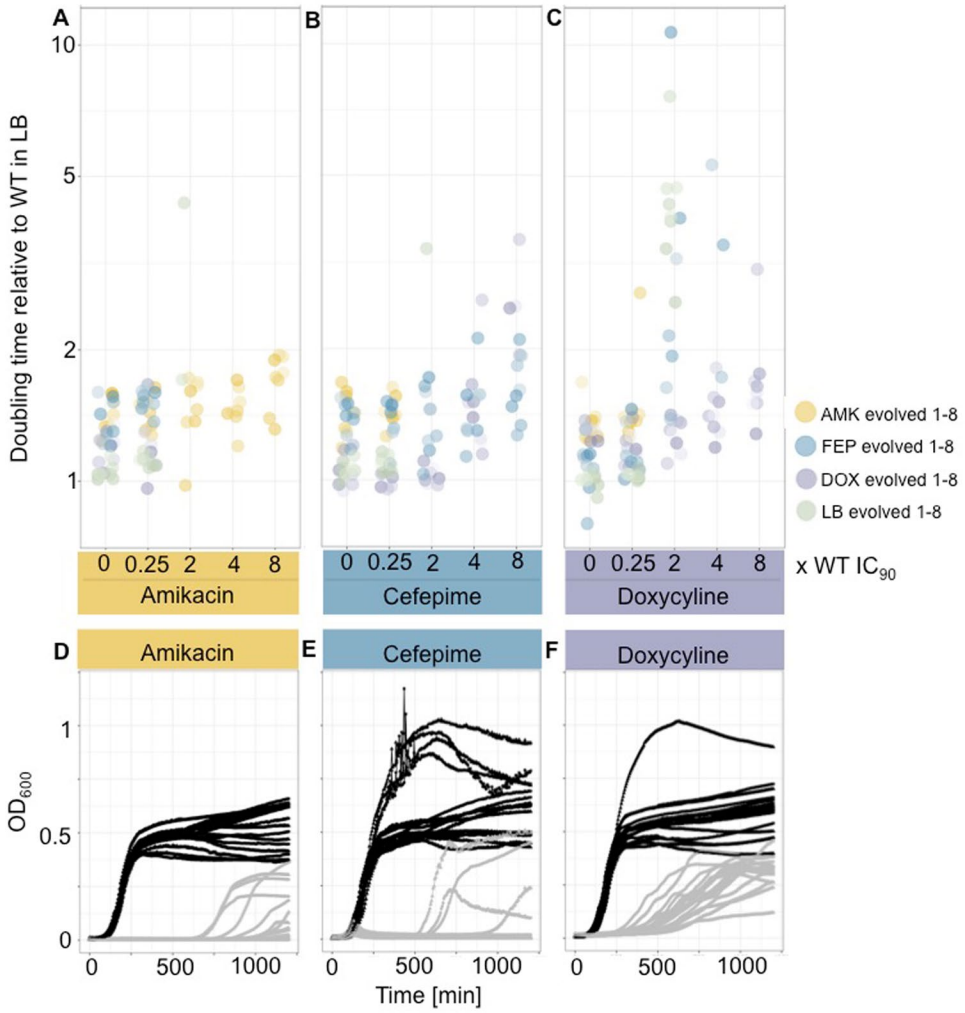

Figure 4. Growth properties of evolved clones. Doubling time of evolved lineages in different concentrations of **(A)** amikacin, **(B)** cefepime and **(C)** doxycycline. The doubling time of the evolved lineages was measured without antibiotic (0 × WT IC_{90}), in sub-inhibitory drug concentrations (0.25 × WT IC_{90}) and in 2, 4 and 8 fold of the WT IC_{90}. The doubling time was normalized to the ancestor WT grown in antibiotic free LB medium. Clones adapted to AMK, FEP, DOX and LB are displayed in yellow, blue, purple and green, respectively. The intensity of the color increases with the resistance level towards the drug they were evolved to. Growth curves of media adapted clones in **(D)** amikacin, **(E)** cefepime and **(F)** doxycycline. The growth curves of all 8 biological and 2 technical replicates of the media adapted clones reveal a huge difference in the growth phenotype in sub-inhibitory drug concentrations (black lines) and 2-fold WT IC_{90} drug concentrations (grey lines).

ones while no correlation between the resistance level and the growth kinetics could be established for FEP evolved clones. In the 2-fold WT IC_{90} drug concentrations some media adapted lineages are unexpectedly able to grow. However, often only one of the technical replicates was able to grow, lag phase was prolonged and the final OD levels were reduced compared to growth in sub-inhibitory concentrations (Fig. 4D–F). These growth patterns could be explained by genotypic differences in the media adapted lineages that could potentially alter their susceptibility patterns[30] or by spontaneous mutations arising during the growth rate measurements. Lineages evolved to DOX and FEP displayed a cross-resistance phenotype as also indicated by the IC_{90} measurements.

Barcoding allows for multiplex phenotyping of evolved strains. By pooling the clones for multiplexed phenotyping based on the barcodes it is possible to reduce the workload needed for the characterization of single clones; especially, when many different conditions are analyzed. We hypothesized that outcomes of the multiplexed analysis would be comparable to our data obtained for each clone tested individually. To test this hypothesis, outgrown overnight cultures of all clones were mixed in equal volumes. A sample of this mixture was frozen as time point 0. Of the remaining mixture, 5 ml of media either without antibiotic, with sub-inhibitory drug concentrations, or 3 different drug concentrations above the WT IC_{90} were inoculated in triplicates for each antibiotic (Fig. 1C). Samples were taken after 2, 4 and 8 hours.

The barcode was amplified and deep sequenced for the whole population subjected to each condition, replicate and time point, and the barcode frequencies were normalized to time point 0. The average of the replicates

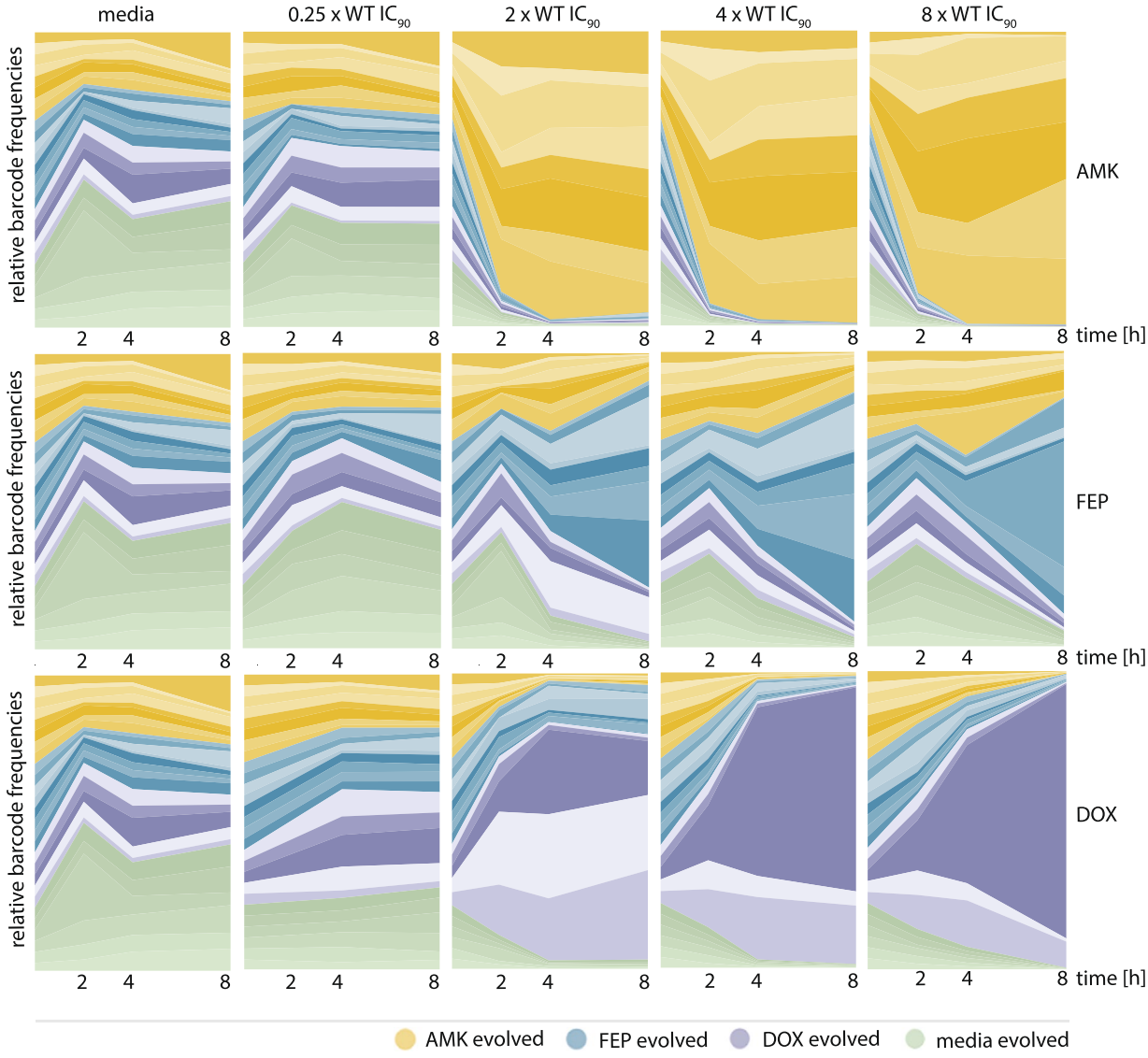

Figure 5. Relative barcode frequencies for each lineage over time in different concentrations of amikacin (AMK), cefepime (FEP) and doxycycline (DOX). Each column represents the different conditions: lineages grown in the media without drug (media), media containing sub-inhibitory drug concentrations (0.25 WT IC90) or three different concentrations above the WT IC_{90} (2×, 4× and 8× WT IC_{90}). The three rows represent the three different drugs. Each plot displays the relative barcode abundance of each lineage over time. Clones adapted to AMK, FEP, DOX and media are displayed in yellow, blue, purple and green, respectively. The intensity of the color increases with the resistance level of each clone towards the drug they were evolved to.

was calculated. In the antibiotic free medium, the LB medium adapted WT appears to be dominating. However, its fitness advantage was not pronounced enough to outcompete the other clones within an 8-hour competition experiment (Fig. 5). The fitness benefit of the WT is only detected in conditions without selection. Under selection clones adapted to the respective drug are clearly favored over time (Fig. 5). The time needed until the drug-adapted lineages dominate the population varies for each drug. In AMK AMK-evolved clones take over the population already within the first 2 hours of growth while 8 hours are not enough for the FEP-adapted clones to fixate despite FEP treatment. The frequencies of the biological replicates adapted to the same drug varied when exposed to different drug concentrations. The most resistant clone for DOX is dominating the population after 8 hours only when the population was exposed to 4 and 8 fold WT IC_{90} drug concentrations but not at 2-fold (Fig. 5). All lineages adapted to AMK and FEP were more resistant than 8 fold of the WT IC_{90} of the respective drug. Drug conditions below the resistance level seem not necessarily to select for the mutant with the highest IC_{90} value and other fitness aspects appear more influential under these conditions.

Interestingly, we observed, in the populations exposed to inhibitory drug concentrations of FEP, that DOX adapted lineages are outcompeted more than AMK adapted lineages. This result stands in contrast to the individual growth kinetics of the clones that did not allow AMK adapted clones to grow under these conditions while DOX adapted lineages were able to grow also in higher FEP concentrations (Figs 4A–C and 5). Consistent with

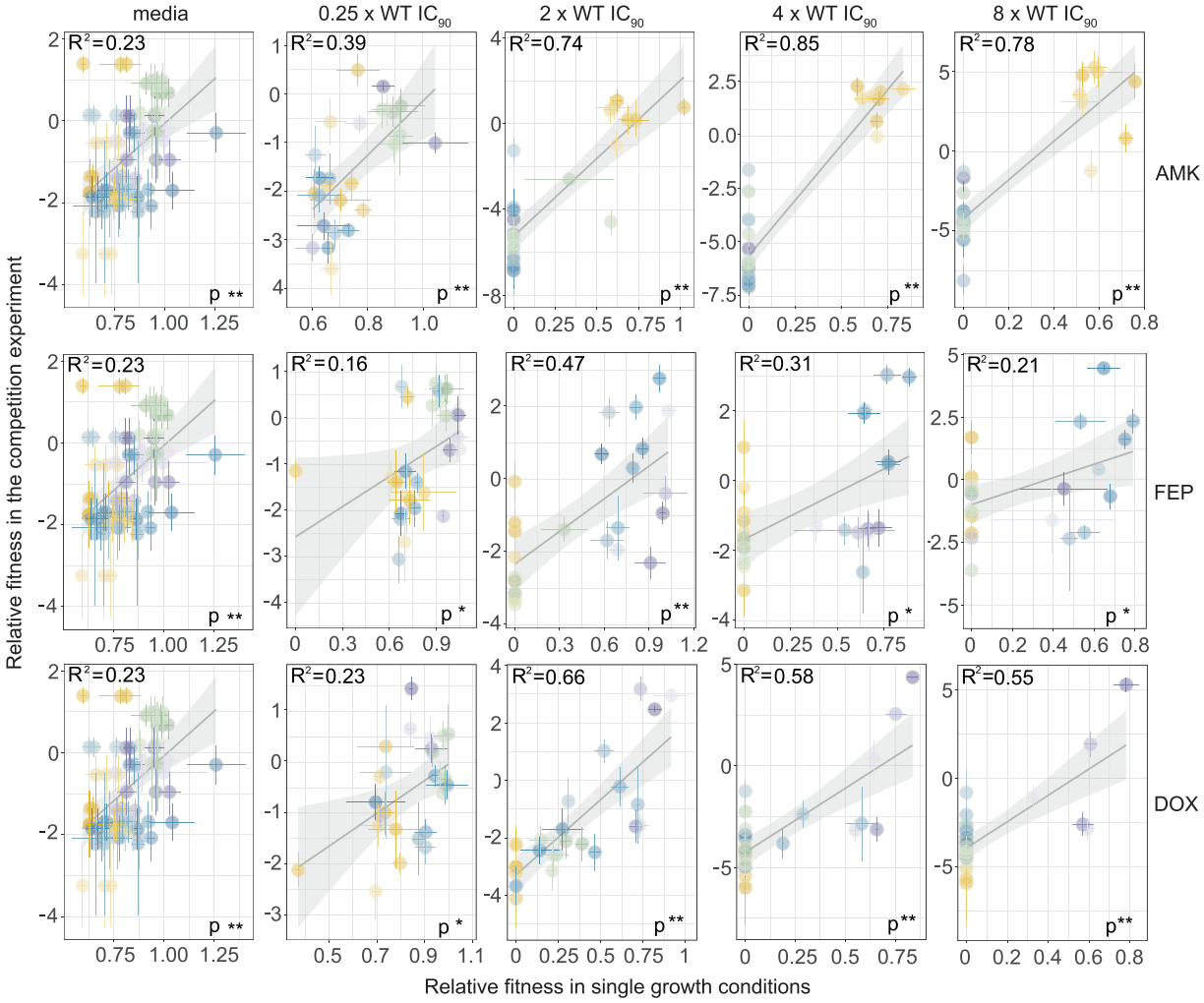

Figure 6. Significant positive correlation of the fitness calculated based on individual and pooled phenotyping. The different columns represent the different conditions: lineages grown in the media, sub-inhibitory drug concentrations or three different concentrations above the WT IC_{90}. The three rows represent the three different drugs. Each plot displays relative fitness calculated from the competition experiment versus the relative fitness derived from individual growth measurments. The coefficient R^2 and the p-value of a Pearson's product-moment correlation are provided for each linear regression model (*$P < 0.05$, **$P < 0.001$). Clones adapted to amikacin (AMK), cefepime (FEP), doxycycline (DOX) and media are displayed in yellow, blue, purple and green, respectively. The intensity of the color increases with the resistance level towards the drug they were evolved to.

the ability of FEP adapted lineages in the single growth kinetic measurements, FEP adapted lineages are also able to grow in low inhibitory concentrations of DOX in the pooled populations (Fig. 5).

In summary the IC_{90} determines largely weather a lineage is able to grow under a specific drug regime. However, other factors influencing the fitness, e.g. the costs of adaptations as well as the interaction with other lineages, decide about the degree of growth under the respective condition.

The results from traditional and multiplexed phenotyping methods are positively correlated. Finally, we tested our hypothesis that pooled and individual clone characterization results in similar outcomes by correlating the fitness of the clones based on the pooled and individual experiments. In the linear regression model we used the fitness derived from the single clone measurements as the predictor and the fitness calculated from the barcode frequencies as a response variable. We find a significant ($P < 0.05$, Pearson's product-moment correlation), positive correlation of the fitness in all conditions after 8 hours of growth (Fig. 6). However, the variability is fairly high and the R^2 varies from 0.16–0.85 dependent on the drug and condition. The variability in the linear regression models for FEP exposed lineages is especially high. As described before we also observed a discrepancy in the phenotypes of the pooled analysis and the single clone measurements for DOX and AMK adapted lineages, which might account for the high variance. The variability would likely decrease by prolonging the competition experiment and therefore allowing the fittest clones more time to outcompete the other lineages.

Due to the high variability in the correlation between growth rates and competition outcomes, a second evaluation of the multiplexed phenotyping was performed. We ranked the fitness of each clone for each drug and

condition from both multiplexed as well as individual phenotyping (SI Table 6). Under conditions with selection (2×, 4× and 8× WT IC_{90}) the best performing clone obtained from the individual growth measurements was among the 5 best performing clones of the competition experiment in the same drug condition. Consequently, picking the best 5 clones for in depth characterization will likely include similar mutants regardless of the fitness assay used.

In conclusion, multiplexed phenotyping of a pooled set of clones correlates with traditional techniques to characterize mutants after ALE experiments and allows identifying the best performing clones under selecting conditions. The barcoded library, created for this study, is consequently a valuable resource for high-throughput ALE experiments as it reduces the workload of subsequent characterization of mutants drastically.

Discussion

Genetically barcoded strains are highly useful to study the population dynamics, also those that result from random processes e.g. population bottlenecks and genetic drift that are not driven by mutant selection, as well as evolutionary processes of heterogenic populations. In addition, barcoded clones can be used to multiplex phenotyping of a larger number of similar strains, e.g. those resulting from ALE experiments. Different strategies for genetic barcoding exist. Yet, to our knowledge all of them depend on the insertion of selection markers or other modifications of the genome[1]. Here, we present a novel approach for inserting genetic barcodes in the genome of *Escherichia coli* without any additional modifications. An unaltered genetic background can be important for example when different antibiotic resistant strains or clones shell be compared in their response to various antibiotics. Moreover, if barcoded clones are used for production strain improvements for example by ALE experiments or transposon mutagenesis and subsequent multiplexed phenotyping, an unaltered genetic background is desired as many production strains already carry genetic alterations and additional selection markers could limit the number of available markers. Additionally, selection markers might burden the cell, which could result in reduced growth rates. Therefore, a strain with as little genetic changes as possible is a desired starting material. To achieve the markerless insertion of genetic barcodes we used *leuD* as selection marker. Even though other selection systems using *sacB*, *galK* or *thyA* are well established they have a narrow compatibility with high escape rates[36], which we did not observe for the native metabolic *leuD* gene. Auxotrophic selection markers can be established in every organism and belong to the standard tools for genome editing in yeast[37,38], highlighting their potential role in genetic engineering of *E. coli* or other microbes.

Multiplexed phenotyping reduces the workload by screening for the fittest mutant under different conditions. While genetic barcodes might not be necessary when genetically distant lineages are used[22], lineages resulting from ALE experiments might differ only in a few nucleotide polymorphisms[29], wherefore genetic barcodes are required to distinguish clones from one another. We could show that multiplexed phenotyping results correlate with traditional phenotyping methods based on individual measurements. Small discrepancies were observed for clones adapted to AMK and DOX exposed to FEP. It should be noted that a shortcoming of the correlation analysis is that the growth rate measurements and pooled competition experiments characterize different aspects of bacterial fitness. While the doubling time is a widely accepted proxy for bacterial fitness[38,39] it is calculated by using only a fraction (steepest part of the growth curve) of the whole growth curve that is taken into account in the competition experiment. Different growth dynamics, especially for strains subjected to antibiotic pressure, including different durations and behaviors of lag, log and stationary phases (Fig. 4 D–F) and interactions with other strains influence the outcome and resolution of competition experiments and might be especially important for physiologically challenged mutants. In fact, we observed altered growth dynamics for some mutants and conditions, especially under exposure to FEP suggesting that growth rate measurements might be a better proxy for fitness under stress free conditions or for mutants that are not physically challenged. Additionally, the presence of other lineages can influence the performance of each clone in a given environment. By pooling all lineages the conditions are less controlled compared to individual growth kinetics, which might be attributed to nutrient availability, the antibiotic exposure and the overall composition of the media changing with metabolites produced from the other cells or through cellular material from lysed cells. Metabolic shifts can result in different tolerance levels for antibiotics[40,41], suggesting that the production of metabolites by a subpopulation might influence the metabolism of susceptible clones increasing or decreasing their tolerance towards a certain antibiotic[41]. For example, it has been found that resistant lineages can produce the compound indole that might increase the tolerance of susceptible clones in the population[42]. Those complex interaction dynamics in bacterial populations are more likely to be detected in pooled phenotyping setups and might more accurately reflect the fitness of bacteria in their natural habitats compared to measurements performed on individual clones.

Multiplexed phenotyping may not completely substitute traditional phenotyping methods. Yet, it can reduce the workload and help to identify promising lineages for in-depth characterization. In addition, it opens ways to study population dynamics, to detect cross-resistance and collateral sensitivity and to identify the fittest mutant in various conditions including challenging environments like urine, wastewater or *in vivo* models. Furthermore, clones adapted to the same condition can be compared in competition experiments, which can help to foster our understanding of the relation between genotype and phenotype.

In conclusion adaptive evolution using barcoded strains harbors a big potential in reducing workload of characterization of evolved strains and opens up the opportunity for a more complex and detailed analysis of the population dynamics of co-existing lineages.

Materials and Methods

Creation of barcoded library. The first step towards the integration of 12-nucleotide long genetic barcodes in *Escherichia coli* was to amplify the chloramphenicol resistance gene from a pZ cloning vector[43] with the following primers: KO_leuD_F: AGGTTAAAGACGTTTGATGACGT-GGACGATAGCGGAAAGCCCG GTCATTTAGTGCTTGGATTCTCACC and KO_leuD_R: TGTG-ACCGGACATTTCGCCGACATTCGCAA

CATTAAATAAGGAGCACACCCTCTGGTAAGGTTGGG, flanking the beginning of the *leuD* gene and the area downstream of the gene. The PCR product was purified with the NucleoSpin Gel and PCR Clean-up kit by Machery-Nagel according to the manufacturers instructions and used for electroporation in MG1655 carrying the pSim6 plasmid[44] allowing the chloramphenicol resistance gene to replace *leuD* through recombeneering. Cells were recovered in lysogeny broth (LB) overnight and plated on LB agar containing chloramphenicol (30 μg/ml) the next day. Colonies were picked and streaked on LB, LB containing ampicillin (100 μg/ml), LB containing chloramphenicol and on Synthetic Complete media (SC) lacking leucine. One clone that grew on all plates except the SC plate lacking leucine, was used to inoculate 5 ml LB containing ampicillin and chloramphenicol. It was used for recombination with another purified PCR product created with primers: Re_tag_leuD_F: GTTATTTCTGTTGTCGCA-TTATTTTTAACCGCAAAGGTTAAAGACGTTTGnnnnnnnnnnnnATGACGT GGACGATAGCGG and Re_leuD_R: TGAACAACGACCGTCTGAATCC using MG1655 WT DNA as a template. The forward primer is carrying the 12-nucleotide long random barcode. After recombination, cells were recovered overnight and plated on LB containing chloramphenicol. More than 1000 colonies were picked and streaked for isolated colonies on LB containing chloramphenicol as well as on SC lacking leucine. Isolated colonies that were sensitive to chloramphenicol and leucine autotrophs were picked and used to inoculate 96-well microtiter plates containing 150 μl of LB. 1 μl of the overnight culture was used for a colony PCR amplifying the barcoded area with the following primers: Re_leuD_F: GGATTTAATGCCTGGAAGAGC and Re_leuD_R. The PCR products were purified using the ZR-96-well DNA Clean-up kit by Zymo Research according to the manufacturers instructions. The purified products were used for Sanger sequencing using the Mix2Seq kit by Eurofins Genomics according the manufacturers instructions including Re_leuD_F as primer and the Sanger sequencing services by BaseClear. Clones that contained the *leuD* gene as well as an unique barcode were transferred to a new 96-well plate containing LB and the position was noted together with the barcode sequence. The clones were frozen in 25% glycerol stocks at −80 °C. Subsequently; these clones were grown at 42 °C to cure them from the pSim6 plasmid[44]. They were streaked on LB agar containing ampicillin and the same toothpick was used to inoculate a well in a 96-well plate. This was repeated until no colonies could be identified on the LB agar containing ampicillin. The final 96-well plate containing the cured clones were replicated into LB containing ampicillin using a 96-well pin-replicator and no growth was detected. The final barcoded library compasses 445 clones each with a unique barcode. A list of all barcodes can be found in SI Table 1. The cured strains were frozen in 25% glycerol stocks at −80 °C.

Adaptive laboratory evolution with barcoded strains. A subset of the barcoded library, 32 clones, were used for an ALE experiment. The clones were exposed to either AMK, FEP, DOX or LB in 8 biological replicates. Another 8 wells contained LB media but were not inoculated to serve as a negative control. All negative control wells stayed uncontaminated throughout the experiment. The antibiotic exposure started at sub-inhibitory drug concentrations and was raised every day by 25%[29] reaching the WT IC_{90} on the 7th day of evolution and ending after 18 days with a >10 fold higher drug concentration than the WT IC_{90}. The exact drug concentrations for each day of the experiment can be found in SI Table 2. The experiment was performed in a volume of 1 ml in 96-deep well plates by Almeco. All plates were prepared with fresh drug stocks prior to the experiment and kept at −20 °C. Every 22 hours, the optical density was measured at a wavelength of 600 nm (OD_{600}) in an ELx808 Absorbance reader (BioTek), 50 μl of the cultures were frozen at −80 C in 25% glycerol and 50 μl were used to inoculate a fresh plate with a higher drug concentration. The new plate was defrosted on the day of usage and preheated to 37 °C. The inoculated plates were incubated at 37 °C and 900 r.p.m. Each lineage was streaked on LB agar after completion of the ALE and an isolated colony was obtained for further experiments.

IC_{90} determination. Each isolated colony was grown in LB overnight and a 96-well pin-replicator (Almeco) was used to inoculate the broth microdilutions in technical replicates. A 2-fold drug gradient was used for each antibiotic. Growth was normalized with the average blank values from the negative controls and the average growth in media without antibiotic as described before[8,29]. Dose response curves were fitted to the data using R[45,46] and the concentration at which the OD_{600} was 10% of the OD_{600} of the positive control, was determined[8,29,47]. All IC_{90} values are presented in SI Table 7 along with MIC values, determined according to standard protocols[48].

Growth rate measurements. 96-well microtiter plates containing 200 μl LB and different antibiotic concentrations (SI Table 8) were inoculated with a 96-well pin-replicator (Almeco) with cells in exponential growth phase. On each plate, 4 wells were reserved to the ancestor WT growing in LB and at least 4 wells served as negative controls. The OD_{600} was measured every 5 min for 20 hours. The plates were kept at 37 °C and 650 r.p.m. The data was analyzed with R[46,49], calculating the doubling time based on the steepest part of the growth curve[29]. The doubling time was normalized to the doubling time of the ancestor WT in LB.

Fitness calculation based on growth kinetics. The fitness was calculated based on the doubling time. The average doubling time of the ancestor WTs growing in LB was divided by the doubling time of each lineage as described before[4]. The average and standard derivation of the replicates was calculated in RStudio (0.99.467).

Competition experiment. For multiplexed phenotyping all clones were grown in LB overnight and mixed in equal volumes. An aliquot of this starting mixture was frozen as time point 0. 50 μl of the mixture were used for inoculation of every triplicate of 4 different (one sub-inhibitory and three inhibitory) drug concentrations for each antibiotic in a total volume of 5 ml. The exact drug concentrations are provided in SI Table 8. The tubes were incubated at 37 °C and 1200 r.p.m. After 2, 4 and 8 hours 500 μl of the cultures were sampled and frozen at −20 °C. Depended on the drug condition and time point varying amounts of the samples (0.5–250 μl) were used for further analysis. 0.5 μl of the samples taken from 0 and 8 hours were mixed with 12.5 μl water. For the other time points varying amounts were spun down so that a tiny pellet was visible in the tube.

The pellet was resuspended in 13 µl of autoclaved miliQ water. All samples were incubated at 99 °C for 7 minutes. A 15-cycle PCR was performed directly on the cells using the following primers 40-fold diluted: Fwd_Primer: TCGTCGGCAGCGTCAGAGTGTATAAGAGACACAATGACCGGGCTTT-CCGC and Rev_Primer: GTCTCGTGGGCTCGGAGATGTGTATAAGAGACAGGGATGCTATGG-TTTCAGG with homology to the NEBNext Multiplex Oligos for Illumina (Index primer sets A and C) (New England BioLabs). The PCR product was directly used for indexing PCR with 20 cycles using the NEBNext Multiplex Oligos for Illumina (Index primer sets A and C) (New England BioLabs) according to the manufacturers instructions. The PCR products were purified using the ZR-96-well DNA Clean-up kit by Zymo Research according to the manufacturers instructions. The DNA quantity was measured with the Qubit dsDNA HS Assay kit (Thermo Fisher Scientific) and samples were pooled in equal amounts of DNA for sequencing on an Illumina MiSeq with 150 bp paired ends.

Determination of the barcode frequencies. The frequencies of the different barcode in each condition were determined in CLC Genomics workbench (Qiagen) and blasting them against a database composed of the barcode sequences (SI Table 9). A p-value of 0.0001 was used as a cut off for the homology to ensure only perfect matches. A table with the number of hits for each barcode was obtained for each condition and time point. The table was extracted and R was used for further analysis. The counts were normalized to time point 0 and the relative abundance of each barcode was calculated for each condition. Few barcodes from the media adapted lineages and well as DOX adapted lineages could not be detected and were therefore excluded from the analysis. The relative barcode frequencies were plotted over time for each condition using R.

Fitness calculation based on barcode frequencies. The fitness of the strains was calculated based on the barcode frequencies from the competition experiment and the calculations were performed according to an adjusted procedure by Wetmore *et al.*[6]. The binary logarithm of the number of reads of a specific barcode at time point 0 was subtracted from the number of reads of the same barcode after 8 hours of growth in a specific condition. The average and standard derivation of the triplicates was calculated.

Statistical tests. The fitness calculated based on the individual growth measurements was used as a predictor variable and the fitness based on the competition experiment served as the response variable for a linear regression model built with ggplot2 in R. The Pearson's correlation coefficient of determination R^2 and the p-value were calculated and added to the plots using two functions (stat_poly_eq() and stat_fit_glance()) from the ggpmisc package[50]. Actual p-values can be found in SI Table 10. Following significance levels were used for the p-value in Fig. 5: *for $p < 0.05$, **for $p < 0.001$. Moreover, the p-values were validated with an additional spearman's correlation (using R statsv3.4.4[49]) that is more robust to non-parametric data and can be found in SI Table 10.

Data availability. The datasets generated during and analyzed during the current study are available from the corresponding author on reasonable request. Barcoded *E. coli* strains can be requested from the corresponding author.

References

1. Blundell, J. R. & Levy, S. F. Beyond genome sequencing: lineage tracking with barcodes to study the dynamics of evolution, infection, and cancer. *Genomics* **104**, 417–430 (2014).
2. Hegreness, M., Shoresh, N., Hartl, D. & Kishony, R. An Equivalence Principle for the Incorporation of Favorable Mutations in Asexual Populations. *Science* **311**, 1615–1617 (2006).
3. Levy, S. F. *et al.* Quantitative evolutionary dynamics using high-resolution lineage tracking. *Nature* **519**, 181–186 (2015).
4. Jaffe, M., Sherlock, G. & Levy, S. F. iSeq: A New Double-Barcode Method for Detecting Dynamic Genetic Interactions inYeast. *G3 Genes Genomes Genet.* **7**, 143–153 (2017).
5. Giaever, G. *et al.* Functional profiling of the Saccharomyces cerevisiae genome. *Nature* **418**, 387–391 (2002).
6. Wetmore, K. M. *et al.* Rapid Quantification of Mutant Fitness in Diverse Bacteria by Sequencing Randomly Bar-Coded Transposons. *mBio* **6**, e00306–15 (2015).
7. Cardinale, S., Tueros, F. G. & Sommer, M. O. A. Genetic-Metabolic Coupling for Targeted Metabolic Engineering. *Cell Rep.* **20**, 1029–1037 (2017).
8. Munck, C., Gumpert, H. K., Wallin, A. I. N., Wang, H. H. & Sommer, M. O. A. Prediction of resistance development against drug combinations by collateral responses to component drugs. *Sci. Transl. Med.* **6**, 262ra156–262ra156 (2014).
9. Barroso-Batista, J. *et al.* The First Steps of Adaptation of Escherichia coli to the Gut Are Dominated by Soft Sweeps. *PLOS Genet.* **10**, e1004182 (2014).
10. Gumpert, H. *et al.* Transfer and Persistence of a Multi-Drug Resistance Plasmid *in situ* of the Infant Gut Microbiota in the Absence of Antibiotic Treatment. *Front. Microbiol.* **8** (2017).
11. Porse, A. *et al.* Genome Dynamics of Escherichia coli during Antibiotic Treatment: Transfer, Loss, and Persistence of Genetic Elements *In situ* of the InfantGut. *Front. Cell. Infect. Microbiol.* **7** (2017).
12. Deppe, U. *et al.* Cell lineages of the embryo of the nematode Caenorhabditis elegans. *Proc. Natl. Acad. Sci.* **75**, 376–380 (1978).
13. Sulston, J. E., Schierenberg, E., White, J. G. & Thomson, J. N. The embryonic cell lineage of the nematode Caenorhabditis elegans. *Dev. Biol.* **100**, 64–119 (1983).
14. Kretzschmar, K. & Watt, F. M. Lineage Tracing. *Cell* **148**, 33–45 (2012).
15. Obersriebnig, M. J., Pallesen, E. M. H., Sneppen, K., Trusina, A. & Thon, G. Nucleation and spreading of a heterochromatic domain in fission yeast. *Nat. Commun.* **7**, 11518 (2016).
16. Buckingham, M. E. & Meilhac, S. M. Tracing Cells for Tracking Cell Lineage and Clonal Behavior. *Dev. Cell* **21**, 394–409 (2011).
17. Ellenbroek, S. I. J. & van Rheenen, J. Imaging hallmarks of cancer in living mice. *Nat. Rev. Cancer* **14**, 406–418 (2014).
18. Progatzky, F., Dallman, M. J. & Lo Celso, C. From seeing to believing: labelling strategies for *in vivo* cell-tracking experiments. *Interface Focus* **3** (2013).
19. Stannek, L., Egelkamp, R., Gunka, K. & Commichau, F. M. Monitoring Intraspecies Competition in a Bacterial Cell Population by Cocultivation of Fluorescently Labelled Strains. *J. Vis. Exp. JoVE*, https://doi.org/10.3791/51196 (2014).

20. Hölscher, T. *et al*. Monitoring Spatial Segregation in Surface Colonizing Microbial Populations., Monitoring Spatial Segregation in Surface Colonizing Microbial Populations. *J. Vis. Exp. JoVE*, https://doi.org/10.3791/54752 (2016).
21. Mwangi, M. M. *et al*. Tracking the *in vivo* evolution of multidrug resistance in Staphylococcus aureus by whole-genome sequencing. *Proc. Natl. Acad. Sci.* **104**, 9451–9456 (2007).
22. Rettedal, E. A., Gumpert, H. & Sommer, M. O. A. Cultivation-based multiplex phenotyping of human gut microbiota allows targeted recovery of previously uncultured bacteria. *Nat. Commun.* **5**, 4714 (2014).
23. Imhof, M. & Schlötterer, C. Fitness effects of advantageous mutations in evolving Escherichia coli populations. *Proc. Natl. Acad. Sci.* **98**, 1113–1117 (2001).
24. Toprak, E. *et al*. Evolutionary paths to antibiotic resistance under dynamically sustained drug selection. *Nat. Genet.* **44**, 101–105 (2011).
25. Imamovic, L. & Sommer, M. O. A. Use of Collateral Sensitivity Networks to Design Drug Cycling Protocols That Avoid ResistanceDevelopment. *Sci. Transl. Med.* **5**, 204ra132–204ra132 (2013).
26. Lazar, V. *et al*. Bacterial evolution of antibiotic hypersensitivity. *Mol. Syst. Biol.* **9**, 700–700 (2014).
27. Oz, T. *et al*. Strength of Selection Pressure Is an Important Parameter Contributing to the Complexity of Antibiotic Resistance Evolution. *Mol. Biol. Evol.* **31**, 2387–2401 (2014).
28. de Evgrafov, M. R., Gumpert, H., Munck, C., Thomsen, T. T. & Sommer, M. O. Collateral resistance and sensitivity modulate evolution of high-level resistance to drug combination treatment in Staphylococcus aureus. *Mol. Biol. Evol.* msv006 (2015).
29. Jahn, L. J., Munck, C., Ellabaan, M. M. H. & Sommer, M. O. A. Adaptive Laboratory Evolution of Antibiotic Resistance Using Different Selection Regimes Lead to Similar Phenotypes and Genotypes. *Front. Microbiol.* **8** (2017).
30. Knöppel, A., Näsvall, J. & Andersson, D. I. Evolution of Antibiotic Resistance without Antibiotic Exposure. *Antimicrob. Agents Chemother.* **61**, e01495–17 (2017).
31. Szybalski, W. & Bryson, V. Genetic Studies on Microbial Cross Resistance to Toxic Agents I. *J. Bacteriol.* **64**, 489–499 (1952).
32. Pál, C., Papp, B. & Lázár, V. Collateral sensitivity of antibiotic-resistant microbes. *Trends Microbiol.* **23**, 401–407 (2015).
33. Knopp, M. & Andersson, D. I. Amelioration of the Fitness Costs of Antibiotic Resistance Due To Reduced Outer Membrane Permeability by Upregulation of Alternative Porins. *Mol. Biol. Evol.* **32**, 3252–3263 (2015).
34. Porse, A., Schønning, K., Munck, C. & Sommer, M. O. A. Survival and Evolution of a Large Multidrug Resistance Plasmid in New Clinical Bacterial Hosts. *Mol. Biol. Evol.* **33**, 2860–2873 (2016).
35. Barbosa, C. *et al*. Alternative Evolutionary Paths to Bacterial Antibiotic Resistance Cause Distinct Collateral Effects. *Mol. Biol. Evol*., https://doi.org/10.1093/molbev/msx158.
36. Gregg, C. J. *et al*. Rational optimization of tolC as a powerful dual selectable marker for genome engineering. *Nucleic Acids Res.* **42**, 4779–4790 (2014).
37. Pronk, J. T. Auxotrophic Yeast Strains in Fundamental and Applied Research. *Appl. Environ. Microbiol.* **68**, 2095–2100 (2002).
38. Jahn, L. J. *et al*. Dependency of Heterochromatin Domains on Replication Factors. *G3 Genes Genomes Genet*., https://doi.org/10.1534/g3.117.300341 (2017).
39. Kawecki, T. J. & Ebert, D. Conceptual issues in local adaptation. *Ecol. Lett.* **7**, 1225–1241 (2004).
40. Hansen, S., Lewis, K. & Vulić, M. Role of global regulators and nucleotide metabolism in antibiotic tolerance in Escherichia coli. *Antimicrob. Agents Chemother.* **52**, 2718–2726 (2008).
41. Meylan, S. *et al*. Carbon Sources Tune Antibiotic Susceptibility in Pseudomonas aeruginosa via Tricarboxylic Acid Cycle Control. *Cell Chem. Biol.* **24**, 195–206 (2017).
42. Lee, H. H., Molla, M. N., Cantor, C. R. & Collins, J. J. Bacterial charity work leads to population-wide resistance. *Nature* **467**, 82–85 (2010).
43. Lutz, R. & Bujard, H. Independent and tight regulation of transcriptional units in Escherichia coli via the LacR/O, the TetR/O and AraC/I1-I2 regulatory elements. *Nucleic Acids Res.* **25**, 1203–1210 (1997).
44. Datta, S., Costantino, N. & Court, D. L. A set of recombineering plasmids for gram-negative bacteria. *Gene* **379**, 109–115 (2006).
45. Ritz, C. & Streibig, J. C. Bioassay analysis using RJ Stat. *Software* **12**, 1–22 (2005).
46. Wickham, H. *ggplot2: elegant graphics for data analysis*. (Springer Science & Business Media, 2009).
47. Ritz, C., Baty, F., Streibig, J. C. & Gerhard, D. Dose-Response Analysis Using R. *PLOS ONE* **10**, e0146021 (2015).
48. Andrews, J. M. Determination of minimum inhibitory concentrations. *J. Antimicrob. Chemother.* **48**(Suppl 1), 5–16 (2001).
49. Team, R. C. R*: A language and environment for statistical computing. R Foundation for Statistical Computing, Vienna, Austria, 2012*. (ISBN 3-900051-07-0, 2014).
50. Learn R …as you learnt your… by Pedro J. Aphalo [PDF/iPad/Kindle]. Available at: https://leanpub.com/learnr. (Accessed: 26th February 2018)
51. Thomason, L. C., Sawitzke, J. A., Li, X., Costantino, N. & Court, D. L. Recombineering: genetic engineering in bacteria using homologous recombination. *Curr. Protoc. Mol. Biol.* **106**, 1.16.1–39 (2014).

Acknowledgements

This work received funding by the European Union's Horizon 2020 research and innovation program under the Marie Sklodowska-Curie grant agreement No 642738, MetaRNA and from the European Union's Horizon 2020 (ERC-2014-StG) under grant agreement 638902, LimitMDR. Moreover, this project was supported from the Danish Free Research Council and from the Novo Nordisk Foundation through the Novo Nordisk Foundation Center for Biosustainability. S.V. received funding from the NNF PhD fellowship grant no. NNF17CC0026768.

Author Contributions

L.J.J., C.M. and M.O.A.S. designed and planned the project. L.J.J. conducted all experimental work with support from A.P. and D.S., L.J.J. analyzed and visualized the data. S.V. calculated the fitness based on the barcode frequencies. L.J.J. wrote the manuscript with critical input from all authors. M.O.A.S. set the direction of the project.

Additional Information

Supplementary information accompanies this paper at https://doi.org/10.1038/s41598-018-25201-5.

Competing Interests: The authors declare no competing interests.

Publisher's note: Springer Nature remains neutral with regard to jurisdictional claims in published maps and institutional affiliations.

Supplemental information

All supplemental tables can be found here: https://www.nature.com/articles/s41598-018-25201-5

Chapter III – Understanding and exploiting genetic responses to antibiotics

Genetic constrains and their exploitation in treatment regimes

The central idea of the work conducted for this thesis was to generate better insights into the genetic evolutionary responses of bacteria to antibiotic treatment and ultimately to answer the question: whether we are able to direct or exploit these responses in any way ideally to limit resistance evolution. Different mechanisms have been proposed that impact and might impair the evolution of resistance such as collateral sensitivity, negative epistasis or cellular hysteresis and accordingly different treatment options such as drug cycling or combination therapy have been explored for their ability to reduce resistance evolution. These different principles and ideas are introduced below followed by experimental work conducted for this thesis.

Collateral sensitivity and collateral resistance

Collateral drug responses are a central biological concept for the research conducted for this thesis (Figure 10). Already in the 1950s and 1960s it was observed that bacteria, resistant to a specific antibiotic, often showed either an increased resistance or increased susceptibility to other antibiotics[195,196]. This phenomenon was further explored in recent years and termed collateral resistance or cross-resistance and collateral sensitivity or hypersensitivity, respectively[164,165]. In *E. coli* and *P. aeruginosa* collateral resistance is often observed for substrates of multi-drug efflux pumps[146,164]. Mutations might be selected that cause an upregulated drug efflux in response to antibiotic induced stress. The increased efflux will provide resistance not only to the drug the bacteria was exposed to but to all substrates of the efflux pump (Figure 10A-B). In general, collateral resistance is about as common as neutral interactions between resistant lineages and other antibiotics (**manuscript 3**). Collateral resistance basically means multi-drug resistance and is therefore quite problematic.

However, besides collateral resistance, also collateral sensitivity occurs. While it is fairly rare compared to collateral resistance and neutral interactions (**manuscript 3**) it is an promising concept that might potentially be exploited for the development of resistance evolution limiting treatment protocols[164]. In *E. coli* collateral sensitivity it was mainly described for lineages adapted to aminoglycoside antibiotics tested against substrates of the AcrB efflux pump such as tetracyclines, flourquinolones, certain beta-lactam antibiotics and macrolides and for lineages adapted to these drugs and tested against peptide antibiotics[165,197]. As the membrane potential and respiration activity are often reduced in aminoglycoside-adapted lineages to limit the uptake of the antibiotic, it was hypothesized that the reduction in

membrane potential reduces the efflux mediated through AcrB, which is proton and energy dependent. The reduced efflux lowers the internal resistance to drugs that are substrates of the broad-range efflux pump ArcB[165] (Figure 10C).

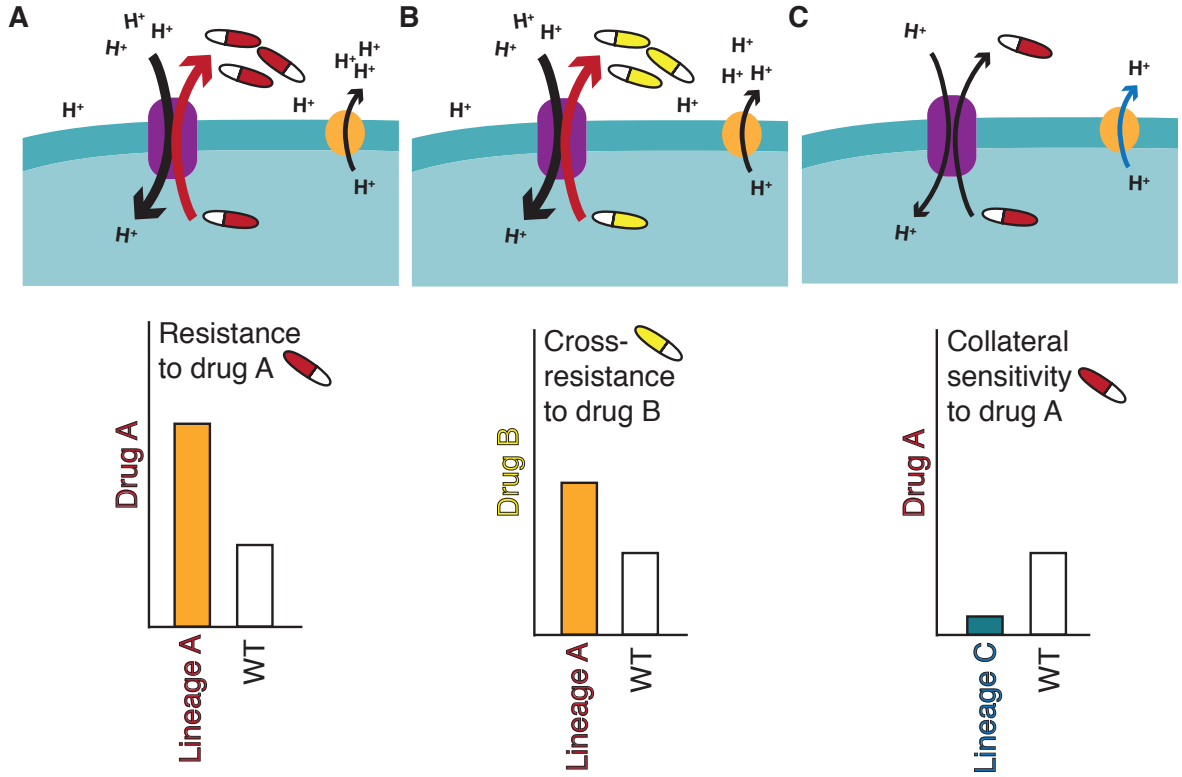

Figure 10: Examples for collateral resistance and sensitivity. A) Lineage A was evolved to drug A. Drug A is a substrate of an efflux pump. Lineage A accumulated mutations resulting in increased efflux activity and therefore increased resistance to drug A compared to the wild type (WT). **B)** The resistance level of lineage A was not only tested against drug A but also against drug B. Drug B is also a substrate of the same efflux pump as drug A. Consequently, efflux of drug B was increased in lineage A compared to the WT wherefore lineage A is collateral resistant to drug B. **C)** Lineage C was evolved to drug C that is not a substrate of the efflux pump. It is an aminoglycoside antibiotic, whose uptake is energy and membrane-potential dependent. As an adaptation to drug C lineage C accumulated mutations that reduce respiration and the membrane potential. Since the drug efflux pump is a proton-antiporter, protons are required for proper function. The activity of the efflux pump is impaired in lineage C compared to the WT and consequently, lineage C is collateral sensitive to drug A, as efflux of drug A was reduced in the lineage.

In *P. aeruginosa* collateral sensitivity is less frequently observed than in *E. coli*, however, mutations in a specific genetic marker, *nfxB*, an efflux regulator, were observed to be associated with collateral sensitivity[146]. By now multiple studies have explored the collateral sensitivity and resistance landscapes of *E. coli* and *P. aeruginosa*[146,163–166]. I compared the results from the literature with my own comprehensive analysis of collateral drug responses in both organisms (Figure 11) (**manuscript 3** and **4**).

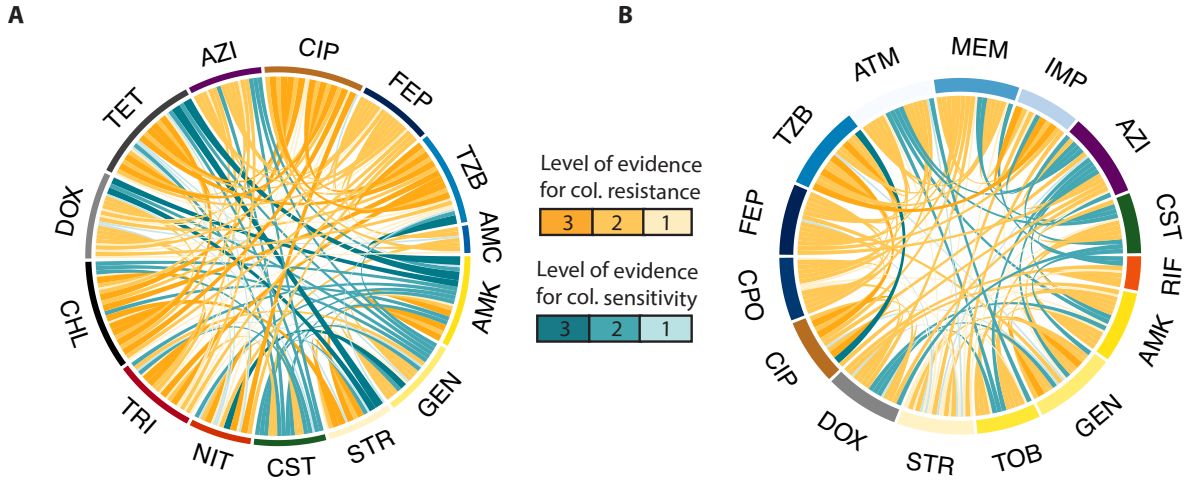

Figure 11: Collateral resistance and sensitivity across the literature in *E. coli* and *P. aeruginosa*. A) Collateral resistance (organge) and collateral sensitivity (blue) between different antibiotics across two to four different scientific studies in *E. coli*. **B)** Collateral resistance (organge) and collateral sensitivity (blue) between different antibiotics across two to three different scientific studies in *P. aeruginosa*. Explanations for the abbreviations for the antibiotics can be found in the supplemental material of **manuscript 3** and **4**.

To compare the different studies I counted the majority of studies that reported the same interaction type and subtracted the number of studies that were disagreeing with the majority of studies. When equal number of studies would have conflicting results the score would be zero. Drug interactions were only included when at least two studies had reported collateral drug responses for these drug pairs. Interestingly, about half of the drug interactions observed were in agreement between all studies. For about a third of the interactions both collateral resistance/sensitivity and neutral interactions were reported and for about 18% of the interactions conflicting results were observed. These differences can either stem from the methodology used to create the resistance lineages[166] or from different methodologies used to determine the collateral response (e.g. growth rate versus MIC)[164,165]. However, it is also plausible that conflicting results are caused by natural variation among biological lineages and different evolutionary trajectories leading to resistance. First of all, it has been shown that collateral sensitivity is determined by genetic adaptations[146,198]. While genetic markers for collateral resistance seem to evolve in parallel[198] genetic adaptations resulting in collateral sensitivity are only selected to a certain probability[199]. In fact, variation in collateral drug responses have been reported among biological replicates adapted in the same study[163,166]. And the parallel evolution of 60 independent lineages revealed that collateral sensitivity is rare and only occurs with a certain likelihood[199]. Moreover, a single study reported that clinical *E. coli* isolates did not display any collateral sensitivity, yet collateral resistance[200]. However, laboratory evolution of clinical isolates repeatedly resulted in comparable collateral resistance

and sensitivity profiles as laboratory evolved strains[164,201]. Interestingly, it was found that the genotype as well as the transcriptome of evolved lineages could predict the phenotypic resistance and sensitivity patterns to a certain extend[198,202,203]. Moreover, the genetic basis for collateral sensitivity was further studied by exposing a gene deletion library of *E. coli* to subinhibitory antibiotic concentrations[204]. Since collateral sensitivity harbors the potential to be exploited in treatment of infections to limit resistance evolution, efforts started to identify novel compounds for their collateral sensitivity profiles[205,206].

Limiting resistance evolution

Since collateral sensitivity is an intriguing phenomenon to potentially exploit and decelerate antibiotic resistance evolution, many studies explored treatment options based on collateral sensitivity. Multiple studies for *E. coli* and *P. aeruginosa* could show that drug cycling between antibiotics that display collateral sensitivity to each other can limit resistance evolution and counter select specific resistance markers both *in vitro* and *in vivo*[146,164,207]. Interestingly, the order in which the antibiotics are applied is important to gain the highest effectiveness[208,209]. In addition, also the duration of the antibiotic exposure is critical[176]. A recent study, suggests that after initial treatment with one drug not the change but the addition of another drug has the best potential to limit resistance evolution[210]. In addition, it was shown that the concentration of the antibiotics utilized is crucial to limit resistance evolution effectively[211]. A mathematical model compared different treatment options in hospitals and found that combination therapy of antibiotics would be even more effective in limiting resistance evolution than drug cycling[212]. Combination therapy has also been extensively studied. Small scale studies provide evidence that combination of antibiotics based on collateral sensitivity can effectively limit resistance evolution in *E. coli* and *P. aeruginosa*[149,213,214]. Besides collateral sensitivity also epistatic drug interactions, that can either be synergistic, additive or antagonistic in comparison to the combined effects of the two antibiotics alone, has been proposed to impact resistance evolution. Yet, results from different studies on the effects of epistatic drug interactions are conflicting suggesting that synergistic combinations limit[213], accelerate[168] or do not impact[149] resistance evolution. In addition to different treatment strategies that were analyzed in regards to their ability to decelerate resistance evolution also the underlying molecular mechanisms have been studied. Epistatic interactions between different genetic changes have been studied and it was found that negative epistasis can reduce the adaptive potential[215,216] but that epistatic interactions in general rather increase the accessibility of multiple fitness peaks[217]. Overall, it can be concluded that collateral sensitivity

and negative genetic epistasis are important to understand and to translate into appropriate treatment protocols as they harbor the potential to decelerate resistance evolution and to prolong the life-time of antibiotics.

Compatibility of evolutionary responses drive resistance evolution during combination therapy

Authors:

Leonie J. Jahn*

Daniel Simon*[1]

Mia Jensen*[2]

Charles Bradshaw*

Mostafa M. H. Ellabaan*

Morten O. A. Sommer*[§]

[§]Corresponding author: msom@bio.dtu.dk

*Author affiliation:

Novo Nordisk Foundation Center for Biosustainability, Technical University of Denmark, Kemitorvet 220, 2800 Kgs. Lyngby, DK

[1]Current affiliation:

Department of Computer Science, New York University Shanghai, 1555 Century Ave, Pudong Xinqu, Shanghai Shi, China, 200122

[2]Current affiliation:

NNIT A/S, Østmarken 3A, 2860 Søborg, DK

Abstract

Antibiotic combinations are considered a relevant strategy to tackle the global antibiotic resistance crisis since they are believed to increase treatment efficacy and reduce resistance evolution[1–3]. However, studies of the evolution of bacterial resistance to combination therapy have focused on a limited number of drugs and have provided contradictory results[4–6]. To address this gap in our understanding, we performed a large-scale laboratory evolution experiment, adapting 460 lineages of *Escherichia coli* to a diverse set of antibiotics and antibiotic pairs. We found that combination therapy significantly limits the evolution of *de novo* resistance in *E. coli,* but that bacteria vary substantially in their ability to evolve resistance to different drug combinations. In contrast to current beliefs, the phenotypic features of drug pairs are weak predictors of resistance evolution and are rarely evolutionarily stable. Instead, the evolvability is driven by the relationship between the evolutionary trajectories that lead to resistance to a drug combination and those that lead to resistance to the component drugs. Drug combinations that require a novel genetic response from target bacteria compared to the individual component drugs significantly reduce resistance evolution. These data support combination therapy as a treatment option to decelerate resistance evolution and they provide a novel framework for selection of optimized drug combinations based on bacterial evolutionary responses.

Introduction

The prevalence of antibiotic resistance has become a global health concern; as such resistance can subvert standard treatments for common bacterial infections, as well as limit effective treatment of chronic infections[7]. As the development of novel antibiotics is expensive in terms of time and resources[8], it is important to use currently available drugs in the best possible way to decelerate antibiotic resistance evolution and to maximize positive treatment outcomes. Empiric combination therapy is believed to improve treatment outcomes via increased potency and reduced evolution of drug resistance[9,10,11]. However, the clinical benefit of combination therapy remains controversial, and several studies have not observed differences in treatment success compared to monotherapy[12–17]. These disparate results might be explained by an incomplete understanding of the factors that drive the evolution of resistance to combination therapy.

The most studied feature of drug combinations is epistatic interaction. Epistatic interactions describe the combined effect of multiple drugs relative to the sum of their individual effects.

Three categories, additive, synergistic and antagonistic, are discriminated based on equal, increased or decreased effects of the drug combinations relative to the sum of their individual effects[18]. To classify drug combinations accordingly the growth rate or susceptibility level are usually determined as effect size for Loewe or Bliss additivity models[5,19]. Epistatic drug interactions potentially drive the evolution of resistance to drug combinations, but their role remains controversial. Some studies have shown that synergistic drug combinations clear infections effectively and limit resistance evolution[20–23], while others provide evidence that synergistic drug pairs do not improve treatment success or reduce resistance evolution[24], and may even accelerate resistance evolution[4]. In addition, it was also reported that epistatic drug interactions do not impact resistance evolution at all[5]. These conflicting results might in part be caused by differing methodologies regarding the assessment of resistance evolution. In order to resolve the opposing findings it would be valuable to determine the effect of epistatic interactions on different aspects of resistance evolution in a systematic and comprehensive manner.

Collateral sensitivity and collateral resistance must also be considered when investigating drug combinations. Collateral sensitivity occurs when a resistance mechanism protects a bacterium from a specific antibiotic but also increases the susceptibility of the bacterium to another drug[25,26]. Collateral resistance, on the other hand, occurs when the evolution of resistance to one drug increases the ability of the bacteria to resist multiple other antibiotics. It has been shown for a limited number of drug combinations that multicomponent drugs with collateral sensitivity between the individual drugs reduce the evolvability in *Escherichia coli* [5,27,28] and that drug cycling based on collateral sensitivity can also reduce the frequency of resistance mutations in clinical settings[29]. However, due to the limited number of drug combinations it remains to be elucidated whether these findings can be generalized.

In addition to the gaps identified above, the genetic response to combination therapy was so far only studied in response to few drug combinations and in light of collateral sensitivity and resistance[5,28]. Wherefore general trends in the evolutionary trajectories followed by bacteria exposed to drug combinations remain to be studied.

In order to address this lack of knowledge, we conducted a systematic high-throughput adaptive laboratory evolution experiment for *Escherichia coli,* an important model organism and human pathogen[30,31], by using 22 individual drugs and 33 drug pairs in eight biological

replicates. We analyzed the phenotypic and genotypic evolutionary responses to single and combinatorial drug exposure and explored the roles of epistatic drug interactions, collateral drug responses, and genetic trajectories as drivers of resistance evolution.

Results

Assessment of evolutionary responses to combination therapy

To identify the underlying features that drive the evolution of resistance to combination therapy, we adapted genetically barcoded lineages[32] of the well-studied model organism *Escherichia coli* K12 MG1655 to a diverse set of 22 different antibiotics and 33 different antibiotic pairs (Table S1, Table S2). These drugs, including both bactericidal (68.18%) and bacteriostatic (31.81%) drugs, covered 11 different drug classes and targeted 6 different bacterial processes (Table S2, Figure 1A). Moreover, the drug combinations covered all three possible epistatic interactions—synergistic (34.4%), additive (28.1%) and antagonistic (37.5%)—and all the possible collateral responses between the individual drugs constituting the pairs (Figure 1A).

Resistance to these drugs and drug combinations was achieved via adaptive laboratory evolution. Even though adaptive evolution experiments simplify the growth conditions in human hosts, they can capture clinically relevant features of resistance evolution[29]. In addition, adaptive evolution reduces the complexity of resistance evolution in clinical settings and allows studying specific parameters systematically under controlled conditions[33]. We performed the evolution experiment in a stepwise manner[34], in eight biological replicates giving a total of 460 lineages (including 20 LB-only controls) (Figure 1B). Every 22 h, the optical density (OD) was measured; a sample of the population was stored; and a new well containing a 25% higher antibiotic concentration was inoculated with a 20-fold dilution[34] (Table S3). The IC_{90} (inhibitory concentration resulting in an OD 10% that of an LB culture without antibiotic) of the ancestral wild type (WT) was reached after 7 days of evolution, and the experiment ended after 18 days, when 10-fold WT IC_{90} was exceeded (Figure 1B). An isolated colony was obtained for each revived endpoint population for subsequent genotypic and phenotypic characterizations (Table S4).

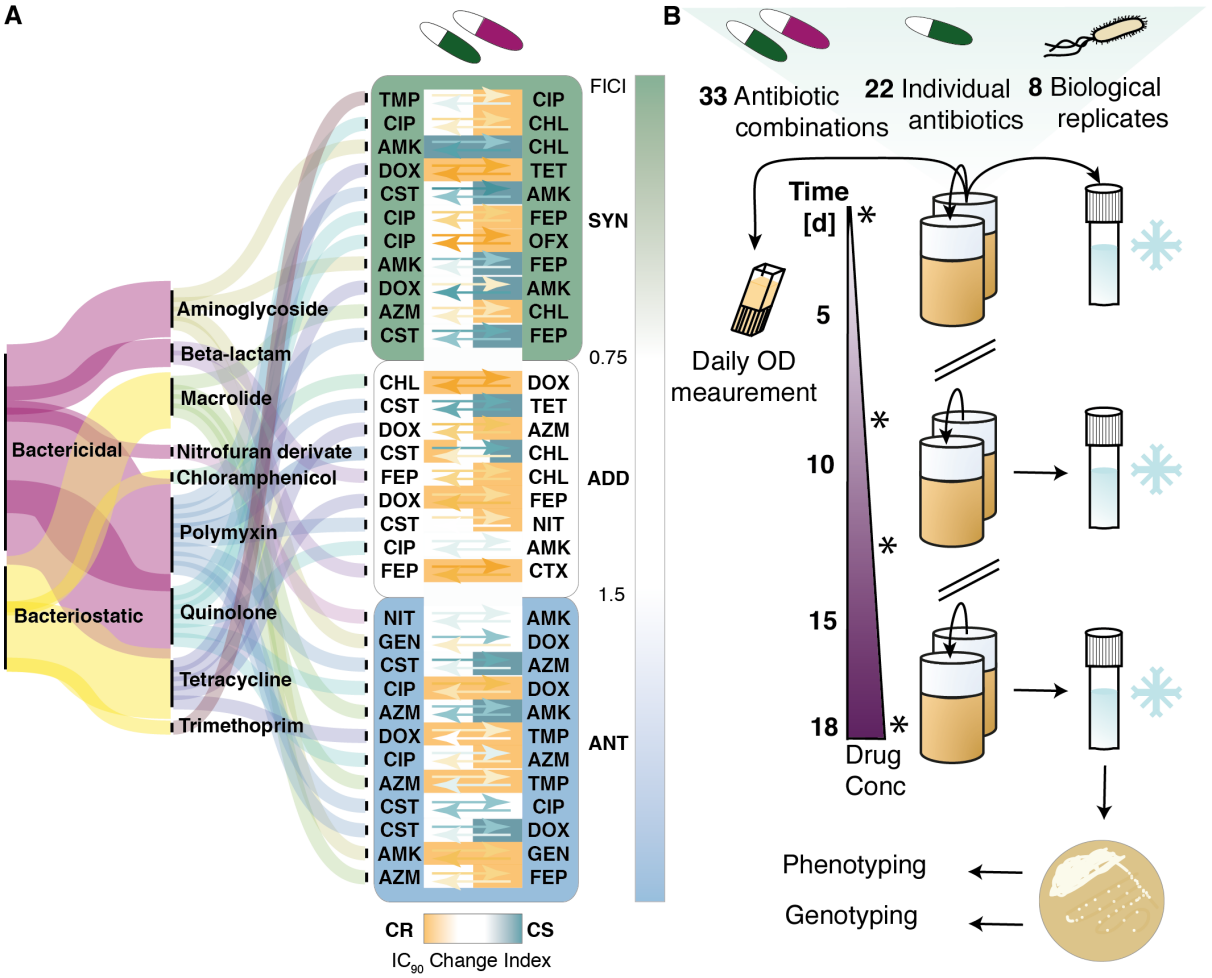

Figure 1: Drug properties and experimental setup. **A** Characteristics of the drugs chosen for adaptive laboratory evolution. The antibiotics were either bactericidal or bacteriostatic and covered nine different drug classes. The drug pairs, shown in ascending order of FICI, exhibit various phenotypic interactions, including synergy (SYN, FICI < 0.75), additivity (ADD, FICI = 0.75-1.5) and antagonism (ANT, FICI > 1.5), as well as collateral resistance (CR), a neutral collateral response and collateral sensitivity (CS). The arrows show the fold increase (orange, more than 2 fold increase in median IC_{90} (inhibitory concentration resulting in an OD 10% that of an LB culture without antibiotic) relative to the ancestral wild type (WT))) or decrease (blue, less than 0.5 fold decrease in median IC_{90} relative to the WT) in resistance compared to the WT. The space around the arrows is colored based on the classification of the drug pairs as CR, CS or neutral according to the IC_{90} change index of each biological replicate. Definitions of antibiotic abbreviations can be found in Table S2. Definitions of the different categories (SYN, ADD, ANT, CS, CR) as well as definitions of the FICI and IC_{90} change index can be found in materials and methods. **B** Adaptive laboratory evolution of antibiotic resistance. Genetically barcoded *E. coli* lineages were evolved in eight biological replicates with 22 different antibiotics and 33 different antibiotic combinations. The lineages were grown in 1 ml of LB containing antibiotic in 96-deep-well-plates. Every 22 h, the cells were transferred to a new plate with 20-fold dilution. In addition, the optical density was measured immediately before each transfer, and an aliquot of the population was saved as a glycerol stock. The evolution of resistance in each population was monitored by measuring the IC_{90} at day 0, 8, 13 and 18, as indicated with stars. The evolution was started at subinhibitory drug concentrations, and the WT IC_{90} was reached on the 7^{th} day of the experiment. The evolution experiment ended after 18 days, when the WT IC_{90} was exceeded by more than 10-fold. Isolated colonies were obtained from frozen endpoints and subsequently used for whole-genome sequencing and susceptibility testing to multiple antibiotics.

While most (68.4%) of the lineages adapted to monodrug exposure exhibited stable growth throughout the evolution experiments (chi-square test of independence, $X^2 = 10.835$, $p < 0.001$), most (59.4%) of the lineages exposed to drug combinations exhibited declining OD

values over time (chi-square test of independence, X^2 = 7.0712, p < 0.01) (Figure S1A-C). Consistent with the observations based on the OD, we found that a majority (67.8%) of the drug-pair-evolved populations, but a minority (23.5%) of the single-drug-evolved populations, only gained resistance levels below the antibiotic concentration they were exposed to during the adaptive laboratory evolution (chi-square test of independence, X^2 = 10.853, p < 0.001) (Figure S1D-F), suggesting a limited capacity of drug-pair-exposed populations to evolve resistance.

Combination therapy reduces resistance evolution

To examine in more detail the effects of drug exposure on evolvability, we analyzed the key factors that impact the adaptive potential: the evolvability index, describing the final phenotypic adaptation level relative to single-drug-evolved lineages[5]; the speed of resistance acquisition inferred from the phenotypic adaptation rate[35]; survival during adaptation[36]; and the number of generations that each lineage underwent during the evolution experiment[4]. All the lineages except those evolved to a combination of ciprofloxacin and azithromycin had a median evolvability index less than 1, indicating that the drug-pair-evolved lineages became less resistant to the two individual drugs than the lineages evolved to these drugs alone (Figure 2A). In fact, for a majority of the drug pairs (87.5%), very limited resistance evolution was observed (evolvability index < 0.5). For 18.75% of the drug pairs, we detected no evolution of resistance to the individual drugs. While the speed of resistance evolution varied among different conditions (Figure S2), drug resistance evolved significantly faster in single-drug-evolved lineages (median phenotypic evolutionary rate of 2.6) than in drug-pair-exposed lineages (median phenotypic evolutionary rate of 1.9) (Mann-Whitney U-test, p < 0.001) (Figure 2B). The variance in the phenotypic evolutionary rate between drug-pair-evolved lineages (2.3) was much lower than the variance between single-drug-evolved lineages (1882.3). In addition, a significantly greater number of lineages became extinct under combination exposure than under single-drug exposure (chi-square test of independence, X^2 = 20.604, p < 0.001) (Figure 2C). Finally, the median relative number of generations of the lineages exposed to a single antibiotic was, at 1.01, almost unchanged compared to the WT, whereas lineages exposed to two antibiotics underwent on average 10% fewer generations (Mann-Whitney U-test, p < 0.001) (Figure 2D).

In summary, all the metrics used to describe the evolvability show that drug pairs in general reduce the adaptive potential of *de novo* antibiotic resistance evolution in *E. coli*. Nevertheless, *E. coli* evolved resistance to specific drug combinations at markedly different rates.

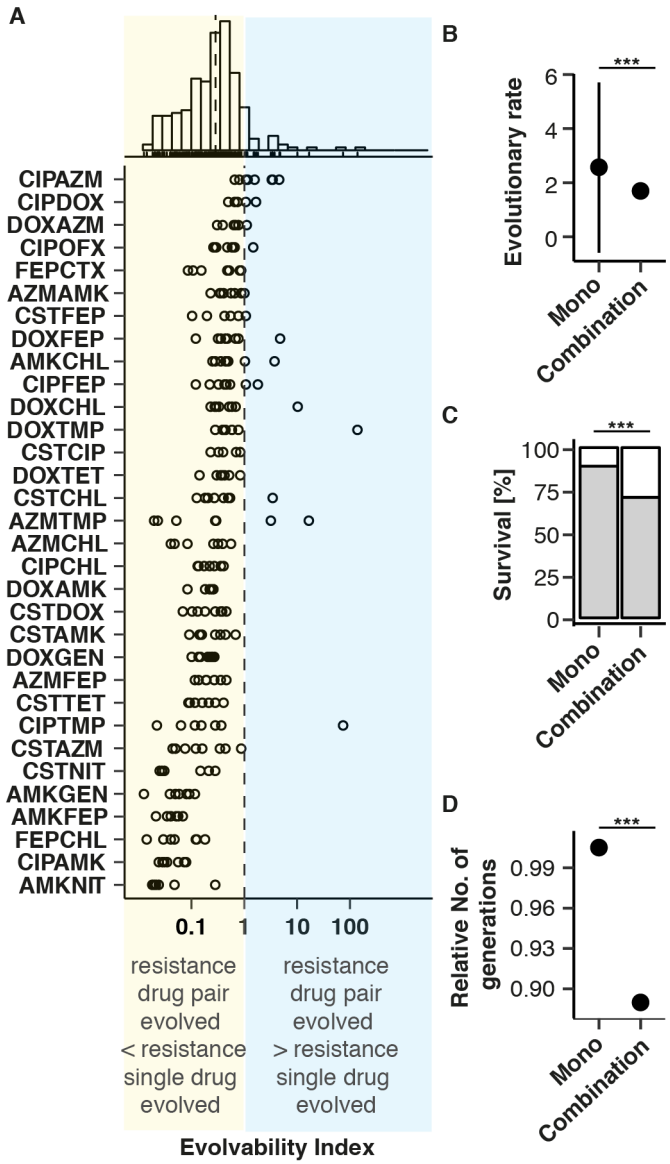

Figure 2: Antibiotic combinations limit resistance evolution. **A** Distribution of the evolvability index of the different biological replicates each represented with a dot for each drug pair. Drug pairs are ordered by median evolvability index. The histogram displays a unimodal right skewed distribution of the lineages over the evolvability index. The dotted line in the histogram indicates the median. **B** Comparison of the median evolutionary rate (±SD) between single-drug-evolved (n = 174) and drug-pair-evolved (n = 262) lineages. Following significance levels were used: * $p < 0.05$, ** $p < 0.01$, *** $p < 0.001$. **C** The percentage of lineages that survived the adaptive laboratory evolution experiment till the end (gray) and of lineages that became extinct before day 18 (white). Following significance levels were used: * $p < 0.05$, ** $p < 0.01$, *** $p < 0.001$. **D** The median number of generations normalized to the WT that evolved in parallel (±SD) in lineages exposed to drug combinations (n = 262) or mono drug exposure (n = 152). Following significance levels were used: * $p < 0.05$, ** $p < 0.01$, *** $p < 0.001$.

Phenotypic parameters are weakly correlated to evolvability and are not evolutionarily stable

Prior studies have suggested that phenotypic drug properties like epistatic drug interactions or collateral drug responses play an important role in explaining the difference in resistance evolution toward drug combinations[5,23,28]. We observed only a minor contribution of epistatic drug interactions on the evolvability of resistance (Figure 3A, Figure S3A-B). The hypothesis

that synergistic drug pairs accelerate resistance evolution was based on accelerated adaptation quantified by the change in growth rate during an adaptive evolution experiment[4]. Consistent with these findings, we observed a significant increase in growth during the adaptation experiment with synergistic drug pairs (Mann-Whitney U-test, $p < 0.001$) (Figure 3B), yet neither the evolvability index (Figure 3A) nor the phenotypic evolutionary rate (Figure S3A) suggest that resistance evolution is accelerated relative to that observed with antagonistic drug combinations (Mann-Whitney-U-test, $p > 0.05$). In addition, epistatic interactions were variable and changed during evolution (Figure 3C). In fact, synergistic drug combinations were highly underrepresented among evolved lineages; highlighting that adaptive responses to such synergistic combinations must be considered when drug combinations are designed in order to prevent insufficient dosage.

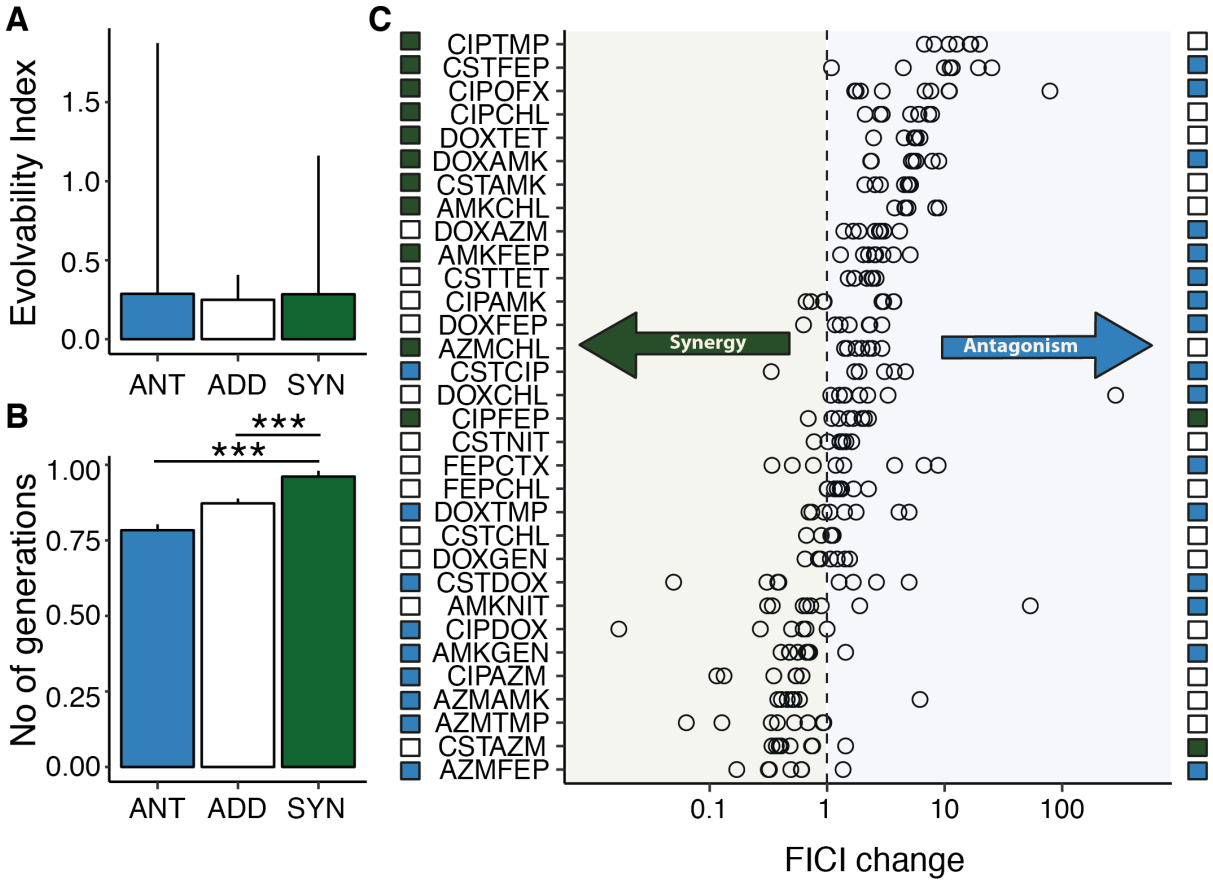

Figure 3: Epistatic drug interactions are weak predictors for resistance evolvability and are evolutionary not robust. **A** The median evolvability indices (±SDs) for drug pairs grouped by epistatic interactions (Mann-Whitney U-test, $p > 0.05$, n = 83, 71, 83). ANT, antagonistic drug pairs; ADD, additive drug pairs; SYN, synergistic drug pairs. **B** The median normalized number of generations (±SD) for drug pairs grouped by epistatic interactions (Mann-Whitney U-test, *** $p < 0.0001$, n = 84, 72, 88). ANT, antagonistic drug pairs; ADD, additive drug pairs; SYN, synergistic drug pairs. **C** The fractional inhibitory concentration index (FICI) change after adaptive evolution. Drug pairs are ordered by median FICI change. The colored boxes to the left of the plot indicate the epistatic interaction based on the FICI: blue is antagonistic (FICI > 1.5), green is synergistic (FICI < 0.75) and neutral is white (FICI = 0.75-1.5). The colored boxes on the right of the plot indicate the epistatic interactions after adaptive evolution according to the same color-coding using the median FICI of the biological replicates.

Next, we assessed the effect of collateral responses on evolution of resistance to drug combinations. Although we observed a limited effect of collateral responses on the evolvability index (Mann-Whitney U-test, $p < 0.05$, $p > 0.05$) (Figure 4A), the evolutionary rate at which resistance to the drug pairs was acquired was significantly higher for drug pairs with collateral resistance than for drug pairs with collateral sensitivity (Mann-Whitney U-test, $p < 0.0001$, $p < 0.05$) (Figure 4B). As resistance to drug combinations consisting of antibiotics with collateral resistance to each other is evolving faster than to other drug combinations, collateral resistance is well-suited to indicate which antibiotic combinations should be avoided.

To analyze the evolutionary robustness of collateral drug responses, we generated a collateral interaction network for all single-drug-evolved lineages (Figure 4C). We counted the occurrence of collateral sensitivity, collateral resistance and neutral interactions for all drug combinations (cutoff: CS < 0.5 x WT IC_{90} < N < 2 x WT IC_{90} < CR, where CS: collateral sensitivity, N: neutral interaction, and CR: collateral resistance). Collateral sensitivity was observed in approximately 20% of all interactions, while collateral resistance and neutral interactions were both observed at frequencies of 40%. Subsequently, we analyzed the biological replicates with regards to their collateral responses. A substantial proportion of the replicates (45.7%) exhibited a homogeneous collateral response. Approximately the same fraction (46.5%) included replicates that had either collateral resistance or collateral sensitivity and neutral interactions, and a minority of 7.8% included both collateral resistance and collateral sensitivity within the biological replicates adapted and tested against the same drugs. We further analyzed significant (ANOVA, $p < 0.05$) differences among biological replicates adapted to the same drug. Significant variation among replicates was less frequently observed for drugs that showed collateral resistance to each other (Figure 4C-D, Figure S3E). Further supporting that collateral resistance is a valid indicator for selection of antibiotic combinations, while collateral sensitivity appears to be less distinctive from neutral interactions and less evolutionary stable.

In summary, epistatic drug interactions as well as collateral sensitivity have limited potential to predict resistance evolution and are evolutionarily not stable, while collateral resistance shows the potential to predict resistance evolution to some extend.

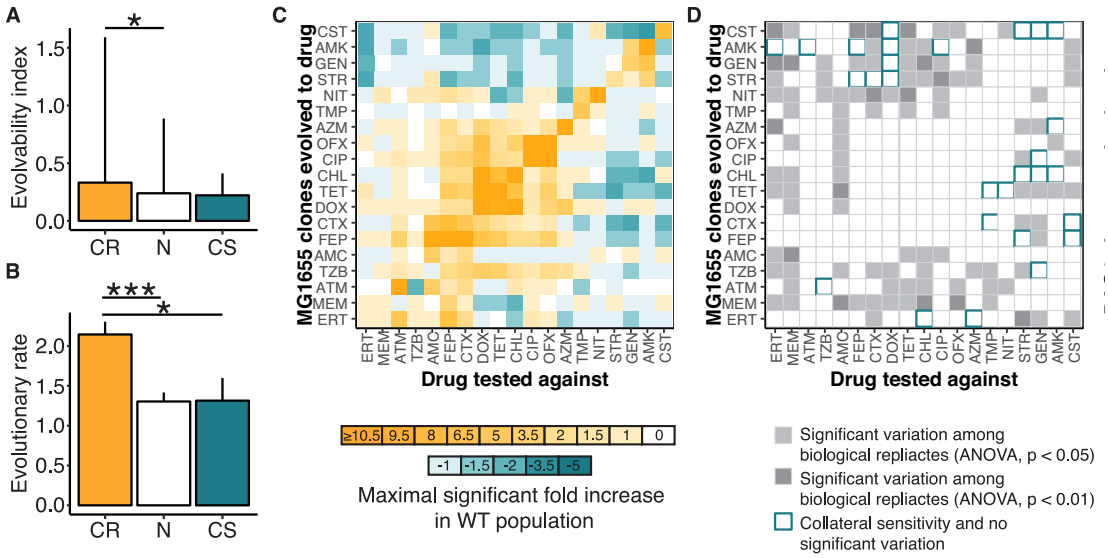

Figure 4: Collateral drug responses weakly predict resistance evolvability. **A** Median evolvability indices (±SDs) for drug pairs grouped by the collateral change index (Mann-Whitney U-test, * $p < 0.05$, n = 108, 110, 19). CR, collateral resistance; N, neutral; CS, collateral sensitivity. **B** The phenotypic evolutionary rate (±SD) for drug pairs grouped by the collateral change index (Mann-Whitney U-test, $p < 0.05$, n = 111, 114, 19). Following significance levels were used: * $p < 0.05$, ** $p < 0.01$, *** $p < 0.001$. CR, collateral resistance; N, neutral; CS, collateral sensitivity. **C** Collateral interaction heatmap of all individual drug-evolved lineages tested against all individual antibiotics. Orange indicates a significant ($p < 0.0001$) fold increase in resistance compared to the WT population, while blue indicates collateral sensitivity. **D** Significant differences (ANOVA, $p < 0.05/0.01$) between the biological replicates evolved to a single drug and tested against all individual antibiotics.

Genetic responses to drug pairs follow distinct patterns

Next, we studied the genotypic responses to antibiotic-induced stress as predictors of the resistance evolvability. Therefore, we performed whole-genome sequencing on 313 isolated lineages that exhibited phenotypic resistance (IC_{90} > 2-fold WT IC_{90}) after an initial screening. We identified five hypermutators with between 21 and 383 mutations. All hypermutators had a mutation in either *mutS* or *mutD* (*dnaQ*) (Table S5), which induce the hypermutator phenotype[37]. On average, we detected approximately 2.5 mutations per lineage, excluding the hypermutators. The gene that was mutated the most (107 times) was *marR* (Table S5), a gene in which mutations can induce a multidrug resistance phenotype[38,39].

We hypothesized that drug-pair-evolved lineages can respond to combination exposure with four different genetic adaptation profiles: (1) mutations conferring resistance to both constituent drugs are the same and are selected by the drug combination (Shared genotype); (2) mutations conferring resistance to both constituent drugs are different, yet are selected by the drug combination (Mixed genotype); (3) mutations conferring resistance to both constituent drugs are different, yet only mutations for one of the constituent drugs are selected by the drug combination (OneDrug genotype); or (4) mutations selected by the drug

combination are different from those selected by each of the constituent drugs (New genotype) (Figure 5A). To classify the drug pairs into these distinct categories, we performed an analysis of similarities (ANOSIM) based on the mutations of each sequenced isolate. ANOSIM is a nonparametric statistical test that is widely used in ecology to identify differences among ecological niches based on ranked dissimilarity matrices[40–42 43]. Here, we used mutated genes as features to identify differences between various adaptation conditions instead of features of an ecological niche.

The Shared group contained two drug pairs for which no significant genotypic differences (R^2 < 0.3 and/or p > 0.005) were observed between single-drug-evolved lineages or between single-drug-evolved lineages and drug-pair-evolved lineages (Figure 5B). For example, key mutations found in doxycycline-adapted lineages were also dominant in chloramphenicol-evolved lineages as well as lineages exposed to both drugs simultaneously. Both drug pairs belonging to the Shared group exhibited collateral resistance to each other (Figure S4), as the genetic alterations provide resistance to both individual drugs as well as to the drug pair.

The Mixed group contained three drug pairs, where a significant difference (R^2 > 0.3 and p < 0.005) between the genotypes of lineages evolved to individual drugs was observed, but no significant difference was observed between the genotypes of drug-pair-evolved lineages and those of lineages evolved to individual drugs (Figure 5C). For example, while the genotypes of lineages evolved to either ciprofloxacin or azithromycin were completely different, the drug-pair-evolved lineages exhibited key mutations that were also found in the lineages exposed to the individual drugs (Figure 5C). This drug combination was also the only one that had a median evolvability index greater than 1, indicating that compatible genetic pathways are unlikely to reduce the evolvability. The three drug pairs with a Mixed genotype exhibited either neutral or collateral resistance to each other, further highlighting that these drug pairs have compatible genetic responses (Figure S4).

The OneDrug group was composed of drug pairs where the genotype exclusively resembled that of lineages evolved to one of the individual drugs (Figure 5D). For example, mutations selected against amikacin were also present in the lineages exposed to amikacin and chloramphenicol, while none of the mutations found in chloramphenicol-adapted lineages were selected in the drug-pair-evolved lineages. Of the 24 drug pairs for which sequencing was performed, 14 (58.33%) were grouped in the OneDrug cluster. Half (50%) of these drug pairs

reached only final exposure levels around the IC_{90} of the individual drugs, mainly due to synergism (Figure S4). This finding indicates that adaptation to highly synergistic drug pairs can be achieved by selection of mutations against one of the drugs constituting the pair. These mutations cause a shift in epistatic interactions, resulting in a lineage that is resistant to one drug and exposed to subinhibitory concentrations of the other drug and does not require selection for additional mutations for survival. Consequently, the evolutionary pressure that we had hoped to impose with the drug pairs was circumvented, highlighting that synergistic drug combinations could also lose efficiency if used at insufficient doses, as previously predicted[6,24]. The remaining drug combinations (50%) that were resistant to both individual drugs and drug pairs were also clustered in the OneDrug group. Drugs belonging to these pairs were substrates of the AcrB efflux pump[44]. While one of the drugs, such as ciprofloxacin, develops resistance primarily via other resistance modes, such as mutations in *gyrA*, the other drug, such as doxycycline, selects for efflux-enhancing mutations. In combination, the efflux mutations are dominant, as these mutations confer resistance to both drugs simultaneously and are therefore likely to be selected. Consequently, the resulting genotype resembles the genotype of the efflux-mutation-selecting single-drug-evolved lineages, even though a shared resistance mechanism is selected.

The New group included drug pairs for which we observed significant ($R^2 > 0.3$, $p < 0.005$) differences in genotypes between individual drugs and between individual drugs and drug pairs (Figure 6E). For example, azithromycin- and trimethoprim-adapted lineages shared almost no mutations, while the lineages evolved to the combination of azithromycin and trimethoprim selected none of these mutations but repeatedly accumulated mutations in the mechanosensitive channel encoding gene *mscM*. Drug pairs with collateral sensitivity were found only in the OneDrug and New groups (Figure S4), highlighting that incompatible genetic trajectories to the individual drugs cannot be co-selected in drug combinations.

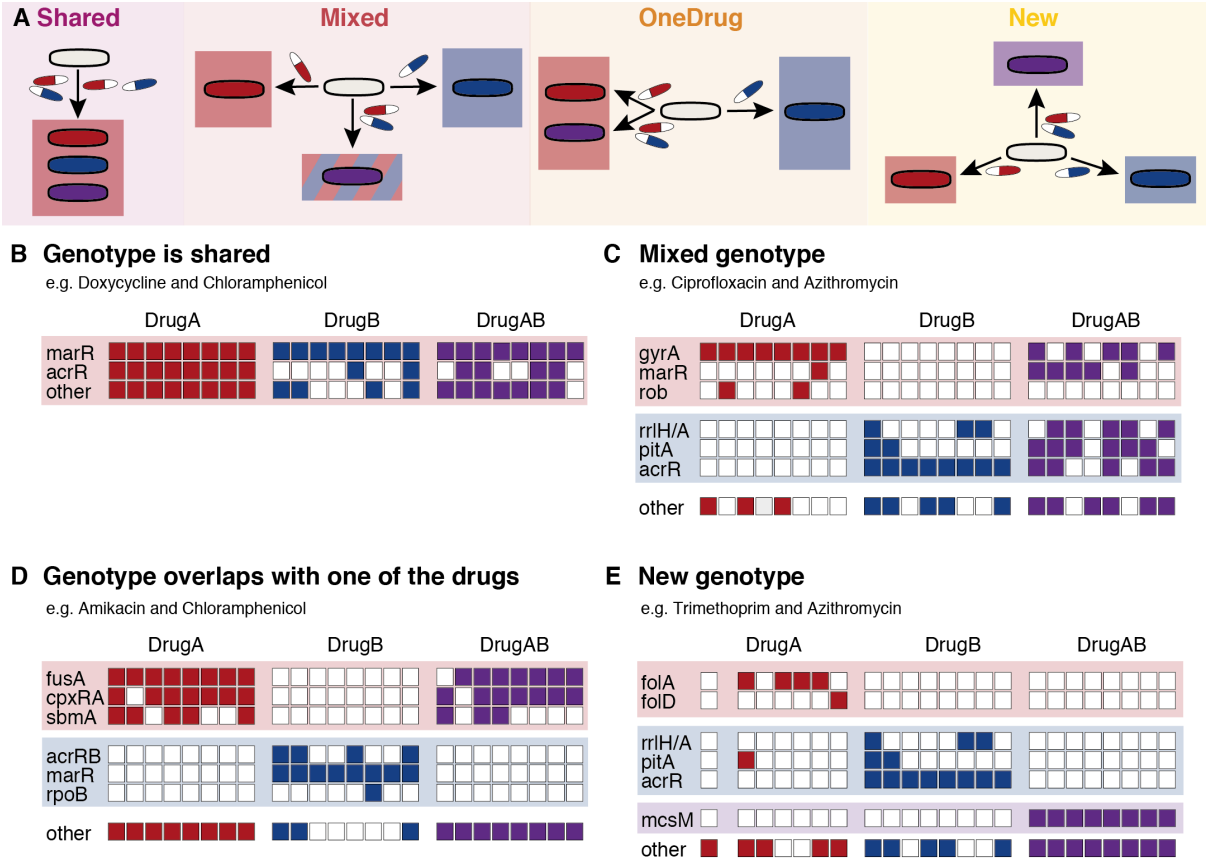

Figure 5: Drug pairs can be grouped in four distinct categories based on their genotypic response in relation to the genotype of lineages adapted to the constituent drugs. **A** Schematic overview of the possible genetic responses of drug-pair-evolved lineages compared to those evolved to the component drugs. **B** – **E** Examples of the genotypes of the eight replicates of single-drug-evolved and drug-pair-evolved lineages for each genetic group

Drug pairs requiring novel genetic responses exhibit the lowest resistance evolvability

To assess the impact of genotypic response on phenotypic evolvability, we analyzed the evolvability of the four different genetic groups. Drug pairs in the New group generally showed a significantly lower evolvability index (Mann-Whitney U-test $p < 0.01$), a lower evolutionary rate (Mann-Whitney U-test $p < 0.05$) and higher extinction rates (chi-square test of independence, $X^2 = 9.1576$, $p < 0.05$) than the other groups (Figure 6). Of the five drug pairs that composed the New genotype group, three exhibited collateral sensitivity to each other in at least one direction and two were defined collateral sensitive based on the IC_{90} change index, All three contained an aminoglycoside antibiotic, like the combination of ciprofloxacin and amikacin (Figure S4). In addition, collateral sensitivity between these drugs did not significantly vary among biological replicates (Figure 4D), suggesting high genetic incompatibility and few genetic alternatives to circumvent the incompatible trajectories. These drug pairs also had the lowest evolvability indices within the group. However, lineages

evolved to azithromycin and trimethoprim also developed a distinct new genotype, despite a lack of collateral sensitivity.

Overall, these findings highlight that drug combinations work best at decelerating resistance evolution when the resistance modes to the individual drugs are incompatible and require a novel genetic response. There appears to be a low probability of selection of these novel responses, as evolvability in this genetic group was significantly lower than that in the other groups (Mann-Whitney U-test $p < 0.01$). By contrast, drug pairs that evolved resistance by selecting for mutations against both drugs, belonging either to the Mixed or Shared group and in part to the OneDrug groups, had higher evolvability indices, higher evolutionary rates and lower extinction rates (Figure 6), demonstrating that combinations of antibiotics that have compatible genetic responses are not well suited to limit resistance evolution.

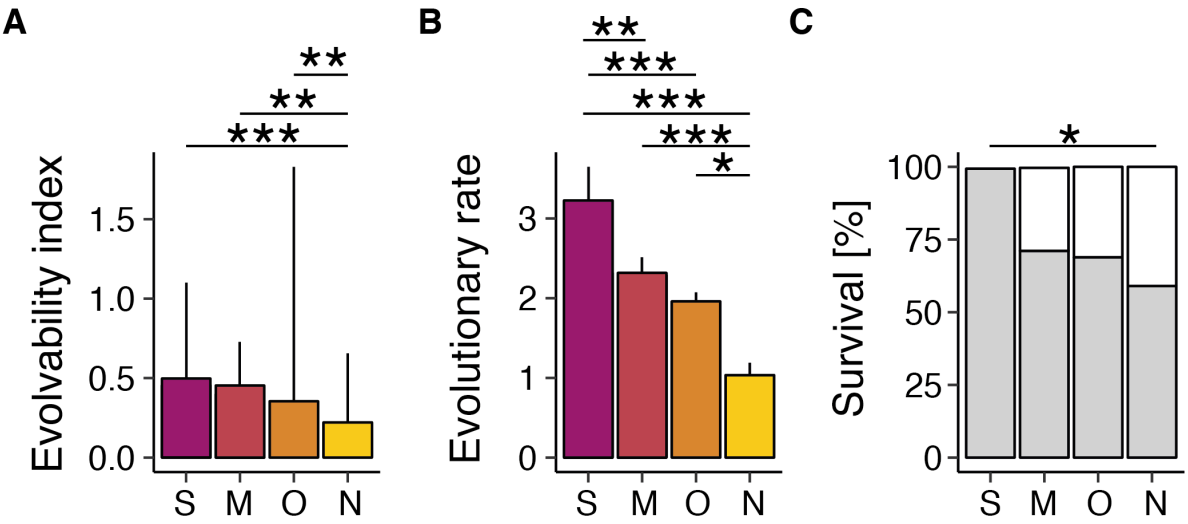

Figure 6: Drug pairs requiring a novel genetic response compared to the constituent drugs have a significantly lower resistance evolvability. **A** The median evolvability index (±SD) of drug combinations grouped by genetic response patterns (n = 16, 21, 101, 38). Following significance levels were used: * $p < 0.05$, ** $p < 0.01$, *** $p < 0.001$. S, Shared genotype; M, Mixed genotype; O, OneDrug genotype; N, New genotype. **B** The median phenotypic evolutionary rate (±SD) of drug combinations grouped by genetic response patterns (n = 16, 21, 106, 39). Following significance levels were used: * $p < 0.05$, ** $p < 0.01$, *** $p < 0.001$. S, Shared genotype; M, Mixed genotype; O, OneDrug genotype; N, New genotype. **C** Survival during the evolution experiment with drug combinations grouped by genetic response patterns (n = 16, 21, 106, 39). Following significance levels were used: * $p < 0.05$, ** $p < 0.01$, *** $p < 0.001$. S, Shared genotype; M, Mixed genotype; O, OneDrug genotype; N, New genotype.

Discussion

This study aimed to clarify the potential of antibiotic combinations in reducing resistance evolution and to identify key properties of these combinations that can predict resistance evolution allowing rational design of antibiotic combinations that limit resistance evolution.

We observed that *de novo* antibiotic resistance evolution is reduced in *E. coli* when two antibiotics are combined. We further assessed the ability of phenotypic parameters such as epistatic drug interactions and collateral responses to predict the evolvability. Previous studies reported conflicting abilities of epistatic drug interactions in limiting resistance evolution[4–6,23,24]. In line with Munck et al. (2014), we find that epistatic drug interactions are weak predictors for resistance evolution. However, our results also agree with findings from Hegreness et al. (2008), who reported increased growth during adaptive evolution in bacteria exposed to synergistic drug combinations. Yet, we do not think that this measure of adaptive potential alone is sufficient and our data on the actual adaptation level like the evolvability index or the phenotypic evolutionary rate do not provide significant differences between synergistic and antagonistic drug pair evolved lineages. Yet, coinciding with findings from experimental and theoretical studies[6,24] we found that synergistic drug combinations harbor the risk of insufficient dosage as epistatic interactions change during resistance evolution. While other studies provide evidence that epistatic interactions are evolutionary stable and robust upon alterations of the genetic background[45], we find that epistatic interactions change during evolution by accumulating resistance adaptations[5]. Our results are further supported by observations that epistatic interactions differ between different organisms[19] and even between different clinical isolates of the same organism[46], highlighting the importance of the genetic background for epistatic interactions. In light of our results, we conclude that epistatic drug interactions are not suitable to predict resistance evolution towards antibiotic combinations and that dosage of synergistic drug pairs should be chosen carefully.

In addition to epistatic drug interactions we also analysed the impact of collateral drug responses on the evolvability of resistance to drug combinations. We found that drug pairs constituted of antibiotics that display collateral resistance to each other can accelerate resistance evolution. This can be further explained by the genetic trajectories that are taken by lineages adapting to drug pairs with collateral resistance to each other. As the evolutionary trajectories to resistance to the individual drugs are compatible or even overlapping, there are fewer constrains for evolving resistance to the drug combination. One the other hand drug pairs that were made up of antibiotics that show collateral sensitivity to each other exclusively grouped in genetic groups like New or OneDrug indicating that the genetic trajectories are incompatible and resistance evolution is more constrained. However, even though drug pairs with collateral sensitivity had a lower evolvability index as neutral or collateral resistant drug pairs, the difference was not significant. One reason might be the fairly small sample size of

collateral sensitive drug pairs, while another reason might be that collateral drug responses are evolutionary not perfectly robust. A recent study explored the collateral responses of 60 parallel-evolved lineages and found that parallel evolution resulting in collateral sensitivity occurs only with a certain probability[47]. This is in line with previous studies that report differences among biological replicates in regards to their collateral response[48,49]. We also found significant differences among biological replicates in this study, highlighting that even though collateral sensitivity is a good first indicator for incompatible and limited resistance evolution in drug pairs as it had been suggested before for a limited number of antibiotic combinations[5,28], genetic adaptations that do not result in collateral sensitivity are open for evolution with a certain probability, wherefore the constrains of collateral sensitivity between drug pairs can be circumvented and resistance evolution is no longer limited.

The instability of phenotypic features of drug combinations highlights that the genetic trajectories ultimately decide whether or not high-level resistance can be achieved. Grouping of drug pairs based on genotypes revealed that resistance evolution to drug pairs that required a New genotypic response was greatly limited. Future work in identifying further evolutionary constrained drug pairs and a framework to predict limited resistance evolution will be needed in order to identify the best drug combinations for limited resistance evolution.

In general, our data provide a comprehensive resource for the exploration of *de novo* resistance evolution in *E. coli* and of the different phenotypic and genotypic adaptations to mono- and combination therapy. However, it would be of great value to test even more antibiotic combinations and multiple organisms to see if the results can be generalized further. Moreover, it remains to be determined whether our findings can be translated to the clinic. Adaptive evolution allows the study of a specific hypothesis under controlled conditions with well-characterized model organisms[33]. This method is frequently used to explore the response to antibiotic exposure[5,25,26,34,48,50]. Recently, findings from adaptive evolution experiments were shown to be applicable in the clinic[29], highlighting the potential of adaptive evolution for the study of clinically relevant scenarios. In addition, clinical isolates were subjected to evolution experiments and similar collateral resistance and sensitivity patterns were observed as reported for laboratory strains[51]. However, other factors, such as horizontal gene transfer, host-pathogen interactions, interactions between bacterial populations, side effects and pharmacodynamics of the antibiotics, as well as patient condition and disease, need to be considered when clinical experiments are conducted. Nonetheless, we

expect that this framework for assessment of evolvability of drug combinations will be the base for further research on the rational design of drug combinations for efficient and resistance-limiting therapies.

Materials and Methods

Bacterial strains and growth conditions

Chromosomally barcoded *Escherichia coli* MG1655 K12[32] were grown in LB at 37 °C and except for the IC_{90} determination at 600 r.p.m. shaking.

Adaptive laboratory evolution (ALE) to individual drugs and drug combinations

E. coli lineages were evolved each in 8 biological replicates to 22 different antibiotics and 33 different antibiotic pairs resulting in 460 individual lineages of which all *E. coli* lineages carried a unique genetic barcode[32]. All antibiotics used in this study, their mechanism of action, solvent and storage conditions are listed in Table S2. For the evolution towards drug combinations, the drugs were combined in a 1:1 ratio based on the WT IC_{90} values of the individual drugs[5]. An overnight culture grown in LB was used to inoculate the ALE experiments. After 22 h of growth at 37 °C and 600 r.p.m., 100 µl were transferred to a 96-well plate and the optical density (OD_{600}) of each lineage was measured in a ELx808 Absorbance Reader (BioTek) at a wavelength of 600 nm. In addition, 50 µl of cells, corresponding to a 20-fold dilution[34,52], were passaged to a new pre-heated 96-deep-well plate containing LB and a 25 % increase in antibiotic concentration in a total volume of 1 ml/well. The WT IC_{90} drug concentration was reached on the 7^{th} day of the ALE and the evolution was stopped after 18 days at a final concentration exceeding 10 fold of the WT IC_{90}[34]. All antibiotic concentrations can be found in Table S3. As a control 20 replicates were evolved to LB media alone. The IC_{90} of the population was measured on day 0, 8, 13 and 18 of the ALE in order to track the resistance evolution on the population level. After each transfer an aliquot of 100 µl was mixed with glycerol to a final glycerol concentration of 12.5 % and stored at -80 °C. Cells were streaked on LB agar from the frozen aliquot saved on the last day with growth (OD_{600} > 0.1). Some cells, were very difficult to revive as observed before[49]. If reviving failed, cells were inoculated into liquid LB before being streaked on LB agar. If cells still failed to revive, cells were streaked from the aliquot saved the day before the last day of growth. Despite the effort, some lineages would not revive at all. A list with all lineages, their last day of growth in the ALE and the day of the ALE they have been revived from can be found in the supplementary

(Table S4). One isolated colony was picked for each lineage, grown in LB and frozen at -80 °C for further characterization. Lineages adapted to the following antibiotics: Erythromycin, Sulfamethoxazole, Fosfomycin as well as the combination of Sulfamethoxazole and Trimethoprim displayed inconsistent phenotypes or did not develop resistance due to technical reasons such as drug stability after freezing. Therefore, these drugs were excluded from this study.

IC_{90} determination

100 µl of LB were inoculated with pin-replicators from frozen stocks of isolated colonies and grown overnight. About 10^5 cells were transferred with pin-replicators into plates containing a 2-fold drug gradient ranging over 10 different concentrations. Plates were grown at 37 °C for 18 h. The OD_{600} was measured for each well. The OD_{600} data was normalized and used to create dose-response curves in R as described before[5]. In brief, percent inhibition was calculated by the following formula: 1 – [(OD_{600} drug exposed – blank)/(OD_{600} media exposed – blank)]. The IC_{90} was defined as the lowest concentration of the drug that inhibited 90% of the growth[5,29]. All IC_{90} values were generated at least in technical replicates. If the WT IC_{90} differed more than 2-fold from the WT IC_{90} value established before the ALE started, the IC_{90} test was repeated along with the ancestor WT. No significant (Student´s t-test, $p > 0.05$) differences between the susceptibility of the WT and the media adapted WT were observed. The IC_{90} values were normalized to the media adapted WT IC_{90}. The heatmap presenting the collateral sensitivity and resistance of the single drug evolved lineages (Figure 5C) displays the times increase of the IC_{90} compared to the media adapted WT with a significance level of at least $p < 0.0001$. Significance levels were obtained as described before[29]. Briefly, by using the growth data OD_{600} of all technical and biological replicates adapted to the same drug for all 10 drug concentrations measured for each drug for the IC_{90} determination compared to the corresponding values of all media adapted technical and biological replicates exposed to the same drug. Within the natural variation of the samples 3000 additional data points were computed to identify robust differences among samples. Times increase or decrease in growth compared to the WT was calculated in steps of 0.5 ranging from -10.5 to 10.5. Pairwise t-tests between drug adapted and media adapted data were performed and the highest times increase/the lowest times decrease with a significance value of at least $p < 0.0001$ was given as output.

Calculation of important variables

Based on the IC_{90} values several calculations were made, that are explained in the following:

The evolvability index was calculated as described before[5]. In short, the following formula was used: ((IC_{90} of AB evolved tested in A normalized to WT/IC_{90} of A evolved tested in A normalized to WT)+(IC_{90} of AB evolved tested in B normalized to WT/IC_{90} of B evolved tested in B normalized to WT))/2. Two replicate lineages evolved to Amikacin and Nitrofurantion, as well as two replicate lineages evolved to Ciprofloxacin and Doxycycline had evolvability indices above 1000. They displayed extremely high IC_{90} values, when tested to one of the individual drugs (Nitrofurantion/Doxycycline). As these values were way outside of a reasonable range of resistance they were treated as technical errors and therefore excluded from the entire analysis.

The phenotypic evolutionary rate was calculated as described by Haldane (1949)[35] except that millions of years in the denominator was replaced by the number of days the lineages were evolved for. The following formula was used: ln((IC_{90} of A evolved tested in A)– ln(IC_{90} of WT tested in A used as starting point for the evolution experiment))/number of days lineage was evolved to A.

Epistatic interactions were determined using a Loewe additivity model and the IC_{90} as effect level. The Loewe additivity model was chosen as it assumes additive effects of identical drugs[5]. This is important as drugs with the same target and drugs from the same drug class were combined in this experiment. The fractional inhibitory concentration index (FICI) was calculated according to the following formula: (IC_{90} of the WT tested in AB * ω/IC_{90} of the WT tested in A) + (IC_{90} of the WT tested in AB * (1-ω) /IC_{90} of the WT tested in B). ω is the molar fraction of A in the drug combination AB. To calculate the FICI change the FICI after the evolution was calculated according to the same formula replacing "WT" by "evolved to AB" divided through the initial FICI. As it was recently shown that additive effects are only robustly detected at a cutoff between 1 and 1.25[53], we applied a low but symmetric cutoff in order to group the drug pairs into synergistic (<0.75), antagonistic (>1.5) and additive (0.75 – 1.5) combinations.

The IC_{90} change was calculated as described before[5]. In short, the following formula was used: ((IC_{90} of B evolved tested in A/IC_{90} of WT tested in A)+(IC_{90} of A evolved tested in B/IC_{90} of WT tested in B))/2. All drug pair evolved lineages were grouped into collateral sensitivity (< 0.5), collateral resistance (>2) and neutral (0.5 – 2) effects according to the IC_{90} change index.

A table including all phenotypic information of the drug pair evolved lineages can be found in the supplement (Table S6).

Whole-genome sequencing and sequence analysis

1 ml LB in each well of a 96-well, deep-well plate was inoculated from frozen stocks of isolated colonies and grown at 37 °C and 600 r.p.m. overnight. Cells were spun down at 2000 r.p.m. for 3 minutes. LB was removed and replaced by DNA shielding buffer (Zymo Research). Samples were sent to BaseClear B.V. for genomic DNA extraction (ZYMO research), Nextera XT library preparation (Illumina) and 125 paired-end whole-genome Illumina HiSeq 2500 sequencing. The resulting fasta reads were used in the following workflow:

(1) Single nucleotide variants (SNPs) and small insertions and deletions (INDELS) were called using CLC Genomics workbench as described before[34]. *E. coli* reads were aligned to the *E. coli* K12 U00096 reference genome[54]. On average, the coverage/base was at least 37 fold. For SNP calling only positions with a phred score of at least 30 at the position where the SNP occurred and at the three neighboring positions were considered. In addition, the SNP had to be detected with a frequency of at least 80 %.

(2) CLC Genomics workbench was further used to detect large insertions and deletions (large INDELS) in the reads using the INDEL function at default settings. The resulting INDELS were considered when they occurred with a frequency of more than 80 % and in more than 5 different reads.

(3) Large insertions were additionally detected by a custom made script used before[34]. The reference genomes of MG1655 as well as all open reading frames were downloaded from the NCBI nucleotide archive and used to cluster all ORFs with cd_hit[55]. The cluster cut off was 90 % identity and coverage. Afterwards the sequenced reads from this study were quality filtered using the FASTX-Toolkit package with a minimum quality of 30 and blasted against the clustered ORFs with a word size of 16 and an e-value of 0.01. Reads, with more than 90% coverage mapping continuously to the genome, that mapped to two different clusters with an

overlap between 30 and 70 % were kept for further analysis. Reads were filtered so they did not cover clusters representing adjacent genes. Finally, large insertions were only counted when they were observed in at least 5 individual reads.

INDELS that were detected by multiple of the parallel analyses were only counted once. Seven WT lineages adapted to the media were sequenced as a control and mutations found in these lineages were excluded from all lineages as they are likely mutations that have been inserted prior to the experiment or are involved in media adaptations. As no significant (Student's-test, $p > 0.05$) phenotypic difference between the resistance level of the ancestor WT and the media adapted WT lineages were identified, those mutations are unlikely to cause antibiotic resistance. Lineages with mutations in genes known to induce a hypermutator phenotype were excluded from the following analysis.

Analysis of similarity

Based on the genetic data, a binary presence absence data matrix was created for each lineage, excluding the hypermutators, and all genes. The matrix was summed for all replicates of the same condition and subsequently used to calculate a dissimilarity matrix with the package "vegan" in R[55] using Euclidian distance. The output was used as input for the anosim function from the package "vegan" in R[56]. Groups were considered to be significantly different when they had a *p*-value smaller than 0.005 and an R statistics greater than 0.3. The results were aggregated with the package "data.table"[57].

Data availability and code

Genomic data will be available in NCBI. All phenotypic data and scripts can be provided upon request. For the calculations and different analysis the following R packages have been utilized: "plyr"[58], "dplyr"[59], "tidyr"[60], "ggplot2"[61], "data.table"[57] "gdata"[62], "SciViews"[63], "drc"[64] "scales"[65], "gridExtra"[66], "cowplot"[67], "stringr"[68], "ggpubr"[69], "magrittr"[70]. For Figure 1 RawGraphs[71] was used to create the figure. All figures were edited in Abode Illustrator.

Supplementary information

Figure S1

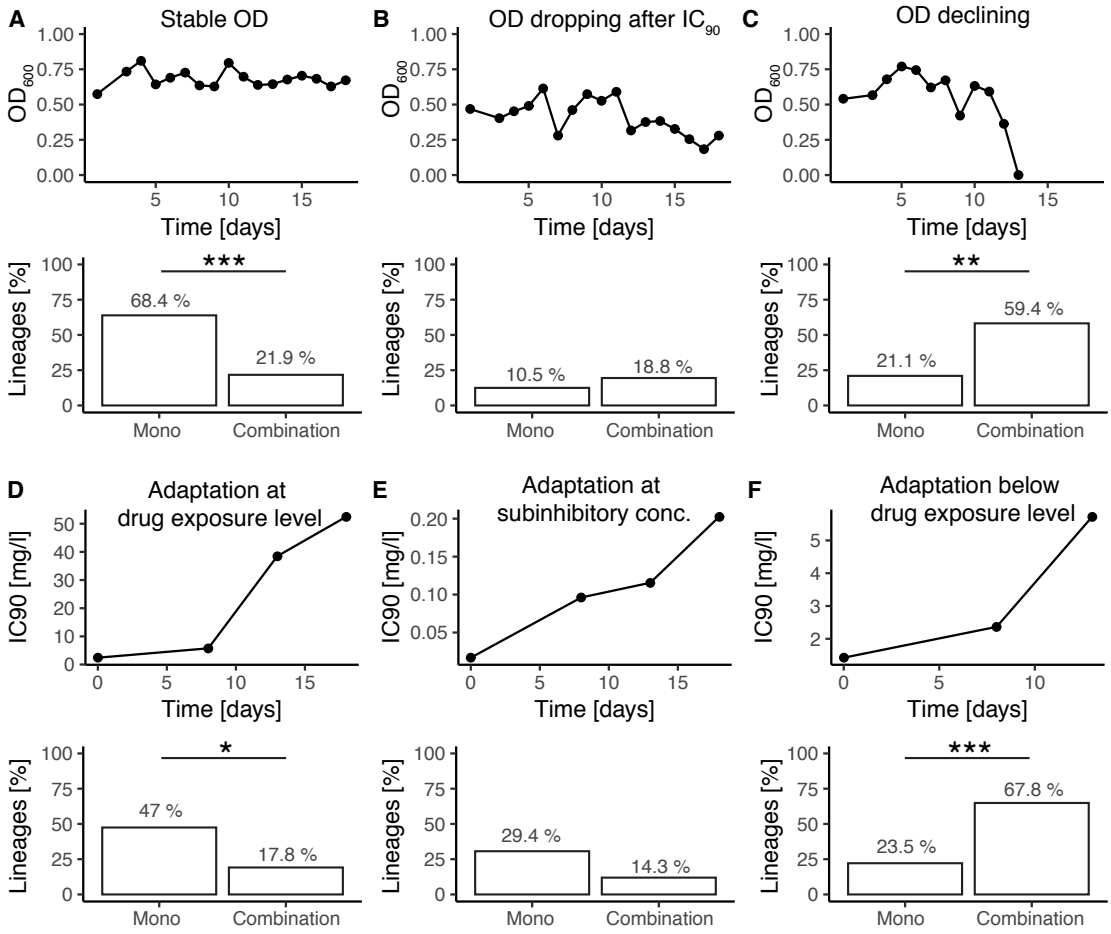

Figure S1: Distribution of optical density and population IC_{90} patterns during the adaptive evolution experiment. **A** Example of stable OD over the experiment (upper panel) (lineage 7 adapted to Ciprofloxacin) and the percentage of populations exposed to mono and combination therapy that exhibited that pattern (lower panel). **B** Example of decrease in OD after the WT IC_{90} was reached (upper panel) (lineage 3 adapted to Getamicin) and the percentage of populations exposed to mono and combination therapy that exhibited that pattern (lower panel). **C** Example of declining OD (upper panel) (lineage 3 adapted to Amoxicillin/Clavulanic acid) and the percentage of populations exposed to mono and combination therapy that exhibited that pattern (lower panel). **D** Example of resistance adaptation at or above the antibiotic exposure level (upper panel) (lineage 8 evolved to Amikacin) and the percentage of populations exposed to mono and combination therapy that exhibited that pattern (lower panel). **E** Example of resistance adaptation at subinhibitory drug concentrations (upper panel) (lineage 3 evolved to Ciprofloxacin) and the percentage of populations exposed to mono and combination therapy that exhibited that pattern (lower panel). **F** Example of resistance adaptation below the antibiotic exposure level (upper panel) (lineage 6 evolved to Amoxicillin/Clavulanic acid) and the percentage of populations exposed to mono and combination therapy that exhibited that pattern (lower panel).

Figure S2

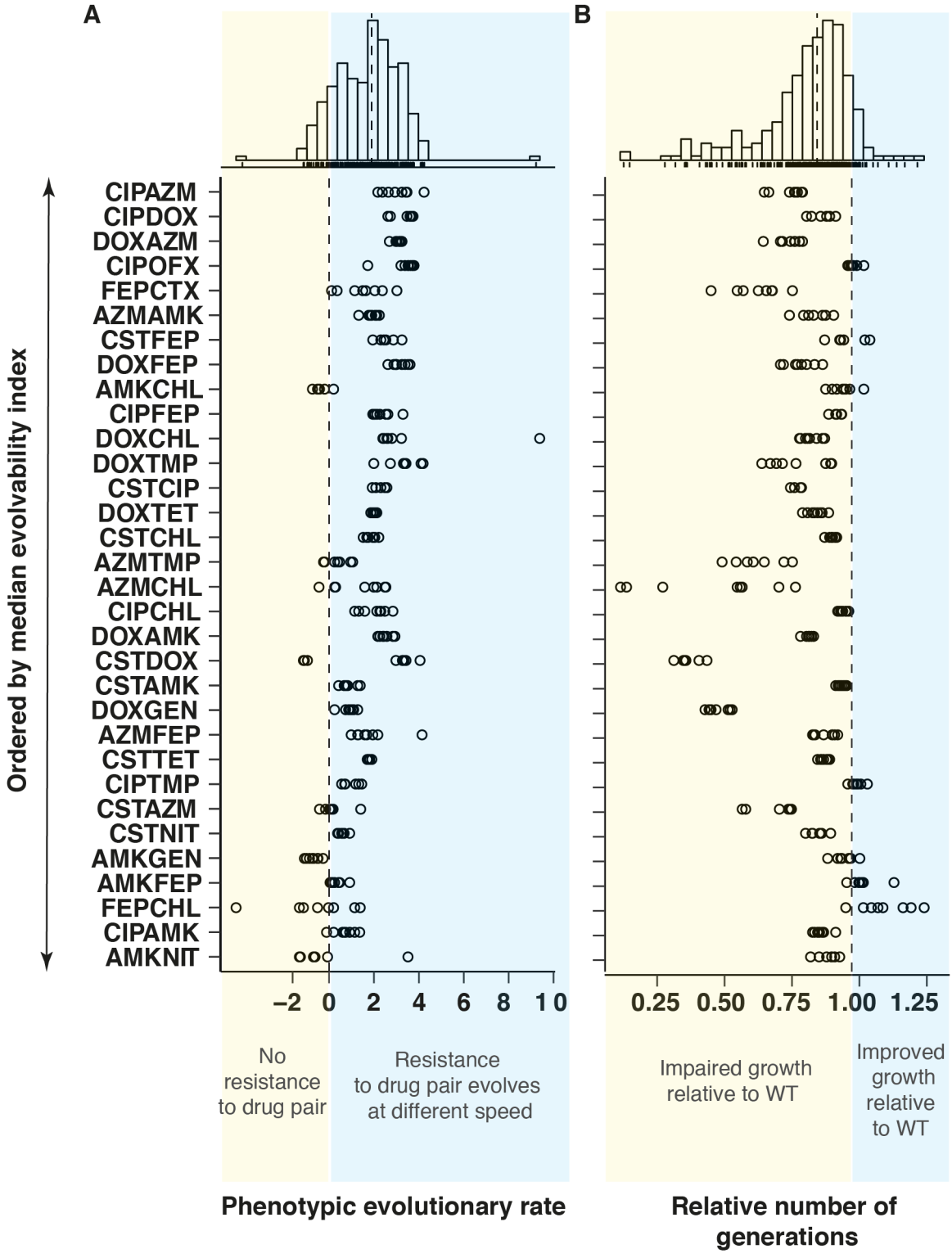

Figure S2: Phenotypic evolutionary rate and relative number of generations during adaptive evolution of all drug pair evolved lineages. **A** The drug pairs are ordered by the evolvability index. The phenotypic evolutionary rate of each biological replicate is presented with a dot for each drug pair. The histogram visualizes a symmetric distribution of the phenotypic evolutionary rate. The median evolutionary rate of all drug pairs and replicates is indicated with a dotted line in the histogram. **B** The relative number of generations of each biological replicate underwent during the adaptive evolution experiment is presented with a dot for each drug pair. The histogram visualizes a left skewed distribution of the relative number of generations The median relative number of generations of all drug pairs and replicates is indicated with a dotted line in the histogram.

Figure S3

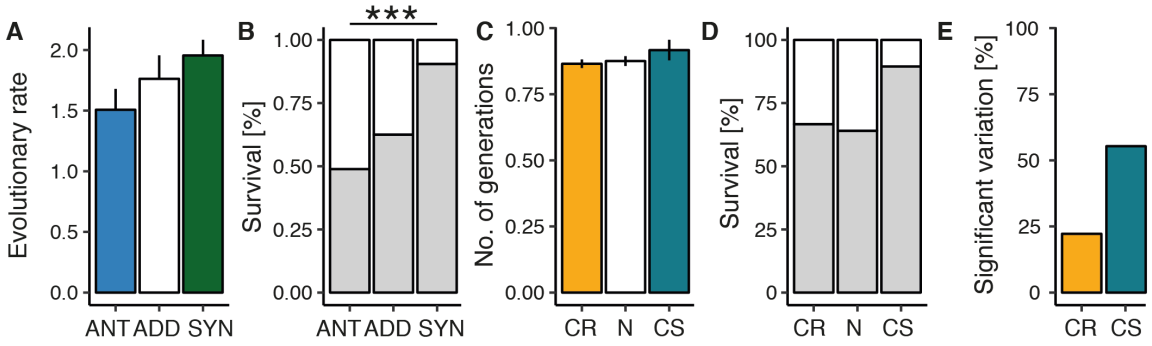

Figure S3: Evolvability features grouped by epistatic and collateral drug interactions. **A** The median phenotypic evolutionary rate (±SD) for drug pairs grouped by epistatic interactions (n = 88, 72, 84). **B** Survival with drug combinations grouped by epistatic interactions (chi-square test, X^2=34.799, *** $p < 0.0001$, n = 88, 72, 84). **C** The normalized number of generations (±SD) with drug pairs grouped by collateral interactions (n = 111, 114, 19). **D** Survival with drug combinations grouped by collateral interactions (n = 111, 114, 19). **E** Proportion of significant variation (ANOVA, $p < 0.05$) among biological replicates exhibiting either CR (n = 152) or CS (n = 68). ANT, antagonistic drug pairs; ADD, additive drug pairs; SYN, synergistic drug pairs; CR, collateral resistance; N, neutral; CS, collateral sensitivity.

Figure S4

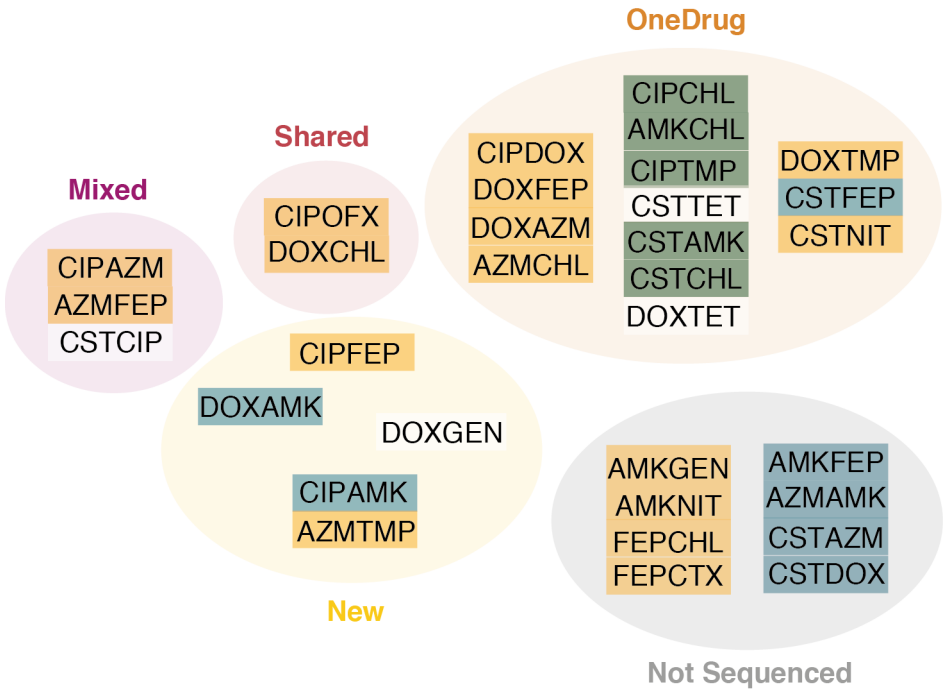

Figure S4: Distribution and features of drug pairs grouped based on genotypic response. The Mixed group contains drug pairs with neutral (white) or collateral resistance (orange) interactions. The Shared group contains only drug pairs with collateral resistance to each other. The OneDrug group is the largest group. Four drug pairs with collateral resistance to each other selected efflux mutations, which could be grouped into a Shared genotype. Half of the drugs in the OneDrug group did not reach high exposure levels to the individual antibiotics, and survival was possible due to a shift in epistatic interactions. The New group contains CIPFEP, which also selected for efflux mutations; therefore, grouping into the Shared group would be appropriate. The other drug pairs exhibited mainly collateral sensitivity (blue). Eight drug pairs were not sequenced due to failure in an initial resistance check. Half of these pairs are collateral resistant, while the other half are collateral sensitive.

Table S1: All antibiotics and antibiotic pairs used for the adaptive evolution experiment.

	Antibiotic	**Antibiotic Pair**
1	Amoxicillin/Clavulanic acid	Amikacin + Cefepime
2	Piperacillin/Tazobactam	Amikacin + Chloramphenicol
3	Meropenem	Amikacin + Gentamicin
4	Ertapenem	Amikacin + Nitrofurantoin
5	Cefotaxime	Azithromycin + Amikacin
6	Cefepime	Azithromycin + Cefepime
7	Aztreonam	Azithromycin + Chloramphenicol
8	Ciprofloxacin	Azithromycin + Trimethoprim
9	Ofloxacin	Cefepime + Cefotaxime
10	Tetracycline	Cefepime + Chloramphenicol
11	Doxycycline	Ciprofloxacin + Amikacin
12	Amikacin	Ciprofloxacin + Azithromycin
13	Gentamicin	Ciprofloxacin + Cefepime
14	Streptomycin	Ciprofloxacin + Chloramphenicol
15	Azithromycin	Ciprofloxacin + Doxycycline
16	Erythromycin	Ciprofloxacin + Trimethoprim
17	Sulfamethoxazole	Ciprofloxacin + Ofloxacin
18	Trimethoprim	Colistin + Amikacin
19	Nitrofurantoin	Colistin + Azithromycin
20	Colistin	Colistin + Cefepime
21	Chloramphenicol	Colistin + Chloramphenicol
22	Fosfomycin	Colistin + Ciprofloxacin
23		Colistin + Doxycycline
24		Colistin + Nitrofurantoin
25		Colistin + Tetracycline
26		Doxycycline + Amikacin
27		Doxycycline + Azithromycin
28		Doxycycline + Cefepime
29		Doxycycline + Chloramphenicol
30		Doxycycline + Gentamicin
31		Doxycycline + Tetracycline

32	Doxycycline + Trimethoprim
33	Sulfamethoxazole + Trimethoprim

Table S2

This table contains a list of all antibiotics and their abbreviations, mechanisms of action, vendors and storage conditions and can be found here: https://www.dropbox.com/preview/Supplementary/TableS2.xlsx?role=work

Table S3

This table provides an overview of all antibiotic concentrations used during the ALE experiment and can be found here:
https://www.dropbox.com/preview/Supplementary/TableS3.xlsx?role=work

Table S4

A list of all lineages and their last day of growth and day of revival can be found here:
https://www.dropbox.com/preview/Supplementary/TableS4.xlsx?role=work

Table S5

A list of all INDELs and SNPs identified in the genome of each lineage after filtering out mutations that were also present in the media-adapted WT lineages can be found here:
https://www.dropbox.com/preview/Supplementary/TableS5.csv?role=work

Table S6

A table with all phenotypic information regarding the drug-pair-evolved lineages can be found here:
https://www.dropbox.com/preview/Supplementary/Table_S6.csv?role=work

Code

Code written for the analysis can be found here:
https://www.dropbox.com/home/Supplementary/CodeEvolvabilityData

References

1. Hesketh, P. J. *et al.* Antiemetics: American Society of Clinical Oncology Clinical Practice Guideline Update. *J. Clin. Oncol.* (2017). doi:10.1200/JCO.2017.74.4789

2. WHO | Updated recommendations on first-line and second-line antiretroviral regimens and post-exposure prophylaxis and recommendations on early infant diagnosis of HIV: interim guidance. *WHO* Available at: http://www.who.int/hiv/pub/guidelines/ARV2018update/en/. (Accessed: 19th December 2018)

3. World Health Organization & Global Tuberculosis Programme. *WHO treatment guidelines for drug-resistant tuberculosis: 2016 update.* (2016).

4. Hegreness, M., Shoresh, N., Damian, D., Hartl, D. & Kishony, R. Accelerated evolution of resistance in multidrug environments. *Proc. Natl. Acad. Sci.* **105**, 13977–13981 (2008).

5. Munck, C., Gumpert, H. K., Wallin, A. I. N., Wang, H. H. & Sommer, M. O. A. Prediction of resistance development against drug combinations by collateral responses to component drugs. *Sci. Transl. Med.* **6**, 262ra156-262ra156 (2014).

6. Lipsitch, M. & Levin, B. R. The population dynamics of antimicrobial chemotherapy. *Antimicrob. Agents Chemother.* **41**, 363–373 (1997).

7. Ventola, C. L. The Antibiotic Resistance Crisis. *Pharm. Ther.* **40**, 277–283 (2015).

8. Luepke, K. H. *et al.* Past, Present, and Future of Antibacterial Economics: Increasing Bacterial Resistance, Limited Antibiotic Pipeline, and Societal Implications. *Pharmacother. J. Hum. Pharmacol. Drug Ther.* **37**, 71–84 (2017).

9. WHO | Treatment of drug-resistant TB: Resources. *WHO* Available at: http://www.who.int/tb/areas-of-work/drug-resistant-tb/treatment/resources/en/. (Accessed: 19th December 2018)

10. Blomberg, B., Spinaci, S., Fourie, B. & Laing, R. The rationale for recommending fixed-dose combination tablets for treatment of tuberculosis. *Bull. World Health Organ.* **79**, 61–68 (2001).

11. Bantar, C. *et al.* Replacement of Broad-Spectrum Cephalosporins by Piperacillin-Tazobactam: Impact on Sustained High Rates of Bacterial Resistance. *Antimicrob. Agents Chemother.* **48**, 392–395 (2004).

12. Beta lactam antibiotic monotherapy versus beta lactam-aminoglycoside antibiotic combination therapy for sepsis - Paul, M - 2014 | Cochrane Library. Available at: https://www.cochranelibrary.com/cdsr/doi/10.1002/14651858.CD003344.pub3/abstract. (Accessed: 21st December 2018)

13. Bliziotis, I. A., Samonis, G., Vardakas, K. Z., Chrysanthopoulou, S. & Falagas, M. E. Effect of Aminoglycoside and β-Lactam Combination Therapy versus β-Lactam Monotherapy on the Emergence of Antimicrobial Resistance: A Meta-analysis of Randomized, Controlled Trials. *Clin. Infect. Dis.* **41**, 149–158 (2005).

14. Leibovici, L. *et al.* Monotherapy versus beta-lactam-aminoglycoside combination treatment for gram-negative bacteremia: a prospective, observational study. *Antimicrob. Agents Chemother.* **41**, 1127–1133 (1997).

15. Skorup, P. *et al.* Beneficial Antimicrobial Effect of the Addition of an Aminoglycoside to a β-Lactam Antibiotic in an E. coli Porcine Intensive Care Severe Sepsis Model. *PLOS ONE* **9**, e90441 (2014).

16. Tepekule, B., Uecker, H., Derungs, I., Frenoy, A. & Bonhoeffer, S. Modeling antibiotic treatment in hospitals: A systematic approach shows benefits of combination therapy over cycling, mixing, and mono-drug therapies. *PLOS Comput. Biol.* **13**, e1005745 (2017).

17. Should the Aminoglycoside β-Lactam Combination Be Abandoned in All Severely Ill Patients With Presumed Gram-Negative Infection? | Clinical Infectious Diseases | Oxford Academic. Available at: https://academic.oup.com/cid/article-abstract/66/3/480/4107422?redirectedFrom=fulltext. (Accessed: 21st December 2018)

18. Wong, A. Epistasis and the Evolution of Antimicrobial Resistance. *Front. Microbiol.* **8**, (2017).

19. Brochado, A. R. *et al.* Species-specific activity of antibacterial drug combinations. *Nature* **559**, 259 (2018).

20. Torella, J. P., Chait, R. & Kishony, R. Optimal Drug Synergy in Antimicrobial Treatments. *PLoS Comput. Biol.* **6**, (2010).

21. Chou, T.-C. Drug Combination Studies and Their Synergy Quantification Using the Chou-Talalay Method. *Cancer Res.* **70**, 440–446 (2010).

22. Lehár, J. *et al.* Synergistic drug combinations tend to improve therapeutically relevant selectivity. *Nat. Biotechnol.* **27**, 659–666 (2009).

23. Barbosa, C., Beardmore, R., Schulenburg, H. & Jansen, G. Antibiotic combination efficacy (ACE) networks for a Pseudomonas aeruginosa model. *PLoS Biol.* **16**, (2018).

24. Pena-Miller, R. *et al.* When the Most Potent Combination of Antibiotics Selects for the Greatest Bacterial Load: The Smile-Frown Transition. *PLoS Biol* **11**, e1001540 (2013).

25. Imamovic, L. & Sommer, M. O. A. Use of Collateral Sensitivity Networks to Design Drug Cycling Protocols That Avoid Resistance Development. *Sci. Transl. Med.* **5**, 204ra132-204ra132 (2013).

26. Lazar, V. *et al.* Bacterial evolution of antibiotic hypersensitivity. *Mol. Syst. Biol.* **9**, 700–700 (2014).

27. de Evgrafov, M. R., Gumpert, H., Munck, C., Thomsen, T. T. & Sommer, M. O. Collateral resistance and sensitivity modulate evolution of high-level resistance to drug combination treatment in Staphylococcus aureus. *Mol. Biol. Evol.* msv006 (2015).

28. Suzuki, S., Horinouchi, T. & Furusawa, C. Suppression of antibiotic resistance acquisition by combined use of antibiotics. *J. Biosci. Bioeng.* **120**, 467–469 (2015).

29. Imamovic, L. *et al.* Drug-Driven Phenotypic Convergence Supports Rational Treatment Strategies of Chronic Infections. *Cell* **172**, 121-134.e14 (2018).

30. Alteri, C. J. & Mobley, H. L. T. Escherichia coli physiology and metabolism dictates adaptation to diverse host microenvironments. *Curr. Opin. Microbiol.* **15**, 3–9 (2012).

31. Bodilsen, J. *et al.* Community-acquired meningitis in adults caused by Escherichia coli in Denmark and The Netherlands. *J. Infect.* **77**, 25–29 (2018).

32. Jahn, L. J. *et al.* Chromosomal barcoding as a tool for multiplexed phenotypic characterization of laboratory evolved lineages. *Sci. Rep.* **8**, 6961 (2018).

33. Jansen, G., Barbosa, C. & Schulenburg, H. Experimental evolution as an efficient tool to dissect adaptive paths to antibiotic resistance. *Drug Resist. Updat.* **16**, 96–107 (2013).

34. Jahn, L. J., Munck, C., Ellabaan, M. M. H. & Sommer, M. O. A. Adaptive Laboratory Evolution of Antibiotic Resistance Using Different Selection Regimes Lead to Similar Phenotypes and Genotypes. *Front. Microbiol.* **8**, (2017).

35. Haldane, J. B. S. Suggestions as to Quantitative Measurement of Rates of Evolution. *Evolution* **3**, 51–56 (1949).

36. Palmer, M. E. & Feldman, M. W. Survivability Is More Fundamental Than Evolvability. *PLOS ONE* **7**, e38025 (2012).

37. Jolivet-Gougeon, A. *et al.* Bacterial hypermutation: clinical implications. *J. Med. Microbiol.* **60**, 563–573 (2011).

38. Praski Alzrigat, L., Huseby, D. L., Brandis, G. & Hughes, D. Fitness cost constrains the spectrum of marR mutations in ciprofloxacin-resistant Escherichia coli. *J. Antimicrob. Chemother.* **72**, 3016–3024 (2017).

39. Woodford, N. & Ellington, M. J. The emergence of antibiotic resistance by mutation. *Clin. Microbiol. Infect.* **13**, 5–18 (2007).

40. Morriën, E. *et al.* Soil networks become more connected and take up more carbon as nature restoration progresses. *Nat. Commun.* **8**, 14349 (2017).

41. Bueno, M. L. *et al.* The environmental triangle of the Cerrado Domain: Ecological factors driving shifts in tree species composition between forests and savannas. *J. Ecol.* **106**, 2109–2120 (2018).

42. de la Torre-Castro, M., Fröcklin, S., Börjesson, S., Okupnik, J. & Jiddawi, N. S. Gender analysis for better coastal management – Increasing our understanding of social-ecological seascapes. *Mar. Policy* **83**, 62–74 (2017).

43. Clarke, K. R. Non-parametric multivariate analyses of changes in community structure. *Aust. J. Ecol.* **18**, 117–143 (1993).

44. Yu, E. W., Aires, J. R. & Nikaido, H. AcrB Multidrug Efflux Pump of Escherichia coli: Composite Substrate-Binding Cavity of Exceptional Flexibility Generates Its Extremely Wide Substrate Specificity. *J. Bacteriol.* **185**, 5657–5664 (2003).

45. Chevereau, G. & Bollenbach, T. Systematic discovery of drug interaction mechanisms. *Mol. Syst. Biol.* **11**, (2015).

46. Nazli, E., Zer, Y. & Eksi, F. In vitro efficacy of various antibiotic combinations against Pseudomonas aeruginosa isolates. *J. Int. Med. Res.* **43**, 217–225 (2015).

47. Nichol, D. *et al.* Antibiotic collateral sensitivity is contingent on the repeatability of evolution. *Nat. Commun.* **10**, 334 (2019).

48. Oz, T. *et al.* Strength of Selection Pressure Is an Important Parameter Contributing to the Complexity of Antibiotic Resistance Evolution. *Mol. Biol. Evol.* **31**, 2387–2401 (2014).

49. Barbosa, C. *et al.* Alternative Evolutionary Paths to Bacterial Antibiotic Resistance Cause Distinct Collateral Effects. *Mol. Biol. Evol.* doi:10.1093/molbev/msx158

50. Toprak, E. *et al.* Evolutionary paths to antibiotic resistance under dynamically sustained drug selection. *Nat. Genet.* **44**, 101–105 (2011).

51. Podnecky, N. L. *et al.* Conserved collateral antibiotic susceptibility networks in diverse clinical strains of Escherichia coli. *Nat. Commun.* **9**, 3673 (2018).

52. Wahl, L. M., Gerrish, P. J. & Saika-Voivod, I. Evaluating the Impact of Population Bottlenecks in Experimental Evolution. *Genetics* **162**, 961–971 (2002).

53. Meletiadis, J., Pournaras, S., Roilides, E. & Walsh, T. J. Defining Fractional Inhibitory Concentration Index Cutoffs for Additive Interactions Based on Self-Drug Additive Combinations, Monte Carlo Simulation Analysis, and In Vitro-In Vivo Correlation Data for Antifungal Drug Combinations against Aspergillus fumigatus. *Antimicrob. Agents Chemother.* **54**, 602–609 (2010).

54. Escherichia coli str. K-12 substr. MG1655, complete genome. (2014).

55. Li, W. & Godzik, A. Cd-hit: a fast program for clustering and comparing large sets of protein or nucleotide sequences. *Bioinformatics* **22**, 1658–1659 (2006).

56. Jari Oksanen, F. Guillaume Blanchet, Michael Friendly, Roeland Kindt, Pierre Legendre, Dan McGlinn, Peter R. Minchin, R. B. O'Hara, Gavin L. Simpson, Peter Solymos, M. Henry H. Stevens, Eduard Szoecs and Helene Wagner (2018). vegan: Community Ecology Package. R package version 2.5-2. https://CRAN.R-project.org/package=vegan

57. Matt Dowle and Arun Srinivasan (2018). data.table: Extension of `data.frame`. R package version 1.11.8. https://CRAN.R-project.org/package=data.table

58. Hadley Wickham (2011). The Split-Apply-Combine Strategy for Data Analysis. Journal of Statistical Software, 40(1), 1-29. URL http://www.jstatsoft.org/v40/i01/.

59. Hadley Wickham, Romain François, Lionel Henry and Kirill Müller (2018). dplyr: A Grammar of DataManipulation. R package version 0.7.7. https://CRAN.R-project.org/package=dplyr

60. Hadley Wickham and Lionel Henry (2018). tidyr: Easily Tidy Data with 'spread()' and 'gather()'Functions. R package version 0.8.2. https://CRAN.R-project.org/package=tidyr

61. H. Wickham. ggplot2: Elegant Graphics for Data Analysis. Springer-Verlag New York, 2016.

62. Gregory R. Warnes, Ben Bolker, Gregor Gorjanc, Gabor Grothendieck, Ales Korosec, Thomas Lumley, Don MacQueen, Arni Magnusson, Jim Rogers and others (2017). gdata: Various R Programming Tools for Data Manipulation. R package version 2.18.0. https://CRAN.R-project.org/package=gdata

63. Grosjean, Ph. (2018). SciViews-R. UMONS, Mons, Belgium. URL http://www.sciviews.org/SciViews-R.

64. Ritz, C., Baty, F., Streibig, J. C., Gerhard, D. (2015) Dose-Response Analysis Using R PLOS ONE, 10(12), e0146021

65. Hadley Wickham (2018). scales: Scale Functions for Visualization. R package version 1.0.0. https://CRAN.R-project.org/package=scales

66. Baptiste Auguie (2017). gridExtra: Miscellaneous Functions for "Grid" Graphics. R package version 2.3. https://CRAN.R-project.org/package=gridExtra

67. Claus O. Wilke (2018). cowplot: Streamlined Plot Theme and Plot Annotations for 'ggplot2'. R package version 0.9.3. https://CRAN.R-project.org/package=cowplot

68. Hadley Wickham (2018). stringr: Simple, Consistent Wrappers for Common String Operations. R package version 1.3.1. https://CRAN.R-project.org/package=stringr

69. Alboukadel Kassambara (2018). ggpubr: 'ggplot2' Based Publication Ready Plots. R packageversion 0.2. https://CRAN.R-project.org/package=ggpubr

70. Stefan Milton Bache and Hadley Wickham (2014). magrittr: A Forward-Pipe Operator for R. R package version 1.5. https://CRAN.Rproject.org/package=magrittr

71. Mauri, M., Elli, T., Caviglia, G., Uboldi, G., & Azzi, M. (2017). RAWGraphs: A Visualisation Platform to Create Open Outputs. In *Proceedings of the 12th Biannual Conference on Italian SIGCHI Chapter* (p. 28:1–28:5). New York, NY, USA: ACM. https://doi.org/10.1145/3125571.3125585

Acknowledgements

C. Munck and L. Imamovice advised on the panel of individual drugs to use and on the adaptive evolution experiment protocol. O. Bitterlin assisted C. Bradshaw in programming the robot used for preparing plates for the evolution experiment and for IC_{90} determination. In addition, we thank J.J. Collins, A. Porse, D. Kell, J. Yang, A. Lopatkin, S. Li, M.A. Misiakou and A.S. Hauser for helpful discussions and input on data representation.

Funding

This work was supported by the European Union's Horizon 2020 research and innovation program under the Marie Sklodowska-Curie grant agreement No 642738, MetaRNA as well from the European Union's Horizon 2020 (ERC-2014-StG) under grant agreement 638902, LimitMDR. In addition, funding was received from the Danish Council for Independent Research, Sapere Aude Program DFF 4004-00213 and from The Novo Nordisk Foundation under NFF grant number: NNF10CC1016517.

Author contribution

MOAS and LJJ conceived the project. CB, LJJ and DS prepared plates used for the adaptive laboratory evolution experiment with help of a Hamilton robot. LJJ, DS and MJ conducted all experimental work. LJJ analyzed and visualized the data. MMHE analyzed the genomic data for large insertions and deletions. LJJ wrote the manuscript with input from MOAS.

Genetic constrains limit resistance evolution in *P. aeruginosa*

Authors:

Leonie J. Jahn*

Daniel Simon*[1]

Mia Jensen*[2]

Charles Bradshaw*

Mostafa M. H. Ellabaan*

Morten O. A. Sommer*[§]

[§]Corresponding author: msom@bio.dtu.dk

*Author affiliation:

Novo Nordisk Foundation Center for Biosustainability, Technical University of Denmark, Kemitorvet 220, 2800 Kgs. Lyngby, DK

[1]Current affiliation:

Department of Computer Science, New York University Shanghai, 1555 Century Ave, Pudong Xinqu, Shanghai Shi, China, 200122

[2]Current affiliation:

NNIT A/S, Østmarken 3A, 2860 Søborg, DK

Abstract

Cystic fibrosis (CF) patients suffer from a rare genetic disease that results in increased amounts of mucus in the lung. The mucus represents an ideal habitat for bacteria wherefore CF patients often experience chronic lung infections that require long-term antibiotic treatment. Lung infections with the opportunistic pathogen *Pseudomonas aeruginosa* are especially problematic, as they are liked to an increased mortality of CF patients. In addition, antibiotic resistance is a serious problem when treating *P. aeruginosa* infections. To limit resistance evolution empirical drug combinations are administered. However, the advantage of combination therapy over single antibiotics remains controversial. Here, we studied the evolutionary trajectories towards antibiotic resistance to 22 single antibiotics and 33 antibiotic combinations in a systematic and controlled manner and found that antibiotic combinations overall limit and decelerate resistance evolution in *P. aeruginosa*. In addition, we studied the evolutionary trajectories towards antibiotic resistance and identified genetic constrains in the evolution that can be exploited by specific antibiotic combinations resulting in a highly limited resistance evolution.

Introduction

Antibiotic resistance is a recognized threat to human health and in particular Gram-negative bacteria are increasingly withstanding standard antibiotic treatments due to intrinsic and acquired resistance. *Pseudomonas aeruginosa* is an opportunistic human pathogen that can cause urinary tract, skin, bloodstream and soft tissue infections in humans (Streeter et al., 2016). In addition, it often colonizes the lungs of cystic fibrosis patients that have increased mucus production in the lungs caused by a rare genetic defect (Jaffé and Bush, 2001). In cystic fibrosis patients *P. aeruginosa* infections are associated with increased morbidity and mortality (Emerson et al., 2002) and treatment of *P. aeruginosa* remains challenging. *P. aeruginosa* is intrinsically resistant to a large number of antibiotics (Köhler et al., 1996; Li et al., 1994; 0kamoto et al., 2001). In addition, it often grows in biofilms, which was shown to decrease antibiotic susceptibility even further (Costerton et al., 1999; Mah et al., 2003; Whiteley et al., 2001). Moreover, antibiotic resistance is usually acquired rapidly either horizontally or vertically often resulting in multi-drug resistant lineages (Breidenstein et al., 2011). It was reported that about 60 % of *P. aeruginosa* isolates from patients suffering from cystic fibrosis are antibiotic resistant to at least one commonly prescribed antibiotic (Pitt et al., 2003). Major routes of resistance acquisition are mutations that increase the intrinsic efflux activity of one of the multiple efflux pumps (MexAB-OprM, MexCD-OprJ, MexEF-OprN , MexXY-OprM, and MexJK-OprM) that all have a broad substrate range (Chuanchuen et al.,

2002; Masuda et al., 2000; Vaez et al., 2014). In the clinic first line treatment of *P. aeruginosa* includes beta-lactams, quinolones, aminoglycosides and polymyxin antibiotics (Sordé et al., 2011). As resistance frequently occurs, empirical drug combinations are usually used (Banerjee and Stableforth, 2000). Yet, the impact of drug combinations on resistance evolution in *P. aeruginosa* has not been systematically studied under controlled conditions. Other treatment strategies have been explored in the laboratory and their applicability in the clinic was also observed (Imamovic et al., 2018). These alternative strategies include induction of metabolic changes in order to increase the susceptibility to specific antibiotics (Meylan et al., 2017), or the sequential cycling of different antibiotics (Imamovic et al., 2018; Roemhild et al., 2015, 2018). The drug cycling is based on the idea that resistance evolution can be limited by negative epistasis of resistance mutations as well as collateral sensitivity (Barbosa et al., 2019; Imamovic et al., 2018). Collateral sensitivity describes antibiotic resistant bacteria that are more susceptible to one or more antibiotics compared to the wild type due to their adaptation to an antibiotic (Szybalski and Bryson, 1952). Contrary, bacteria can also be collateral resistant when they adapted resistance to one antibiotic, which renders them more resistant to other antibiotics simultaneously (Szybalski and Bryson, 1952). It has been shown in *E. coli*, *S. aureus* and *P. aeruginosa* that collateral sensitivity in combination therapy can limit resistance evolution (Barbosa et al., 2018; de Evgrafov et al., 2015; Munck et al., 2014). In this study we examined the genetics underlying collateral sensitivity and resistance and the genetic constrains imposed by drug combinations with different collateral effects.

Results and Discussion

Collateral sensitivity and resistance are connected to genetic markers

In order to identify drug combinations that show diverse collateral relationships to each other, we evolved *P. aeuginosa* PAO1 in eight biological replicates to 22 different single antibiotics, spanning 9 different drug classes (Table S1), following the same evolution protocol as performed previously in *E. coli* (**manuscript 3**) and determined the collateral drug responses of all evolved lineages (Figure 1A). As observed before (Imamovic et al., 2018), lineages adapted to beta-lactam antibiotics display collateral resistance to each other and also to a certain extend to other drug classes such as quinolones, tetracyclines or macrolides. These drug classes were also repeatedly collateral resistant to each other but were at the same time often associated with mild collateral sensitivity to polymyxin and aminoglycoside antibiotics. While aminoglycoside evolved lineages often displayed collateral resistance to other aminoglycoside

antibiotics and some degree of collateral sensitivity to antibiotics of other drug classes. No significant increase in resistance was observed across the biological replicates adapted to polymyxin antibiotics in this study. It has previously been discussed that the disruption of gene *cprA* might hinder resistance evolution to colistin in PAO1 (Gutu et al., 2015). Another study observed that the killing efficiency of colistin is population density dependent, suggesting that inoculum effect might shield the population from colistin induced killing (Bulitta et al., 2010). Overall, it should be noticed that collateral resistance is more prevalent and collateral sensitivity less pronounced in *P. aeruginosa* compared *E. coli* (Imamovic and Sommer, 2013; Lázár et al., 2013, **manuscript 3**).

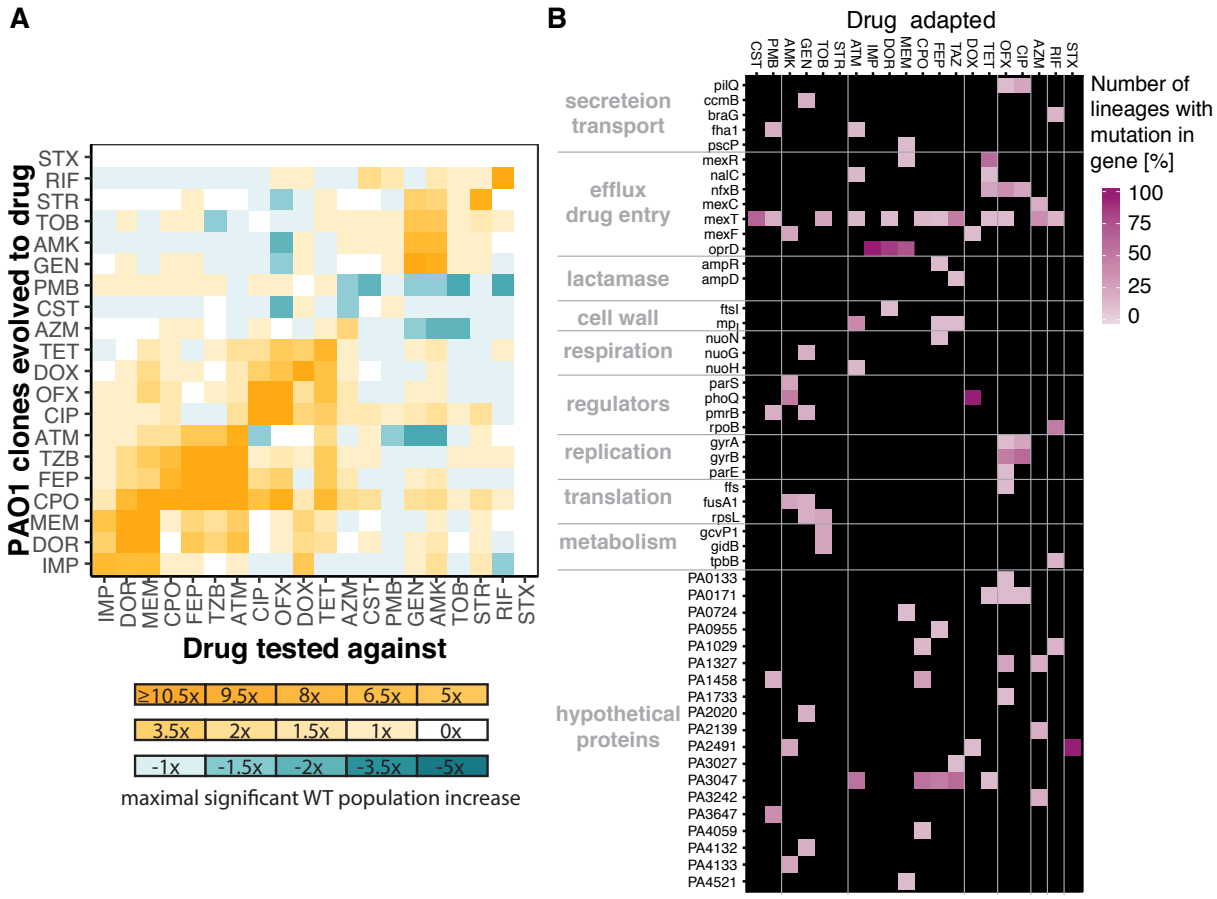

Figure 1: Phenotypic drug responses and genotypic adaptations after antibiotic adaptation. A Degree of significant collateral sensitivity (blue), neutral (white) or collateral resistance (orange) phenotypes of drug adapted PAO1 lineages compared to the wild type. **B** Mutations, functionally grouped, identified in the adapted lineages. The color intensity shows the percentage of biological replicates carrying a mutation in this gene per drug. Black indicates that the gene was not mutated in response to the antibiotic.

Moreover, it was shown in *E. coli* that collateral resistance and sensitivity can be linked to specific genetic mutations (Lázár et al., 2013, 2014). However, especially collateral resistance in *P. aeruginosa* might also occur in lineages whose genotypes are not overlapping (Barbosa et

al., 2017), highlighting the diverse routes of resistance acquisition in *P. aeruginosa*, which might also explain the dominance of collateral resistance in this pathogen. While collateral resistance seems difficult to be linked to specific genetic traits, markers for collateral sensitivity have been identified (Barbosa et al., 2017; Imamovic et al., 2018). It has been shown that a mutation in the regulator encoding gene *nfxB*, conferring resistance to quinolones, tetracyclines and macrolides, also increases susceptibility towards aminoglycosides, colistin and beta-lactam antibiotics (Imamovic et al., 2018; Masuda et al., 2001). Moreover, mutations in *pmrB* and *mexZ* causing resistance to aminoglycoside antibiotics exhibit also collateral sensitivity towards beta-lactam antibiotics (Barbosa et al., 2017). On the other hand, a deletion in *nalC* observed to increase resistance to beta-lactam antibiotics was linked to higher susceptibility to aminoglycoside antibiotics (Barbosa et al., 2017). In order to identify novel genetic markers for collateral sensitivity and resistance, we performed whole-genome sequencing on 123 single drug evolved lineages. While one study reported that parallel evolution between lineages adapted to different antibiotic classes was rare (Barbosa et al., 2017), another study found convergent evolution (Imamovic et al., 2018) in line with reports on resistance evolution in *E. coli* (Lázár et al., 2014). Our findings also indicate parallel evolution across lineages evolved to different antibiotics (Figure 1B). The highest prevalence across almost all tested antibiotics was observed for mutations in the regulator *mexT* that was shown to regulate efflux pumps, virulence factors and that is involved in stress response (Fargier et al., 2012; Jin et al., 2011; Tian et al., 2009). In addition, also mutations in the antagonist of *mexT* *mexS* (PA2491) were repeatedly identified. In general functional grouping of the mutations revealed that mutations affecting efflux and drug entry through porins were observed in response to all antibiotic classes. Mutations targeting secretion and transport as well as regulators, especially two-component systems, were also repeatedly observed in response to several drug classes. A few hypothetical proteins were also mutated after adaptation to at least two different antibiotic classes such as PA0171, probably involved in motility twitching (Shan et al., 2004) and PA1327 a probable protease (Winsor et al., 2016). On the other hand, mutations affecting the expression of beta-lactamases or cell wall composition were exclusive to lineages evolved to beta-lactam antibiotics. Replication was only affected in response to quinolone antibiotics and the translation machinery was only mutated in lineages exposed to aminoglycoside antibiotics (Figure 1B). In addition, our data supports the studies mentioned earlier as we can confirm mild collateral sensitivity towards aminoglycosides for lineages that carry mutations in *nfxB* or a frameshift mutation in *nalC* (Table 1). Interestingly, a missense mutation in *nalC* was not associated with collateral sensitivity to aminoglycosides (Table 1).

We can also confirm collateral resistance between lineages carrying mutations in the two-component system *pmrB* and aminoglycosides or polymyxin B, respectively (Abraham and Kwon, 2009; López-Causapé et al., 2018) (Table 1) and moderate collateral sensitivity against some beta-lactam antibiotics (Table 1) (Barbosa et al., 2017). In addition, we identified that mutations in the outer membrane protein PA3647 in response to polymyxin B that conferred a small increase in colistin resistance and that has been identified before in response to colistin exposure (Dößelmann et al., 2017), was associated with strong collateral sensitivity to nearly all other drug classes (Table 1). Finally, we also observed that mutations in *gyrB* in response to quinolone antibiotics resulted in increased collateral sensitivity towards aminoglycosides and imipenem (Table 1).

Table 1: Genetic markers for collateral sensitivity and resistance and their phenotypic resistance profiles. Abbreviations for antibiotics are explained in Table S1. Values are fold change compared to the wild type and colors indicate collateral sensitivity (blue) or collateral resistance (orange).

Gene	Position	Lineage	Genetic background	AMK	GEN	TOB	STR	CST	PMB	FEP	TZB	CPO	IMP	DOR	MEM	ATM	CIP	OFX	TET
nfxB	Insertion	PA_OFX_1	*gyrA*	0.7	0.5	0.7	0.6	0.8	2	6.4	1.2	7.6	0.7	1.7	0.88	0.2	34	30	2.6
nfxB	Insertion	PA_OFX_3	*ffs, PA0133*	0.8	0.5	0.5	0.5	0.6	1.3	4.9	1.7	9.4	0.5	1.5	0.82	0.46	37	16	3.3
nfxB	Insertion nfxB promoter	PA_OFX_8	*pilQ*	0.2	0.5	0.4	0.4	0.5	0.6	7.7	1.4	16	0.5	NA	4.92	3.06	32	29	7.5
nfxB	Tyr101*	PA_TET_2		0.6	0.8	0.7	0.6	0.7	1	5.3	1.1	18	0.9	1	0.68	0.7	26	8.1	9
nfxB	Arg23*	PA_TET_8	*PA0171*	0.6	0.4	0.4	0.4	0.6	1.1	4.5	0.9	11	0.2	1.5	0.79	NA	18	10	5
nfxB	Deletion	PA_CIP_1	*gyrB*	0.8	0.7	0.8	0.6	0.6	1.3	5.2	1.4	7.6	0.8	1.5	1.66	0.45	23	19	2.7
nfxB	Deletion	PA_CIP_5	*gyrB*	0.8	0.8	2.3	0.7	0.8	1.5	2.6	1.1	5.9	0.9	1.4	1.15	1.09	18	15	1.7
nalC	Leu203Gln	PA_TET_3		0.7	1.2	1.1	1.3	1	2.1	2.4	3.2	1.9	0.9	2	1.44	2.39	2.3	2.4	2.3
nalC	Tyr157*	PA_ATM_6		0.9	0.7	0.7	0.8	0.8	2.1	13	3.3	NA	1.1	16	10.3	26	3.5	3.1	5.7
pmrB	Met292Thr	PA_PMB_3	*fha1, mexT*	3.3	5.9	3.4	1.8	1.4	1.3	0.5	0.7	0.7	0.5	1	0.66	0.26	3.1	1	1.2
pmrB	Ser80Asn	PA_GEN_3	*nuoG*	28	57	13	44	0.9	18	2.8	1	3.7	0.6	3.8	1.27	0.23	3.7	1.9	1
PA3647	Asn57fs	PA_PMB_6		0.8	0.6	0.6	0.4	2.3	0.9	0.5	1	0.6	0.3	0.8	0.75	0.46	0.9	0.6	0.2
PA3647	Gln70*	PA_PMB_8		0.8	0.6	0.6	0.3	2.2	0.9	NA	0.4	0.5	0.3	0.5	0.74	0.13	0.6	0.2	0.2
gyrB	Glu468Asp	PA_CIP_1	*nfxB*	0.8	0.7	0.8	0.6	0.6	1.3	5.2	1.4	7.6	0.8	1.5	1.66	0.45	23	19	2.7
gyrB	Glu468Asp	PA_CIP_4		0.9	0.6	0.9	0.5	0.9	1.6	5.4	2.4	12	0.8	1.6	0.92	1.84	47	44	3.6
gyrB	Ser466Phe	PA_CIP_5	*nfxB*	0.8	0.8	2.3	0.7	0.8	1.5	2.6	1.1	5.9	0.9	1.4	1.15	1.09	18	15	1.7
gyrB	Pro749Ser	PA_CIP_6		1.6	0.6	0.6	0.4	0.6	1.6	5.2	1.5	8.5	0.4	1.8	0.81	0.42	38	18	5
gyrB	Val469Phe	PA_CIP_7	*pilQ*	1	0.5	0.7	0.6	0.5	2.4	5.5	1.4	8.3	0.7	2.3	0.93	0.3	41	25	5.3
gyrB	Gly784_Asp785insGly	PA_OFX_2		0.2	0.3	0.2	0.3	0.9	0.5	4.9	1.1	9.5	0.1	1.6	0.8	0.29	34	20	13
gyrB	Glu468Val	PA_OFX_5	*PA1327*	0.9	0.5	0.5	0.5	0.5	0.5	3.8	1.2	13	0.2	1.5	0.85	0.29	43	29	11
gyrB	Ser466Phe	PA_OFX_6		0.7	1.8	0.8	1.3	0.8	2.5	5.2	NA	10	0.8	3.3	NA	3.9	37	24	8.5
gyrB	Thr510Ile	PA_OFX_8	*PA0171, pilQ, nfxB*	0.2	0.5	0.4	0.4	0.5	0.6	7.7	1.4	16	0.5	NA	4.92	3.06	32	29	7.5

In short, we observed collateral resistance and parallel evolution across multiple drug classes in PAO1 in response to antibiotic exposure but also identified collateral sensitivity relationships that could be linked to known and unknown genetic markers.

Antibiotic combination therapy limits resistance evolution

In order to test our hypothesis that collateral sensitivity might constrain resistance evolution in drug combinations, we performed a second adaptive laboratory evolution experiment, following the same protocol as before, adapting PAO1 in eight biological replicates towards 33 different drug combinations (Table S2). The antibiotic pairs covered a broad variety in their collateral resistance and sensitivity profile (Figure S1). A previous study on the impact of collateral sensitivity on resistance evolution towards drug combinations in *P. aeruginosa* used

growth during the adaptive evolution experiment and extinction as parameters to evaluate the evolvability (Barbosa et al., 2018). Both parameters have been previously described as measures for evolvability (Hegreness et al., 2008; Palmer and Feldman, 2012). However, it was recently demonstrated that these parameters alone might not be sufficient to characterize the evolvability and that final resistance phenotypes towards the individual as well as to the drug pairs are equally important to quantify the evolvability precisely (**manuscript 3**). Consequently, we analysed the adaptive potential of *P. aeruginosa* towards drug combinations with the evolvability index (de Evgrafov et al., 2015; Munck et al., 2014, **manuscript 3**), the phenotypic evolutionary rate (Haldane, 1949, **manuscript 3**), extinction (Palmer and Feldman, 2012), and by the number of generations underwent during the evolution experiment, normalized to the wild type (**manuscript 3**). We found as described for *E. coli* that the evolvability varies dependent on the characteristics of the drug pair (**manuscript 3**), but that overall the phenotypic evolutionary rate, extinction rates and growth during the evolution experiment suggest that combination therapy generally limits resistance evolution in *P. aeruginosa* (Figure 2).

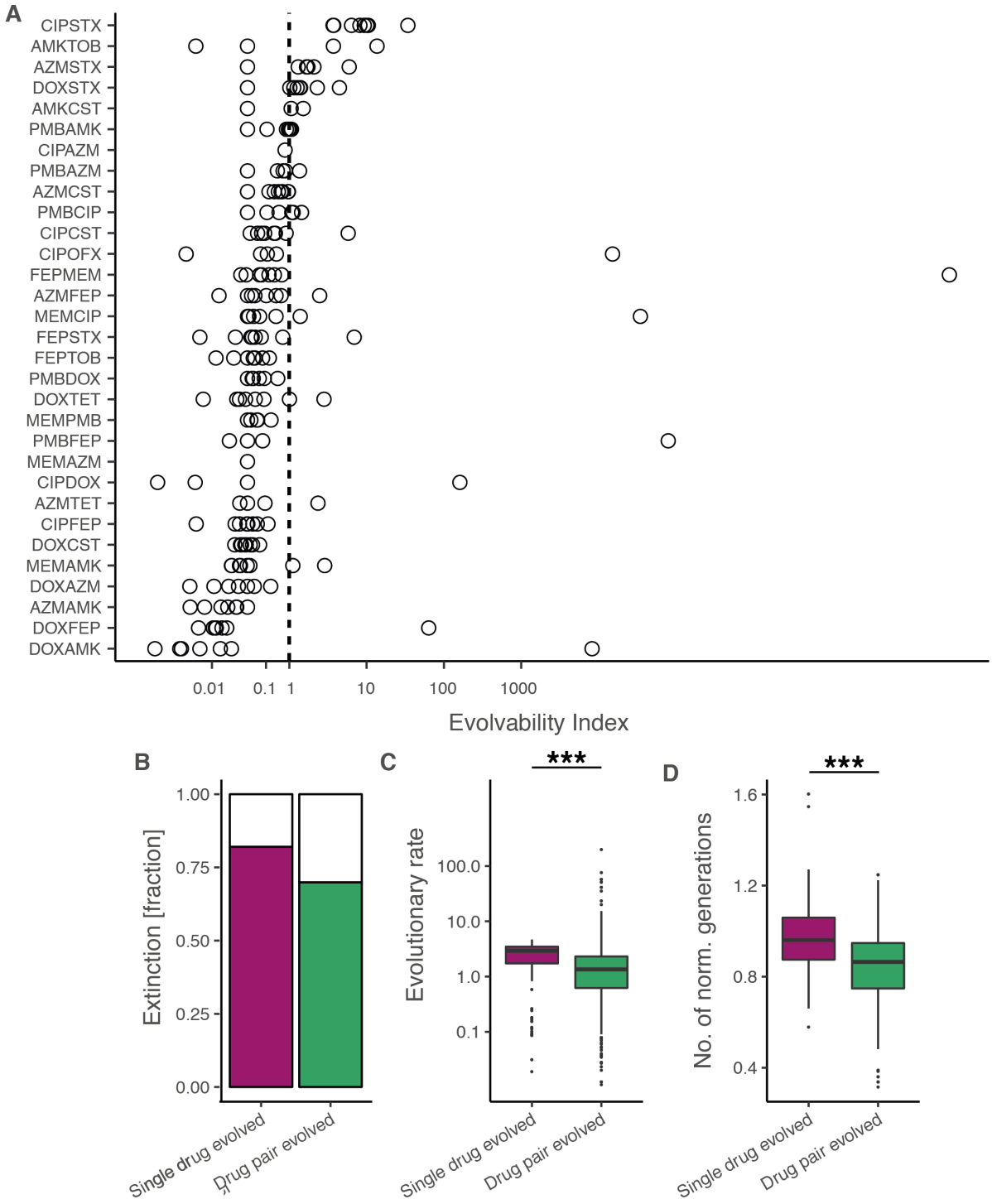

Figure 2: Evolvability of PAO1 in response to antibiotic combinations. A Drug pairs are ordered by their median evolvability index. Abbreviations for the antibiotics can be found in table S2. Dots represent the evolvability index of the biological replicates evolved to a certain drug combination. Dots in the blue area are below 1 indicating reduced resistance evolution compared to resistance evolution to individual antibiotics and dots in the orange area have increased resistance evolution. **B** Fraction of lineages that went extinct during the adaptive laboratory evolution experiment in response to single drug (purple) or drug pair (green) exposure. **C** The phenotypic evolutionary rate of lineages exposed to single (purple) or paired (green) antibiotics. The difference is significant (Kruskal-Wallis test, $p < 0.001$). **D** Number of generations underwent during the evolution experiment normalized to the WT evolved in parallel between lineages exposed to individual drugs (purple) or drug pairs (green). The difference is significant (Mann-Whitney-U-test, $p < 0.001$).

Drug pairs with collateral sensitivity decelerate resistance evolution

To test weather collateral drug responses impact resistance evolution, we grouped the drug pairs according to their collateral drug responses (Figure S1) and analysed their impact on the different features of evolvability as well as on the growth rate (Figure 3). In line with recent findings in *E. coli* we do see a small decrease in the evolvability in drug pairs with collateral sensitivity, yet not significant (**manuscript 3**) (Figure 3A). The phenotypic evolutionary rate however was significantly decreased in drug pairs with collateral sensitivity (Mann-Whitney-U-test, $p < 0.001$) (Figure 3B) similar to findings in *E. coli* (**manuscript 3**). In addition, extinction occurred more often and earlier in lineages exposed to drug pairs with collateral sensitivity (Figure 3C). The doubling time in LB was slightly (Mann-Whitney-U-test, $p > 0.05$) increased in lineages after adaptation to drug pairs with collateral sensitivity (Figure 3E) and the overall growth during the evolution experiment was significantly reduced (Mann-Whitney-U-test, $p < 0.001$) in agreement with previous reports (Barbosa et al., 2018). These findings suggest, that collateral sensitivity of individual drug adapted lineages can limit resistance evolution in *P. aeruginosa* better compared to drug pairs with collateral resistance.

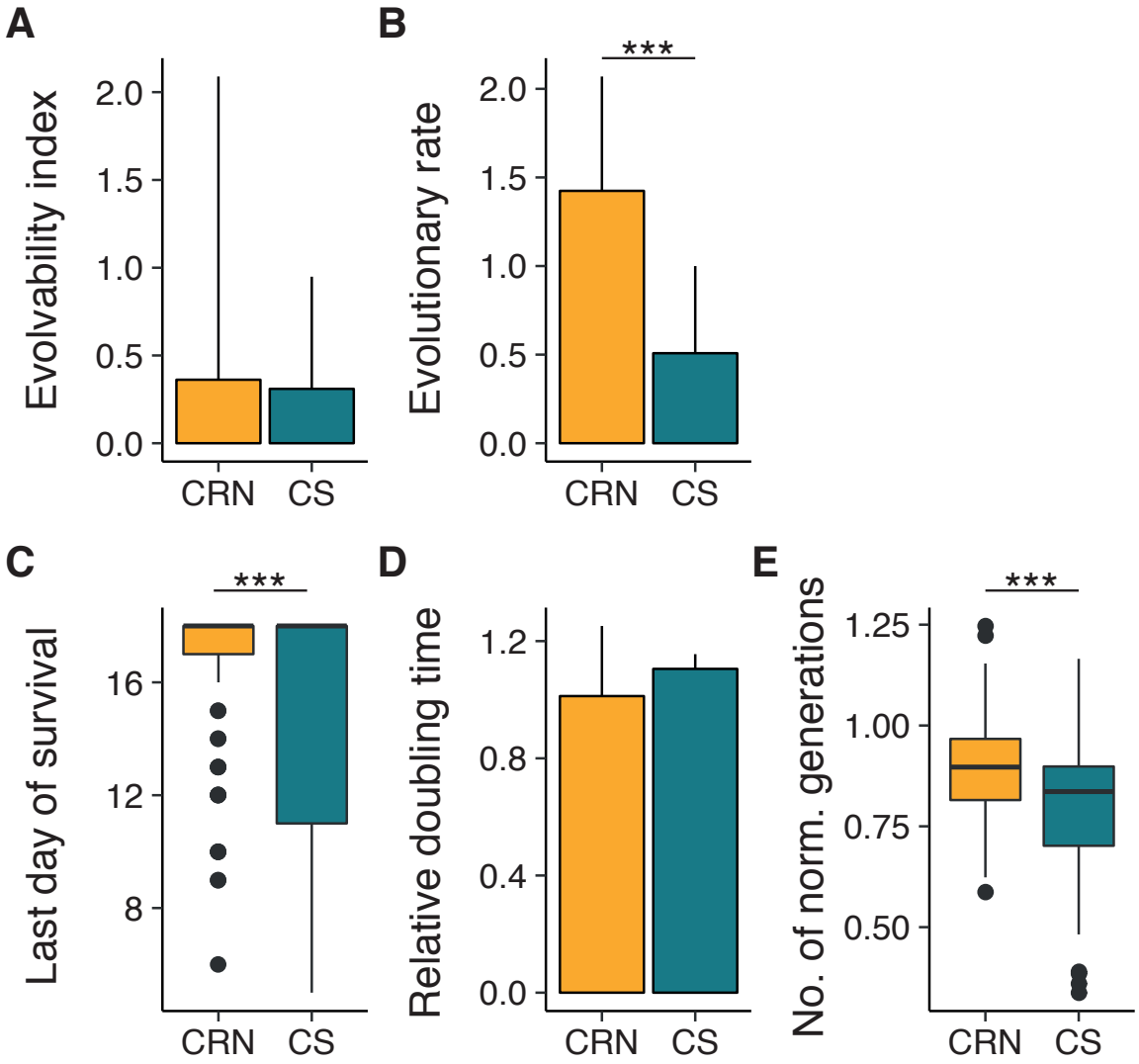

Figure 3: Effect of collateral resistance and sensitivity on the evolvability towards drug combinations. A Drug pairs were divided into collateral sensitivity and resistance according to Figure S1. Lineages evolved to drug pairs in the collateral sensitivity (blue) group had a lower evolvebility index (Mann-Whitney-U-test, $p > 0.05$) compared to lineages evolved to drugs in the collateral resistant group (orange). **B** Drug pairs were divided into collateral sensitivity and resistance according to Figure S1. Lineages evolved to drug pairs in the collateral sensitivity (blue) group had a significantly lower evolutionary rate (Mann-Whitney-U-test, $p < 0.001$) compared to lineages evolved to drugs in the collateral resistant group (orange) **C** Drug pairs were divided into collateral sensitivity and resistance according to Figure S1. Lineages evolved to drug pairs in the collateral sensitivity (blue) group went extinct significantly earlier (Mann-Whitney-U-test, $p < 0.001$) compared to lineages evolved to drugs in the collateral resistant group (orange). **D** Drug pairs were divided into collateral sensitivity and resistance according to Figure S1. Lineages evolved to drug pairs in the collateral sensitivity (blue) group had a higher doubling time in LB (Mann-Whitney-U-test, $p > 0.05$) compared to lineages evolved to drugs in the collateral resistant group (orange). **E** Drug pairs were divided into collateral sensitivity and resistance according to Figure S1. Lineages evolved to drug pairs in the collateral sensitivity (blue) group underwent significantly fewer generations (Mann-Whitney-U-test, $p < 0.001$) compared to lineages evolved to drugs in the collateral resistant group (orange).

Nonetheless, it was recently shown that collateral sensitivity occurs only with a certain probability (Nichol et al., 2019) and that multiple trajectories are open to resistance evolution in drug pairs, wherefore collateral sensitivity alone might not be sufficient to predict limited resistance evolution (**manuscript 3**). And indeed, we also observed some drug pairs, e.g. polymyxin B or colistin mixed with azithromycin with collateral sensitivity to each other that displayed a high evolvability index and moderate evolutionary rate, despite their collateral sensitivity (Figure S1, Figure 1, Table S3). As it was shown that the genetic trajectories leading to drug resistance are better suited to identify drug combinations that limit resistance evolution (**manuscript 3**), we also performed whole-genome sequencing on 132 lineages adapted to antibiotic pairs (Table S4). We compared the genomes of the drug pair evolved lineages to those that were adapted to the individual dugs constituting the pairs and identified examples of how collateral sensitivity and resistance can shape resistance evolution towards antibiotic pairs. The drug combination cefepime and tobramycin displayed reciprocal collateral sensitivity, suggesting genetic incompatibility between the trajectories towards the individual drugs. Interestingly, all lineages evolved to this drug combinations went extinct early on in the evolution experiment (average last day of survival = 6.4, ±SD 0.5, Table S3) further highlighting constrains in adapting resistance to this drug combination. Sequencing of the adapted lineages revealed a high degree of parallel evolution and no variation among the biological replicates, suggesting that the evolutionary space to accumulate mutations against this drug combination is highly limited. All lineages carried mutations in the two-component system encoding gene *phoQ* (Table S4) that was previously described to confer aminoglycoside resistance (Macfarlane et al., 2000). Our findings are in line with reports stating that tobramycin can suppress resistance evolution towards cefepime (Drusano et al., 2012). It was shown that beta-lactamase expression is reduced through tobramycin and it is believed that this might contribute to the resistance suppressing phenotype (Drusano et al., 2012). In addition, our data suggests that resistance evolution is further suppressed by incompatible genetic trajectories that are usually taken when resistance is evolved to the individual drugs. Another example of limited resistance evolution is the drug combination polymyxin B and amikacin. A mutation in the two-component system encoding gene *pmrB* was found in response to gentamicin as well as polymyxin B exposure (Table 1). Mutations in *pmrB* resulted in mild collateral resistance between polymyxin B and gentamicin evolved lineages (Table S1), yet in absence of *pmrB* mutations lineages would be either neutral or even collateral sensitive to each other, highlighting genetic constrains for other genotypic

adaptations. Interestingly, we observed that in response to the combination of polymyxin B and amikacin lineages were evolving highly similarly, only accumulating mutations in *pmrB* and no other target (Table S4). This observation underlines that genetic constrains guide resistance evolution to combination therapy and that collateral sensitivity and resistance shape genetic responses to drug combinations in *P. aeruginosa*. In summary, even though collateral sensitivity by itself is likely not sufficient to predict limited resistance evolution in PAO1, it impacts the genotypic adaptations to single drugs and antibiotic combinations and can therefore be an valid starting point to identify treatment regimes that drive genetic trajectories during resistance evolution rationally and eventually decelerate resistance evolution.

Materials and Methods

Bacterial strains and growth conditions

P. aeruginosa PAO1 was grown at 37 °C shaking at 300 r.p.m. in LB.

Adaptive laboratory evolution (ALE)

The evolution experiment was conducted as described before in more detail (**manuscript 3**). In short, eight biological replicates were exposed to either 22 individual antibiotics (Table S1) or 33 different antibiotic pairs (Table S2) in LB in a total volume of 1 ml in 96-deep-well plates. In addition, 20 wild type populations were evolved in parallel in LB to control for media adaptations. The antibiotic concentration was increased by 25 % after 24 hours when cells were transferred in a 20-fold dilution to a fresh plate. After each transfer 50 µl of the remaining population were saved as a glycerol stock and stored at -80 °C. The antibiotic concentration at which 10 % of growth based on the optical density (OD_{600}) measured in an ELx808 Absorbance reader (BioTek), was reached compared to growth in LB without antibiotic (IC_{90}) of the wild type was reached after 7 days of evolution. The evolution experiment was continued for in total 18 days when the wild type IC_{90} was exceeded at least 10 times. Lineages were streaked on LB agar from the last day of growth during the evolution experiment and an isolated colony was saved as glycerol stock for subsequent characterization. However, some lineages would fail to revive as reported previously (Barbosa et al., 2017, **manuscript 3**). When lineages would not grow, they were recovered in liquid LB first or a previous day of the evolution experiment was used. Yet, this did not result in recovery of all replicates. A list with the last day of growth and day of revival can be found in table S5.

IC_{90} determination

The IC_{90} was determined as described before (Munck et al., 2014) in technical replicates. Isolated colonies were grown over night in LB and approximately 10^6 cells were transferred with pin-replicators (Almeco) to a 10-step 2-fold gradient and LB without antibiotic as growth control. Plates were incubated at 37 °C and the OD_{600} was determined. Growth was normalized to growth in the LB control and the growth inhibition by the antibiotic was calculated. A dose-response curve was fitted on the data and used to identify the IC_{90}. Significant increases in IC_{90} compared to the wild type were calculated using bootstrapping and a p-value cutoff of $p < 0.0001$ as described before (Imamovic et al., 2018, **manuscript 3**).

Evolvability index and evolutionary rate

The evolvability index was calculated by dividing the sum of normalized IC_{90} values of the drug pair evolved lineages to the individual drugs constituting the pair with the sum of IC_{90} values of the individual drug evolved lineages of the corresponding antibiotics (Munck et al., 2014). The phenotypic evolutionary rate was calculated by subtracting the natural logarithm of the IC_{90} before the evolution was started from the natural logarithm of the IC_{90} after the evolution experiment was ended of the drug or drug pair that the lineage was evolved against. Thereafter, this value was divided by the number of days the lineage was evolved for (**manuscript 3**).

Determination of doubling time

The doubling time was measured of isolated colonies after the adaptive evolution experiment. Cells were grown overnight in LB, diluted on the next day and when exponential growth phase was reached used to inoculate 150 µl LB with pin-replicators. Plates were grown at 37 °C shaking and the OD_{600} was measured every 5 minutes for 24 hours. Based on the OD data the doubling time during exponential growth phase was calculated as described before (Jahn et al., 2017).

Whole-genome sequencing and sequence analysis

Cells were sent for genome extraction and 125 paired-end whole-genome Illumina HiSeq 2500 sequencing to BaseClear B.V.. Fasta reads were analysed as described previously (**manuscript 3**). In short, CLC Genomics workbench was used to identify single nucleotide polymorphisms at a frequency of 80% or higher as well as large insertions and deletions at default parameters. Insertions and deletions were included when they occurred in 80% of the reads and at least in 5 different reads. Mutations found in the media adapted lineages were removed from the

dataset as they are likely media adaptations. The sequencing data will be available at NCBI upon publication.

Data availability and code

The code used for the analysis will be available at GitHub. Data will be shared upon request.

Supplementary information

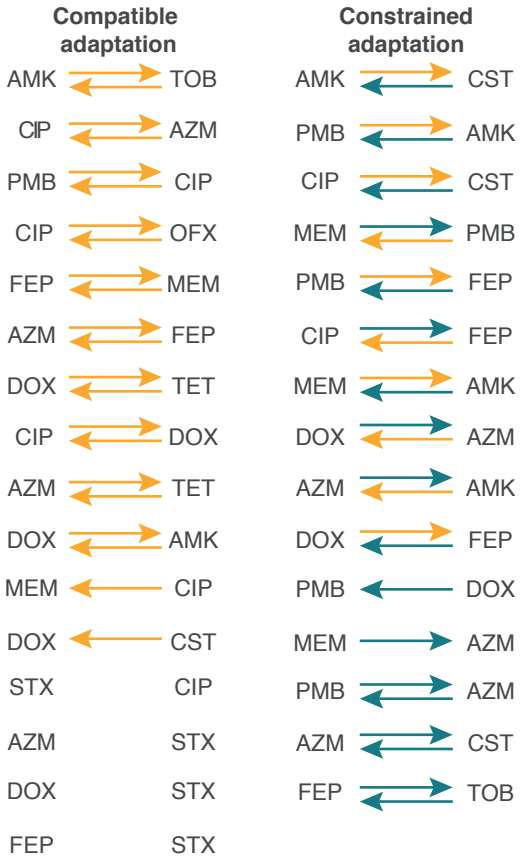

Figure S1: Drug pairs with neutral (no arrow) or collateral resistant (orange arrow) relationships are grouped as collateral resistant, while drug pairs with collateral sensitivity (blue arrow) in at least one direction form their own group. Abbreviations of antibiotics can be found in table S1 and S2.

All supplemental tables can be accessed under:

https://www.dropbox.com/home/Supplementary/PAO1_Supplemental_files

References

Abraham, N., and Kwon, D.H. (2009). A single amino acid substitution in PmrB is associated with polymyxin B resistance in clinical isolate of Pseudomonas aeruginosa. FEMS Microbiol. Lett. *298*, 249–254.

Banerjee, D., and Stableforth, D. (2000). The treatment of respiratory pseudomonas infection in cystic fibrosis: what drug and which way? Drugs *60*, 1053–1064.

Barbosa, C., Trebosc, V., Kemmer, C., Rosenstiel, P., Beardmore, R., Schulenburg, H., and Jansen, G. (2017). Alternative Evolutionary Paths to Bacterial Antibiotic Resistance Cause Distinct Collateral Effects. Mol. Biol. Evol. *34*, 2229–2244.

Barbosa, C., Beardmore, R., Schulenburg, H., and Jansen, G. (2018). Antibiotic combination efficacy (ACE) networks for a Pseudomonas aeruginosa model. PLoS Biol. *16*.

Barbosa, C., Roemhild, R., Rosenstiel, P., and Schulenburg, H. (2019). Evolutionary stability of collateral sensitivity to antibiotics in the model pathogen Pseudomonas aeruginosa. BioRxiv 570663.

Breidenstein, E.B.M., de la Fuente-Núñez, C., and Hancock, R.E.W. (2011). Pseudomonas aeruginosa: all roads lead to resistance. Trends Microbiol. *19*, 419–426.

Bulitta, J.B., Yang, J.C., Yohonn, L., Ly, N.S., Brown, S.V., D'Hondt, R.E., Jusko, W.J., Forrest, A., and Tsuji, B.T. (2010). Attenuation of Colistin Bactericidal Activity by High Inoculum of Pseudomonas aeruginosa Characterized by a New Mechanism-Based Population Pharmacodynamic Model. Antimicrob. Agents Chemother. *54*, 2051–2062.

Chuanchuen, R., Narasaki, C.T., and Schweizer, H.P. (2002). The MexJK Efflux Pump of Pseudomonas aeruginosa Requires OprM for Antibiotic Efflux but Not for Efflux of Triclosan. J. Bacteriol. *184*, 5036–5044.

Costerton, J.W., Stewart, P.S., and Greenberg, E.P. (1999). Bacterial Biofilms: A Common Cause of Persistent Infections. Science *284*, 1318–1322.

Dößelmann, B., Willmann, M., Steglich, M., Bunk, B., Nübel, U., Peter, S., and Neher, R.A. (2017). Rapid and Consistent Evolution of Colistin Resistance in Extensively Drug-Resistant

Pseudomonas aeruginosa during Morbidostat Culture. Antimicrob. Agents Chemother. *61*, e00043-17.

Drusano, G.L., Bonomo, R.A., Bahniuk, N., Bulitta, J.B., Vanscoy, B., Defiglio, H., Fikes, S., Brown, D., Drawz, S.M., Kulawy, R., et al. (2012). Resistance emergence mechanism and mechanism of resistance suppression by tobramycin for cefepime for Pseudomonas aeruginosa. Antimicrob. Agents Chemother. *56*, 231–242.

Emerson, J., Rosenfeld, M., McNamara, S., Ramsey, B., and Gibson, R.L. (2002). Pseudomonas aeruginosa and other predictors of mortality and morbidity in young children with cystic fibrosis. Pediatr. Pulmonol. *34*, 91–100.

de Evgrafov, M.R., Gumpert, H., Munck, C., Thomsen, T.T., and Sommer, M.O. (2015). Collateral resistance and sensitivity modulate evolution of high-level resistance to drug combination treatment in Staphylococcus aureus. Mol. Biol. Evol. msv006.

Fargier, E., Aogáin, M.M., Mooij, M.J., Woods, D.F., Morrissey, J.P., Dobson, A.D.W., Adams, C., and O'Gara, F. (2012). MexT Functions as a Redox-Responsive Regulator Modulating Disulfide Stress Resistance in Pseudomonas aeruginosa. J. Bacteriol. *194*, 3502–3511.

Gutu, A.D., Rodgers, N.S., Park, J., and Moskowitz, S.M. (2015). Pseudomonas aeruginosa high-level resistance to polymyxins and other antimicrobial peptides requires cprA, a gene that is disrupted in the PAO1 strain. Antimicrob. Agents Chemother. *59*, 5377–5387.

Haldane, J.B.S. (1949). Suggestions as to Quantitative Measurement of Rates of Evolution. Evolution *3*, 51–56.

Hegreness, M., Shoresh, N., Damian, D., Hartl, D., and Kishony, R. (2008). Accelerated evolution of resistance in multidrug environments. Proc. Natl. Acad. Sci. *105*, 13977–13981.

Imamovic, L., and Sommer, M.O.A. (2013). Use of Collateral Sensitivity Networks to Design Drug Cycling Protocols That Avoid Resistance Development. Sci. Transl. Med. *5*, 204ra132-204ra132.

Imamovic, L., Ellabaan, M.M.H., Dantas Machado, A.M., Citterio, L., Wulff, T., Molin, S., Krogh Johansen, H., and Sommer, M.O.A. (2018). Drug-Driven Phenotypic Convergence Supports Rational Treatment Strategies of Chronic Infections. Cell *172*, 121-134.e14.

Jaffé, A., and Bush, A. (2001). Cystic fibrosis: review of the decade. Monaldi Arch. Chest Dis. Arch. Monaldi Mal. Torace *56*, 240–247.

Jahn, L.J., Munck, C., Ellabaan, M.M.H., and Sommer, M.O.A. (2017). Adaptive Laboratory Evolution of Antibiotic Resistance Using Different Selection Regimes Lead to Similar Phenotypes and Genotypes. Front. Microbiol. *8*.

Jin, Y., Yang, H., Qiao, M., and Jin, S. (2011). MexT Regulates the Type III Secretion System through MexS and PtrC in Pseudomonas aeruginosa. J. Bacteriol. *193*, 399–410.

Köhler, T., Kok, M., Michea-Hamzehpour, M., Plesiat, P., Gotoh, N., Nishino, T., Curty, L.K., and Pechere, J.C. (1996). Multidrug efflux in intrinsic resistance to trimethoprim and sulfamethoxazole in Pseudomonas aeruginosa. Antimicrob. Agents Chemother. *40*, 2288–2290.

Lázár, V., Pal Singh, G., Spohn, R., Nagy, I., Horváth, B., Hrtyan, M., Busa-Fekete, R., Bogos, B., Méhi, O., Csörgő, B., et al. (2013). Bacterial evolution of antibiotic hypersensitivity. Mol. Syst. Biol. *9*, 700.

Lázár, V., Nagy, I., Spohn, R., Csörgő, B., Györkei, Á., Nyerges, Á., Horváth, B., Vörös, A., Busa-Fekete, R., Hrtyan, M., et al. (2014). Genome-wide analysis captures the determinants of the antibiotic cross-resistance interaction network. Nat. Commun. *5*, 4352.

Li, X.Z., Livermore, D.M., and Nikaido, H. (1994). Role of efflux pump(s) in intrinsic resistance of Pseudomonas aeruginosa: resistance to tetracycline, chloramphenicol, and norfloxacin. Antimicrob. Agents Chemother. *38*, 1732–1741.

López-Causapé, C., Rubio, R., Cabot, G., and Oliver, A. (2018). Evolution of the Pseudomonas aeruginosa Aminoglycoside Mutational Resistome In Vitro and in the Cystic Fibrosis Setting. Antimicrob. Agents Chemother. *62*, e02583-17.

Macfarlane, E.L., Kwasnicka, A., and Hancock, R.E. (2000). Role of Pseudomonas aeruginosa PhoP-phoQ in resistance to antimicrobial cationic peptides and aminoglycosides. Microbiol. Read. Engl. *146 (Pt 10)*, 2543–2554.

Mah, T.-F., Pitts, B., Pellock, B., Walker, G.C., Stewart, P.S., and O'Toole, G.A. (2003). A genetic basis for Pseudomonas aeruginosa biofilm antibiotic resistance. Nature *426*, 306.

Masuda, N., Sakagawa, E., Ohya, S., Gotoh, N., Tsujimoto, H., and Nishino, T. (2000). Substrate Specificities of MexAB-OprM, MexCD-OprJ, and MexXY-OprM Efflux Pumps in Pseudomonas aeruginosa. Antimicrob. Agents Chemother. *44*, 3322–3327.

Masuda, N., Sakagawa, E., Ohya, S., Gotoh, N., and Nishino, T. (2001). Hypersusceptibility of the Pseudomonas aeruginosa nfxB Mutant to β-Lactams Due to Reduced Expression of the AmpC β-Lactamase. Antimicrob. Agents Chemother. *45*, 1284–1286.

Meylan, S., Porter, C.B.M., Yang, J.H., Belenky, P., Gutierrez, A., Lobritz, M.A., Park, J., Kim, S.H., Moskowitz, S.M., and Collins, J.J. (2017). Carbon Sources Tune Antibiotic Susceptibility in Pseudomonas aeruginosa via Tricarboxylic Acid Cycle Control. Cell Chem. Biol. *24*, 195–206.

Munck, C., Gumpert, H.K., Wallin, A.I.N., Wang, H.H., and Sommer, M.O.A. (2014). Prediction of resistance development against drug combinations by collateral responses to component drugs. Sci. Transl. Med. *6*, 262ra156-262ra156.

Nichol, D., Rutter, J., Bryant, C., Hujer, A.M., Lek, S., Adams, M.D., Jeavons, P., Anderson, A.R.A., Bonomo, R.A., and Scott, J.G. (2019). Antibiotic collateral sensitivity is contingent on the repeatability of evolution. Nat. Commun. *10*, 334.

Okamoto, K., Gotoh, N., and Nishino, T. (2001). Pseudomonas aeruginosa Reveals High Intrinsic Resistance to Penem Antibiotics: Penem Resistance Mechanisms and Their Interplay. Antimicrob. Agents Chemother. *45*, 1964–1971.

Palmer, M.E., and Feldman, M.W. (2012). Survivability Is More Fundamental Than Evolvability. PLOS ONE *7*, e38025.

Pitt, T.L., Sparrow, M., Warner, M., and Stefanidou, M. (2003). Survey of resistance of Pseudomonas aeruginosa from UK patients with cystic fibrosis to six commonly prescribed antimicrobial agents. Thorax *58*, 794–796.

Roemhild, R., Barbosa, C., Beardmore, R.E., Jansen, G., and Schulenburg, H. (2015). Temporal variation in antibiotic environments slows down resistance evolution in pathogenic Pseudomonas aeruginosa. Evol. Appl. *8*, 945–955.

Roemhild, R., Gokhale, C.S., Dirksen, P., Blake, C., Rosenstiel, P., Traulsen, A., Andersson, D.I., and Schulenburg, H. (2018). Cellular hysteresis as a principle to maximize the efficacy of antibiotic therapy. Proc. Natl. Acad. Sci. *115*, 9767–9772.

Shan, Z., Xu, H., Shi, X., Yu, Y., Yao, H., Zhang, X., Bai, Y., Gao, C., Saris, P.E.J., and Qiao, M. (2004). Identification of two new genes involved in twitching motility in Pseudomonas aeruginosa. Microbiol. Read. Engl. *150*, 2653–2661.

Sordé, R., Pahissa, A., and Rello, J. (2011). Management of refractory Pseudomonas aeruginosa infection in cystic fibrosis. Infect. Drug Resist. *4*, 31–41.

Streeter, K., Genecology Research Centre, Faculty of Science, Health, Education and Engineering, University of the Sunshine Coast, Maroochydore DC, Queensland, Australia, Katouli, M., and Genecology Research Centre, Faculty of Science, Health, Education and Engineering, University of the Sunshine Coast, Maroochydore DC, Queensland, Australia (2016). Pseudomonas aeruginosa: A review of their Pathogenesis and Prevalence in Clinical Settings and the Environment. Infect. Epidemiol. Med. *2*, 25–32.

Szybalski, W., and Bryson, V. (1952). GENETIC STUDIES ON MICROBIAL CROSS RESISTANCE TO TOXIC AGENTS I.: Cross Resistance of Escherichia coli to Fifteen Antibiotics1, 2. J. Bacteriol. *64*, 489.

Tian, Z.-X., Mac Aogáin, M., O'Connor, H.F., Fargier, E., Mooij, M.J., Adams, C., Wang, Y.-P., and O'Gara, F. (2009). MexT modulates virulence determinants in Pseudomonas aeruginosa independent of the MexEF-OprN efflux pump. Microb. Pathog. *47*, 237–241.

Vaez, H., Faghri, J., Isfahani, B.N., Moghim, S., Yadegari, S., Fazeli, H., Moghofeei, M., and Safaei, H.G. (2014). Efflux pump regulatory genes mutations in multidrug resistance Pseudomonas aeruginosa isolated from wound infections in Isfahan hospitals. Adv. Biomed. Res. *3*.

Whiteley, M., Bangera, M.G., Bumgarner, R.E., Parsek, M.R., Teitzel, G.M., Lory, S., and Greenberg, E.P. (2001). Gene expression in Pseudomonas aeruginosa biofilms. Nature *413*, 860.
PA1327 - Serine protease - Pseudomonas aeruginosa (strain ATCC 15692 / DSM 22644 / CIP 104116 / JCM 14847 / LMG 12228 / 1C / PRS 101 / PAO1) - PA1327 gene & protein.

Acknowledgements

We would like to thank Lejla Imamovic and Christian Munck in guiding the decision of the drugs used and for suggestions to the adaptive laboratory evolution experiment. Moreover, we thank Olivier Bitterlin in assisting C.B. in preparing the plates used for adaptive evolution and IC_{90} determination.

Funding

This work was supported by the European Union's Horizon 2020 research and innovation program under the Marie Sklodowska-Curie grant agreement No 642738, MetaRNA as well from the European Union's Horizon 2020 (ERC-2014-StG) under grant agreement 638902, LimitMDR. In addition, funding was received from the Danish Council for Independent Research, Sapere Aude Program DFF 4004-00213 and from The Novo Nordisk Foundation under NFF grant number: NNF10CC1016517.

Author contribution

M.O.A.S and L.J.J. conceived the project. C.B., L.J.J. and D.S. prepared all plates used for the adaptive evolution experiment and resistance determination. L.J.J., D.S and M.J. performed the experimental work. L.J.J. analyzed and visualized the data. M.M.H.E. calculated significance values for the resistance data. L.J.J. wrote the manuscript.

Dominant resistance and negative epistasis limit the co-selection of vertically and horizontally acquired antibiotic resistance factors

Authors:

Andreas Porse*[1†]

Leonie J. Jahn*[†]

Mostafa M. H. Ellabaan*

Morten O. A. Sommer*[§]

[§]Corresponding author: msom@bio.dtu.dk

*Author affiliation:

Novo Nordisk Foundation Center for Biosustainability, Technical University of Denmark, Kemitorvet 220, 2800 Kgs. Lyngby, DK

[1]Current affiliation:

SNIPR Biome, Lersø Parkallé 44, 2100 Copenhagen, Denmark

[†]Equal contribution.

Abstract

Due to the increasing public health threat posed by multidrug-resistant bacteria, it is of vital importance to understand the fundamental mechanisms underlying the evolution of antibiotic resistance. While much attention has been devoted to the study of vertically acquired antibiotic resistance conferred by chromosomal mutations or horizontally acquired antibiotic resistance provided through antibiotic resistance genes (ARGs), little is known about the interactions between the two, which may constrain or enhance the evolution of antibiotic resistance. Here, we employ a multiplexed barcoded approach to rapidly assess the fitness of 144 mutant-ARG combinations in *Escherichia coli* subjected to eight different antibiotics at 11 different concentrations and identify significant interactions for 12 % of the mutant-ARG combinations. We found that ARGs conferring resistance under a given set of conditions tend to dominate less-fit mutations at low drug concentrations. However, we observed that when a mutant has a low fitness cost and is conferring high resistance, mutants are preferentially selected over ARGs, as shown for a *gyrA* mutation that is widely present in clinical *E. coli* isolates. Finally, we identified strong negative epistasis between two unrelated resistance mechanisms: the *tetA* tetracycline resistance gene and loss-of-function *nuo* mutations involved in aminoglycoside tolerance. We propose that the TetA-induced aminoglycoside sensitivity is caused by a general increase in membrane permeability and show that other drug efflux pumps can have similar effects. Our study demonstrates that epistatic interactions between horizontally and vertically acquired resistance are rare. However, when these interactions do occur, dominant and negative epistasis are the most commonly observed dynamics, highlighting important constraints that may allow better prediction and control of antibiotic resistance evolution.

Introduction

Bacterial evolution is driven by two main mechanisms: selection of genomic mutations (vertical evolution) and the acquisition of foreign DNA through horizontal gene transfer (HGT). These two modes of adaptation provide the genetic plasticity that allows bacteria to inhabit virtually all ecological niches on the planet. However, the rapid adaptation of bacteria can also be problematic, as the emergence of antibiotic-resistant pathogenic bacteria has increasingly compromised our ability to treat infections[1,2].

The acquisition and retention of genes or mutations that confer antibiotic resistance is strongly affected by the genetic context. For example, chromosomal mutations leading to antibiotic resistance most often occur at multiple loci[3], and interactions between different

mutations can increase resistance levels or reduce the fitness cost of initially costly mutations[4,5]. Similarly, the transfer of most plasmids, including those carrying individually cloned ARGs, initially has a negative impact on host fitness[6–10], and these costs may be ameliorated by compensatory mutations in either the plasmid or the chromosomes[5,6,11,12]. Intriguingly, while ARGs have evolved to function in a broad range of genomic contexts, and genomic mutations leading to resistance are host-specific, the resulting resistance mechanisms often overlap[13]. For example, a protein targeted by an antibiotic may be altered via mutation(s) to avoid inhibition; and the same result can be achieved through the horizontal acquisition of effectors that modify or replace the target, thereby rendering the cell resistant[14]. Taken together, these observations suggest that chromosomal mutations and HGT events could interact to contribute to the development of antibiotic resistance.

In addition to promoting antibiotic resistance development, epistatic interactions between resistance determinants or collateral sensitivity can also limit resistance evolution during sequential treatment regimes in individual patients[15–18]. For example, mutations associated with aminoglycoside resistance confer sensitivity towards multiple antibiotic drug classes, including beta-lactams, quinolones and tetracyclines[17–19], and this sensitivity is thought to arise from a reduction in the proton motive force (PMF) that reduces the uptake of aminoglycoside, while simultaneously decreasing multidrug efflux[18].

Thus, it is reasonable to hypothesize that horizontally and vertically acquired resistance factors could interact in a similar way to affect antibiotic resistance or sensitivity. However, little is known about the direct interactions that may occur between ARGs and mutations that confer antibiotic resistance. Whereas no previous work has looked into the interactions between ARGs and resistance mutations directly, a study by Silva *et al.* investigated the fitness effects of combining conjugative plasmids with resistance-conferring mutations in the *gyrA, rpoB* and *rpsL* genes of *Escherichia coli*[20]. The results from this study suggested that the coexistence of these mutations and conjugative plasmids had an overall positive effect on bacterial fitness. However, it is unclear to what extent the observed epistatic effects are caused by the plasmid-encoded ARGs or other components of the large plasmid backbones and weather these interactions are maintained during antibiotic selection.

Given the importance of chromosomal mutations and acquired resistance genes in the evolution of multidrug resistance, there is a need to assess both modes of resistance simultaneously on a broader scale[21]. To shed light on the specific epistatic interactions

between resistance genes and resistance mutations, we developed a multiplexed competition approach to assess the fitness of a panel of ARG-mutant combinations against a representative set of antibiotics at a variety of clinically relevant concentrations.

Results

To study epistatic interactions between resistance mutations and resistance genes, we selected 11 different chromosomally barcoded mutants, adapted to resist different antibiotics (**manuscript 3**), and 11 synthetic ARGs[10,22]. The mutants and ARGs were chosen to represent a wide range of mutational targets and biochemical resistance mechanisms (**Supplementary Tables 1 and 2**). To assess the effect of each mutational background on the function of each ARG, we created a combined library containing each barcoded host transformed with each ARG, comprising a total of 144 combinations of ARGs and resistance mutations, including the background strain (wild-type, WT) and an empty vector control. To assess the effect of potential interactions on resistance phenotypes, we subjected each ARG-mutant combination to selection by antibiotics representing eight different clinically important drug classes, including both bactericidal and bacteriostatic antibiotics, at 11 different concentrations (**Figure 1**).

Initially, all ARG-mutant pools subjected to antibiotics at concentrations just above the minimal inhibitory concentration (MIC) of the WT strain carrying the empty vector backbone, and at the highest drug concentration with growth were selected for further characterization for each antibiotic tested. The barcoded genomic region of each ARG-mutant pool was sequenced in order to quantify the relative abundance; reflecting the fitness of each ARG and resistance mutation combination under each selective condition. A control without antibiotics was included to quantify the fitness of each combination in the absence of drug selection (**Supplementary Figure 1**).

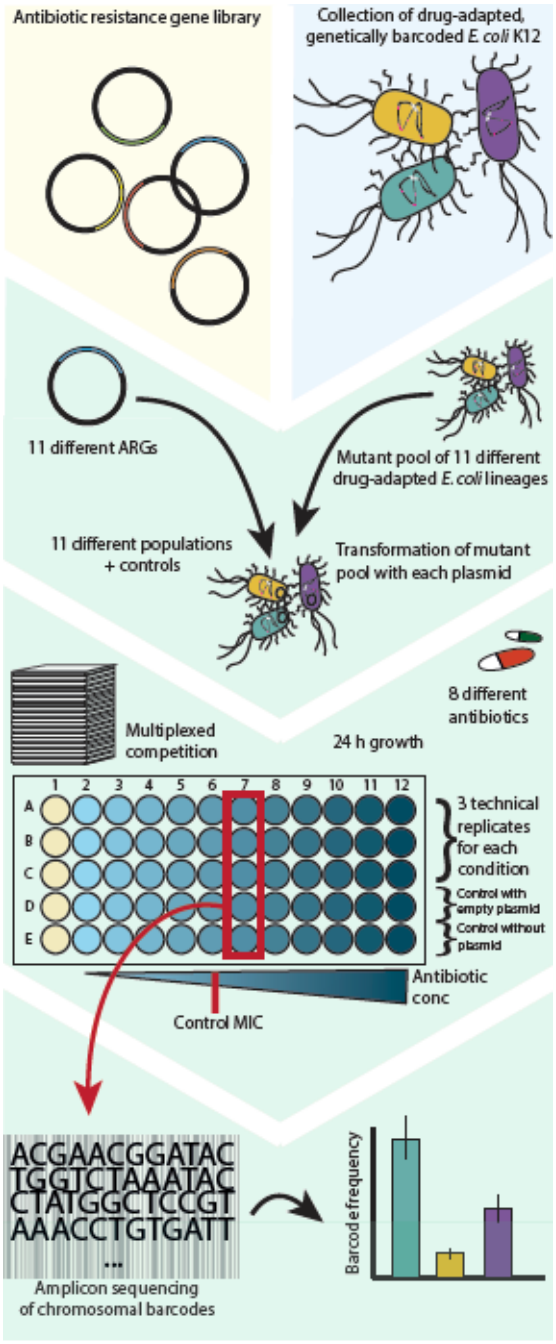

Figure 1. Experimental overview. 11 pools of 11 different mutants were individually transformed with 11 ARGs to create 121 unique ARG-mutant combinations. Additionally, 2 combinations containing either the empty vector or the background *E. coli* MG1655 WT strain were made. The mutant pools containing each ARG were subjected to eight different drugs, as well as an antibiotic-free condition. At least two replicates of the individual pools were then sequenced to determine the abundance of each mutant barcode.

ARG-mutant interactions promote differential mutant selection during antibiotic exposure

An important aspect of resistance evolution is how different genotypes interact during antibiotic treatment. Such epistatic interactions may cause preferential selection or counterselection of certain genotypic combinations in a manner that would not be predicted

from their individual effects. To test the effect of different antibiotics on the selection of ARG-mutant combinations, we quantified the frequencies of each mutant by sequencing after 24 h of incubation in each antibiotic at a concentration two-fold higher than the WT MIC to obtain an overview of potential ARG-mutant interactions (**Figure 2**).

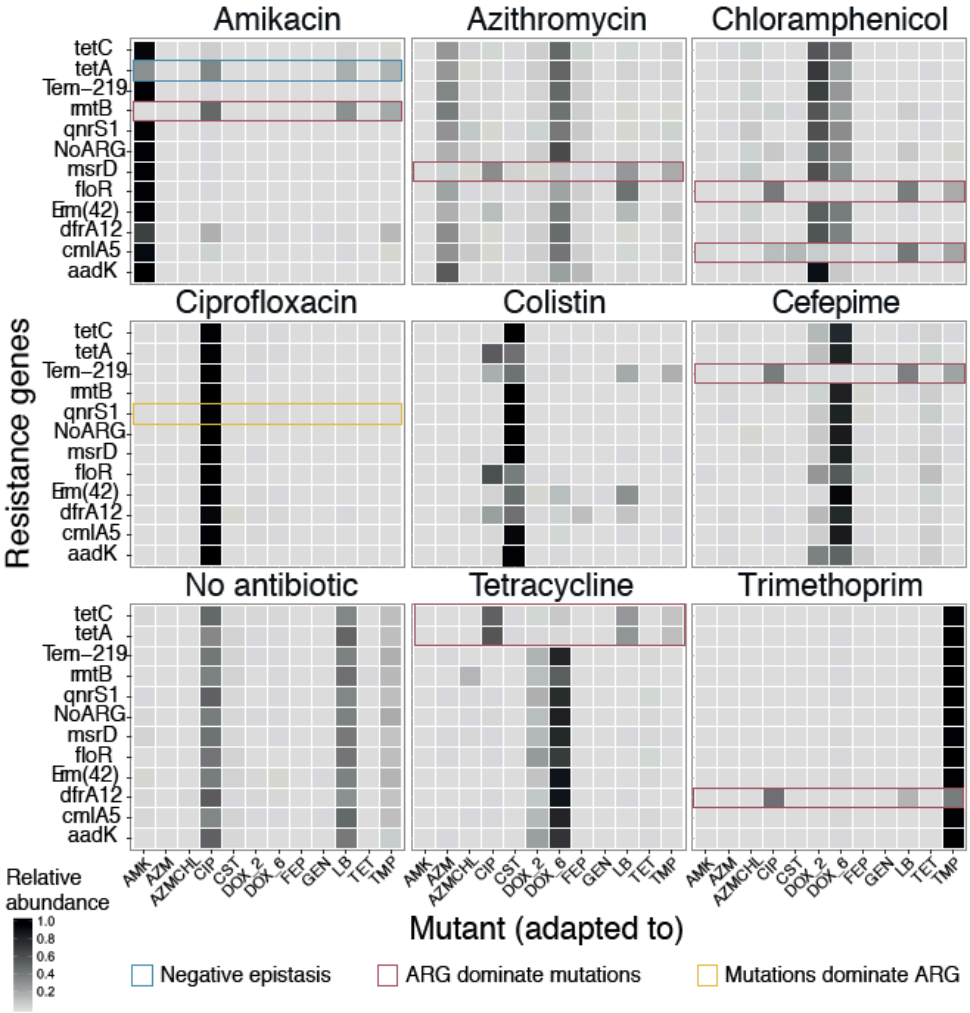

Figure 2. Selective patterns of mutant pools transformed with antibiotic resistance genes. Each ARG-mutant pool was subjected to different drugs (indicated above the panels) at a concentration twice that of the WT MIC. The color intensity illustrates the relative abundance of each mutant within each ARG-associated mutant pool. Highlighted combinations (except yellow) show the significant deviations (ANOVA, $p < 0.05$) from the null-hypothesis of no ARG influence across at least two replicates. Combinations highlighted in red illustrate the cases where the ARG shields the selection of the mutant that would otherwise be selected. Blue highlights situations in which an ARG that does not confer resistance to the antibiotic tested reduces the selection of the mutant; suggesting a negative interaction between the mutant and the ARG. Cases highlighted in yellow demonstrate the selection of the resistant mutant despite the presence of a resistance gene conferring resistance to the antibiotic tested, suggesting a dominant effect of the mutant over the resistance gene. AMK (amikacin), AZM (azithromycin), AZMCHL (azithromycin and chloramphenicol), CIP (ciprofloxacin), CST (colistin), DOX_2 (doxycycline – low resistance), DOX_6 (doxycycline – high resistance), FEP (cefepime), GEN (gentamycin), LB (Medium without antibiotics), TET (tetracycline), TMP (trimethoprim).

Based on the resulting abundance profiles of barcodes in each population, we observed three overall phenomena of altered selection in ARG-mutant pairs. The most common (nine out of 11 cases) being the selection of a mutant distribution similar to the non-selective (LB)

condition. However, a case of mutant dominance was also observed for the *qnrS1* gene present in the *gyrA* ciprofloxacin resistant background and a case of strong negative epistasis was observed for the *tetA* gene in the amikacin evolved background (**Figure 2**). Testing for the differences in selection patterns between each mutant carrying different ARGs, revealed an overall deviation of 12 % of the ARG-mutant combinations from mutants transformed with the empty vector control (ANOVA, $P < 0.004$, Bonferroni corrected). In the absence of antibiotic selection, we did not observe any significant difference in fitness between the 11 different mutants carrying a specific ARG after 24 h of growth (ANOVA, $P > 0.05$).

In summary, these results suggests that while most chromosomal resistance mutations and ARGs did not interact to a detectable extent, strong interactions do occur that may alter the long-term coexistence of such mutant-ARG pairs.

ARGs tend to dominate mutants in an additive fashion

The previous results suggested that the selection of mutants in the presence of a given ARG would depend largely on the ARGs ability to confer resistance to the presented drug challenge. The selection patterns observed suggests that ARGs dominate the resistance phenotype of the mutants and that, accordingly, the selection of mutants would depend on their fitness in the condition without antibiotics (**Supplementary Figure 2**).

To investigate this phenomenon further, we determined mutant selection patterns in the presence or absence of the ARGs $bla_{\text{TEM-219}}$, *floR* and *qnrS1* at concentrations ranging from sub-MIC levels to 256 times the WT MIC of cefepime, chloramphenicol and ciprofloxacin, respectively. From the selection patterns observed at the different drug concentrations, it is clear that mutants were selected for at very low (sub-MIC) drug concentrations in the absence of a protective ARG (**Figure 3**). A clear pattern of concentration-dependent mutant selection was observed, which corresponded well with the relative fitness cost of each mutant in the absence of antibiotics, as well as the respective antibiotic resistance profile (**Supplementary Figure 2 and Supplementary Table 3**).

For mutants carrying the $bla_{\text{TEM-219}}$or *floR* resistance genes, the presence of the ARG substantially enhanced the resistance of all of the mutants of the pool, resulting in the selection of mutants based on their fitness rather than on their resistance level to the drug over a wide concentration range. Consequently, the ARGs shield the selective dynamics that

occur in the absence of the ARG (**Supplementary Figure 3 A and B**). However, at high drug concentrations, when the antibiotic exposure approached the resistance level conferred by the ARG, the resistance gene no longer shielded the mutants, and differential selection of mutants resistant to the specific antibiotic was observed (**Figure 3 A and B**).

Interestingly, the *qnrS1* ciprofloxacin resistance gene confers lower resistance to ciprofloxacin than the low-cost *gyrA* (ciprofloxacin-adapted) mutation and does not provide substantial protective benefits to sensitive hosts (**Figure 3 C**). Because the *gyrA* mutant is highly resistant and its fitness cost is low, the resistance gene adds only a minimal amount of resistance to the mutant pool. Therefore, only a marginal shift in mutant selection is observed in the presence of *qnrS1*, resulting in a small additive effect dominated by the resistant mutant (**Supplementary Figure 3**).

Taken together, these results suggest that mutant fitness and the resistance capacity of an ARG are the main factors determining which mode of resistance is selected at a particular concentration and that these parameters dictate when additive effects occur. The fact that most ARGs confer high levels of resistance means that resistance mutations may be redundant when ARGs are present in environments exposed to low drug concentrations.

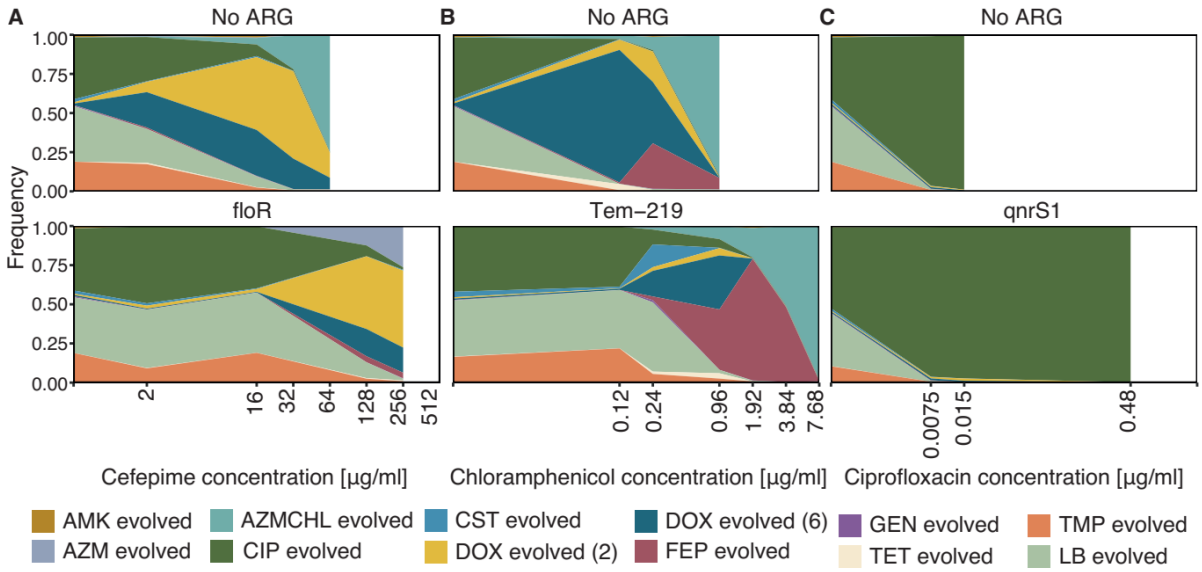

Figure 3. Concentration-dependent mutant selection with and without ARG shielding. Mutant pools with and without expression of Tem-219 beta-lactamase (A) or the FloR efflux pump (B) at different concentrations of either cefepime (Tem-219) or chloramphenicol (FloR) were sequenced to determine the mutant selection patterns. (C) Shows the dynamics of mutant selection in the presence of the *qnrS1* conferring low resistance compared to the *gyrA* mutation. Mutants were evolved in AMK (amikacin), AZM (azithromycin), AZMCHL (azithromycin and chloramphenicol), CIP (ciprofloxacin), CST (colistin), DOX_2 (doxycycline – low resistance), DOX_6 (doxycycline – high resistance), FEP (cefepime), GEN (gentamycin), LB (Medium without antibiotics), TET (tetracycline), TMP (trimethoprim).

Negative epistasis of TetA and mutations in aminoglycoside-adapted strains is due to mutations in the respiratory *nuo* genes

To explore the dynamics of mutant fitness and ARG resistance capacity in more detail, we looked into the example of strong negative epistasis between the amikacin-evolved mutant (Amk3) and the tetracycline efflux pump TetA. Amk3 was not selected in the presence of amikacin to the same extent when the TetA gene was present (> 75 % decrease in relative abundance compared to the control) as when the other ARGs were present; demonstrating a negative epistatic interaction (**Figure 2**).

To identify the causal mutation of the TetA-induced aminoglycoside sensitivity, we used multiplexed automated genome engineering (MAGE) to simultaneously reverse all individual mutations of the amikacin-resistant mutant to their respective WT sequence in the presence of the *tetA* gene. The Amk3 mutant had point mutations in *nuoH*, *cpxR*, *crr*, *fusA* and *rffG,* as well as a small deletion in *lrhA*. While the effect of *crr*, *rffG* and *lrhA* mutations are not clear, the *fusA*, *cpxR* and *nuoH* mutations are often associated with resistance towards aminoglycosides[18,19,23]. The *nuo* genes encode subunits of NADH:quinone oxidoreductase I, which maintains the PMF to fuel respiration[24]. The PMF is required for aminoglycoside uptake, and mutations of the *nuo* genes can lead to a decreased PMF, resulting in a high tolerance towards aminoglycosides[18]. After one MAGE cycle, a *tetA*-carrying MAGE pool containing the reversed mutants was selected on amikacin to identify the causal mutation leading to the TetA-induced amikacin sensitivity. Sequencing the targeted loci of four surviving colonies revealed that the *nuoH* mutation had been reversed to the WT sequence, suggesting that this mutation interacts antagonistically with *tetA* in the presence of amikacin (**Supplementary Table 4**).

To test if this negative interaction with TetA might apply to the other genes in the *nuo* cluster, we selected a different aminoglycoside-resistant mutant (Amk4), which carried mutations in *nuoF* and *fusA* only. This mutant showed similar properties to the Amk3 (*nuoH)* mutant, including reduced growth at sub-MIC concentrations of aminoglycosides, which was especially pronounced for streptomycin, when *tetA* was present (**Figure 4 A**). This suggests that several members of the *nuo* pathway may be involved in the sensitivity. To confirm the involvement of the *nuo* mutant in this sensitive phenotype, we measured the competitive fitness of the *tetA*-carrying mutant in competition with the same *fusA* background but with the *nuoF* allele reverted to WT (**Figure 4 B**). Here, the *nuoF* mutant showed a marked

competitive disadvantage at streptomycin concentrations above 4 µg/ml, with complete suppression at 32 µg/ml. Additionally, the presence of tetracycline did not have a significant effect on the selection patterns.

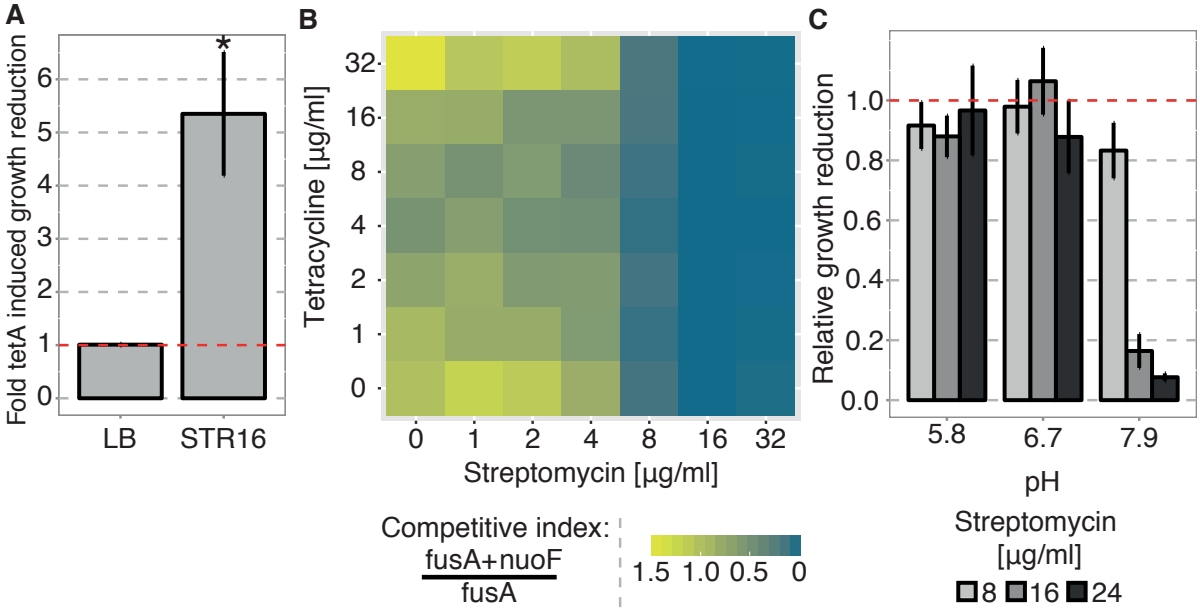

Figure 4. The presence of TetA-induces *nuoF*-dependent sensitivity to aminoglycosides. (A) Doubling time of the Amk4 mutant grown in media in the presence (STR16) or absence (LB) of a sub-MIC concentration of streptomycin (16 µg/ml). Error bars display the standard error of the mean (n = 8). The dotted line shows the baseline growth without antibiotics. The asterisk indicates statistical significance compared to the baseline (Wilcoxon rank sum test, $P < 0.05$). **(B)** Fitness landscape of *nuoF*-reversed mutants competing against their ancestor at different concentrations of tetracycline and streptomycin. **(C)** Relative growth reduction of the *tetA*-carrying *nuoF* mutant compared to the corresponding mutant carrying an empty vector at different streptomycin concentrations and pH values. Error bars show the standard-error of the mean (n = 3).

We speculated that the effect of *tetA* on the *nuo* mutants was connected to the PMF, in which case it would be dependent on the external proton concentration (pH). To test this idea, we measured the effect of the growth medium pH on the growth of the *tetA*-carrying nuoF mutant at different streptomycin concentrations (**Figure 4 C**). By measuring the growth reduction relative to growth in the *tetA*-free background for each set of conditions, we observed an increase in the *tetA*-conferred sensitivity with increasing pH.

To obtain an idea of the broader implications of such negative epistasis on the occurrence of the *nuo* and *tetA* resistance factors in natural isolates, we analyzed their co-occurrences in all 13,500 sequenced *E. coli* genomes. In these geneomes, *tetA* was never observed together with the single nucleotide polymorphisms (SNPs) in *nuoF* and *nuoH* that were observed in this study, nor with any other mutation expected to result in loss of function in the *nuo* pathway (e.g., stop codons and INDELS). For example, *tetA* was observed 377 times and *nuoF* mutants

661 times; however, they were never observed together, although they would be expected to co-occur in 18 genomes by chance.

These results suggest that the presence of *tetA* alters the resistance level of aminoglycoside resistance mutants, carrying mutations in the *nuo* operon, in a PMF-dependent manner and that such interactions may limit their co-selection in natural *E. coli* isolates.

Several major facilitator superfamily transporters induce streptomycin sensitivity at high expression levels

Given the strong effect of *tetA* in a genetic context in which a *nuo*-family gene is mutated when exposed to streptomycin, we hypothesized that such negative epistatic interactions with the *nuo* genes could be a more general attribute of antibiotic efflux pumps. To test this, we subjected the *tetC* and *tetG* tetracycline pumps and the chloramphenicol efflux pumps *cmlA5* and *floR,* which share 39 %, 43 %, 17 % and 18 % amino acid sequence identity with *tetA*, respectively, to high expression in the *nuoF* background. Although these efflux pumps vary substantially in their primary structure, they all belong to the major facilitator superfamily (MFS) of transporters that comprises the largest group of acquired antibiotic transporters[25]. These were expressed in the *nuoF* background, and the sensitivity of these strains was compared to that of the empty vector control when grown in media containing streptomycin. For the *cmlA5*, *floR* and *tetC*, we observed significant sensitivity towards streptomycin (Wilcoxon rank sum test, $P < 0.05$), suggesting that this phenotype is not exclusive to *tetA* (**Figure 5 A**). These data suggest that MFS transporters other than TetA may facilitate the uptake of compounds in an unspecific manner.

Therefore, to assess the effect of the selected efflux pumps on general membrane permeability, we measured the accumulation of Hoechst 33342 in the *nuoF* mutant expressing the same MFS transporters as tested in the streptomycin sensitivity assay. Compared to the empty vector control, all efflux pumps increased the membrane permeability of the indicator dye Hoechst 33342 by 17.8 % on average (Wilcoxon rank sum test, $P < 0.001$) (**Figure 5 B**). This increase in membrane permeability, induced by a diverse set of efflux pumps, suggests that the uptake is not determined by their specific functionality but rather by a more general effect, e.g. their perforation of the inner membrane, which may supplement the intrinsic routes of aminoglycoside uptake.

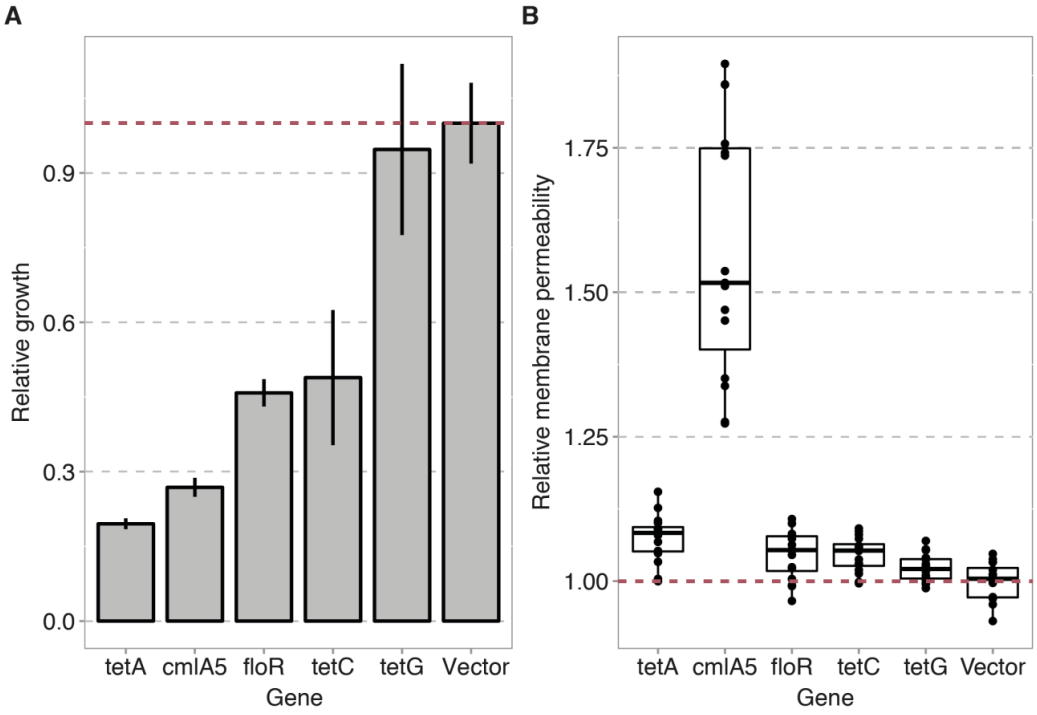

Figure 5. Effect of different MFS efflux pumps on streptomycin sensitivity and membrane permeability in the Amk4 mutant. Various genes encoding MFS pumps were independently expressed in the *E. coli nuoF+fusA* mutant strain. Growth **(A)** and membrane permeability **(B)** were measured and are displayed relative to those of the same *E. coli* strain carrying an empty vector. Membrane permeability was measured as the increase in fluorescence resulting from Hoechst 33342 uptake. The data are represented as the mean and standard error of two replicates **(A)**, and as the interquartile range between the first and third quartiles and median (internal line) with dots representing individual fluorescence measurements (n=16).

Discussion

Both genomic mutations and HGT contribute to the emergence of multidrug-resistant bacteria, yet the relative contribution of each evolutionary mechanism to clinical resistance problems remains to be determined. Using a multiplexed barcoded approach, we were able to simultaneously test multiple ARG-mutant combinations under multiple conditions to describe epistatic interactions that may direct antibiotic resistance evolution.

While a previous study[20] reported strong epistatic effects on fitness for combinations of conjugative plasmids with *gyrA, rpoB* and *rpsL* mutants, our study focused specifically on ARG-mutant interactions and suggests that such effects are unlikely to stem from ARG-mutant interactions, but rather from the remaining portion of the large plasmid backbones. This notion is supported by previous studies of plasmid-host evolution that describe interactions between the host chromosome and several plasmid components not related to antibiotic resistance[6,26,27]. Contrary to the study by *Silva et al.*[20] we did not find any significant effect of ARG-mutant co-existence on fitness in the absence of antibiotics. While it is possible that our 24 h competition assay could not detect minor effects on combined ARG-mutant

fitness, we were able to detect the subtle fitness differences between low-cost mutants e.g., in those with mutations in *folA* and *gyrA*, compared to the susceptible ancestor (**Supplementary Figure 2**), suggesting that potential effects missed by our assay where minor.

The coexistence of ARGs and chromosomal mutations that confer resistance towards the same condition will be selected only if they interact in a favorable manner to increase overall resistance or fitness. In the majority of cases, when an ARG conferred resistance to a given drug, we saw a concentration-dependent additive effect of the ARG on the mutants. This interaction can allow mutants to survive at higher antibiotic concentrations and thus be beneficial in combination with the ARG at high drug concentrations. However, they do also render the shielded mutations subject to negative selection at low antibiotic concentrations where costly mutations are not beneficial. The observed dynamics are likely dictated, at least in part, by the fitness cost of mutations and the degree of positive drug selection needed to compensate for the cost shifted by the resistance conferred by the ARG. These dynamics were also demonstrated for the interaction of *qnrS1* with the *gyrA* mutant challenged with ciprofloxacin, which is an exception to the shielding phenotype observed for most of the ARGs we tested, yet it conforms with our model predicting the dominance of the fittest resistant determinant. Such mutant domination is likely due to the low resistance level conferred by the *qnrS1* gene, whereby the shift in mutant selection caused by the addition of the ARG is only marginal in our assay. In line with our observations, previous studies suggest an additive effect of *qnr* genes and *gyrA* mutant interactions[28,29]. However, this interaction is beneficial only at high ciprofloxacin concentrations, when the resistance provided by the *gyrA* mutant is exceeded.

The counterselection of *nuoF* and *nuoH* mutants in the presence of *tetA* and aminoglycoside selection is an interesting example of negative epistasis between genes with unrelated resistance functionalities. TetA has previously been shown to increase the uptake of different compounds, including aminoglycosides, when highly expressed[30,31]. However, the increase in the sensitivity of aminoglycoside-resistant mutants has not been described before. Importantly, loss-of-function *nuo* mutants are known to arise during aminoglycoside treatment and have shown a strong increased tolerance towards aminoglycosides in addition to a more general drug persistence phenotype that is likely due to the decrease in respiration resulting from a decreased PMF[23,32]. Because the presence of MFS efflux pumps such as TetA

may lower the PMF threshold needed for aminoglycoside tolerance, a broad range of efflux pumps could render selection of *nuo* mutations less favorable during drug treatments (**Figure 5 A**). This antagonistic relationship was supported by our genomic mining of *E. coli* genomes, where *tetA* and loss-of-function *nuo* mutants were not observed together. As drug tolerance is believed to be a critical first step towards drug resistance[33,34], incorporating knowledge of how ARG-mutant interactions may curb this transition will be necessary to fully understand resistance evolution.

It has previously been shown that high *tetA* expression increases aminoglycoside uptake without altering the membrane potential[30]. This, along with the data presented here, indicates that the increased sensitivity towards aminoglycosides is not due to *tetA* altering the membrane potential itself, but rather to the cells expressing *tetA* increasing aminoglycoside uptake with the PMF gradient to a higher extent than cells lacking *tetA*. While we observed a high sensitivity towards especially streptomycin, the degree of sensitivity likely relates to properties of both the drug and efflux pump, as is evident from the diverse sensitivity profiles of the tested efflux pumps and drugs.

Although we have aimed to represent a mechanistically diverse and representative set of ARGs and mutants in a bacterium of high medical relevance, there are still countless conditions left to be explored before we can fully comprehend the interplay between mutational and horizontally acquired antibiotic resistance. The exact selective dynamics of ARG-mutant associations should also depend on factors such as ARG expression levels, growth conditions and other genetic determinants, which we did not fully consider in this study.

In conclusion, our data suggest that while strong interactions between ARGs and chromosomal resistance mutations may be rare, ARGs tend to be more effective and dominate chromosomal mutations, especially at low antibiotic concentrations. The ability of certain MFS efflux pumps to increase aminoglycoside sensitivity in a *nuo* mutant background provides a good example of collateral sensitivity that may guide medical interventions to limit resistance evolution. Further studies should seek to understand antibiotic resistance in a broader genomic context, and we hope that the methodology and results presented here will inspire others to adopt a more nuanced view on antibiotic resistance evolution. Considering the breadth of genomic contexts in which resistance may evolve will ultimately lead to increased accuracy in our ability to understand, predict and prevent antibiotic resistance evolution.

Materials and Methods

Strains and plasmids

Twelve isolated colonies of chromosomally barcoded *E. coli* MG1655 K12 lineages were chosen from the endpoint of a large-scale adaptive evolution experiment based on the diversity of their mutation profile[22] **(manuscript 3)**. Eleven strains were adapted to different antibiotics and now carry between one and six chromosomal mutations (**Supplementary Table 1**) affecting, among other processes and parameters: drug uptake, efflux, the drug target and global transcription levels. One strain was adapted in LB medium as a control to include effects of adaptations to the growth medium. The 12 strains were pooled in equal cell numbers, and aliquots of this mutant pool were transformed via electroporation with a medium copy number plasmid (p15A replicon) carrying one of 11 different ARGs cloned according to *Porse et al.* (**Supplementary Table 1**) [10]. The 11 ARGs were chosen to confer resistance to a broad selection of antibiotics via different mechanisms, and were expressed from a weak promoter to simulate realistic ARG expression levels (**Supplementary Table 2**)[10]. Two aliquots of the mutant pool served as controls: one was transformed with the empty vector, while the other remained untransformed. A selection of the includedARGs encoding efflux pumps was also cloned into a high-copy vector (pZE21)[35] and transformed into the Amk4 (*fusA* + *nuoF*) mutant strain obtained in Jahn et al.[22]

Multiplexed competition experiment

First, 150 µl of medium with or without added antibiotics was inoculated with approximately 10^6 cells from an overnight culture of the transformed mutant pools and incubated for 18 h at 37 °C without shaking. Each mutant pool was subjected to a two-fold concentration gradient ranging over 11 different concentrations of eight different antibiotics, resulting in more than 3000 competition experiments in at least two replicates. The antibiotics used cover a wide range of clinically important drug classes and mechanisms, including both bactericidal and bacteriostatic antibiotics (**Supplementary Table 5**). In addition, cells were grown in LB alone. For all conditions, 40 µg/ml zeocin was added to prevent plasmid loss, and no bias in mutant selection was observed at this concentration of zeocin (**Supplementary Figure 1**).

Amplicon sequencing

Amplicon sequencing of the mutant pools was performed before and after each transformation. In addition, at least two replicates of each mutant pool were sequenced after growth at antibiotic concentrations two-fold the WT MIC, as well as at the highest antibiotic

concentration that displayed growth. Based on interesting trends derived from the sequencing data, the DNA of samples incubated at additional concentrations was also sequenced for certain ARG-mutant pools. The pools of sequenced samples and conditions under which they were incubated are listed in **Supplementary Table 5**. Amplicon sequencing was performed as previously described[22]. Briefly, the barcoded region in the genome was amplified by colony PCR using the following primers: Fwd_Primer: TCGTCGGCAGCGTCAGAGTGTATAAGAGACACAATGACCGGGCTTTCCGC and Rev_Primer: GTCTCGTGGGCTCGGAGATGTGTATAAGAGACAGGGATGCTATGGTTTCAGG, which are amplified by the NEBNext Multiplex Oligos for Illumina sequencing (New England BioLabs, Massachusetts, USA). These primers were subsequently used for indexing PCRs. Samples were purified and pooled into aliquots with equal DNA concentrations, then sequenced on an Illumina MiSeq. The barcode frequencies for each condition were determined as the number of reads containing each barcode relative to the total number of barcoded reads.

Mutant repair using multiplexed automated genome engineering (MAGE)

The mutations found in the amikacin-evolved (Amk3) mutant were repaired using single-stranded oligo recombineering as previously described[36]. Briefly, the AMK mutant was transformed with the pMA7 vector, which carried the λ recombineering system[37]. The recombineering system was induced in mid-log phase by adding 0.2 % w/v arabinose and incubating for an additional 15 min. Competent cells were prepared by three rounds of washing at 4 °C, and electroporation of a pool of oligos was performed (**Supplementary Table 4**). The transformed cultures were allowed to recover for 4 h before plating on 10 μg/ml amikacin LB plates to select resistant clones.

Growth rate determination

Optical density (OD) measurements were conducted in 96-well plates containing 150 μl of LB medium per well using the *ELx808* plate reader (BioTek, USA). The OD at 600 nm (OD_{600}) was measured over 5 min intervals for a maximum of 20 h, and the plates were incubated at the medium shaking setting at 37 °C between measurements. Media with varying pH values were prepared by diluting HEPES buffer to a concentration of 50 mM in LB and subsequently adjusting the pH with NaOH and HCl. The final pH was measured just before inoculation. Sensitivity measurements of MFS efflux pumps in the *fusA+ nuoF* background were performed at different concentrations of streptomycin (0-64 μg/ml) in two-fold increments, and the exponential growth rate was normalized to that of the antibiotic-free (LB) samples for each

concentration. The average sensitivity was then calculated as the average relative reduction in the LB-normalized growth rate relative to the growth rate of the empty vector control at all concentrations where the empty vector control displayed growth (< 32 μg/ml).

2D competitive fitness assay

The *tetA*-carrying *fusA*+*nuoF* mutant and the *nuoF*-repaired mutants were transformed with *gfp*- and *rfp*-expressing pZE21 plasmids, respectively[35]. Each strain was grown to an OD_{600} of 0.5, diluted 1000x and mixed equally before inoculation into a 96-well clear-bottomed black plate containing a 2D gradient of two-fold dilutions of streptomycin and tetracycline in 200 μl LB medium per well. Fluorescence (at 528 nm and 615 nm with excitation at 485 nm and 580 nm for GFP and RFP, respectively) and OD_{600} were measured for 10 h using the *Synergy H1* plate reader (BioTek, USA). The RFP to GFP signal ratio after 8 h of growth is reported as the competitive index.

Membrane permeability assay

The DNA-intercalating dye Hoechst 33342 changes its fluorescent properties upon DNA binding and has been applied to measure the membrane permeability of bacterial cells[18,38,39]. The accumulation of Hoechst 33342 is sensitive to the activity of endogenous multidrug efflux systems, such as the AcrAB–TolC system of *E. coli*, and to membrane-piercing structures, such as porins, that ease dye entry[38,39]. Cultures were grown to an OD_{600} of 0.3, and 100 μl of each strain was transferred to a clear-bottomed black plate. Using a 96-channel pipette (INTEGRA VIAFLO 96), 100 μl of additional LB medium containing 5 μM Hoechst 33342 was simultaneously added to each well. The plate was incubated at 37 °C with shaking in a *Synergy H1* plate reader (BioTek, USA), and fluorescence and OD_{600} were read every 5 min. Fluorescence was read from the bottom of the plate using 355 nm and 450 nm excitation and emission filters, respectively[38]. The membrane permeability was then calculated as the area under the fluorescence/OD curve.

Resistance gene and mutation co-occurrence analysis in sequenced *E. coli* genomes

Approximately 13,500 complete *E. coli* genomes were downloaded from the NCBI RefSeq database (June 2018). BLAST analysis was performed to identify ARGs (clustered at 95 % identity) and mutations associated with the genes mutated in this study (**Supplementary Table 1**). BLAST identification of ARGs and genes involved in mutational resistance was performed at 99 % ID. INDELs and stop codons within a reading frame were regarded as having similar (loss-of-function) outcomes. The statistical analysis was performed using the

Cooccur package of R to conduct the co-occurrence analysis[38]. Here, the p-value cut-off for interaction-type classification was Bonferroni-adjusted based on the number of total interactions.

Acknowledgement

This work was supported by the European Union's Horizon 2020 research and innovation program under the Marie Sklodowska-Curie grant agreement No 642738, MetaRNA as well from the European Union's Horizon 2020 (ERC-2014-StG) under grant agreement 638902, LimitMDR. In addition, funding was received from the Danish Council for Independent Research, Sapere Aude Program DFF 4004-00213 and from The Novo Nordisk Foundation under NFF grant number: NNF10CC1016517. M.O.A.S also acknowledges funding by the Lundbeck foundation.

Author contributions

A.P., L.J.J. and M.O.A.S. designed the study. A.P. and L.J.J. performed the experiments and analyzed the data with input from M.O.A.S.. M.M.H.E. constructed the genome database and performed BLAST searches. A.P. and L.J.J. wrote the paper with input from M.O.A.S..

References

1. Davies, J. & Davies, D. Origins and evolution of antibiotic resistance. *Microbiol. Mol. Biol. Rev.* **74,** 417–433 (2010).

2. O'Neill, J. Tackling drug-resistant infections globally: final report and recommendations. *Rev. Antimicrob. Resist.* 84 (2016). doi:10.1016/j.jpha.2015.11.005

3. Thulin, E., Sundqvist, M. & Andersson, D. I. Amdinocillin (mecillinam) resistance mutations in clinical isolates and laboratory-selected mutants of Escherichia coli. *Antimicrob. Agents Chemother.* **59,** 1718–1727 (2015).

4. Hughes, D. & Andersson, D. I. Evolutionary Trajectories to Antibiotic Resistance. 579–596 (2017). doi:10.1146/annurev-micro-090816

5. Andersson, D. I. The biological cost of mutational antibiotic resistance: any practical conclusions? *Curr. Opin. Microbiol.* **9,** 461–465 (2006).

6. Porse, A., Schønning, K., Munck, C. & Sommer, M. O. A. Survival and Evolution of a Large Multidrug Resistance Plasmid in New Clinical Bacterial Hosts. *Mol. Biol. Evol.* **33,** 2860–2873 (2016).

7. Gumpert, H. *et al.* Transfer and Persistence of a Multi-Drug Resistance Plasmid in situ of the Infant Gut Microbiota in the Absence of Antibiotic Treatment. *Front. Microbiol.* **8,** (2017).

8. Porse, A. *et al.* Genome Dynamics of Escherichia coli during Antibiotic Treatment: Transfer, Loss, and Persistence of Genetic Elements In situ of the Infant Gut. *Front. Cell. Infect. Microbiol.* **7126,** 1–12 (2017).

9. San Millan, A. & MacLean, R. C. Fitness Costs of Plasmids: a Limit to Plasmid Transmission. *Microbiol. Spectr.* **5,** 1–12 (2017).

10. Porse, A., Schou, T. S., Munck, C., Ellabaan, M. M. H. & Sommer, M. O. A. Biochemical mechanisms determine the functional compatibility of heterologous genes. *Nat. Commun.* **9,** (2018).

11. Yano, H. *et al.* Evolved plasmid-host interactions reduce plasmid interference cost. *Mol. Microbiol.* **101,** 743–756 (2016).

12. Harrison, E. & Brockhurst, M. a. Plasmid-mediated horizontal gene transfer is a coevolutionary process. *Trends Microbiol.* **20,** 262–7 (2012).

13. Munita, J. M., Arias, C. A., Unit, A. R. & Santiago, A. De. Mechanisms of Antibiotic Resistance. *Microbiol Spectr* **4,** 1–37 (2016).

14. Kumar, S. & Varela, M. F. Molecular mechanisms of bacterial resistance to antimicrobial agents. *Microb. Pathog. Strateg. Combat. them Sci. Technol. Educ.* 522–534 (2013).

15. Imamovic, L. *et al.* Drug-Driven Phenotypic Convergence Supports Rational Treatment Strategies of Chronic Infections. *Cell* **172,** 121–134.e14 (2018).

16. Podnecky, N. L. *et al.* Conserved collateral antibiotic susceptibility networks in diverse clinical strains of Escherichia coli. *Nat. Commun.* **9,** (2018).

17. Munck, C., Gumpert, H. K., Wallin, A. I. N., Wang, H. H. & Sommer, M. O. A. Prediction of resistance development against drug combinations by collateral responses to component drugs. *Sci. Transl. Med.* **6,** 262ra156-262ra156 (2014).

18. Lázár, V. *et al.* Bacterial evolution of antibiotic hypersensitivity. *Mol. Syst. Biol.* **9,** (2013).

19. Jahn, L. J., Munck, C., Ellabaan, M. M. H. & Sommer, M. O. A. Adaptive laboratory evolution of antibiotic resistance using different selection regimes lead to similar phenotypes and genotypes. *Front. Microbiol.* **8,** 1–14 (2017).

20. Silva, R. F. *et al.* Pervasive sign epistasis between conjugative plasmids and drug-resistance chromosomal mutations. *PLoS Genet.* **7,** e1002181 (2011).

21. Wong, A. Epistasis and the evolution of antimicrobial resistance. *Front. Microbiol.* **8,** 1–12 (2017).

22. Jahn, L. J. *et al.* Chromosomal barcoding as a tool for multiplexed phenotypic characterization of laboratory evolved lineages. *Sci. Rep.* **8,** (2018).

23. Van Den Bergh, B. *et al.* Frequency of antibiotic application drives rapid evolutionary adaptation of Escherichia coli persistence. *Nat. Microbiol.* **1,** 1–7 (2016).

24. Friedrich, T., Steinmüller, K. & Weiss, H. The proton-pumping respiratory complex I of bacteria and mitochondria and its homologue in chloroplasts. *FEBS Lett.* **367,** 107–111 (1995).

25. Fluman, N. & Bibi, E. Bacterial multidrug transport through the lens of the major facilitator superfamily. *Biochim. Biophys. Acta - Proteins Proteomics* **1794,** 738–747 (2009).

26. Harrison, E., Guymer, D., Spiers, A. J., Paterson, S. & Brockhurst, M. A. Parallel Compensatory Evolution Stabilizes Plasmids across the Parasitism-Mutualism Continuum. *Curr. Biol.* **25,** 2034–2039 (2015).

27. San Millan, A., Toll-Riera, M., Qi, Q. & MacLean, R. C. Interactions between horizontally acquired genes create a fitness cost in Pseudomonas aeruginosa. *Nat. Commun.* **6,** 6845 (2015).

28. Martinez-Martinez, L., Pascual, A., Garcia, I., Tran, J. & Jacoby, G. A. Interaction of plasmid and host quinolone resistance [1]. *J. Antimicrob. Chemother.* **51,** 1037–1039 (2003).

29. Machuca, J. *et al.* Interplay between plasmid-mediated and chromosomal-mediated fluoroquinolone resistance and bacterial fitness in Escherichia coli. *J. Antimicrob. Chemother.* **69,** 3203–3215 (2014).

30. Merlin, T. L., Davis, G. E., Anderson, W. L., Moyzis, R. K. & Griffith, J. K. Aminoglycoside uptake increased by tet gene expression. *Antimicrob. Agents Chemother.* **33,** 1549–1552 (1989).

31. Stavropoulos, T. a & Strathdee, C. a. Expression of the tetA(C) tetracycline efflux pump in Escherichia coli confers osmotic sensitivity. *FEMS Microbiol. Lett.* **190,** 147–50 (2000).

32. Shan, Y., Lazinski, D., Rowe, S., Camilli, A. & Lewis, K. Genetic basis of persister tolerance to aminoglycosides in Escherichia coli. *MBio* **6,** 1696–1699 (2015).

33. Levin-Reisman, I. *et al.* Antibiotic tolerance facilitates the evolution of resistance. *Science (80-.).* **355,** 826–830 (2017).

34. Cohen, N. R., Lobritz, M. A. & Collins, J. J. Microbial persistence and the road to drug resistance. *Cell Host Microbe* **13,** 632–42 (2013).

35. Lutz, R. & Bujard, H. Independent and tight regulation of transcriptional units in escherichia coli via the LacR/O, the TetR/O and AraC/I1-I2 regulatory elements. *Nucleic Acids Res.* **25,** 1203–1210 (1997).

36. Wang, H. H. & Church, G. M. *Multiplexed genome engineering and genotyping methods: Applications for synthetic biology and metabolic engineering*. *Methods in Enzymology* **498,** (Elsevier Inc., 2011).

37. Lennen, R. M. *et al.* Transient overexpression of DNA adenine methylase enables efficient and mobile genome engineering with reduced off-target effects. *Nucleic Acids Res.* **44,** 1–14 (2015).

38. Coldham, N. G., Webber, M., Woodward, M. J. & Piddock, L. J. V. A 96-well plate fluorescence assay for assessment of cellular permeability and active efflux in Salmonella enterica serovar Typhimurium and Escherichia coli. *J. Antimicrob. Chemother.* **65,** 1655–1663 (2010).

39. Krishnamoorthy, G. *et al.* Synergy between Active Efflux and Outer Membrane Diffusion Defines Rules Negative Bacteria. *MBio* **8,** 1–16 (2017).

Supplemental material

Supplementary Figure 1 – ARG-mutant unselected fitness. Normalized to the fitness of mutants carrying the empty vector.

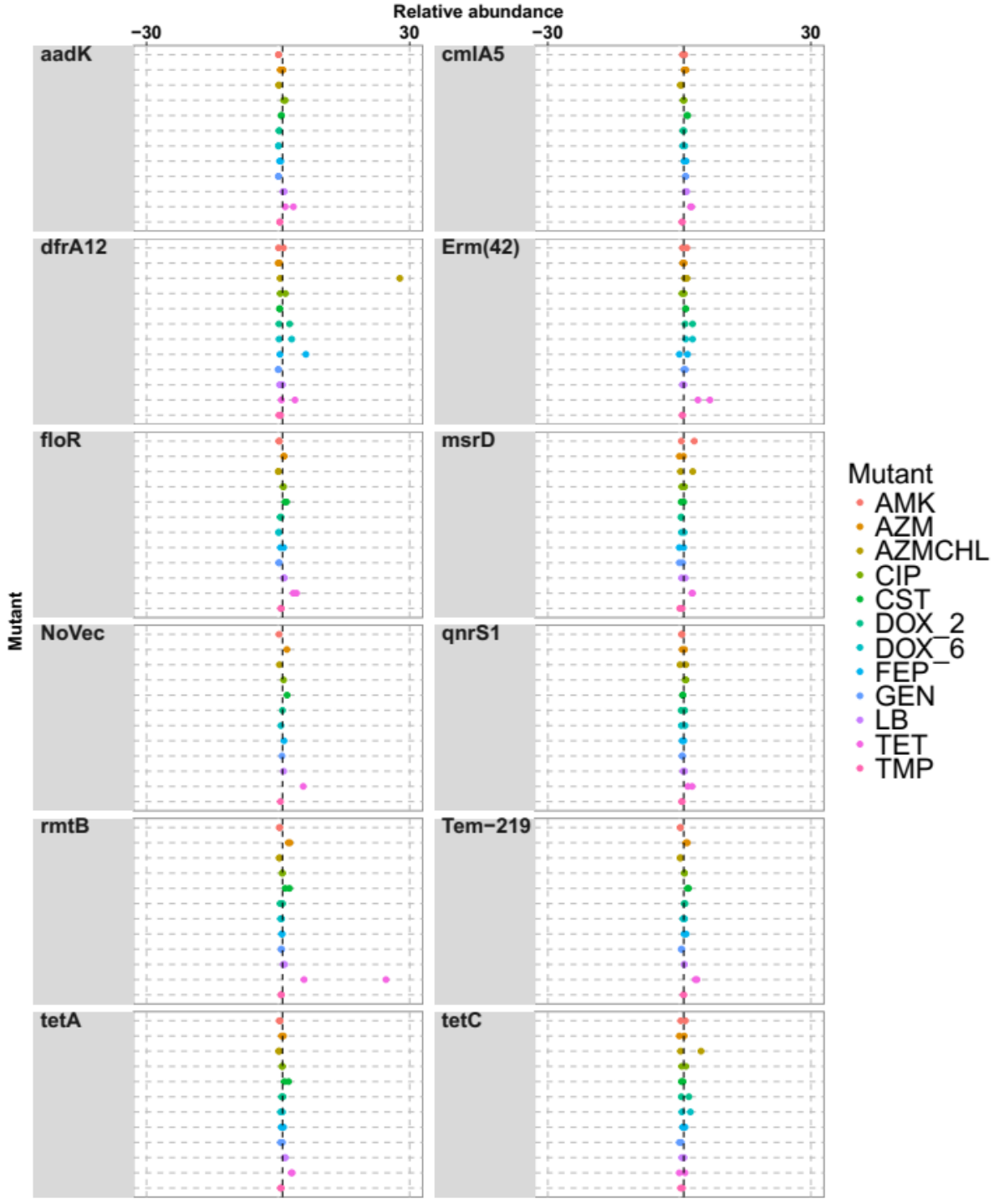

Supplementary Figure 2
The relative fitness of each mutant without ARGs after 24h of growth in the absence of selection.

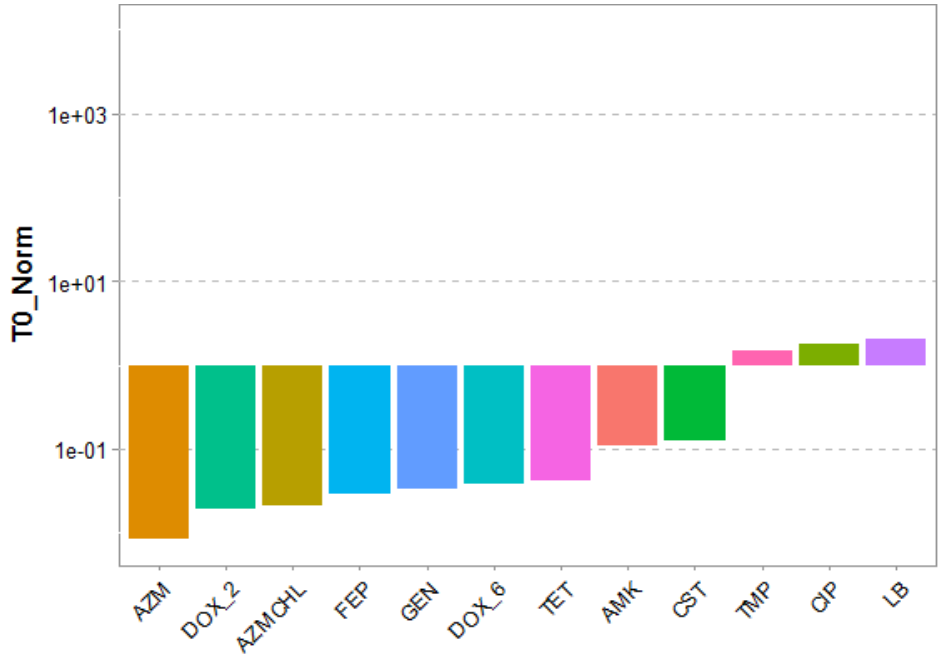

Supplementary Figure 3
Schematic depicting the influence of fitness and resistance level on the preferential selection of ARGs or mutations. (A) and (B) The WT is selected over the Cefepime/Chloramphenicol resistant mutant in low drug concentrations at which the WT has a fitness advantage. However, the mutant is selected in higher concentrations at which its resistance provides an advantage and concentration dependent increase in fitness. The addition of a resistance gene shifts the resistance level of both the WT and the mutant in an additive manner, wherefore the fitness advantage of the WT causes selection of the WT in a wider concentration range. Only at very high concentrations the mutant is selected. (C) The fitness advantage of the WT without antibiotic exposure over the Ciprofloxacin evolved mutant is smaller compared to most other mutants. In addition, the mutant is highly resistant while the resistance gene only adds marginal resistance to both the mutant and the WT. While still an additive interaction between the resistance gene and the mutant can be detected, only a marginal shift in mutant selection is observed.

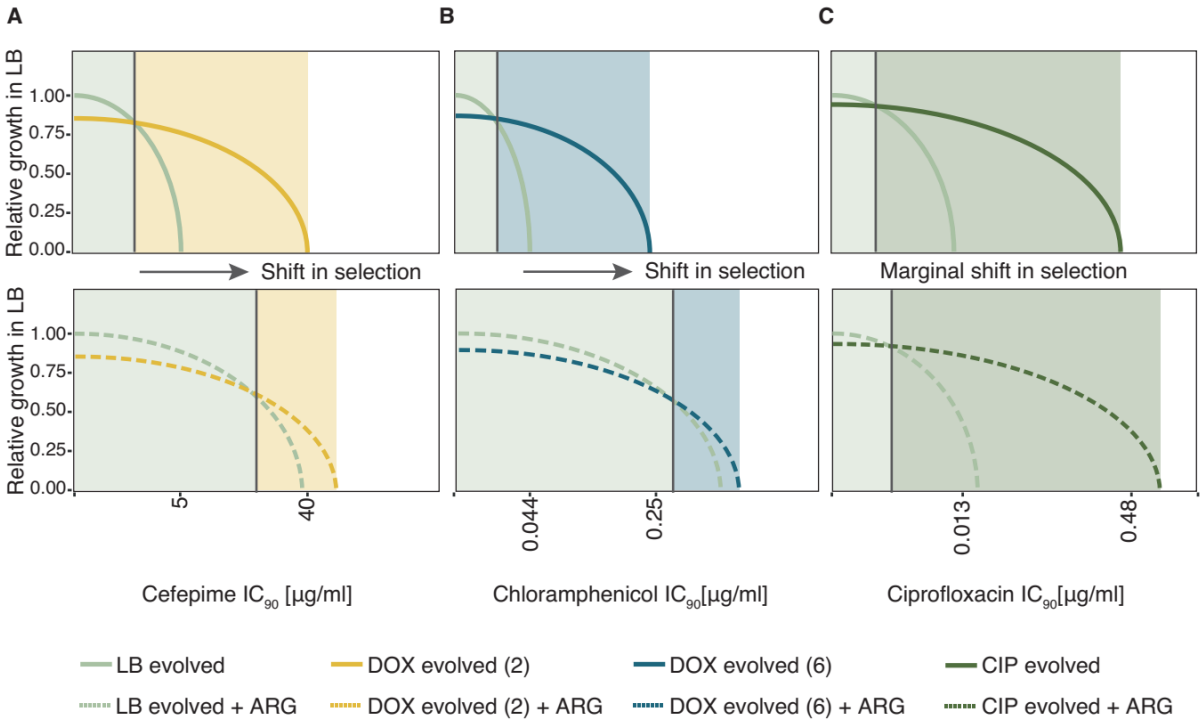

Supplementary Table 1 – Drug evolved mutant lineages

Strain	Adapted to	Increase in MIC	Mutated genes	Position in gene	Mechanism	PMID
MG_CST_5	Colistin	45	basR	Gly53Glu	two component system, sensor, kinase, results in positively charged LPS	28629229
MG_FEP_1	Cefepime	22	acrR, ompC, ompF	INDEL, Gln171*, INDEL	membrane porin	19100346
MG_GEN_1	Gentamycin	3	nuoG, fusA	Ala302fs, Phe593Leu	proton pump, elongation factor	7515367 24169403
MG_AMK_3	Amikacin	24	nuoH, lrhA, crr, fusA, rffG, cpxR	Trp187*, Ala32_Ala34del, Met1?, Pro610Gln, Gly11Trp, Met53Thr	Membrane potential, stress and elongation factor	7515367 24169403
MG_AZM_6	Azithromycin	9	acrR, rrlA	Thr5Ala, INDEL	transcriptional regulator for acrAB genes	12183262
MG_CIP_5	Ciprofloxacin	55	gyrA, parE	Ser83Leu, INDEL	DNA gyrase subunit	15352551
MG_TMP_6	Trimethoprim	NA	folA	Trp30Gly	Folate metabolism	17451440
MG_TET_6	Tetracycline	43	ybaO, marR, lrhA	Met107Arg, Leu114*, Gln47Glu	Regulation and efflux	24523773
MG_DOX_2	Doxycycline	14	acrR, marR, rob, trkA	INDEL, INDEL, Thr184Lys, INDEL	Transcription factor. Stress tolerance	25391482
MG_DOX_6	Doxycycline	46	lon, arcR, marR,	Pro480Leu, Phe52Val, Gly104Asp,	Protease, regulators of efflux,	26989065

			rpsJ	Val57Leu	translation	
MG_AZMCHL_2	Azithromycin and Chloramphenicol	9	acrR, marR, ompR, rpoB	Leu158Val, Leu46His, Arg110fs, Arg451Ser	transcriptional regulator of efflux, porin,	29764951
MG_LB_6	No antibiotics	0	-		-	

Supplementary Table 2 – Antibiotic resistance genes (ARGs)

Gene	Resistance	Mechanism
Tem-219	Beta lactams	Drug inactivation
Erm(42)	Macrolides, clindamycin	Ribosomal modification
aadk	Aminoglycosides (Str)	Drug inactivation
rmtB	Aminoglycosides (Gen,Str)	Ribosomal modification
tetA	Tetracycline	Efflux
floR	Chloramphenicol	Efflux
cmlA5	Chloramphenicol	Efflux
qnrS1	Fluoroquinolones	Gyrase protection
drfA12	Trimethoprim	Target replacement
tetC	Tetracycline	Efflux
msrD	Macrolides	Ribosomal protection
Vector	(Zeocin)	

Supplementary Table 3 – Antibiotics and concentrations used

Antibiotic	Abbreviation	Concentration range [µg/ml]	Concentration chosen for sequencing [µg/ml]
Amikacin	Amk	0.5 to 512	16; 256
Azithromycin	Azm	0.5 to 512	8; 512
Cefepime	Fep	0.0075 to 7.68	0.06; 3.84
Chloramphenicol	Chl	1 to 1024	16; 256
Ciprofloxacin	Cip	0.0019 to 1.92	0.0075; 0.48
Colistin	Col	0.0625 to 64	1; 4
Tetracycline	Tet	0.125 to 128	2; 128
Trimethoprim	Tmp	0.0625 to 64	8; 64

Supplementary Table 4 – MAGE oligoes

Oligo	gene	Genome position
TGATCTTCTGGACGACAGCATTGATTTACTTTTGCTTGACGTAAtGATGCCGAAGAAAAATGGTATCGACACATTAAAAGCACTTCGCCA	cpxR	4105525
CACCGCGTCGCTCGTTTCGTTGATGATATAACGCACCAGCGCCGAGCCAATAAACCcGGCACCACCTGTTATCAGAATTTTTCTCATCAG	rffg	3972564
ACGTCACCGGTGTTCTCTTCCGGAGTTTCTACTTCAACCTTCATGATCGGCTCAAGCAGAACTggTTTCGCTTTCTTAAAGCCTTCTTTA	fusA	3471698
TGCTAATCCACGAGATGCGGCCCAATTTACTGCTTAGGAGAAGATCATGGGTTTGTTCGATAAACTGAAATCTCTGGTTTCCGACGACAAGAAG	crr	2535848
GCATTTGCTGACTTACGGCGGACTGAGTACGACACACAGCGGCAGCTGCGGCAGCAAAAGTGTTCAGATCGGCAACAGCAACAAATGTTCTC	IrhA	2406554
CGATGGCAAAGGTAATAAAACCAAAGAATTGCGGGATAACGTTCcACACATGCGCCTGGCTGTTGACGATGTCGGTCATGTTGAATGAACCGG	nuoH	2396895

Chapter IV – Improving efficiency of CRISPR-based antimicrobials

Alternatives to compound antibiotics

As antibiotic resistance is a threat to human health, it is important to continuously screen for novel antibiotics but also to explore new approaches for treatment of bacterial infections. Besides antibiotics, nanomaterials have been explored as potential antimicrobials[218], moreover antibodies either used for passive immunization[219] or as antibody-antibiotic conjugates show a vast potential in extending current treatment options[220]. In addition, phage therapy is a promising alternative to antibiotics[221]. Moreover, the fast development in the fields of synthetic biology since the discovery of the CRISPR-Cas system provide a synthetic and rational framework to specifically target pathogenic or antibiotic resistant bacteria[222]. CRISPR stands for clustered regularly interspaced short palindromic repeats. These repeats are found in prokaryotic genomes and derive likely from viruses[223]. Cas9 (CRISPR-associated 9) is an enzyme that recognizes DNA sequences guided by the CRISPR arrays and is able to insert DNA double strand-breaks. Naturally, the CRISPR machinery is believed to be an immune system of bacteria helping bacteria to survive phage infections and entry of foreign DNA[223]. The system was recently exploited to advance synthetic biology as it can be used as a valuable tool for genome editing in multiple organisms[224]. It may also be used for the development of CRISPR-based antimicrobials, which are built on the ability of the CRISPR system to create DNA double strand breaks that cannot be repaired, as most bacteria are lacking non-homologous end joining repair pathways[225]. Advantages of CRISPR-based antimicrobials are that a DNA sequence can be designed to specifically target pathogenic or antibiotic resistant bacteria. Consequently, the microbiome, whose role in human health is becoming increasingly valued[226], is less burdened and resistant bacteria can be eliminated from bacterial populations. Yet, there are many challenges before CRISPR-based antimicrobials can be used as antimicrobials, including legislative problems, DNA delivery into the bacteria and low efficiency[222]. In order to increase the efficiency of CRISPR-based antimicrobials, we set out to analyze the impact of different features on the efficiency and tried to explore ways to finally improve the system resulting in higher efficiency and greater limitations for resistance evolution (**manuscript 6**).

Mechanism of bacterial resistance to CRISPR-Cas antimicrobials

Authors:
Ruben Vazquez-Uribe*†,
Christin Rathmer*†,
Leonie J. Jahn*†,
Simone Li*,
Morten O.A. Sommer*§

§Corresponding author: msom@bio.dtu.dk

*Author affiliation:
Novo Nordisk Foundation Center for Biosustainability, Technical University of Denmark, Kemitorvet 220, 2800 Kgs. Lyngby, DK

†Equal contribution.

Abstract

As antibiotic resistance is an emerging threat to human health, it is important to explore alternative treatment options for infectious diseases. Promising alternatives are CRISPR-based antimicrobials. The CRISPR-machinery can induce highly selective double strand breaks in the bacterial DNA, finally resulting in cell death. The high selectivity is very advantageous as pathogenic bacteria could be specifically targeted reducing the burden of broad-spectrum antibiotics on the microbiome. In addition, antibiotic resistant bacteria could be removed from an infecting bacterial population, restoring the efficiency of commonly used antibiotics. However, CRISPR-based antimicrobials often have high escape rates, requiring further research to optimize the killing efficiency. In this study, we systematically identified and explored various parameters that impact efficiency and tried to exploit the generated knowledge in order to optimize the CRISPR-induced killing efficiency.

Introduction

Antibiotic resistance is undermining the achievements of modern medicine as infectious diseases are becoming increasingly life threatening again due to the global rise of antibiotic resistant pathogens (Bush et al., 2011). The crisis is further enhanced by a lack of new therapeutics. The development of novel antibiotics is a cost and time intensive venture and only few companies invest in antibiotic drug discovery today (Bush et al., 2011). However, new treatment strategies against antibiotic resistant bacteria are urgently needed in order to combat resistant bacteria.

A fast development in the field of synthetic biology based on CRISPR (clustered regularly interspaced short palindromic repeats) systems might revolutionize the way we treat disease in the future. The promising technology stems from the adaptive immune systems from bacteria and archae (Horvath and Barrangou, 2010). Their Cas (CRISPR-associated) nucleases recognize a specific sequence of DNA or RNA by forming a complex with a small guide RNA (gRNA) that has sequence homology to the target (Jiang et al., 2013). The RNA-guided nuclease binds to the target and introduces a DNA break. Due to the precision of the CRISPR-Cas system and ease of programmability, CRISPR-based tools for genome editing have been successfully applied in eukaryotes and prokaryotes, where damaged DNA is repaired via homologous recombination using a matching copy of DNA (Cong et al., 2013; Jiang et al., 2013; Mali et al., 2013). Alternatively, eukaryotic cells can repair DNA breaks using the error-prone non-homologues end joining (NHEJ) mechanisms (Davis and Chen, 2013). However, most

prokaryotes lack NHEJ mechanisms, wherefore continuous DNA damage leads to cell death if not repaired through homologous recombination (HR) (Ayora et al., 2011). This phenomenon has been exploited for the development of CRISPR-Cas based antimicrobials (Bikard et al., 2014; Citorik et al., 2014; Gomaa et al., 2014).

CRISPR-Cas antimicrobials have the advantage over antibiotics to discriminate and eliminate specific bacteria at the strain level (Bikard et al., 2014). Antibiotic treatment is often associated with a change in the human microbiome leading to a temporary reduction of diversity, which might increase the risk for other diseases like *Clostridium difficile* infection (Jakobsson et al., 2010; Johnson, 2009). Therefore, a drug that specifically targets pathogenic bacteria would be highly beneficial. Moreover, resistant bacteria could be targeted specifically, clearing them from the infection and leaving antibiotic susceptible bacteria that can be targeted by standard antibiotic treatments (Bikard et al., 2014). In addition, the technique could also be used for targeted microbiome engineering (Hidalgo-Cantabrana et al., 2017), highlighting the potential of CRISPR-Cas based medicine to not only treat infectious diseases but also multiple microbiome-related conditions such as diabetes, obesity, inflammation, and cancer (Cho and Blaser, 2012).

The basic design of CRISPR-Cas antimicrobials consist of a gRNA encoded in a DNA vector and an endogenously or exogenously provided CRISPR-Cas effector. CRISPR-Cas systems are remarkably diverse in both the structural components and functions. The different effector modules of these systems target DNA, RNA or both (Makarova et al., 2015 and 2017). The most commonly studied effector protein is the DNA endonuclease Cas9 from *Streptococcus pyogenes* (Marraffini, 2016). In previous reports, Cas9 has been reprogrammed and successfully deployed to induced bacterial cell death in antibiotic resistant and clinically relevant bacteria (Bikard et al., 2014; Citorik et al., 2014; Gomaa et al., 2014).

Yet, one of the main challenges of this technology is the relatively high rate of bacteria escaping CRISPR-Cas antimicrobials potentially due to mutations in CRISPR-Cas effector protein, gRNA or the target sequence (Bikard et al., 2014; Citorik et al., 2014; Gomaa et al., 2014; Caliando & Voigt, 2015; Lauritsen et al., 2017). Furthermore, in many cases escaper bacteria are the result of intrinsic resistance or tolerance to CRISPR-Cas antimicrobial that is associated to gRNA efficiency and the activity of recA-mediated DNA repair (Cui and Bikard, 2016; Guo et al., 2018; Moreb et al., 2017). After DNA damage, the ubiquitous recA system repairs the break using an intact chromosomal copy of the cleaved DNA strand (Cui and

Bikard, 2016), therefore if a weak gRNA is used, the rate of recA-mediated DNA repair will be higher than Cas9 induced double stranded breaks (DSB) resulting in a higher survival rate.

As acquired mutational resistance is frequently observed as an immediate response to *in vitro* treatment of bacteria with CRISPR-Cas based antimicrobials, it is crucial to understand the underlying mechanisms in order to improve the therapeutic efficiency.

We set to systematically study the different parameters affecting the CRISPR-Cas antimicrobial resistance patterns. We focused on CRISPR-Cas antimicrobials that use Cas9 from *S. pyogenes* (spCas9), the effector protein from the type II CRISPR-Cas systems (Deltcheva et al., 2011; Jinek et al., 2012). Based on the observed resistance patterns we tested different mechanisms for potential improvement in the design of CRISPR-Cas antimicrobials. Our findings contribute to the development of more efficient CRISPR-based antimicrobials for controlling the composition of complex microbial populations or fighting the rise of antibiotic resistance.

Results

CRISPR-Cas9 expression impacts killing efficiency

Tolerance against DNA damage caused by CRISPR-Cas antimicrobial is often associated with gRNA efficiency and the activity of recA-mediated DNA repair (Cui and Bikard, 2016; Moreb et al., 2017; Guo et al., 2018). However, one parameter often overlooked is the level of spCas9 expression. It has been reported that some bacteria can tolerate an active self-targeting gRNA that directs spCas9 to cleave the chromosome, without up-regulating DNA repair genes, when spCas9 was mildly expressed (Hullahalli et al., 2018). We investigated the role of spCas9 expression level for the intrinsic resistance or tolerance associated to CRISPR-spCas9 antimicrobials. Therefore, we designed three genetic circuits based on different promoter strengths previously characterized (Anderson collection). We choose the promoters J23116, J23111 and J23100 for weak, intermediate and strong expression of spCas9, respectively. Expression was tightly controlled by the addition of a translational theophylline riboswitch between the promoter and the coding sequencing (Suess et al., 2004). Furthermore, expression of a gRNA targeting the chromosome (CRT6) was also regulated using an arabinose inducible expression system, and an additional strain with a non-targeting gRNA (CRT0) was included as a control (Table S2).

In order to determine the surviving fraction of *E. coli* carrying the different genetic circuits, serial dilutions of overnight cultures were plated with or without inducers. The fraction of surviving bacteria was determined after induction of gRNA and spCas9 compared to the uninduced control. The expression strength was clearly linked to the killing efficiency of the system (Figure 1). Moreover, we also observed a difference in the non-targeting strains indicating that the sole expression of spCas9 represented a burden for the cells. The survival rate amounted ~80 % which describes the average toxicity of Cas9.

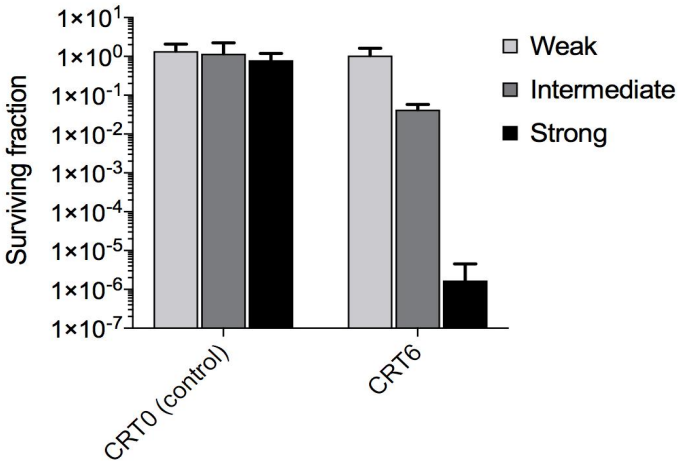

Figure1: The surviving fraction from different expression levels of spCas9. The fraction of bacteria surviving spCas9-mediated death was determined by plating the same dilution of cells on agar plates with and without the inducers (2mM of theophylline and 1% arabinose). CRT0 (control) is a guide RNA that has no target site in the chromosome of *E. coli* MG1655. CRT6 is a guide RNA with strong activity and a single target site. SpCas9 was expressed from 3 promoters with distinct strength based on the scores from the Anderson collection (http://parts.igem.org/Promoters/Catalog/Anderson) : weak (J23116), medium (J23111) and strong(J23100) promoters.

Efficiency of gRNA with multiple genomic targets

The number of target sites has been previously linked to the killing efficiency of CRISPR-Cas based antimicrobials (Caliando and Voigt, 2015). To systematically analyse the impact of DSB quantity on cell killing, 13 different gRNAs were randomly selected with between 1 and 15 target sites in the genome of *E. coli* MG1655 K12 derivate (EC0000096) (CRT1-13) (Figure 2A). In addition, a strain with a missing PAM region was designed to control for Cas9 toxicity (control/CRT0). The different gRNAs pair with the type II effector protein Cas9 to introduce DSBs. The expression of Cas9 was coupled to a theophylline riboswitch allowing induction of

killing at a defined time point. The killing efficiency was determined after induction of gRNA and Cas9 compared to an uninduced control.

In contrast to our hypothesis that the number of target sites would be linked to the killing efficiency, no correlation was observed (Figure 2B). Overall the killing efficiency was with around 99.99 % fairly high. However, two CRTs (CRT2 and CRT5) had much higher survival rates (Figure 2B). Their killing efficiency was only slightly higher compared to the toxic effects of Cas9 expression by itself. Both targeted only one genomic site. Interestingly, CRT6, had also only one target site and its performance was with 99.999% the highest (Figure 2B).

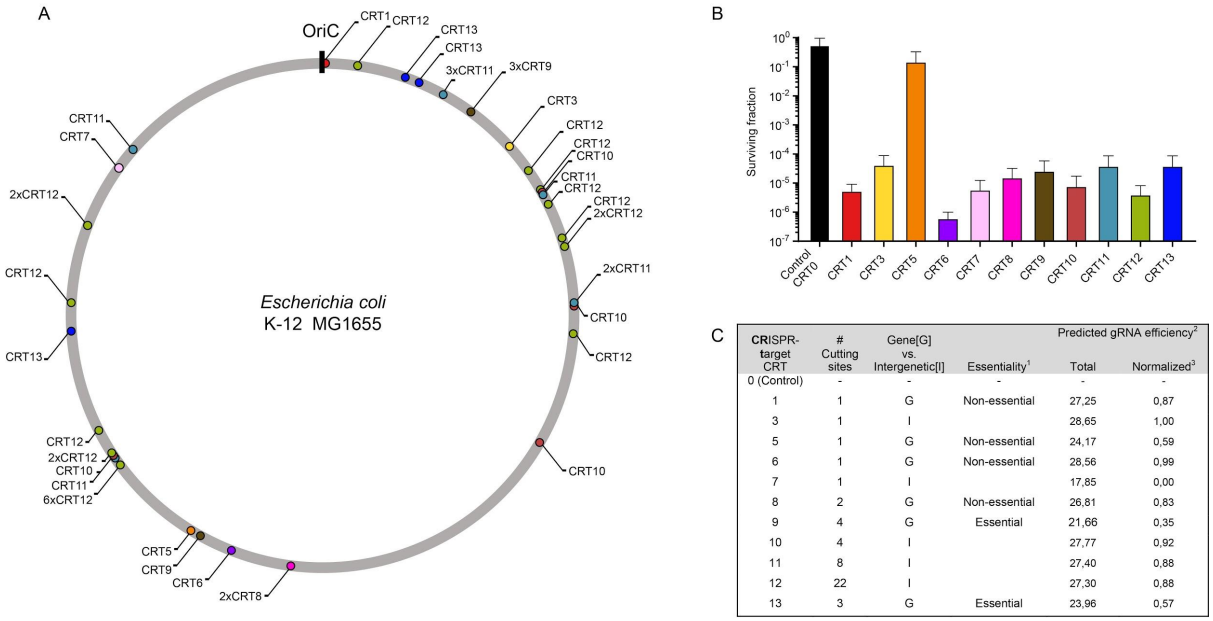

CRISPR-target CRT	# Cutting sites	Gene[G] vs. Intergenetic[I]	Essentiality[1]	Predicted gRNA efficiency[2] Total	Normalized[3]
0 (Control)	-	-	-	-	-
1	1	G	Non-essential	27,25	0,87
3	1	I		28,65	1,00
5	1	G	Non-essential	24,17	0,59
6	1	G	Non-essential	28,56	0,99
7	1	I		17,85	0,00
8	2	G	Non-essential	26,81	0,83
9	4	G	Essential	21,66	0,35
10	4	I		27,77	0,92
11	8	I		27,40	0,88
12	22	I		27,30	0,88
13	3	G	Essential	23,96	0,57

Figure 2. Chromosomal targets in *E.coli* K-12 MG1655. (A) Chromosomal map of *E.coli* K-12 MG1655 indicating the oriC and the cutting sites of the different CRISPR targets (CRTs). (B) Efficiency of the CRTs determined by the surviving fraction, the CRTs are ordered by the number of cutting sites. CRT0 indicated as a black bar served as a control gRNA with a non-targeting sequence. (C) A table, describing the CRTs used in this study. 1-Essentiality of a gene was based on the information available on Ecocyc. 2-The predicted efficiency of the CRTs was determined using the model developed by Guo et al. 2018 and was normalized against the range of values obtained for this dataset.

As a study by Gomes et al. (2016) highlighted that distance to the origin of replication (oriC) as well as coding versus non-coding regions influence the accessibility of the DNA, the target sites were chosen in a manner that they were randomly spread around the whole genome and located in both coding and noncoding regions (Figure 1A). However, neither the location of the target site nor coding versus non-coding regions in the genome could explain the differences between the killing efficiencies. This can be illustrated by comparing CRT1 and CRT2 which sole target sites are located in close proximity (500 bp difference) around 0.79 Mbp from the OriC. Yet, their killing efficiency differs by around 30 %. Moreover, CRT2 and

CRT5, the worst performing strains, both have a single target site, yet located in a non-coding region and a coding region, respectively.

Previous studies showed that activity of the gRNA that is targeting the genome has a high impact on the killing efficiency (Cui and Bikard, 2016; Moreb et al., 2017). The design rules for strong activity are not well understood, however several parameters are believed to influence the activity of the gRNA:Cas9 complex in the genome, for instance supercoiling of DNA and torsional constrains are potential biophysical factors affecting the accessibility of the target (Farasat and Salis, 2016). Libraries of thousands of gRNAs allowed scoring the activity of targets across the genome of *E.coli* (Moreb et al., 2017; Guo et al., 2018). These scores were further utilized to built a model that can predict gRNA activity to a certain extend. We also compared our measured efficiency with the predicted values based on a model by Guo et al. (2018). While some results are overlapping such as a low activity for CRT5, no clear correlation could be obtained (Figure 2C). The differences between the predicted activity scores and our results could be attributed to the differences in the experimental set-up, for instance Guo et al. (2018) used a weaker promoter (J23113) to express spCas9 and their model does not account for targets with multiple cutting sites.

In summary, no correlation between the number of target sites, the predicted gRNA efficiency, the distance to the OriC and location in coding or non-coding regions of the target sites could be established to predict killing efficiency.

Cas9 effector is the preferred target for mutations

While the majority of the bacterial population was killed through the CRISPR-induced DSBs, some cells escaped and survived. We further investigated the fraction of bacteria that survived spCas9-mediated DSB breaks. *E. coli* escapers can survive chromosomal DSBs by continuously repairing them through recA-mediated HR (Cui and Bikard, 2016; Maul and Sutton, 2005). However, we assumed that a fraction of the surviving bacteria would have acquired mutations instead of tolerating the DSB. We hypothesized, that the genetic adaptations in *E. coli* would predominantly occur in the sequence of spCas9, gRNA or in the chromosomal target site. Thus, in order to distinguish bacteria tolerating DSB from the ones that acquired beneficial mutations, we subjected 40 escaper colonies of each experiment from: CRT0 (control), CRT6, CRT11, CRT12 and CRT13 to a second round of spCas9-induced DSB. Interestingly, the frequency of transiently tolerant bacteria was fairly low (Figure 3A). The majority of bacteria

were insensitive to spCas9-induced killing after the second round of exposure, indicating that they likely acquired a genotypic adaptation that mediated their survival (Figure 3A).

As spCas9 is encoded by a long genetic sequence, we assumed that it would be the part of the genetic circuit that is most prone to accumulate mutations. In order to test this hypothesis, we functionally tested if the escape mutants disrupted the expression or activity of spCas9. We picked 14 mutants from each experiment and replaced the genetic circuit with an intact version of the plasmid but with a different selection marker. The new strains were subjected to spCas9-DSB, demonstrating in most cases that the mutant strains regained sensitivity to spCas9 mediated killing (Figure 2B). Remarkably, 4 mutants of CRT6 were able to escape even when an intact copy of spCas9 was reintroduced, indicating that they gained resistance through a different mechanism. As CRT6 had only one cutting site in the genome, it might have been more prone to mutations also in the chromosomal target site than the other CRTs, indicating that a single target makes the system more likely to fail.

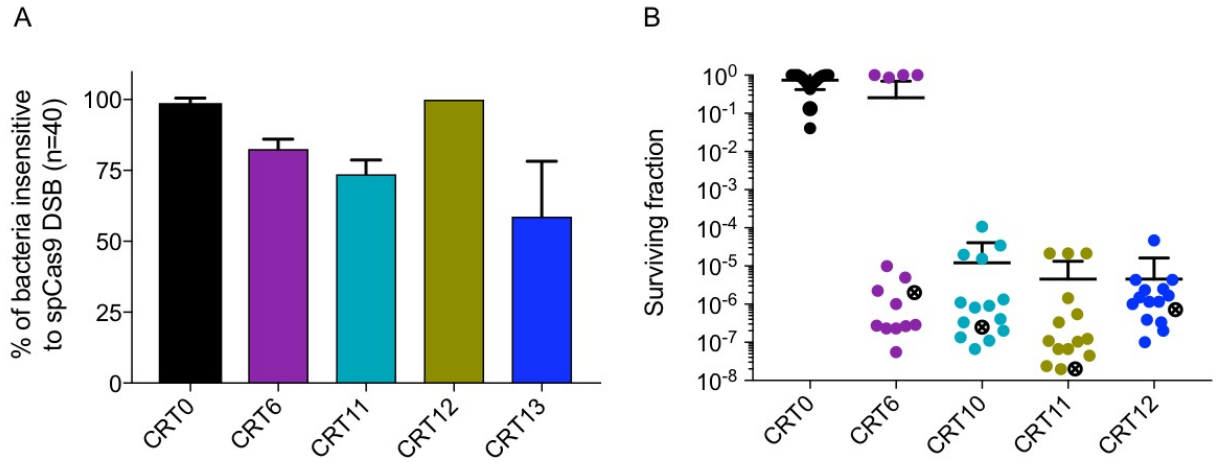

Figure 3. Functional validation of escaping mutants. (A) Percentage of bacteria that acquired a mutation inactivating the effect of the antimicrobial. (B) Surviving fraction of 14 mutants after reintroduction of an intact spCas9 copy.

To further investigate the genetic adaptations, we subjected the cells that survived also the second exposure to the CRISPR-system to whole-genome sequencing. The majority of replicates had accumulated mutations in spCas9, as suggested by our functional test (Table S1).

In short, we determined that most escaping bacteria acquired mutational resistance against CRISPR-antimicrobials and that spCas9 was the preferred target for mutations. In addition, we

found that gRNAs with multiple chromosomal targets prove to be a successful strategy to reduce mutations at the target site.

Redundant Cas9 lowers probability of nuclease failure

We hypothesized, that adding redundancy in the effector module of the system might lower the probability of acquiring a mutation that results in system failure. Accordingly, we constructed a plasmid with two spCas9 copies. However, in order to avoid recombination events between the two genes, we used a codon optimized version for yeast, spCas9-Y (Jakočiūnas et al., 2015). This copy has a different sequence at the nucleotide level, but the translated product is identical to bacterial spCas9. The effector proteins were expressed from separate promoters of identical expression strength. The efficiency of the redundant and individual systems were tested separately (Figure 4A). Unexpectedly, the single spCas9-Y and the redundant system were less efficient than the previous version of spCas9 alone (Figure 4). We observed a negative effect of expressing both effectors inside *E. coli*, which might be attributed to the detrimental effect of expressing the codon-optimized version for yeast (Boël et al., 2016).

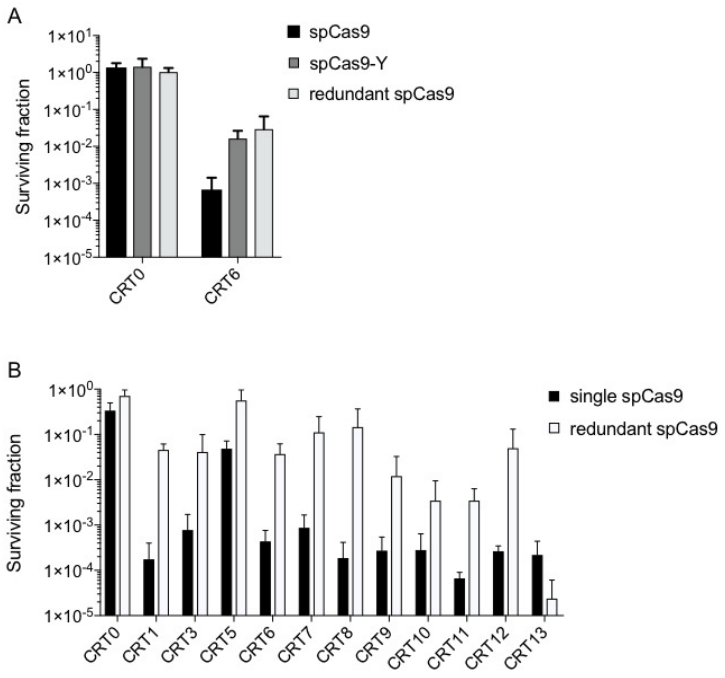

Figure 4: Redundant system. (A) Comparison of the plasmid systems expressing a single Cas9 from bacteria, single Cas9 codon-optimized for yeast and together in a redundant system. (B) Surviving fraction of bacteria as result of different gRNAs. Comparison of single and redundant system.

Discussion

CRISPR-Cas9 antimicrobials have shown great potential (Bikard et al., 2014 and Citorik et al., 2014). Yet, several challenges must be overcome before taking this technology to clinical applications. For instance, the importance of the expression of the system has been overlooked previously. Here, we demonstrate that lower spCas9 expression contributes to the transient non-lethal resistance state. We determined that in order to maximize the effect of the gRNA it is required to have high expression of spCas9. Nonetheless, this might be different depending on the organism used and could explain the apparent failure of spCas9 observed in some organisms (Jiang et al., 2018; Noduthodi et al., 2018).

Besides tolerance to DSB through RecA-mediated DNA repair, *E. coli* can acquire mutations that allow it to escape the antimicrobial effect. We found that the majority of escapers indeed accumulated mutational resistance. Further, we characterized the genetic adaptations and found that spCas9 was the preferred target for mutations. We also detected that gRNA with multiple chromosomal targets prove to be a successful strategy to reduce mutations at the target site. However, adding redundancy in the effector module did not improve the performance of the antimicrobial. The low efficiency of the redundant system might be explained by the overall effect in gene expression by the codon-optimized version of spCas9 for yeast. Expression of the second copy could be negatively affecting the expression of the bacterial spCas9 by deviating resources from it.

The escapers characterized in this study immediately mutated spCas9 or other genomic targets to allow their survival. However, antibiotic resistance is often only acquired after prolonged exposure to the antibiotic. Therefore, it would be interesting to perform a long-term evolution study to identify further mutations that might contribute to CRISPR-antimicrobial survival. In addition, other sources of resistance can be expected when the system will be applied linked to the delivery system or anti-CRISPRs acquired through horizontal gene transfer.

CRISPR-Cas antimicrobials are a promising alternative to antibiotic therapy. Therefore, research on optimizing efficiency of this potential drug is of great value. We hope that the results from this study might help designing more robust CRISPR-Cas antimicrobials in future.

Methods

Cell growth conditions

If not stated otherwise overnight cultures were used to inoculate all experiments. Cells were grown at 37 °C, 250 rpm for around 18 h. Glycerol stocks were made of overnight cultures from isolated colonies in a final glycerol concentration of 25 % and stored at -80°C.

Blunt-end ligation

Blunt-end ligation was used to create the pDual4 with different CRT's (Table S2). The reaction was incubated at 37 °C for 30 min followed by incubation at RT °C for 1 h and inactivation by incubation at 65 °C for 20 min. The ligated plasmid was transformed via electroporation in *E. coli* Top10.

Cloning of selection system

Construction of pDual plasmids for the different CRTs containing the arabinose inducible gRNA was constructed by USER cloning.The primers were design with the AMUSER web tool (Jiang et al., 2013). For amplification of backbone and DNA fragment Phusion U Polymerase from Thermofisher Scientific was used. The chimeric gRNA under a pBAD inducible system and terminator were synthesized from IDT (5'-**CTATAACCAGACCGTTCAGC**GTTTTAGAGCTAGAAATAGCAAGTTAAAATAAGGCTAGTCCG TTATCAACTTGAAAAAGTGGCACCGAGTCGGTGCTTTTTTT-3'). The backbone of the plasmid was amplified from pSEVA3610, a plasmid that contains a chloramphenicol resistance gene (cat), an arabinose inducible expression system and a low copy number origin of replication p15A (Martinez-Garcia et al., 2015).

Construction of pCasesn3 plasmid containing spCas9 was performed in a single step using USER cloning (Genee et al., 2014). The fragment containing spCas9 was amplified from DS-SPcas addgene ID48645 (Esvelt et al., 2013) and cloned into the backbone of pSEVA47 containing the low copy number origin of replication pSC101 and the antibiotic resistance gene *aadA* that confers resistance against Spectinomycin (Martinez-Garcia et al., 2015). The theophylline riboswitch was placed in front of Cas9 using a long forward primer from IDT (5'-AAGTCTAGCGAACCGCACTTAATACGACTCACTATAGGTACCGGTGATACCAGCATCGTCTTG ATGCCCTTGGCAGCACCCTGCTAAGGTAACAACAAGATGATGGATAAGAAATACTCAATAGG CTTAGATATCGGCAC-3'). Additionally, a sigma70 constitutive promoter was also introduced using a reverse primer in order to introduce a different promoter for Cas9 (5'-

ctctagTagctagcactgtacctaggactgagctagccgtcaaGTTAGCTGTGCTCTAGAAGCTAGCAG-3').

Survival-assay

Overnight culutures of the strains subjected to the survival-assay were diluted up to 10^{-8}. 5 µL of the dilution series were spotted in technical repliactes on agar plates containing the required antibiotics and inducers (2mM theophylline and 1% arabinose). As control the same dilution series were spotted on agar plates only containing the required antibiotics. The plates were incubated overnight at 37 °C. For evaluation of the Colony-forming units (CFUs), surviving cells were counted and normalized to the uninduced control. Experiments were repeated three times on independent days.

Functional-testing of Cas9-Mutations

Cells surviving the survival-assay under induced conditions were picked and a new Cas9 plasmid with a different antibiotic selection marker was introduced via electroporation. Colonies of the transformation were randomly picked and an overnight culture was prepared. The overnight cultures were used to perform the survival-assay as described above once in technical replicates. The survival rate of the escape mutants with reintroduced Cas9 was compared to the respective untreated ancestor strain as control. Significance levels were determined with GraphpadPrism7.

Prediction of gRNA activity

The activity of the gRNA for each CRT was predicted using the model developed by Guo et al. 2018. Using the CRTs spacers in Supp. Table S3 and applying the default parameters. https://github.com/zhangchonglab/sgRNA-cleavage-activity-prediction

Statistical analysis

For the statistical analysis (e.g. One-way ANOVA) GraphpadPrism7 software was used.

Whole-genome-sequencing

Washed pellets of overnight cultures were sent for genomic DNA extraction (ZYMO research), Nextera XT library preparation (Illumina) and 125 paired-end whole-genome Illumina HiSeq 2500 sequencing to BaseClear B.V.. The resulting fasta reads were used to identify single nucleotide polymorphisms, small insertions and deletions by CLC genomic workbench. We

included only positions with a phred-score greater 30 also at the neighboring three bases and filtered for a frequency of at least 80 %. Other parameters were kept at default conditions.

Supplementary

Supplementary table S1. Mutations identified in escapers. Supplemenary table can be found here: https://www.dropbox.com/preview/Supplementary/S1_CRISPR.csv?role=work

Supplementary table S2. Strain and plasmids used in this study.

Strain	Description	Reference
Escherichia coli Top 10	F- *mcr*A Δ(*mrr-hsd*RMS-mcrBC) Φ80l*ac*ZΔM15 Δ *lac*X74 *rec*A1 *ara*D139 Δ(*araleu*)7697 *gal*U *gal*K *rps*L (Str^R) *en*dA1 *nup*G	Thermofisher Scientific®
Escherichia coli MG1655	Wild-type *E. coli* MG1655 derived from *E. coli* K12	Blattner et. al. 1997

Plasmids	Description	Reference
pCaSens3Spec	$Spec^r$;bacterial *cas*9; RBS_{Theo}; CloDF1	This study
pCaSens3Kan	Kan^r ;bacterial *cas*9; RBS_{Theo}; CloDF1	This study
PCaSens6Spec	$Spec^r$;bacterial *cas*9; yeast-like *cas*9; RBS_{Theo}; CloDF1	This study
pCaSens7Spec	$Spec^r$;yeast-like *cas*9; RBS_{Theo}; CloDF1	This study
pDual4CRT#0	Cm^r; gRNA (5'agttctggcaagcgcggtaa 3') P_{BAD}; p15a	This study
pDual4CRT#1	Cm^r; gRNA (5'tggggctatcgataaactcg 3') P_{BAD}; p15a	This study
pDual4CRT#3	Cm^r; gRNA (5'cacttcagttctttctcatc 3') P_{BAD}; p15a	This study
pDual4CRT#5	Cm^r; gRNA (5'ctatgcgctggatacctta 3') P_{BAD}; p15a	This study
pDual4CRT#6	Cm^r; gRNA (5' tgacgactgacttaacgctc 3') P_{BAD}; p15a	This study
pDual4CRT#7	Cm^r; gRNA (5' cggcatctgcacctcgccac 3')	This study

	P_{BAD}; p15a	
pDual4CRT#8	Cm^r; gRNA (5' cgcggatcaacctgttcttc 3') P_{BAD} ; p15a	This study
pDual4CRT#9	Cm^r; gRNA (5'cgaactcgcgaccccgacct 3') P_{BAD}; p15a	This study
pDual4CRT#10	Cm^r; gRNA (5' tttgtaggcctgataagacg 3') P_{BAD}; p15a	This study
pDual4CRT#11	Cm^r; gRNA (5' gacgcggcaagcgtcgcatc 3') P_{BAD}; p15a	This study
pDual4CRT#12	Cm^r; gRNA (5' aagacgcgccagcgtcgcatc 3') P_{BAD}; p15a	This study
pDual4CRT#	Cm^r gRNA(5' agacgcgccagcgtcgcatc 3') P_{BAD}; p15a	This study
pFLP	Flipase activity	Kuhlman and Cox 2009
pTKred	recombeneering	Kuhlman and Cox 2009

Supplementary table S3. Detailed information of CRTs

CRT	# of cutting sites	sequence	PAM	Gene vs. Intergenetic location	Function	Predicted RNA cleavage efficiency
CRT0 (Control)	-	-	-	-	catabolic process	25.69
1	1	tggggctatcgataaactcg	agg	G	Protein MioC, electron transporter	27.24
3	1	cacttcagttctttctcatc	ggg	I		28.64
5	1	ctatgcgctggatacctta	cgg	G	Flagellar protein FliL, bacterial-type flagellum-dependent swarming motility	24.17
6	1	tgacgactgacttaacgctc	agg	G	Long-chain-fatty-acid-CoA ligase	28.55
7	2	cggcatctgcacctcgccac	cgg	I		17.84

Acknowledgments

This work was supported by the European Union's Horizon 2020 research and innovation program under the Marie Sklodowska-Curie grant agreement No 642738, MetaRNA. In addition, funding was received from the Danish Council for Independent Research, Sapere Aude Program DFF 4004-00213 and from The Novo Nordisk Foundation under NFF grant number: NNF10CC1016517.

Author contributions

R.V., L.J.J. and M.O.A.S conceived and designed the project. R.V., C.R., and L.J.J. conducted the experimental work. R.V. and C.R. analyzed and visualized the phenotypic data. L.J.J. and S.L. analyzed the genomic data. R.V., L.J.J. and C.R. wrote the manuscript.

References

Ayora, S., Carrasco, B., Cárdenas, P.P., César, C.E., Cañas, C., Yadav, T., Marchisone, C., and Alonso, J.C. (2011). Double-strand break repair in bacteria: a view from Bacillus subtilis. FEMS Microbiol. Rev. *35*, 1055–1081.

Bikard, D., Euler, C.W., Jiang, W., Nussenzweig, P.M., Goldberg, G.W., Duportet, X., Fischetti, V.A., and Marraffini, L.A. (2014). Exploiting CRISPR-Cas nucleases to produce sequence-specific antimicrobials. Nat. Biotechnol. *32*, 1146–1150.

Bush, K., Courvalin, P., Dantas, G., Davies, J., Eisenstein, B., Huovinen, P., Jacoby, G.A., Kishony, R., Kreiswirth, B.N., Kutter, E., et al. (2011). Tackling antibiotic resistance. Nat. Rev. Microbiol. *9*, 894–896.

Cho, I., and Blaser, M.J. (2012). The human microbiome: at the interface of health and disease. Nat. Rev. Genet. *13*, 260–270.

Citorik, R.J., Mimee, M., and Lu, T.K. (2014). Sequence-specific antimicrobials using efficiently delivered RNA-guided nucleases. Nat. Biotechnol. *32*, 1141–1145.

Cong, L., Ran, F.A., Cox, D., Lin, S., Barretto, R., Habib, N., Hsu, P.D., Wu, X., Jiang, W., Marraffini, L.A., et al. (2013). Multiplex genome engineering using CRISPR/Cas systems. Science *339*, 819–823.

Cui, L., and Bikard, D. (2016). Consequences of Cas9 cleavage in the chromosome of Escherichia coli. Nucleic Acids Res. *44*, 4243–4251.

Davis, A.J., and Chen, D.J. (2013). DNA double strand break repair via non-homologous end-joining. Transl. Cancer Res. *2*, 130–143.

Deltcheva, E., Chylinski, K., Sharma, C.M., Gonzales, K., Chao, Y., Pirzada, Z.A., Eckert, M.R., Vogel, J., and Charpentier, E. (2011). CRISPR RNA maturation by *trans*-encoded small RNA and host factor RNase III. Nature *471*, 602–607.

Farasat, I., and Salis, H.M. (2016). A Biophysical Model of CRISPR/Cas9 Activity for Rational Design of Genome Editing and Gene Regulation. PLOS Comput. Biol. *12*, e1004724.

Gomaa, A.A., Klumpe, H.E., Luo, M.L., Selle, K., Barrangou, R., and Beisel, C.L. (2014). Programmable Removal of Bacterial Strains by Use of Genome-Targeting CRISPR-Cas Systems. MBio *5*, e00928-13.

Guo, J., Wang, T., Guan, C., Liu, B., Luo, C., Xie, Z., Zhang, C., and Xing, X.-H. (2018). Improved sgRNA design in bacteria via genome-wide activity profiling. Nucleic Acids Res. *46*, 7052–7069.

Hidalgo-Cantabrana, C., O'Flaherty, S., and Barrangou, R. (2017). CRISPR-based engineering of next-generation lactic acid bacteria. Curr. Opin. Microbiol. *37*, 79–87.

Horvath, P., and Barrangou, R. (2010). CRISPR/Cas, the Immune System of Bacteria and Archaea. Science *327*, 167–170.

Hullahalli, K., Rodrigues, M., Nguyen, U.T., and Palmer, K. (2018). An Attenuated CRISPR-Cas System in Enterococcus faecalis Permits DNA Acquisition. MBio *9*, e00414-18.

Jakobsson, H.E., Jernberg, C., Andersson, A.F., Sjölund-Karlsson, M., Jansson, J.K., and Engstrand, L. (2010). Short-Term Antibiotic Treatment Has Differing Long-Term Impacts on the Human Throat and Gut Microbiome. PLOS ONE *5*, e9836.

Jiang, W., Bikard, D., Cox, D., Zhang, F., and Marraffini, L.A. (2013). RNA-guided editing of bacterial genomes using CRISPR-Cas systems. Nat. Biotechnol. *31*, 233–239.

Jinek, M., Chylinski, K., Fonfara, I., Hauer, M., Doudna, J.A., and Charpentier, E. (2012). A programmable dual-RNA-guided DNA endonuclease in adaptive bacterial immunity. Science *337*, 816–821.

Johnson, S. (2009). Recurrent Clostridium difficile infection: A review of risk factors,

treatments, and outcomes. J. Infect. *58*, 403–410.

Lauritsen, I., Porse, A., Sommer, M.O.A., and Nørholm, M.H.H. (2017). A versatile one-step CRISPR-Cas9 based approach to plasmid-curing. Microb. Cell Factories *16*, 135.

Mali, P., Yang, L., Esvelt, K.M., Aach, J., Guell, M., DiCarlo, J.E., Norville, J.E., and Church, G.M. (2013). RNA-Guided Human Genome Engineering via Cas9. Science *339*, 823–826.

Marraffini, L.A. (2016). The CRISPR-Cas system of Streptococcus pyogenes: function and applications. In Streptococcus Pyogenes : Basic Biology to Clinical Manifestations, J.J. Ferretti, D.L. Stevens, and V.A. Fischetti, eds. (Oklahoma City (OK): University of Oklahoma Health Sciences Center), p.

Maul, R.W., and Sutton, M.D. (2005). Roles of the Escherichia coli RecA protein and the global SOS response in effecting DNA polymerase selection in vivo. J. Bacteriol. *187*, 7607–7618.

Moreb, E.A., Hoover, B., Yaseen, A., Valyasevi, N., Roecker, Z., Menacho-Melgar, R., and Lynch, M.D. (2017). Managing the SOS Response for Enhanced CRISPR-Cas-Based Recombineering in E. coli through Transient Inhibition of Host RecA Activity. ACS Synth. Biol. *6*, 2209–2218.

Suess, B., Fink, B., Berens, C., Stentz, R., and Hillen, W. (2004). A theophylline responsive riboswitch based on helix slipping controls gene expression in vivo. Nucleic Acids Res. *32*, 1610–1614.

Chapter V - Conclusion and perspective

Conclusion and perspective

This thesis conveyed that antibiotic resistance challenges the global public health and that action in various forms, including basic research, is needed in order to tackle the antibiotic resistance crisis. The research conducted in this thesis might provide a piece of the puzzle in how to solve the antibiotic resistance crisis by contributing to our basic understanding in various areas. These areas included: how antibiotic resistance evolves (**manuscript 1**, **3**, **4** and **6**); what the limitations and constrains in the evolution of antibiotic resistance are (**manuscript 3**, **4** and **5**); which limitations and constrains could potentially be exploited to decelerate antibiotic resistance evolution in future (**manuscript 3** and **4**) or help to improve antimicrobial therapy with novel agents, by circumventing specific resistance mechanisms (**manuscript 6**). However, the work conducted incorporated basic research, which needs to be further investigated in more complex and natural settings to be verified, especially to provide clinical context. Consequently, basic and applied research needs to be continued in future to provide solutions to the antibiotic resistance crisis.

Looking on Pubmed publications using the term "antibiotic resistance" one can see that the abundance of literature in this field is fairly high, e.g. comparing it to "hot" biology topics such as CRISPR, reassuring that many scientists in the world base their work around antibiotic resistance and contribute to the improvement of the resistance crisis (Figure 12). Yet, lately the trend is descending and I hope that it will stabilize again at a high level in the future.

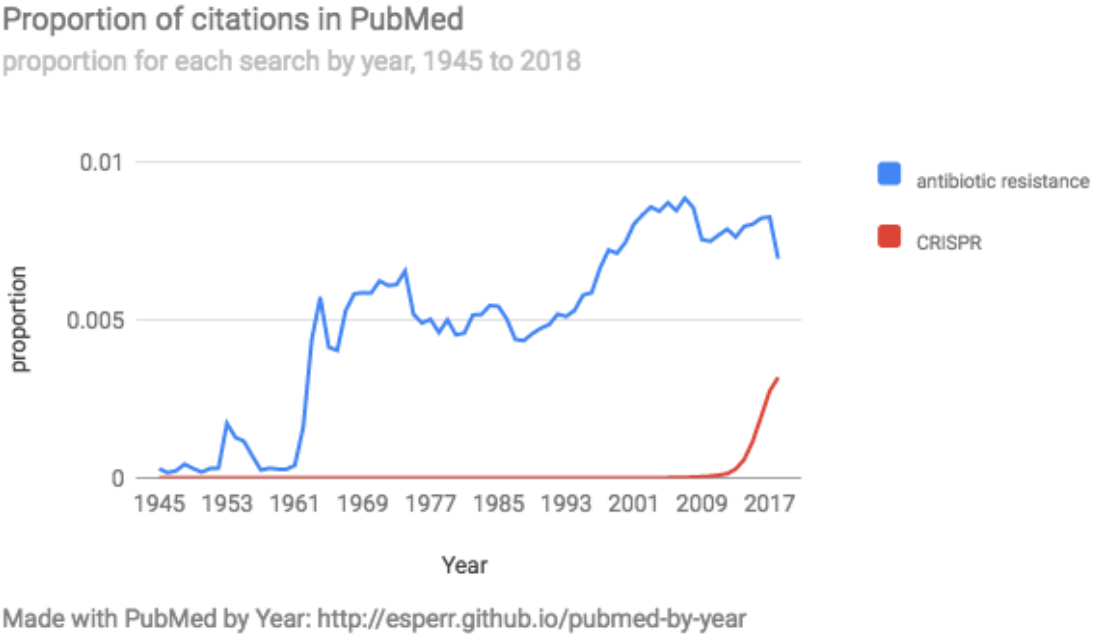

Figure 12: Proportion of citations of papers about antibiotic resistance (blue) or CRISPR (red) in pubmed over time. The figure was obtained from PubMed by Year.

Furthermore, recently a lot of research has been conducted in order to develop strategies to make antibiotic development more competitive and attractive for companies[227–232]. And interestingly, the trend of a reduction in novel antibiotic approvals is indeed slowly overcome. In the recent years, increasing numbers of novel antibiotics are entering the market (Figure 13) e.g. in 2018 5 novel antibiotics have been approved by the FDA[233], including urgently needed agents against Gram-negative bacteria[234]. Overall the number of FDA approved antibiotics seems to increase almost linearly (Figure 13).

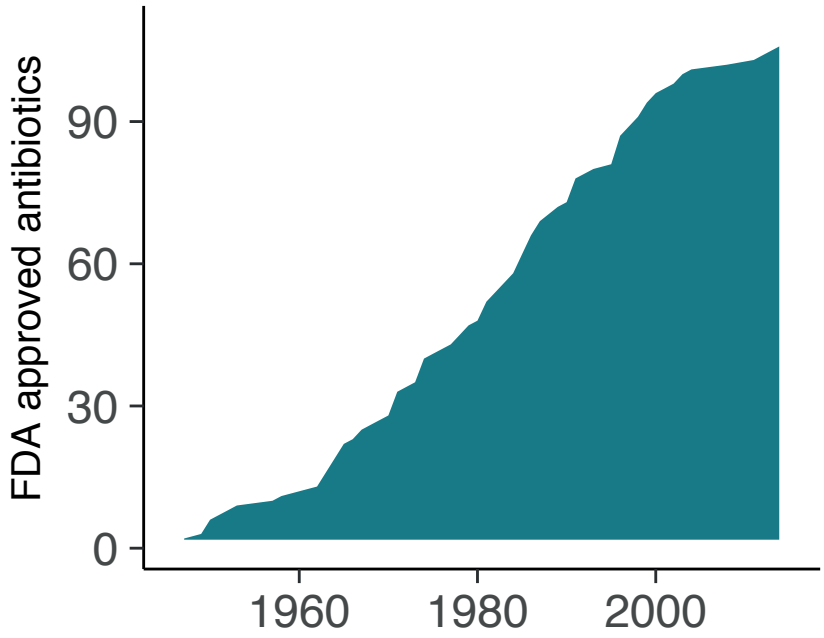

Figure 13: FDA approved antibiotics over time. The data was obtained by searching Drugbank[14] for all antibacterial agents and using their names to retrieve all FDA approved antibiotics from the orange book of the FDA[20].

Combined with the medial attention, public health efforts and global action plans, I think we are on a good path in order to combat the antibiotic resistance crisis. Yet, the resistance crisis is often compared to the "Red Queen's Race" a scene from "Through the looking-glass" by Lewis Caroll, where Alice and the red queen are running but staying at the same spot (Figure 14). This image is well suited to visualize the deadly race between adapting bacteria and humans developing answers to these adaptations. Consequently, it is important to be aware that even if we are on a good path now to control the resistance crisis that we can never stop

running; we need to continue our efforts in research, communication, education and novel drug development in order to keep our ability to treat infectious diseases also in future generations.

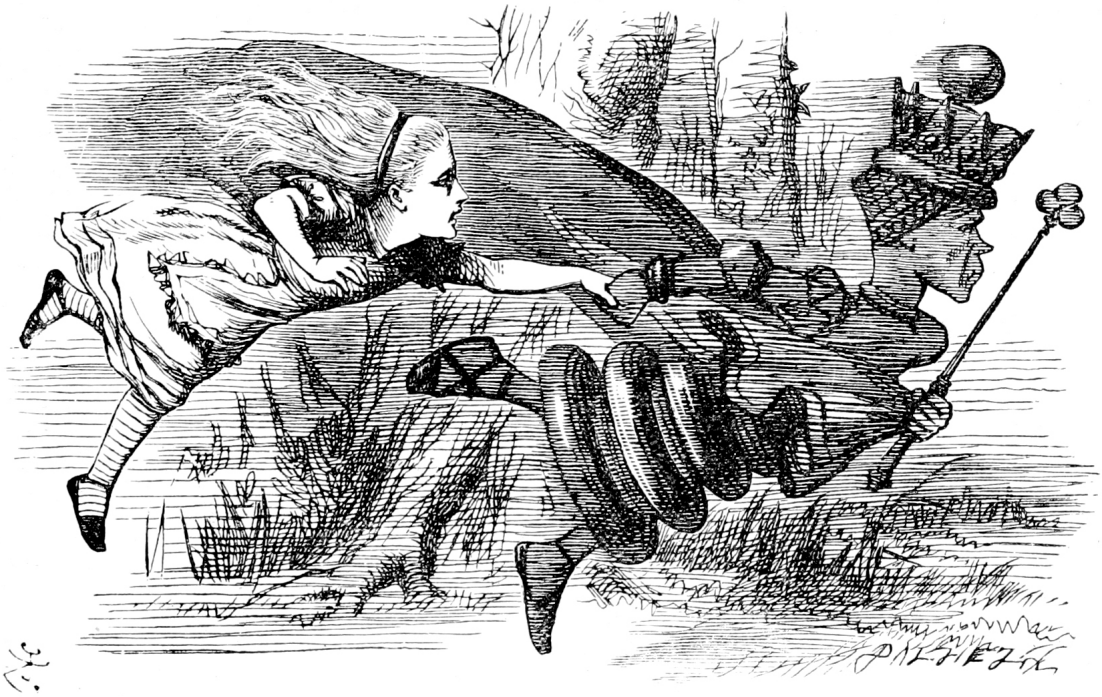

Figure 14: Red Queens Race. The illustration was made by John Tenniel[235], the illustration is public domain since John Tenniel died more than 100 years ago in 1914.

Acknowledgement

I would like to thank Alexander Hauser for providing me with the tittle figure for my thesis as well as with DrugBank and FDA approval data that I used to create multiple figures in this thesis. I am also thankful for his constructive comments on the thesis. In addition, I am extremely grateful that Andreas Porse, Mari Rodriguez de Evgrafov, Simone Li and Vanessa Rees were proofreading this thesis and provided their critical input. Finally, I would like to thank Andreas Porse for the translation of the Dansk Resumé.

References

1. Blundell, J. R. & Levy, S. F. Beyond genome sequencing: lineage tracking with barcodes to study the dynamics of evolution, infection, and cancer. *Genomics* **104**, 417–430 (2014).
2. R. Julian, T. Environmental transmission of diarrheal pathogens in low and middle income countries. *Environ. Sci. Process. Impacts* **18**, 944–955 (2016).
3. Solo-Gabriele, H. M. *et al.* Beach sand and the potential for infectious disease transmission: observations and recommendations. *J. Mar. Biol. Assoc. U. K.* **96**, 101–120 (2016).
4. Wolfe, N. D., Dunavan, C. P. & Diamond, J. Origins of major human infectious diseases. *Nature* **447**, 279–283 (2007).
5. Conly, J. & Johnston, B. Where are all the new antibiotics? The new antibiotic paradox. *Can. J. Infect. Dis. Med. Microbiol.* **16**, 159–160 (2005).
6. Runcie, H. Infection in a Pre-Antibiotic Era. *J. Anc. Dis. Prev. Remedies* **03**, (2015).
7. Hughes, D. & Karlén, A. Discovery and preclinical development of new antibiotics. *Ups. J. Med. Sci.* **119**, 162–169 (2014).
8. Waksman, S. A. The Role of Antibiotics in Nature. *Perspect. Biol. Med.* **4**, 271–287 (1961).
9. Sengupta, S., Chattopadhyay, M. K. & Grossart, H.-P. The multifaceted roles of antibiotics and antibiotic resistance in nature. *Front. Microbiol.* **4**, (2013).
10. Mlot, C. Antibiotics in Nature: Beyond Biological Warfare. *Science* **324**, 1637–1639 (2009).
11. Clardy, J., Fischbach, M. & Currie, C. The natural history of antibiotics. *Curr. Biol. CB* **19**, R437–R441 (2009).

12. Lewis, K. Platforms for antibiotic discovery. *Nat. Rev. Drug Discov.* **12**, 371–387 (2013).
13. Etebu, E. & Arikekpar, I. Antibiotics: Classification and mechanisms of action with emphasis on molecular perspectives. *Int J Appl Microbiol Biotechnol Res* **4**, 90–101 (2016).
14. Wishart, D. S. *et al.* DrugBank 5.0: a major update to the DrugBank database for 2018. *Nucleic Acids Res.* **46**, D1074–D1082 (2018).
15. Danishuddin, M. & Khan, A. U. Virtual screening strategies: a state of art to combat with multiple drug resistance strains. *MOJ Proteomics Bioinforma.* **2**, 1–0 (2015).
16. Norfloxacin: a fluoroquinolone carboxylic acid antimicrobial agent. *Am. J. Med.* **82**, 1–92 (1987).
17. Wright, P. M., Seiple, I. B. & Myers, A. G. The Evolving Role of Chemical Synthesis in Antibacterial Drug Discovery. *Angew. Chem. Int. Ed Engl.* **53**, 8840–8869 (2014).
18. Towse, A. *et al.* Time for a change in how new antibiotics are reimbursed: Development of an insurance framework for funding new antibiotics based on a policy of risk mitigation. *Health Policy* **121**, 1025–1030 (2017).
19. Sharland, M. *et al.* Classifying antibiotics in the WHO Essential Medicines List for optimal use—be AWaRe. *Lancet Infect. Dis.* **18**, 18–20 (2018).
20. Research, C. for D. E. and. Orange Book Data Files. *FDA* (2019).
21. Rosenblatt-Farrell, N. The Landscape of Antibiotic Resistance. *Environ. Health Perspect.* **117**, A244–A250 (2009).
22. Hopwood, D. A. How do antibiotic-producing bacteria ensure their self-resistance before antibiotic biosynthesis incapacitates them? *Mol. Microbiol.* **63**, 937–940 (2007).

23. Allen, H. K. *et al.* Call of the wild: antibiotic resistance genes in natural environments. *Nat. Rev. Microbiol.* **8**, 251–259 (2010).

24. Fair, R. J. & Tor, Y. Antibiotics and Bacterial Resistance in the 21st Century. *Perspect. Med. Chem.* **6**, 25–64 (2014).

25. Berglund, B. Environmental dissemination of antibiotic resistance genes and correlation to anthropogenic contamination with antibiotics. *Infect. Ecol. Epidemiol.* **5**, 28564 (2015).

26. Jasovský, D., Littmann, J., Zorzet, A. & Cars, O. Antimicrobial resistance—a threat to the world's sustainable development. *Ups. J. Med. Sci.* **121**, 159–164 (2016).

27. Naylor, N. R. *et al.* Estimating the burden of antimicrobial resistance: a systematic literature review. *Antimicrob. Resist. Infect. Control* **7**, 58 (2018).

28. Teillant, A., Gandra, S., Barter, D., Morgan, D. J. & Laxminarayan, R. Potential burden of antibiotic resistance on surgery and cancer chemotherapy antibiotic prophylaxis in the USA: a literature review and modelling study. *Lancet Infect. Dis.* **15**, 1429–1437 (2015).

29. Taylor, J. *et al.* Estimating the economic costs of antimicrobial resistance. (2014). Available at: https://www.rand.org/pubs/research_reports/RR911.html. (Accessed: 28th January 2019)

30. Lee, B. Y. *et al.* The economic burden of community-associated methicillin-resistant Staphylococcus aureus (CA-MRSA). *Clin. Microbiol. Infect. Off. Publ. Eur. Soc. Clin. Microbiol. Infect. Dis.* **19**, 528–536 (2013).

31. Jansen, G., Barbosa, C. & Schulenburg, H. Experimental evolution as an efficient tool to dissect adaptive paths to antibiotic resistance. *Drug Resist. Updat.* **16**, 96–107 (2013).

32. Darwin, C. On the origin of species by means of natural selection. (1859).

33. Enright, M. C. & Spratt, B. G. Extensive variation in the ddl gene of penicillin-resistant Streptococcus pneumoniae results from a hitchhiking effect driven by the penicillin-binding protein 2b gene. *Mol. Biol. Evol.* **16**, 1687–1695 (1999).
34. Freese, P. D., Korolev, K. S., Jiménez, J. I. & Chen, I. A. Genetic Drift Suppresses Bacterial Conjugation in Spatially Structured Populations. *Biophys. J.* **106**, 944–954 (2014).
35. Lande, R. Natural Selection and Random Genetic Drift in Phenotypic Evolution. *Evolution* **30**, 314–334 (1976).
36. Baquero, F. & Blázquez, J. Evolution of antibiotic resistance. *Trends Ecol. Evol.* **12**, 482–487 (1997).
37. Baquero, F., Negri, M.-C., Morosini, M.-I. & Blázquez, J. Antibiotic-Selective Environments. *Clin. Infect. Dis.* **27**, S5–S11 (1998).
38. Livermore, D. M. Linezolid in vitro: mechanism and antibacterial spectrum. *J. Antimicrob. Chemother.* **51 Suppl 2**, ii9-16 (2003).
39. Meylan, S. *et al.* Carbon Sources Tune Antibiotic Susceptibility in Pseudomonas aeruginosa via Tricarboxylic Acid Cycle Control. *Cell Chem. Biol.* **24**, 195–206 (2017).
40. Nguyen, D. *et al.* Active Starvation Responses Mediate Antibiotic Tolerance in Biofilms and Nutrient-Limited Bacteria. *Science* **334**, 982–986 (2011).
41. Lee, H. H., Molla, M. N., Cantor, C. R. & Collins, J. J. Bacterial charity work leads to population-wide resistance. *Nature* **467**, 82–85 (2010).
42. Que, Y.-A. *et al.* A Quorum Sensing Small Volatile Molecule Promotes Antibiotic Tolerance in Bacteria. *PLOS ONE* **8**, e80140 (2013).
43. Stewart, P. S. Antimicrobial Tolerance in Biofilms. *Microbiol. Spectr.* **3**, (2015).

44. Aminov, R. I. & Mackie, R. I. Evolution and ecology of antibiotic resistance genes. *FEMS Microbiol. Lett.* **271**, 147–161 (2007).

45. Jiang, X. *et al.* Dissemination of antibiotic resistance genes from antibiotic producers to pathogens. *Nat. Commun.* **8**, 15784 (2017).

46. Lacroix, B. & Citovsky, V. Transfer of DNA from Bacteria to Eukaryotes. *mBio* **7**, e00863-16 (2016).

47. Nikolaidis, N., Doran, N. & Cosgrove, D. J. Plant expansins in bacteria and fungi: evolution by horizontal gene transfer and independent domain fusion. *Mol. Biol. Evol.* **31**, 376–386 (2014).

48. von Wintersdorff, C. J. H. *et al.* Dissemination of Antimicrobial Resistance in Microbial Ecosystems through Horizontal Gene Transfer. *Front. Microbiol.* **7**, (2016).

49. Martinez, J. L. & Baquero, F. Mutation frequencies and antibiotic resistance. *Antimicrob. Agents Chemother.* **44**, 1771–1777 (2000).

50. Johnson, J. R., Johnston, B., Clabots, C., Kuskowski, M. A. & Castanheira, M. Escherichia coli Sequence Type ST131 as the Major Cause of Serious Multidrug-Resistant E. coli Infections in the United States. *Clin. Infect. Dis.* **51**, 286–294 (2010).

51. Tenaillon, O., Skurnik, D., Picard, B. & Denamur, E. The population genetics of commensal Escherichia coli. *Nat. Rev. Microbiol.* **8**, 207–217 (2010).

52. UCSB Science Line. Available at: https://scienceline.ucsb.edu/getkey.php?key=3775. (Accessed: 11th February 2019)

53. Sommer, M. O. A., Munck, C., Toft-Kehler, R. V. & Andersson, D. I. Prediction of antibiotic resistance: time for a new preclinical paradigm? *Nat. Rev. Microbiol.* **15**, 689–696 (2017).

54. Son, M. S., Matthews, W. J., Kang, Y., Nguyen, D. T. & Hoang, T. T. In Vivo Evidence of Pseudomonas aeruginosa Nutrient Acquisition and Pathogenesis in the Lungs of Cystic Fibrosis Patients. *Infect. Immun.* **75**, 5313–5324 (2007).

55. Robinson, D. A., Feil, E. J. & Falush, D. *Bacterial Population Genetics in Infectious Disease*. (John Wiley & Sons, 2010).

56. Jayaraman, R. Mutators and hypermutability in bacteria: the Escherichia coli paradigm. *J. Genet.* **88**, 379–391 (2009).

57. Baquero, M.-R. *et al.* Polymorphic Mutation Frequencies in Escherichia coli: Emergence of Weak Mutators in Clinical Isolates. *J. Bacteriol.* **186**, 5538–5542 (2004).

58. Denamur, E. *et al.* High Frequency of Mutator Strains among Human Uropathogenic Escherichia coli Isolates. *J. Bacteriol.* **184**, 605–609 (2002).

59. Mena, A. *et al.* Genetic Adaptation of Pseudomonas aeruginosa to the Airways of Cystic Fibrosis Patients Is Catalyzed by Hypermutation. *J. Bacteriol.* **190**, 7910–7917 (2008).

60. Chopra, I., O'Neill, A. J. & Miller, K. The role of mutators in the emergence of antibiotic-resistant bacteria. *Drug Resist. Updat.* **6**, 137–145 (2003).

61. JAYARAMAN, R. Hypermutation and stress adaptation in bacteria. *J. Genet.* **90**, 383–391 (2011).

62. Eliopoulos, G. M. & Blázquez, J. Hypermutation as a factor contributing to the acquisition of antimicrobial resistance. *Clin. Infect. Dis.* **37**, 1201–1209 (2003).

63. Blazquez, J., Oliver, A. & Gomez-Gomez, J.-M. Mutation and Evolution of Antibiotic Resistance: Antibiotics as Promoters of Antibiotic Resistance? (2002). doi:info:doi/10.2174/1389450023347579

64. Kohanski, M. A., DePristo, M. A. & Collins, J. J. Sublethal Antibiotic Treatment Leads to Multidrug Resistance via Radical-Induced Mutagenesis. *Mol. Cell* **37**, 311–320 (2010).

65. Edlund, T. & Normark, S. Recombination between short DNA homologies causes tandem duplication. *Nature* **292**, 269 (1981).

66. Sandegren, L. & Andersson, D. I. Bacterial gene amplification: implications for the evolution of antibiotic resistance. *Nat. Rev. Microbiol.* **7**, 578–588 (2009).

67. Koskiniemi, S., Sun, S., Berg, O. G. & Andersson, D. I. Selection-Driven Gene Loss in Bacteria. *PLoS Genet* **8**, e1002787 (2012).

68. Török, M., Chantratita, N. & Peacock, S. Bacterial gene loss as a mechanism for gain of antimicrobial resistance. *Curr. Opin. Microbiol.* **15**, 583–587 (2012).

69. Vandecraen, J., Chandler, M., Aertsen, A. & Houdt, R. V. The impact of insertion sequences on bacterial genome plasticity and adaptability. *Crit. Rev. Microbiol.* **43**, 709–730 (2017).

70. Nicoloff, H., Perreten, V. & Levy, S. B. Increased Genome Instability in Escherichia coli lon Mutants: Relation to Emergence of Multiple-Antibiotic-Resistant (Mar) Mutants Caused by Insertion Sequence Elements and Large Tandem Genomic Amplifications. *Antimicrob. Agents Chemother.* **51**, 1293–1303 (2007).

71. Andersson, D. I. & Hughes, D. Antibiotic resistance and its cost: is it possible to reverse resistance? *Nat. Rev. Microbiol.* (2010). doi:10.1038/nrmicro2319

72. Barbosa, T. M. & Levy, S. B. The impact of antibiotic use on resistance development and persistence. *Drug Resist. Updat.* **3**, 303–311 (2000).

73. Andersson, D. I. Persistence of antibiotic resistant bacteria. *Curr. Opin. Microbiol.* **6**, 452–456 (2003).

74. Andersson, D. I. & Levin, B. R. The biological cost of antibiotic resistance. *Curr. Opin. Microbiol.* **2**, 489–493 (1999).

75. Andersson, D. I. & Hughes, D. Persistence of antibiotic resistance in bacterial populations. *FEMS Microbiol. Rev.* **35**, 901–911 (2011).

76. Horinouchi, S., Byeon, W. H. & Weisblum, B. A complex attenuator regulates inducible resistance to macrolides, lincosamides, and streptogramin type B antibiotics in Streptococcus sanguis. *J. Bacteriol.* **154**, 1252–1262 (1983).

77. Wong, A. Epistasis and the Evolution of Antimicrobial Resistance. *Front. Microbiol.* **8**, (2017).

78. Lopatkin, A. J. *et al.* Persistence and reversal of plasmid-mediated antibiotic resistance. *Nat. Commun.* **8**, 1689 (2017).

79. Lau, B. T. C., Malkus, P. & Paulsson, J. New quantitative methods for measuring plasmid loss rates reveal unexpected stability. *Plasmid* **70**, 353–361 (2013).

80. Lee, J.-Y., Park, Y. K., Chung, E. S., Na, I. Y. & Ko, K. S. Evolved resistance to colistin and its loss due to genetic reversion in *Pseudomonas aeruginosa*. *Sci. Rep.* **6**, 25543 (2016).

81. Meka, V. G. *et al.* Reversion to susceptibility in a linezolid-resistant clinical isolate of Staphylococcus aureus. *J. Antimicrob. Chemother.* **54**, 818–820 (2004).

82. Patel, A. B., Hill, E., Simpson, E. L. & Hanifin, J. M. Reversion of Methicillin-Resistant Staphylococcus aureus Skin Infections to Methicillin-Susceptible Isolates. *JAMA Dermatol.* **149**, 1167–1171 (2013).

83. Schrag, S. J., Perrot, V. & Levin, B. R. Adaptation to the fitness costs of antibiotic resistance in Escherichia coli. *Proc. R. Soc. Lond. B Biol. Sci.* **264**, 1287–1291 (1997).

84. Schulz zur Wiesch, P., Engelstadter, J. & Bonhoeffer, S. Compensation of Fitness Costs and Reversibility of Antibiotic Resistance Mutations. *Antimicrob. Agents Chemother.* **54**, 2085–2095 (2010).

85. Davies, N. G., Flasche, S., Jit, M. & Atkins, K. E. Within-host dynamics shape antibiotic resistance in commensal bacteria. *Nat. Ecol. Evol.* 1 (2019). doi:10.1038/s41559-018-0786-x

86. Mongkolrattanothai, K. *et al.* Simultaneous carriage of multiple genotypes of Staphylococcus aureus in children. *J. Med. Microbiol.* **60**, 317–322 (2011).

87. Porse, A., Schou, T. S., Munck, C., Ellabaan, M. M. H. & Sommer, M. O. A. Biochemical mechanisms determine the functional compatibility of heterologous genes. *Nat. Commun.* **9**, 522 (2018).

88. Spoor, L. E. *et al.* Livestock Origin for a Human Pandemic Clone of Community-Associated Methicillin-Resistant Staphylococcus aureus. *mBio* **4**, e00356-13 (2013).

89. Harrison, E. M. *et al.* Genomic surveillance reveals low prevalence of livestock-associated methicillin-resistant Staphylococcus aureus in the East of England. *Sci. Rep.* **7**, 7406 (2017).

90. Holmes, A. H. *et al.* Understanding the mechanisms and drivers of antimicrobial resistance. *The Lancet* **387**, 176–187 (2016).

91. Coll, F. *et al.* Longitudinal genomic surveillance of MRSA in the UK reveals transmission patterns in hospitals and the community. *Sci. Transl. Med.* **9**, eaak9745 (2017).

92. Eveillard, M., Martin, Y., Hidri, N., Boussougant, Y. & Joly-Guillou, M.-L. Carriage of Methicillin-Resistant Staphylococcus aureus Among Hospital Employees:

Prevalence, Duration, and Transmission to Households. *Infect. Control Hosp. Epidemiol.* **25**, 114–120 (2004).

93. Bengtsson-Palme, J. *et al.* The Human Gut Microbiome as a Transporter of Antibiotic Resistance Genes between Continents. *Antimicrob. Agents Chemother.* **59**, 6551–6560 (2015).
94. von Wintersdorff, C. J. H. *et al.* High Rates of Antimicrobial Drug Resistance Gene Acquisition after International Travel, the Netherlands. *Emerg. Infect. Dis.* **20**, 649–657 (2014).
95. Chang, Q., Wang, W., Regev-Yochay, G., Lipsitch, M. & Hanage, W. P. Antibiotics in agriculture and the risk to human health: how worried should we be? *Evol. Appl.* **8**, 240–247 (2015).
96. Edelsberg, J. *et al.* Prevalence of antibiotic resistance in US hospitals. *Diagn. Microbiol. Infect. Dis.* **78**, 255–262 (2014).
97. Friedman, M. Antibiotic-Resistant Bacteria: Prevalence in Food and Inactivation by Food-Compatible Compounds and Plant Extracts. *J. Agric. Food Chem.* **63**, 3805–3822 (2015).
98. Marti, E., Jofre, J. & Balcazar, J. L. Prevalence of Antibiotic Resistance Genes and Bacterial Community Composition in a River Influenced by a Wastewater Treatment Plant. *PLOS ONE* **8**, e78906 (2013).
99. Munck, C. *et al.* Limited dissemination of the wastewater treatment plant core resistome. *Nat. Commun.* **6**, 8452 (2015).
100. Sommer, M. O. A., Dantas, G. & Church, G. M. Functional Characterization of the Antibiotic Resistance Reservoir in the Human Microflora. *Science* **325**, 1128–1131 (2009).

101. Cavaco, L. M. *et al.* Prevalence of Quinolone Resistance Mechanisms and Associations to Minimum Inhibitory Concentrations in Quinolone-Resistant Escherichia coli Isolated from Humans and Swine in Denmark. *Microb. Drug Resist.* **14**, 163–169 (2008).

102. Chen, J.-Y. *et al.* Molecular Epidemiology and Mutations at gyrA and parC Genes of Ciprofloxacin-Resistant Escherichia coli Isolates from a Taiwan Medical Center. *Microb. Drug Resist.* **7**, 47–53 (2001).

103. Lautenbach, E. *et al.* The Prevalence of Fluoroquinolone Resistance Mechanisms in Colonizing Escherichia coli Isolates Recovered from Hospitalized Patients. *Clin. Infect. Dis.* **51**, 280–285 (2010).

104. Livermore, D. M. Multiple Mechanisms of Antimicrobial Resistance in Pseudomonas aeruginosa: Our Worst Nightmare? *Clin. Infect. Dis.* **34**, 634–640 (2002).

105. Pirnay, J.-P. *et al.* Analysis of the Pseudomonas aeruginosa oprD gene from clinical and environmental isolates. *Environ. Microbiol.* **4**, 872–882 (2002).

106. Tam, V. H. *et al.* Prevalence, Resistance Mechanisms, and Susceptibility of Multidrug-Resistant Bloodstream Isolates of Pseudomonas aeruginosa. *Antimicrob. Agents Chemother.* **54**, 1160–1164 (2010).

107. Blair, J. M. A., Webber, M. A., Baylay, A. J., Ogbolu, D. O. & Piddock, L. J. V. Molecular mechanisms of antibiotic resistance. *Nat. Rev. Microbiol.* **13**, 42–51 (2015).

108. Nikaido, H. Molecular basis of bacterial outer membrane permeability revisited. *Microbiol. Mol. Biol. Rev. MMBR* **67**, 593–656 (2003).

109. Hancock, R. E. W. & Bell, A. Antibiotic Uptake into Gram-Negative Bacteria. in *Perspectives in Antiinfective Therapy* (eds. Jackson, G. G., Schlumberger, H. D. & Zeiler, H.-J.) 42–53 (Springer Berlin Heidelberg, 1989).

110. Zgurskaya, H. I. & Nikaido, H. Multidrug resistance mechanisms: drug efflux across two membranes. *Mol. Microbiol.* **37**, 219–225 (2000).

111. Lindgren, P. K., Marcusson, L. L., Sandvang, D., Frimodt-Moller, N. & Hughes, D. Biological Cost of Single and Multiple Norfloxacin Resistance Mutations in Escherichia coli Implicated in Urinary Tract Infections. *Antimicrob. Agents Chemother.* **49**, 2343–2351 (2005).

112. Okusu, H., Ma, D. & Nikaido, H. AcrAB efflux pump plays a major role in the antibiotic resistance phenotype of Escherichia coli multiple-antibiotic-resistance (Mar) mutants. *J. Bacteriol.* **178**, 306–308 (1996).

113. Su, C.-C., Rutherford, D. J. & Yu, E. W. Characterization of the multidrug efflux regulator AcrR from Escherichia coli. *Biochem. Biophys. Res. Commun.* **361**, 85–90 (2007).

114. Nikaido, H. Multidrug Resistance in Bacteria. *Annu. Rev. Biochem.* **78**, 119–146 (2009).

115. Elkins, C. A. & Nikaido, H. Substrate Specificity of the RND-Type Multidrug Efflux Pumps AcrB and AcrD of Escherichia coli Is Determined Predominately by Two Large Periplasmic Loops. *J. Bacteriol.* **184**, 6490–6498 (2002).

116. Munita, J. M. & Arias, C. A. Mechanisms of Antibiotic Resistance. *Microbiol. Spectr.* **4**, (2016).

117. Schmidtke, A. J. & Hanson, N. D. Role of ampD Homologs in Overproduction of AmpC in Clinical Isolates of Pseudomonas aeruginosa. *Antimicrob. Agents Chemother.* **52**, 3922–3927 (2008).

118. Bush, K. Past and Present Perspectives on β-Lactamases. *Antimicrob. Agents Chemother.* **62**, e01076-18 (2018).

119. Worthington, R. J. & Melander, C. Overcoming Resistance to β-Lactam Antibiotics. *J. Org. Chem.* **78**, 4207–4213 (2013).

120. Conrad, S. *et al.* gyrA mutations in high-level fluoroquinolone-resistant clinical isolates of Escherichia coli. *J. Antimicrob. Chemother.* **38**, 443–455 (1996).

121. Weisblum, B. Erythromycin resistance by ribosome modification. *Antimicrob. Agents Chemother.* **39**, 577–585 (1995).

122. Barbosa, T. M. & Levy, S. B. Differential Expression of over 60 Chromosomal Genes in Escherichia coli by Constitutive Expression of MarA. *J. Bacteriol.* **182**, 3467–3474 (2000).

123. Hirakawa, H., Nishino, K., Hirata, T. & Yamaguchi, A. Comprehensive studies of drug resistance mediated by overexpression of response regulators of two-component signal transduction systems in Escherichia coli. *J. Bacteriol.* **185**, 1851–1856 (2003).

124. Raivio, T. L., Leblanc, S. K. D. & Price, N. L. The Escherichia coli Cpx Envelope Stress Response Regulates Genes of Diverse Function That Impact Antibiotic Resistance and Membrane Integrity. *J. Bacteriol.* **195**, 2755–2767 (2013).

125. Mahoney, T. F. & Silhavy, T. J. The Cpx Stress Response Confers Resistance to Some, but Not All, Bactericidal Antibiotics. *J. Bacteriol.* **195**, 1869–1874 (2013).

126. Abu Sin, M. *et al.* Globale und nationale Strategien gegen Antibiotikaresistenzen. *Bundesgesundheitsblatt - Gesundheitsforschung - Gesundheitsschutz* **61**, 507–514 (2018).

127. WHO publishes list of bacteria for which new antibiotics are urgently needed. Available at: https://www.who.int/news-room/detail/27-02-2017-who-publishes-list-of-bacteria-for-which-new-antibiotics-are-urgently-needed. (Accessed: 18th February 2019)

128. Jang, J. *et al.* Environmental Escherichia coli: ecology and public health implications-a review. *J. Appl. Microbiol.* **123**, 570–581 (2017).

129. Kaper, J. B., Nataro, J. P. & Mobley, H. L. T. Pathogenic *Escherichia coli*. *Nat. Rev. Microbiol.* **2**, 123–140 (2004).

130. Bodilsen, J. *et al.* Community-acquired meningitis in adults caused by Escherichia coli in Denmark and The Netherlands. *J. Infect.* **77**, 25–29 (2018).

131. Flores-Mireles, A. L., Walker, J. N., Caparon, M. & Hultgren, S. J. Urinary tract infections: epidemiology, mechanisms of infection and treatment options. *Nat. Rev. Microbiol.* **13**, 269–284 (2015).

132. Tandogdu, Z. & Wagenlehner, F. M. E. Global epidemiology of urinary tract infections. *Curr. Opin. Infect. Dis.* **29**, 73 (2016).

133. Nickel, J. C. Practical Management of Recurrent Urinary Tract Infections in Premenopausal Women. *Rev. Urol.* **7**, 11–17 (2005).

134. Sezonov, G., Joseleau-Petit, D. & D'Ari, R. Escherichia coli Physiology in Luria-Bertani Broth. *J. Bacteriol.* **189**, 8746–8749 (2007).

135. Baba, T. *et al.* Construction of Escherichia coli K-12 in-frame, single-gene knockout mutants: the Keio collection. *Mol. Syst. Biol.* **2**, 2006.0008 (2006).

136. Tamae, C. *et al.* Determination of Antibiotic Hypersensitivity among 4,000 Single-Gene-Knockout Mutants of Escherichia coli. *J. Bacteriol.* **190**, 5981–5988 (2008).

137. Frimodt-Møller, J. *et al.* Mutations causing low level antibiotic resistance ensure bacterial survival in antibiotic-treated hosts. *Sci. Rep.* **8**, (2018).

138. Jochumsen, N. *et al.* The evolution of antimicrobial peptide resistance in Pseudomonas aeruginosa is shaped by strong epistatic interactions. *Nat. Commun.* **7**, 13002 (2016).

139. Marvig, R. L., Madsen Sommer, L. M., Jelsbak, L., Molin, S. & Johansen, H. K. Evolutionary insight from whole-genome sequencing of Pseudomonas aeruginosa from cystic fibrosis patients. *Future Microbiol.* **10**, 599–611 (2015).

140. Mojsoska, B. *et al.* High persister phenotype of Pseudomonas Aeruginosa is associated with increased fitness in cystic fibrosis airways. *Pediatr. Pulmonol.* **53**, 315–315 (2018).

141. Gellatly, S. L. & Hancock, R. E. W. Pseudomonas aeruginosa: new insights into pathogenesis and host defenses. *Pathog. Dis.* **67**, 159–173 (2013).

142. Lyczak, J. B., Cannon, C. L. & Pier, G. B. Lung Infections Associated with Cystic Fibrosis. *Clin. Microbiol. Rev.* **15**, 194–222 (2002).

143. Driscoll, J. A., Brody, S. L. & Kollef, M. H. The Epidemiology, Pathogenesis and Treatment of Pseudomonas aeruginosa Infections. *Drugs* **67**, 351–368 (2007).

144. Morita, Y., Tomida, J. & Kawamura, Y. Responses of Pseudomonas aeruginosa to antimicrobials. *Front. Microbiol.* **4**, (2014).

145. Moreau-Marquis, S., Stanton, B. A. & O'Toole, G. A. Pseudomonas aeruginosa biofilm formation in the cystic fibrosis airway. *Pulm. Pharmacol. Ther.* **21**, 595–599 (2008).

146. Imamovic, L. *et al.* Drug-Driven Phenotypic Convergence Supports Rational Treatment Strategies of Chronic Infections. *Cell* **172**, 121-134.e14 (2018).

147. Reller, L. B., Weinstein, M., Jorgensen, J. H. & Ferraro, M. J. Antimicrobial Susceptibility Testing: A Review of General Principles and Contemporary Practices. *Clin. Infect. Dis.* **49**, 1749–1755 (2009).

148. Haeili, M. *et al.* Copper Complexation Screen Reveals Compounds with Potent Antibiotic Properties against Methicillin-Resistant Staphylococcus aureus. *Antimicrob. Agents Chemother.* **58**, 3727–3736 (2014).

149. Munck, C., Gumpert, H. K., Wallin, A. I. N., Wang, H. H. & Sommer, M. O. A. Prediction of resistance development against drug combinations by collateral responses to component drugs. *Sci. Transl. Med.* **6**, 262ra156-262ra156 (2014).

150. Samuels, D. S., Marconi, R. T., Huang, W. M. & Garon, C. F. gyrB mutations in coumermycin A1-resistant Borrelia burgdorferi. *J. Bacteriol.* **176**, 3072–3075 (1994).

151. Alexander, H. K. & MacLean, C. Stochastic bacterial population dynamics prevent the emergence of antibiotic resistance. *bioRxiv* (2019). doi:10.1101/458547

152. Levin, B. R. & Udekwu, K. I. Population Dynamics of Antibiotic Treatment: a Mathematical Model and Hypotheses for Time-Kill and Continuous-Culture Experiments. *Antimicrob. Agents Chemother.* **54**, 3414–3426 (2010).

153. van Dijk, E. L., Jaszczyszyn, Y., Naquin, D. & Thermes, C. The Third Revolution in Sequencing Technology. *Trends Genet.* **34**, 666–681 (2018).

154. Mercier-Darty, M., Boutolleau, D., Lepeule, R., Rodriguez, C. & Burrel, S. Utility of ultra-deep sequencing for detection of varicella-zoster virus antiviral resistance mutations. *Antiviral Res.* **151**, 20–23 (2018).

155. Alemany, A., Florescu, M., Baron, C. S., Peterson-Maduro, J. & van Oudenaarden, A. Whole-organism clone tracing using single-cell sequencing. *Nature* **556**, 108–112 (2018).

156. Gardy, J. L. & Loman, N. J. Towards a genomics-informed, real-time, global pathogen surveillance system. *Nat. Rev. Genet.* **19**, 9–20 (2018).

157. Köser, C. U. *et al.* Routine Use of Microbial Whole Genome Sequencing in Diagnostic and Public Health Microbiology. *PLOS Pathog.* **8**, e1002824 (2012).

158. Coll, F. *et al.* Rapid determination of anti-tuberculosis drug resistance from whole-genome sequences. *Genome Med.* **7**, 51 (2015).

159. Andersson, D. I. & Hughes, D. Evolution of antibiotic resistance at non-lethal drug concentrations. *Drug Resist. Updat.* **15**, 162–172 (2012).

160. Porse, A., Schønning, K., Munck, C. & Sommer, M. O. A. Survival and Evolution of a Large Multidrug Resistance Plasmid in New Clinical Bacterial Hosts. *Mol. Biol. Evol.* **33**, 2860–2873 (2016).

161. Satta, G. *et al.* Mycobacterium tuberculosis and whole-genome sequencing: how close are we to unleashing its full potential? *Clin. Microbiol. Infect.* **24**, 604–609 (2018).

162. San Millan, A., Escudero, J. A., Gifford, D. R., Mazel, D. & MacLean, R. C. Multicopy plasmids potentiate the evolution of antibiotic resistance in bacteria. *Nat. Ecol. Evol.* **1**, 0010 (2016).

163. Barbosa, C. *et al.* Alternative Evolutionary Paths to Bacterial Antibiotic Resistance Cause Distinct Collateral Effects. *Mol. Biol. Evol.* doi:10.1093/molbev/msx158

164. Imamovic, L. & Sommer, M. O. A. Use of Collateral Sensitivity Networks to Design Drug Cycling Protocols That Avoid Resistance Development. *Sci. Transl. Med.* **5**, 204ra132-204ra132 (2013).

165. Lazar, V. *et al.* Bacterial evolution of antibiotic hypersensitivity. *Mol. Syst. Biol.* **9**, 700–700 (2014).

166. Oz, T. *et al.* Strength of Selection Pressure Is an Important Parameter Contributing to the Complexity of Antibiotic Resistance Evolution. *Mol. Biol. Evol.* **31**, 2387–2401 (2014).

167. de Evgrafov, M. R., Gumpert, H., Munck, C., Thomsen, T. T. & Sommer, M. O. Collateral resistance and sensitivity modulate evolution of high-level resistance to drug combination treatment in Staphylococcus aureus. *Mol. Biol. Evol.* msv006 (2015).

168. Hegreness, M., Shoresh, N., Damian, D., Hartl, D. & Kishony, R. Accelerated evolution of resistance in multidrug environments. *Proc. Natl. Acad. Sci.* **105**, 13977–13981 (2008).

169. Baym, M. *et al.* Spatiotemporal microbial evolution on antibiotic landscapes. *Science* **353**, 1147–1151 (2016).

170. Toprak, E. *et al.* Evolutionary paths to antibiotic resistance under dynamically sustained drug selection. *Nat. Genet.* **44**, 101–105 (2011).

171. Alonso, A., Campanario, E. & Martínez, J. L. Emergence of multidrug-resistant mutants is increased under antibiotic selective pressure in Pseudomonas aeruginosa. *Microbiology* **145**, 2857–2862 (1999).

172. Knöppel, A., Näsvall, J. & Andersson, D. I. Evolution of Antibiotic Resistance without Antibiotic Exposure. *Antimicrob. Agents Chemother.* **61**, e01495-17 (2017).

173. Ahmed, M. N., Porse, A., Sommer, M. O. A., Høiby, N. & Ciofu, O. Evolution of Antibiotic Resistance in Biofilm and Planktonic Pseudomonas aeruginosa Populations Exposed to Subinhibitory Levels of Ciprofloxacin. *Antimicrob. Agents Chemother.* **62**, e00320-18 (2018).

174. Bergh, B. V. den *et al.* Frequency of antibiotic application drives rapid evolutionary adaptation of *Escherichia coli* persistence. *Nat. Microbiol.* **1**, nmicrobiol201620 (2016).

175. Levin-Reisman, I. *et al.* Antibiotic tolerance facilitates the evolution of resistance. *Science* **355**, 826–830 (2017).

176. Roemhild, R. *et al.* Cellular hysteresis as a principle to maximize the efficacy of antibiotic therapy. *Proc. Natl. Acad. Sci.* **115**, 9767–9772 (2018).

177. Wistrand-Yuen, E. *et al.* Evolution of high-level resistance during low-level antibiotic exposure. *Nat. Commun.* **9**, 1599 (2018).

178. Adler, M., Anjum, M., Andersson, D. I. & Sandegren, L. Combinations of mutations in envZ, ftsI, mrdA, acrB and acrR can cause high-level carbapenem resistance in Escherichia coli. *J. Antimicrob. Chemother.* **71**, 1188–1198 (2016).

179. Vogwill, T., Kojadinovic, M., Furió, V. & MacLean, R. C. Testing the Role of Genetic Background in Parallel Evolution Using the Comparative Experimental Evolution of Antibiotic Resistance. *Mol. Biol. Evol.* **31**, 3314–3323 (2014).

180. Knopp, M. & Andersson, D. I. Amelioration of the Fitness Costs of Antibiotic Resistance Due To Reduced Outer Membrane Permeability by Upregulation of Alternative Porins. *Mol. Biol. Evol.* **32**, 3252–3263 (2015).

181. Sekowska, A., Wendel, S., Fischer, E. C., Nørholm, M. H. H. & Danchin, A. Generation of mutation hotspots in ageing bacterial colonies. *Sci. Rep.* **6**, 2 (2016).

182. Ghaddar, N., Hashemidahaj, M. & Findlay, B. L. Access to high-impact mutations constrains the evolution of antibiotic resistance in soft agar. *Sci. Rep.* **8**, 17023 (2018).

183. Tenaillon, O., Toupance, B., Nagard, H. L., Taddei, F. & Godelle, B. Mutators, Population Size, Adaptive Landscape and the Adaptation of Asexual Populations of Bacteria. *Genetics* **152**, 485–493 (1999).

184. Huseby, D. L. *et al.* Mutation Supply and Relative Fitness Shape the Genotypes of Ciprofloxacin-Resistant Escherichia coli. *Mol. Biol. Evol.* **34**, 1029–1039 (2017).

185. Wahl, L. M., Gerrish, P. J. & Saika-Voivod, I. Evaluating the Impact of Population Bottlenecks in Experimental Evolution. *Genetics* **162**, 961–971 (2002).

186. Hansen, S., Lewis, K. & Vulić, M. Role of global regulators and nucleotide metabolism in antibiotic tolerance in Escherichia coli. *Antimicrob. Agents Chemother.* **52**, 2718–2726 (2008).

187. Linares, J. F. *et al.* The global regulator Crc modulates metabolism, susceptibility to antibiotics and virulence in Pseudomonas aeruginosa. *Environ. Microbiol.* **12**, 3196–3212 (2010).

188. Wagner, V. E., Bushnell, D., Passador, L., Brooks, A. I. & Iglewski, B. H. Microarray Analysis of Pseudomonas aeruginosa Quorum-Sensing Regulons: Effects of Growth Phase and Environment. *J. Bacteriol.* **185**, 2080–2095 (2003).

189. Gad, F., Zahra, T., Hasan, T. & Hamblin, M. R. Effects of Growth Phase and Extracellular Slime on Photodynamic Inactivation of Gram-Positive Pathogenic Bacteria. *Antimicrob. Agents Chemother.* **48**, 2173–2178 (2004).

190. Kobayashi, A., Hirakawa, H., Hirata, T., Nishino, K. & Yamaguchi, A. Growth Phase-Dependent Expression of Drug Exporters in Escherichia coli and Its Contribution to Drug Tolerance. *J. Bacteriol.* **188**, 5693–5703 (2006).

191. Thulin, E., Sundqvist, M. & Andersson, D. I. Amdinocillin (Mecillinam) Resistance Mutations in Clinical Isolates and Laboratory-Selected Mutants of Escherichia coli. *Antimicrob. Agents Chemother.* **59**, 1718–1727 (2015).

192. Wang, H., Dzink-Fox, J. L., Chen, M. & Levy, S. B. Genetic characterization of highly fluoroquinolone-resistant clinical Escherichia coli strains from China: role of acrR mutations. *Antimicrob. Agents Chemother.* **45**, 1515–1521 (2001).

193. Warner, D. M. *et al.* Involvement of MarR and YedS in carbapenem resistance in a clinical isolate of Escherichia coli from China. *Antimicrob. Agents Chemother.* **57**, 1935–1937 (2013).

194. Winstanley, C., O'Brien, S. & Brockhurst, M. A. Pseudomonas aeruginosa Evolutionary Adaptation and Diversification in Cystic Fibrosis Chronic Lung Infections. *Trends Microbiol.* **24**, 327–337 (2016).

195. Beutner, E. H., Doyle, W. M. & Evander, L. C. Collateral Susceptibility of Isoniazid-Resistant Tubercle Bacilli To Nitrofurans. *Am. Rev. Respir. Dis.* **88**, 712–715 (1963).

196. Szybalski, W. & Bryson, V. GENETIC STUDIES ON MICROBIAL CROSS RESISTANCE TO TOXIC AGENTS I. ,. *J. Bacteriol.* **64**, 489–499 (1952).

197. Lázár, V. *et al.* Antibiotic-resistant bacteria show widespread collateral sensitivity to antimicrobial peptides. *Nat. Microbiol.* **3**, 718–731 (2018).

198. Lázár, V. *et al.* Genome-wide analysis captures the determinants of the antibiotic cross-resistance interaction network. *Nat. Commun.* **5**, 4352 (2014).

199. Nichol, D. *et al.* Antibiotic collateral sensitivity is contingent on the repeatability of evolution. *Nat. Commun.* **10**, 334 (2019).

200. Obolski, U., Dellus-Gur, E., Stein, G. Y. & Hadany, L. Antibiotic cross-resistance in the lab and resistance co-occurrence in the clinic: Discrepancies and implications in E.coli. *Infect. Genet. Evol. J. Mol. Epidemiol. Evol. Genet. Infect. Dis.* **40**, 155–161 (2016).

201. Podnecky, N. L. *et al.* Conserved collateral antibiotic susceptibility networks in diverse clinical strains of Escherichia coli. *Nat. Commun.* **9**, 3673 (2018).

202. Horinouchi, T. *et al.* Prediction of Cross-resistance and Collateral Sensitivity by Gene Expression profiles and Genomic Mutations. *Sci. Rep.* **7**, 14009 (2017).

203. Suzuki, S., Horinouchi, T. & Furusawa, C. Prediction of antibiotic resistance by gene expression profiles. *Nat. Commun.* **5**, 5792 (2014).

204. Liu, A. *et al.* Antibiotic Sensitivity Profiles Determined with an Escherichia coli Gene Knockout Collection: Generating an Antibiotic Bar Code. *Antimicrob. Agents Chemother.* **54**, 1393–1403 (2010).

205. Chait, R., Craney, A. & Kishony, R. Antibiotic interactions that select against resistance. *Nature* **446**, 668–671 (2007).

206. Colclough, A., Corander, J., Sheppard, S., Bayliss, S. & Vos, M. Patterns of cross-resistance and collateral sensitivity between clinical antibiotics and natural antimicrobials. (2019). doi:10.1111/eva.12762

207. Fuentes-Hernandez, A. *et al.* Using a Sequential Regimen to Eliminate Bacteria at Sublethal Antibiotic Dosages. *PLoS Biol* **13**, e1002104 (2015).

208. Nichol, D. *et al.* Steering Evolution with Sequential Therapy to Prevent the Emergence of Bacterial Antibiotic Resistance. *PLOS Comput. Biol.* **11**, e1004493 (2015).

209. Roemhild, R., Barbosa, C., Beardmore, R. E., Jansen, G. & Schulenburg, H. Temporal variation in antibiotic environments slows down resistance evolution in pathogenic Pseudomonas aeruginosa. *Evol. Appl.* **8**, 945–955 (2015).

210. Barbosa, C., Roemhild, R., Rosenstiel, P. & Schulenburg, H. Evolutionary stability of collateral sensitivity to antibiotics in the model pathogen Pseudomonas aeruginosa. *bioRxiv* 570663 (2019). doi:10.1101/570663

211. Udekwu, K. I. & Weiss, H. Pharmacodynamic considerations of collateral sensitivity in design of antibiotic treatment regimen. *Drug Des. Devel. Ther.* **12**, 2249–2257 (2018).

212. Tepekule, B., Uecker, H., Derungs, I., Frenoy, A. & Bonhoeffer, S. Modeling antibiotic treatment in hospitals: A systematic approach shows benefits of combination therapy over cycling, mixing, and mono-drug therapies. *PLOS Comput. Biol.* **13**, e1005745 (2017).

213. Barbosa, C., Beardmore, R., Schulenburg, H. & Jansen, G. Antibiotic combination efficacy (ACE) networks for a Pseudomonas aeruginosa model. *PLoS Biol.* **16**, (2018).

214. Suzuki, S., Horinouchi, T. & Furusawa, C. Suppression of antibiotic resistance acquisition by combined use of antibiotics. *J. Biosci. Bioeng.* **120**, 467–469 (2015).

215. Dellus-Gur, E. *et al.* Negative Epistasis and Evolvability in TEM-1 β-Lactamase—The Thin Line between an Enzyme's Conformational Freedom and Disorder. *J. Mol. Biol.* **427**, 2396–2409 (2015).

216. Khan, A. I., Dinh, D. M., Schneider, D., Lenski, R. E. & Cooper, T. F. Negative Epistasis Between Beneficial Mutations in an Evolving Bacterial Population. *Science* **332**, 1193–1196 (2011).

217. Palmer, A. C. *et al.* Delayed commitment to evolutionary fate in antibiotic resistance fitness landscapes. *Nat. Commun.* **6**, 7385 (2015).

218. Hemeg, H. A. Nanomaterials for alternative antibacterial therapy. *Int. J. Nanomedicine* **12**, 8211–8225 (2017).

219. Berghman, L. R., Abi-Ghanem, D., Waghela, S. D. & Ricke, S. C. Antibodies: an alternative for antibiotics? *Poult. Sci.* **84**, 660–666 (2005).

220. Mariathasan, S. & Tan, M.-W. Antibody–Antibiotic Conjugates: A Novel Therapeutic Platform against Bacterial Infections. *Trends Mol. Med.* **23**, 135–149 (2017).

221. Lin, D. M., Koskella, B. & Lin, H. C. Phage therapy: An alternative to antibiotics in the age of multi-drug resistance. *World J. Gastrointest. Pharmacol. Ther.* **8**, 162–173 (2017).

222. Pursey, E., Sünderhauf, D., Gaze, W. H., Westra, E. R. & Houte, S. van. CRISPR-Cas antimicrobials: Challenges and future prospects. *PLOS Pathog.* **14**, e1006990 (2018).

223. Richter, C., Chang, J. T. & Fineran, P. C. Function and Regulation of Clustered Regularly Interspaced Short Palindromic Repeats (CRISPR) / CRISPR Associated (Cas) Systems. *Viruses* **4**, 2291–2311 (2012).

224. Doudna, J. A. & Charpentier, E. Genome editing. The new frontier of genome engineering with CRISPR-Cas9. *Science* **346**, 1258096 (2014).

225. Gomaa, A. A. *et al.* Programmable Removal of Bacterial Strains by Use of Genome-Targeting CRISPR-Cas Systems. *mBio* **5**, e00928-13 (2014).

226. Cho, I. & Blaser, M. J. The human microbiome: at the interface of health and disease. *Nat. Rev. Genet.* **13**, 260–270 (2012).

227. Kozak, M. L. & Larsen, J. C. Economic Incentives for Antibacterial Drug Development: Alternative Market Structures to Promote Innovation. in *Antimicrobial Resistance in the 21st Century* (eds. Fong, I. W., Shlaes, D. & Drlica, K.) 721–753 (Springer International Publishing, 2018). doi:10.1007/978-3-319-78538-7_24

228. Lum, K., Bhatti, T., Holland, S., Guthrie, M. & Sassman, S. Diagnosis Confirmation Model: A Value-Based Pricing Model for Inpatient Novel Antibiotics. *J. Law. Med. Ethics* **46**, 66–74 (2018).

229. Minssen, T. & Nordberg, A. *Rules and Tools in the Battle Against Superbugs - A Call for Integrated Strategies and Enhanced International Collaboration to Promote Antimicrobial Drug Development*. (Social Science Research Network, 2018).

230. Monnier, A. A. *et al.* Ensuring Antibiotic Development, Equitable Availability, and Responsible Use of Effective Antibiotics: Recommendations for Multisectoral Action. *Clin. Infect. Dis.* doi:10.1093/cid/ciy824

231. Piddock, L. J. The crisis of no new antibiotics—what is the way forward? *Lancet Infect. Dis.* **12**, 249–253 (2012).

232. Storehagen, L., Aftab, F., Årdal, C., Savic, M. & Røttingen, J.-A. Should Antibiotics Be Controlled Medicines? Lessons from the Controlled Drug Regimen. *J. Law. Med. Ethics* **46**, 81–94 (2018).

233. Drug Innovation - Novel Drug Approvals for 2018. Available at: https://www.fda.gov/drugs/developmentapprovalprocess/druginnovation/ucm592464.htm. (Accessed: 25th February 2019)

234. Zhanel, G. G. *et al.* Review of Eravacycline, a Novel Fluorocycline Antibacterial Agent. *Drugs* **76**, 567–588 (2016).

235. The Red Queen was right: We have to run to keep in place. Available at: https://phys.org/news/2013-06-red-queen.html. (Accessed: 25th April 2019)